Summary of Activities

2016

CANADA-NUNAVUT GEOSCIENCE OFFICE
ᑲᓇᑕᐅᑉ-ᓄᓇᕗᑦᒧ ᐅᔭᖅᑲᓂᒃ ᖃᐅᔨᓴᖅᑎᖏᑦ
BUREAU GÉOSCIENTIFIQUE CANADA-NUNAVUT
KANATAMI-NUNAVUMI GEOSCIENCE TITIGAKVIIT

CANADA-NUNAVUT
GEOSCIENCE OFFICE

ᑲᓇᑕᐅᑉ-ᓄᓇᕘᓪᓗ
ᐅᔾᖅᑲᓂᒃ ᖃᐅᔨᓴᖅᑎᕐᕕᑦ

BUREAU GÉOSCIENTIFIQUE
CANADA-NUNAVUT

KANATAMI-NUNAVUMI
GEOSCIENCE TITIGAKVIIT

SUMMARY OF ACTIVITIES 2016

This publication is also available, free of charge, as colour digital files in Adobe Acrobat® PDF format from the Canada-Nunavut Geoscience Office website: www.cngo.ca/

Every reasonable effort is made to ensure the accuracy of the information contained in this report, but Natural Resources Canada does not assume any liability for errors that may occur. Source references are included in the report and users should verify critical information.

When using information from this publication in other publications or presentations, due acknowledgment should be given to Canada-Nunavut Geoscience Office. The recommended reference is included on the title page of each paper. The complete volume should be referenced as follows:

Canada-Nunavut Geoscience Office (2016): Canada-Nunavut Geoscience Office Summary of Activities 2016; Canada-Nunavut Geoscience Office, 140 p.

ISSN 2291-1235 Canada-Nunavut Geoscience Office Summary of Activities (Print)
ISSN 2291-1243 Canada-Nunavut Geoscience Office Summary of Activities (Online)

Front cover photo: Measuring ice-flow indicators on glacially polished quartzite outcrop near the Keewatin Ice Divide, south of Wager Bay, Nunavut. Photo by Iyse Randour, Université du Québec à Montréal.

Back cover photo: Grey carbonate interbedded with yellow to red siltstone (1–5 cm thick) at the base of the Laddie formation in the Paleoproterozoic Belcher Group on western Tukarak Island, Nunavut. Photo by Lauren Timlick, University of Manitoba.

Foreword

I am pleased to be releasing this 2016 *Summary of Activities* volume of the Canada-Nunavut Geoscience Office (CNGO). This marks the fifth year for the volume's release, although only the second year for me, as Chief Geologist, to be releasing it. I am very proud of, and grateful to, all of the hard-working CNGO professionals, and the other researchers and collaborators who contribute in so many ways to help us understand various aspects of Nunavut's geology. I have heard from many mineral industry and government stakeholders that this volume is always well received.

The Canada-Nunavut Geoscience Office was established in 1999 and is a partnership between Natural Resources Canada, Earth Sciences Sector (NRCan-ESS); Indigenous and Northern Affairs Canada (INAC); and the Government of Nunavut, Economic Development and Transportation (GN-EDT). Nunavut Tunngavik Incorporated (NTI) is an ex-officio member of the office. The CNGO is co-managed and co-funded by the three partners; operational direction and activities are assisted by a Management Board consisting of representatives from NRCan, INAC, GN-EDT, NTI and the Chief Geologist. This office also has a Technical Advisory Committee that meets at least annually to discuss research and strategic ideas for the office.

The CNGO consists of six full-time professionals with expertise in Precambrian, Paleozoic and Quaternary geology, GIS and cartography, and online data dissemination. The mandate of the office is to provide Nunavut with accessible geoscience information and expertise to support 1) responsible resource exploration and development, 2) responsible infrastructure development, 3) geoscience capacity building, 4) geoscience education and training, and 5) geoscience awareness and outreach.

The papers in each annual volume document findings and results from a variety of research conducted by the CNGO with and by our partners and other collaborators in the past year. We have successfully disseminated these data in a timely manner and, starting with last year's volume, before the end of the calendar year in which the activities took place.

Collectively, this high-quality research increases the level of geological knowledge in Nunavut and ensures that the new geoscience information is accessible for making land-use decisions in the future. Additionally, this information allows evaluations of resource potential for a variety of commodities, including diamonds and other gemstones, base and precious metals, industrial minerals, carving stone and aggregates. These activities also aim to assist northerners by providing geoscience training to college and university students.

The office finished a two-year geoscience program (2014–2016) this past spring and recently received approval for an additional two years of programming (2016–2018) that will focus on activities to support responsible exploration and development of natural resources, allow responsible infrastructure development to occur and be protected, and disseminate geoscience data and information.

The 12 papers in this 2016 volume are grouped under four topics—'Regional Geoscience', 'Geoscience for Infrastructure', 'Carving Stone' and 'Outreach'—that all support the mandate of the office. All papers are available for download, free of charge, at www.cngo.ca. In 2013, the CNGO introduced a new publication series, the 'Geoscience Data Series', that disseminates digital data such as analytical datasets, point data, polygon and metadata files. Data that support the research work and papers in this volume continue to be released through this additional avenue.

For the 'Regional Geoscience' research, six papers focus on targeted bedrock mapping, surficial geology studies, sediment and water sampling, and other thematic studies. The first paper deals with continuing research on microfossils (conodonts) within carbonate xenoliths found in the Chidliak kimberlites. This research is providing additional data to help understand the emplacement processes and cooling history of the kimberlites. The second paper, surficial geological mapping in the Sylvia Grinnell Lake area, reports on the analyses of samples of till, stream sediments, lake sediments, stream water and lake water for determining the surficial landforms and history for this area. Papers three to five report findings from the Tehery Lake–Wager Bay mapping project in central Nunavut. Geological mapping discussed in the third paper focuses on characterizing the rock units and features in this area; several new discoveries were made that will help resolve its enigmatic geological history. The fourth paper discusses the use of gravity and magnetic data to identify shallow crustal structures, and preliminary results from a thematic study of the postglacial marine limit are discussed in the fifth paper. The final paper of this section reports on a continuing study in Frobisher Bay to map the regional seafloor geoscience. Understanding the seabed geology, geohazards in the area and the geological processes affecting the seafloor will aid in future development in this region.

In recognition of climate change and warming conditions occurring in the North, the 'Geoscience for Infrastructure' section has four papers that discuss a variety of these effects and conditions. The first two papers discuss permafrost in the Rankin Inlet area of central Nunavut, and the latter two document preliminary findings in the Niaqunguk River (commonly referred to unofficially as the Apex river) watershed. The first paper on permafrost reports on the recording of observations and selection of sites for permafrost and ground-temperature monitoring stations. A workshop held in February of this year in Rankin Inlet is reported upon in the second paper. This workshop involved understanding permafrost conditions through integration of local and traditional observations with geoscience data. The third paper presents preliminary findings about snow hydrology in the Niaqunguk River watershed. This work is conducted through the 'Partnership for Integrated Hydrological and Water Quality Monitoring, Research and Training'. Research for the fourth paper in this section took a methodological approach to understanding groundwater movement by characterizing flow paths and water sources during the active-layer thaw period. The research for these latter two papers was conducted in the Niaqunguk River watershed, a river that could be a supplemental source of potable water for Iqaluit and Apex.

Stone that is suitable for carving has been the focus of recent targeted work in Nunavut to determine the characteristics (quality and quantity) of the stone for Nunavut's artists. In 2016, a team of geologists from the Qikqitani Inuit Association and the CNGO, and a geology student from the University of Manitoba visited four carving stone sites in the Belcher Islands to survey the landscape, map out the carving stone deposits and try to understand how the carving stone was formed.

The final paper in this volume discusses an initiative that took place outside the Hamlet of Taloyaok this past summer. A pilot program for a community field school was conducted in preparation for bedrock mapping by the Geological Survey of Canada and the CNGO in 2017 and 2018. This field school provided northerners with opportunities to see how geological data are collected in the field and how these data can assist with future decision-making in a manner that does not necessarily impose a significant impact on the environment.

I hope everyone who reads these papers enjoys learning about the variety of high-quality research conducted by this office, and our partners and collaborators.

Acknowledgments

The CNGO staff thanks all authors of papers in this fifth *Summary of Activities*. Their dedication is greatly appreciated, and is critical in helping the CNGO deliver such a quality product. RnD Technical is also thanked for their technical editing and assembling of the volume. In addition, special thanks are extended to reviewers of papers:

Vaughn Barrie	Geological Survey of Canada
Janet Campbell	Geological Survey of Canada
Kate Clark	Geological Survey of Canada
Carl Guilmette	Université Laval
David Mate	Polar Knowledge Canada
Martin McCurdy	Geological Survey of Canada
Peter Morse	Geological Survey of Canada
Greg Oldenborger	Geological Survey of Canada
J. Kelly Russell	University of British Columbia
Wendy Sladen	Geological Survey of Canada
Mike Thomas	Geological Survey of Canada
Tommy Tremblay	Canada-Nunavut Geoscience Office

Linda Ham
Chief Geologist
Canada-Nunavut Geoscience Office
www.cngo.ca/

Préface

Il me fait plaisir d'annoncer la publication de l'édition 2016 du *Sommaire des activités* du Bureau géoscientifique Canada-Nunavut. Il y a maintenant cinq ans que le Bureau publie ce volume bien que, dans mon cas, il ne s'agisse que de la seconde année pour laquelle je suis responsable de sa parution à titre de géologue en chef. Je suis extrêmement fière de tous les professionnels consciencieux qui œuvrent au sein du Bureau, ainsi que de tous les autres collaborateurs et chercheurs qui contribuent de diverses façons à l'acquisition de connaissances au sujet de la géologie qui caractérise le Nunavut, et je les en remercie. J'ai appris de la part de nombreux intervenants des secteurs de l'industrie minérale et du gouvernement à quel point ce volume est toujours bien accueilli.

Le Bureau géoscientifique Canada-Nunavut, fondé en 1999, est le fruit d'une collaboration entre le Secteur des Sciences de la Terre relevant de Ressources naturelles Canada, les Affaires autochtones et du Nord Canada et le ministère du Développement économique et des Transports relevant du Gouvernement du Nunavut. La société Nunavut Tunngavik Incorporated est un membre d'office du Bureau, lequel est géré et subventionné à la fois par les trois partenaires. Un Conseil de gestion constitué de représentants de tous ces organismes, aussi bien gouvernementaux que privé, et du géologue en chef procure son soutien aux travaux et à la direction opérationnelle du Bureau, lequel dispose en outre d'un Comité consultatif technique dont les membres se rencontrent au moins une fois l'an en vue de discuter des orientations stratégiques et en matière de recherche.

Le Bureau compte actuellement six employés professionnels à plein temps dont les connaissances spécialisées portent sur la géologie du Précambrien, du Paléozoïque et du Quaternaire, ainsi que sur la cartographie et les systèmes d'information géographique, et la diffusion de données géoscientifiques en ligne. Le Bureau a pour mandat de fournir de l'information et des connaissances spécialisées en géosciences au Nunavut en vue de promouvoir 1) la poursuite de travaux d'exploration et de mise en valeur responsables des ressources, 2) le développement responsable des infrastructures, 3) le renforcement des capacités géoscientifiques, 4) l'éducation et les possibilités de formation dans le domaine des sciences de la Terre et 5) la mise en place de programmes de sensibilisation du public en matière de géosciences.

Les articles paraissant dans les volumes annuels présentent les constatations et les résultats liés aux recherches menées par le Bureau dans divers domaines, ainsi que provenant de travaux réalisés au cours de cette année par nos partenaires et autres collaborateurs, ou conjointement avec ces derniers. Nous avons réussi à diffuser ces données en temps opportun et, depuis l'édition de l'an passé, cela même avant la fin de l'année civile au cours de laquelle se sont déroulés ces travaux.

Ces travaux de recherche de haute qualité forment un tout qui vient s'ajouter à la base de connaissances au sujet de la géologie du Nunavut, tout en assurant l'accès à de nouveaux renseignements de nature géoscientifique susceptibles d'aider à la prise de décisions en matière d'utilisation des terres à l'avenir. En outre, grâce à ces renseignements, il est possible de procéder à des évaluations de la présence possible de ressources correspondant à toute une gamme d'éléments utiles, notamment les diamants et autres gemmes, les métaux communs et précieux, les minéraux industriels, la pierre à sculpter et les agrégats. Ces travaux ont également pour objet d'aider les habitants du Nord en offrant aux étudiants des niveaux collégial et universitaire une occasion d'acquérir une formation en sciences de la Terre.

Un programme géoscientifique de deux ans (2014–2016) prenait fin au printemps et le Bureau recevait peu après l'approbation de le poursuivre pour un autre deux ans (2016–2018); les travaux porteront sur l'exploration et la mise en valeur responsables des ressources naturelles, la mise en place responsable et la protection de projets de développement des infrastructures et la diffusion de l'information et de données géoscientifiques.

La présente édition du volume regroupe un total de 12 articles répartis en fonction des sujets suivants, qui tous concordent avec le mandat du Bureau : « Études géoscientifiques régionales », « Études géoscientifiques liées à l'infrastructure », « Pierre à sculpter » et « Sensibilisation du public ». Tous les articles sont publiés (en anglais seulement, accompagnés de résumés en français) sur Internet et peuvent être téléchargés sans frais depuis le www.cngo.ca. Le Bureau a lancé en 2013 une nouvelle série, la *Série des données géoscientifiques*, qui permet la diffusion d'ensembles de données numériques tels les ensembles de données analytiques, polygonales ou ponctuelles et les fichiers de métadonnées. Les données appuyant les travaux de recherche entrepris et décrits dans les articles présentés dans le volume sont ainsi également mises en circulation par le biais de cette autre série.

Dans la section portant sur les travaux entrepris dans le cadre des « Études géoscientifiques régionales », six articles font état de projets ciblés de cartographie du substratum rocheux, d'études de la géologie de surface, d'échantillonnage des sédiments et de l'eau, et d'autres études de nature thématique. Le premier article traite de la poursuite de recherches sur les

microfossiles (conodontes) que renferment les xénolites carbonatés au sein des kimberlites de Chidliak. Ces travaux fournissent des données complémentaires qui aident à mieux comprendre les processus responsables de la mise en place des kimberlites ainsi que l'histoire de leur refroidissement. Le second article porte sur des travaux de cartographie de la géologie de surface dans la région du lac Sylvia Grinnell et présente les résultats d'analyses d'échantillons de till, de sédiments fluviatiles et lacustres, et d'eau de ruisseau et de lacs en vue d'établir l'histoire de la région et des accidents de terrain qui s'y trouvent. Les trois articles qui suivent font état de résultats acquis dans le cadre du projet de cartographie de la région du lac Tehery et de la baie Wager, qui se situe au centre du Nunavut. Les travaux de cartographie géologique présentés dans le troisième article mettent l'accent sur l'identification des unités rocheuses et des caractéristiques de la région et les nouvelles découvertes qui ont été faites aideront à résoudre l'énigme entourant ses origines géologiques. Le quatrième article souligne comment le recours aux données gravimétriques et magnétiques a permis d'identifier des structures peu profondes de la croûte terrestre, alors que les premiers résultats provenant d'une étude thématique de la limite marine postglaciaire est le sujet du cinquième article. Le dernier article paraissant dans cette section fait état d'une étude qui se poursuit dans la baie Frobisher en vue d'y dresser la carte des éléments géoscientifiques caractérisant le plancher océanique. Une meilleure compréhension de la géologie du fond de l'océan, des géorisques dans la région et des processus géologiques ayant une incidence sur le plancher océanique contribuera grandement à la mise en valeur future de la région.

En reconnaissance des changements climatiques et des conditions de réchauffement qui se manifestent dans l'ensemble du Nord, la section ayant trait aux « Études géoscientifiques liées à l'infrastructure » regroupe quatre articles dans lesquels sont présentés quelque uns de ces effets et de ces conditions. Les deux premiers portent sur le pergélisol aux alentours de Rankin Inlet, une région située au centre du Nunavut, et les deux derniers font état de résultats préliminaires provenant de recherches entreprises dans le bassin hydrographique de la rivière Niaqunguk (communément appelée de façon officieuse la rivière Apex). Le premier article portant sur le pergélisol note le résultat d'observations et de la sélection de sites se prêtant à la mise en place de stations de surveillance du pergélisol et de la température au sol. Un atelier qui a eu lieu en février à Rankin Inlet est le sujet du second article. L'atelier avait pour objet d'acquérir une meilleure compréhension des processus régissant le pergélisol en combinant les observations locales et traditionnelles aux données géoscientifiques. Le troisième article fait état de résultats préliminaires découlant d'une étude hydrologique liée à la neige réalisée dans le bassin hydrographique de la rivière Niaqunguk. Ces travaux ont pu être réalisés grâce à un partenariat poursuivant des études intégrées de suivi, de recherche et de formation en matière d'hydrologie et de la qualité de l'eau. Les recherches entreprises dans le cadre du quatrième article de cette section se sont penchées sur la circulation de l'eau souterraine et, ayant recours à une approche méthodologique, ont tenté de caractériser les voies empruntées par cette dernière et d'identifier les sources d'eau au cours de la saison de dégel de la couche active. Les recherches afférant à ces deux derniers articles ont été réalisées dans le bassin hydrographique de la rivière Niaqunguk, soit la rivière qui a été désignée à titre de source complémentaire d'eau potable pour les collectivités d'Iqaluit et d'Apex.

La pierre se prêtant à la sculpture a récemment fait l'objet de travaux ciblés au Nunavut afin d'en déterminer les caractéristiques (qualité et quantité) à l'intention des artistes du Nunavut. En 2016, une équipe formée de géologues de la Qikqitani Inuit Association et du Bureau, accompagnée par un étudiant en géologie de l'Université du Manitoba, a visité quatre emplacements de pierre à sculpter dans les îles Belcher afin d'y étudier le paysage, de dresser la carte des gisements de pierre à sculpter et de tenter de mieux comprendre les processus à l'origine de la formation de la pierre.

Le dernier article du volume traite d'une initiative qui a eu lieu à l'extérieur du hameau de Taloyaok au cours de l'été. Un programme expérimental d'école de terrain communautaire s'est déroulé en guise de préparation des campagnes de cartographie du substratum rocheux prévues par la Commission géologique du Canada et le Bureau en 2017 et 2018. Cette école de terrain a permis aux habitants du Nord d'apprécier eux-mêmes les méthodes utilisées afin de recueillir des données géologiques sur le terrain et de voir exactement comment ces dernières peuvent servir à des prises de décisions à l'avenir qui se feront sans nécessairement avoir d'incidence néfaste sur l'environnement.

J'ose espérer que tous et chacun découvriront et apprécieront en lisant ces articles à quel point est variée la recherche de haute qualité entreprise aussi bien par le Bureau, que par ses partenaires et collaborateurs.

Remerciements

Le Bureau géoscientifique Canada-Nunavut tient à remercier les auteurs des articles publiés dans cette cinquième édition du *Sommaire des activités*. Leur dévouement est extrêmement apprécié et c'est grâce à eux qu'il nous est possible de publier un document d'une telle qualité. Merci à RnD Technical d'avoir vu à l'édition technique et à l'assemblage de ce numéro. Nos remerciements s'adressent également aux personnes suivantes, lecteurs critiques des articles :

Vaughn Barrie	Commission géologique du Canada
Janet Campbell	Commission géologique du Canada
Kate Clark	Commission géologique du Canada
Carl Guilmette	Université Laval
David Mate	Savoir polaire Canada
Martin McCurdy	Commission géologique du Canada
Peter Morse	Commission géologique du Canada
Greg Oldenborger	Commission géologique du Canada
J. Kelly Russell	Université de Colombie-Britannique
Wendy Sladen	Commission géologique du Canada
Mike Thomas	Commission géologique du Canada
Tommy Tremblay	Bureau géoscientifique Canada-Nunavut

Linda Ham
Géologue en chef
Bureau géoscientifique Canada-Nunavut
www.cngo.ca/

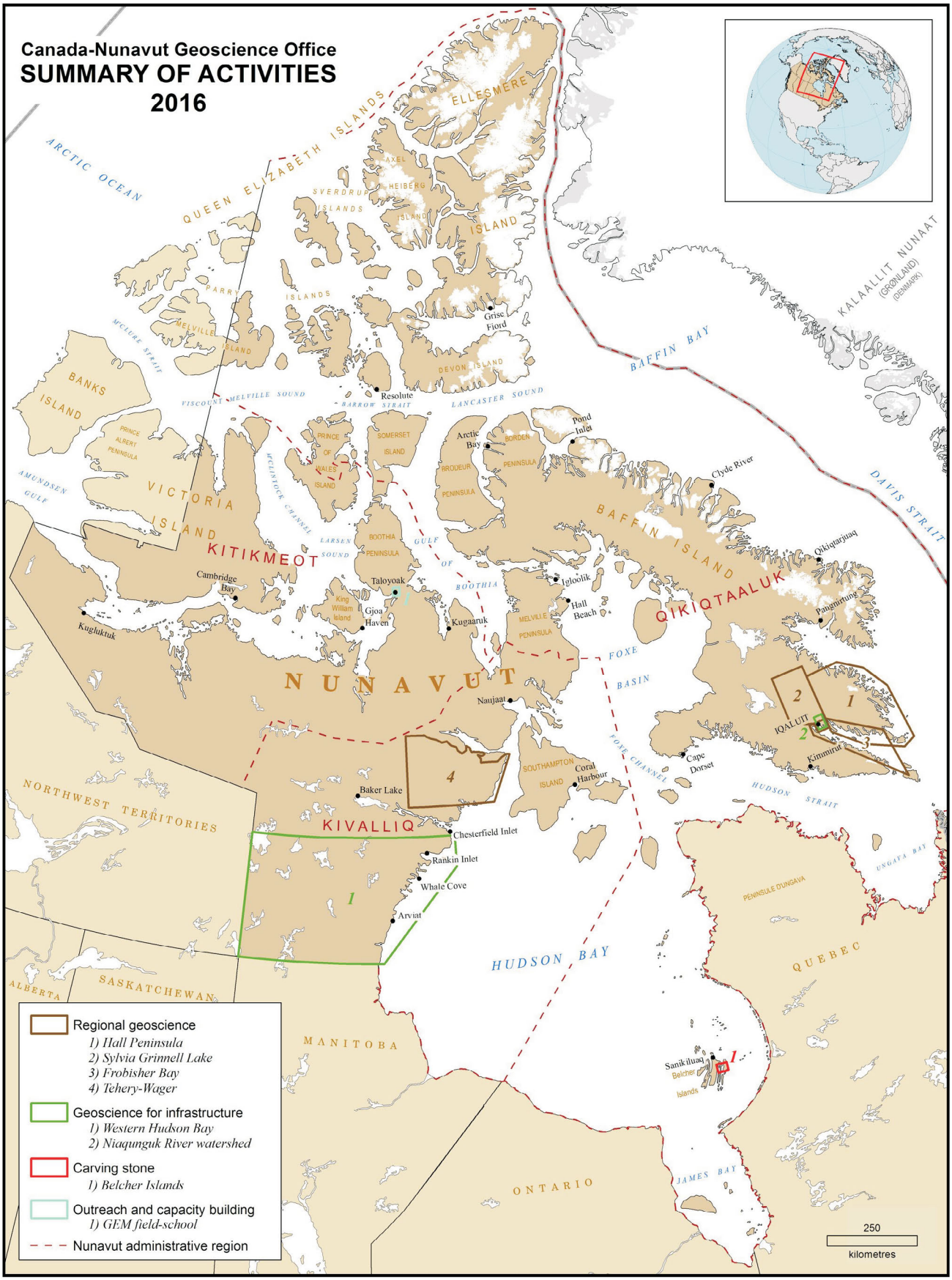
Canada-Nunavut Geoscience Office
SUMMARY OF ACTIVITIES
2016
ARCTIC OCEAN
QUEEN ELIZABETH ISLANDS
ELLESMERE ISLAND
AXEL HEIBERG ISLAND
SVERDRUP ISLANDS
PARRY ISLANDS
MELVILLE ISLAND
M'CLURE STRAIT
BANKS ISLAND
PRINCE ALBERT PENINSULA
VICTORIA ISLAND
AMUNDSEN GULF
KITIKMEOT
VISCOUNT MELVILLE SOUND
BARROW STRAIT
LANCASTER SOUND
PRINCE OF WALES ISLAND
SOMERSET ISLAND
M'CLINTOCK CHANNEL
LARSEN SOUND
BOOTHIA PENINSULA
GULF OF BOOTHIA
BORDEN PENINSULA
BRODEUR PENINSULA
MELVILLE PENINSULA
DEVON ISLAND
Grise Fiord
Resolute
Arctic Bay
Pond Inlet
Clyde River
BAFFIN BAY
DAVIS STRAIT
KALAALLIT NUNAAT (GRØNLAND) (DENMARK)
BAFFIN ISLAND
QIKIQTAALUK
Qikiqarjuaq
Pangnirtung
Iqaluit
Kimmirut
Cape Dorset
Igloolik
Hall Beach
Taloyoak
King William Island
Gjoa Haven
Kugaaruk
Cambridge Bay
Kugluktuk
NUNAVUT
FOXE BASIN
FOXE CHANNEL
Naujaat
SOUTHAMPTON ISLAND
Coral Harbour
Baker Lake
KIVALLIQ
Chesterfield Inlet
Rankin Inlet
Whale Cove
Arviat
HUDSON STRAIT
UNGAVA BAY
PENINSULE D'UNGAVA
QUEBEC
HUDSON BAY
NORTHWEST TERRITORIES
ALBERTA
SASKATCHEWAN
MANITOBA
ONTARIO
JAMES BAY
Sanikiluaq
Belcher Islands
1
2
3
4
Regional geoscience
1) Hall Peninsula
2) Sylvia Grinnell Lake
3) Frobisher Bay
4) Tehery-Wager
Geoscience for infrastructure
1) Western Hudson Bay
2) Niaqunguk River watershed
Carving stone
1) Belcher Islands
Outreach and capacity building
1) GEM field-school
Nunavut administrative region
250
kilometres

Contents

Conodonts and their colour alteration index values from carbonate xenoliths in four kimberlites on Hall Peninsula, Baffin Island, Nunavut

S. Zhang[1] and J. Pell[2]

[1]*Canada-Nunavut Geoscience Office, Iqaluit, Nunavut, shunxin.zhang@canada.ca*

[2]*Peregrine Diamonds Ltd., Vancouver, British Columbia*

This work is part of the Hall Peninsula Integrated Geoscience Program (HPIGP), led by the Canada-Nunavut Geoscience Office (CNGO) in collaboration with the Government of Nunavut, Indigenous and Northern Affairs Canada, Dalhousie University, University of Alberta, Université Laval, University of Manitoba, University of Ottawa, University of Saskatchewan, University of New Brunswick, Nunavut Arctic College and the Geological Survey of Canada. It is supported logistically by several local, Inuit-owned businesses and the Polar Continental Shelf Program. The focus is on bedrock and surficial geology mapping (1:100 000 scale). In addition, a range of thematic studies is being conducted, including Archean and Paleoproterozoic tectonics, geochronology, landscape uplift and exhumation, microdiamonds, sedimentary rock xenoliths and permafrost. The goal is to increase the level of geological knowledge and better evaluate the natural resource potential in this frontier area.

Zhang, S. and Pell, J. 2016: Conodonts and their colour alteration index values from carbonate xenoliths in four kimberlites on Hall Peninsula, Baffin Island, Nunavut; *in* Summary of Activities 2016, Canada-Nunavut Geoscience Office, p. 1–12.

Abstract

Hall Peninsula, located on southeastern Baffin Island, Nunavut, is host to the newly discovered Chidliak kimberlite province. The region is underlain by Precambrian basement and the original Paleozoic cover has been removed by erosion. The earlier presence of Paleozoic carbonate strata is indicated by the presence of carbonate xenoliths—many of which contain numerous conodont microfossils—in the Chidliak kimberlites. The present study is a continuation of work done on conodonts recovered from Hall Peninsula kimberlites and their colour alteration index (CAI) values. This paper summarizes the results recovered from 12 drillholes in 4 kimberlites, including 10 new drillholes in 3 of the 11 kimberlites previously studied and 2 drillholes in a kimberlite that have not been previously reported on. Of the 59 collected samples, 43 contain conodonts, from which nearly 600 identifiable conodont specimens have been recovered with conodont CAI values ranging from 4 to 8. These provide additional data to understating the kimberlite emplacement processes and cooling history.

Résumé

La péninsule Hall, située au sud de l'île de Baffin, au Nunavut, renferme la province de kimberlites de Chidliak, qui vient tout récemment d'être découverte. La région repose sur du socle précambrien dont la couverture paléozoïque originale a été complètement enlevée par l'érosion. Des xénolites de calcaire, seuls témoins de la présence antérieure de couches carbonatées paléozoïques, renferment de nombreux microfossiles (conodontes). La présente étude poursuit des travaux portant sur des conodontes provenant d'échantillons de kimberlites recueillis dans la péninsule Hall et examine les valeurs de l'indice d'altération de la couleur (IAC) qui les caractérisent. Le rapport résume les résultats acquis des douze trous de forage creusés dans quatre unités de kimberlites, notamment dix nouveaux trous forés dans trois des onze unités de kimberlite déjà étudiées et deux autres forés dans une unité de kimberlites qui n'a pas encore fait l'objet d'études. Des 59 échantillons recueillis, 43 renfermaient des conodontes, parmi lesquels presque 600 spécimens de conodontes identifiables, dont l'IAC varie de 4 à 8, ont pu être récupérés. Ces spécimens fournissent des renseignements supplémentaires, grâce auxquels il est possible de mieux comprendre les processus en jeu lors de la mise en place des kimberlites et l'histoire de leur refroidissement.

Introduction

The Chidliak kimberlite province covers a 40 by 70 km area on Hall Peninsula, southeastern Baffin Island, Nunavut, between Frobisher Bay on the southwest and Cumberland Sound on the northeast (Figure 1). More than 70 kimberlites have been found since the first kimberlite discovery in 2008. As a byproduct of the exploration programs, a number of carbonate xenoliths have been found in many of the kimberlite pipes on the Hall Peninsula. In addi-

This publication is also available, free of charge, as colour digital files in Adobe Acrobat® PDF format from the Canada-Nunavut Geoscience Office website: http://cngo.ca/summary-of-activities/2016/.

tion, many of the xenoliths yield very well preserved Late Ordovician–Early Silurian conodont microfossils (Zhang and Pell, 2013, 2014). These are direct evidence that Paleozoic rocks were present on Hall Peninsula at the time of kimberlite emplacement (Late Jurassic and Early Cretaceous). The Paleozoic strata were subsequently eroded away between the time of emplacement of the kimberlites and the present (Zhang and Pell, 2013, 2014).

In previous studies (Zhang and Pell, 2013, 2014), a total of 109 carbonate xenolith samples were collected from 19 drillholes in 11 of the Chidliak kimberlites (CH-06, CH-07, CH-17, CH-28, CH-31, CH-33, CH-44, CH-45, CH-56, CH-55 and CH-58). More than 1300 conodont specimens were recovered from 76 conodont-bearing carbonate xenolith samples, in which 32 species representing 23 genera were recognized (Zhang and Pell, 2014). These conodonts have a wide range of colour alteration index (CAI) values, from 1.5 to 8 (Zhang and Pell, 2014). Based on these data, Zhang and Pell (2014)

- reconstructed the Paleozoic stratigraphy on Hall Peninsula by means of the discovered conodont species;
- estimated the total thickness of the Paleozoic strata that have been eroded from Hall Peninsula by using the known stratigraphic data from other areas around the Foxe Basin;
- estimated the erosion rate on Hall Peninsula; and
- provided unique information about the effects of thermal alteration of conodonts by the kimberlites in the Chidliak kimberlite province.

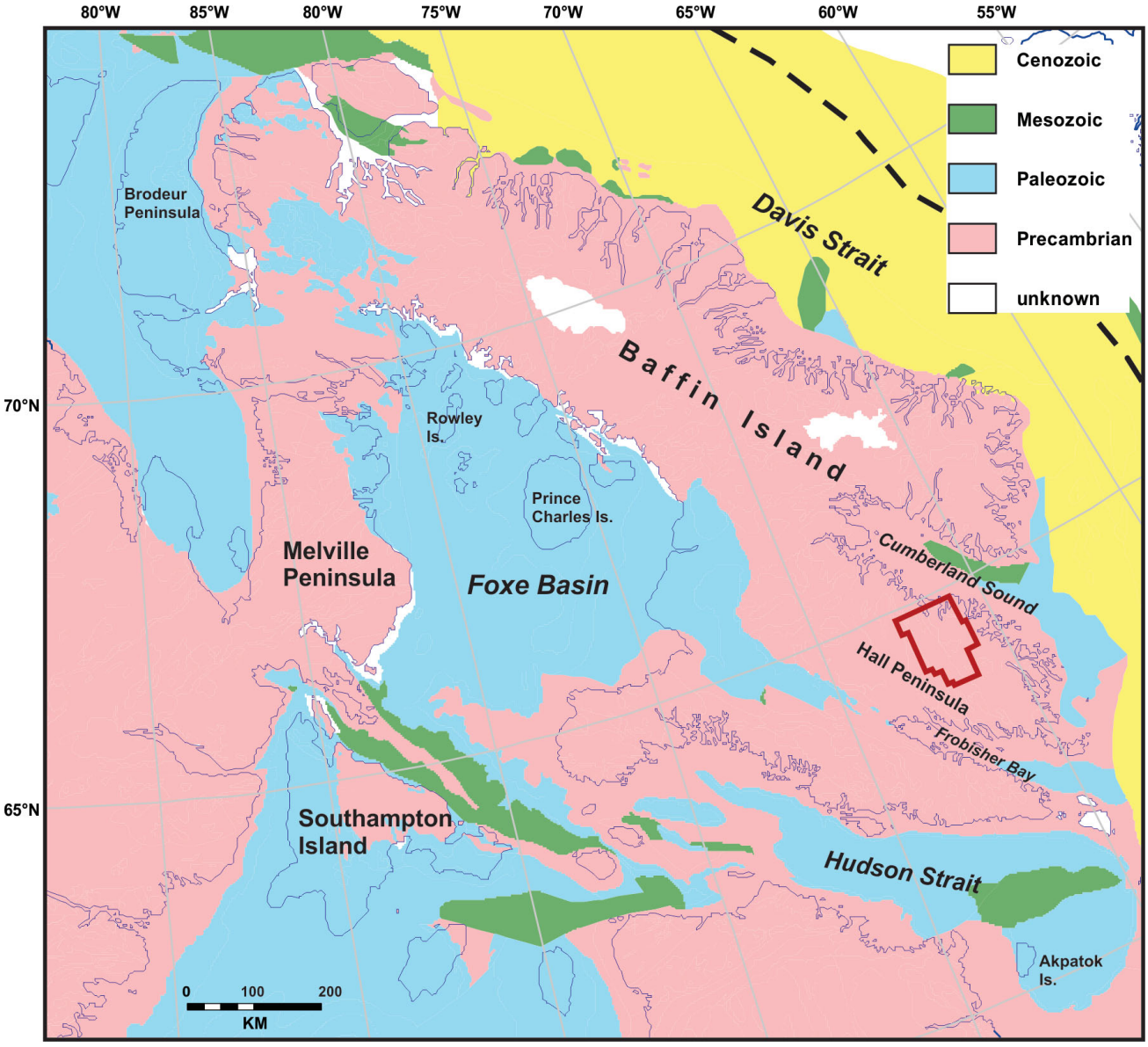

Figure 1: Simplified geological map of the Foxe Basin and vicinity (modified from Wheeler et al., 1997), showing the location of Chidliak project area (red polygon).

Furthermore, Pell et al. (2015) used the conodont CAI values to build thermal models for cooling of the Chidliak kimberlite pipes and synchronous heating of conodont-bearing xenoliths.

This paper will present new conodont data collected from 12 drillholes in 4 kimberlites (CH-06, CH-07, CH-44, CH-46) in 2012 and 2014, in addition to those in Zhang and Pell (2013, 2014), and focus on the conodont CAI values and their implication on the heating of conodont-bearing xenoliths within the kimberlites.

Geological setting

Based on early work and a reconnaissance geochronology study (Scott, 1996), Hall Peninsula was divided into three major crustal entities (Scott, 1996, 1999; St-Onge et al., 2006), which, from west to east, are the Cumberland Batholith, a belt of Paleoproterozoic metasedimentary rocks and a gneissic terrane now termed the Hall Peninsula block (Figure 2; Whalen et al., 2010). This tectonic framework had been maintained during the remapping of the southern part of the peninsula in 2012 (Machado et al., 2013), and northern part of the peninsula, including the Chidliak region, in 2013 (Steenkamp and St-Onge, 2014).

The Hall Peninsula block (Figure 2) comprises Archean orthogneissic and supracrustal rocks with a ca. 2.92–2.80 Ga age, and possibly younger clastic rocks that have been tectonically reworked to some degree (Scott, 1999). The block hosts 74 kimberlites discovered on Hall Peninsula between 2008 and 2015. This region is referred to as the Chidliak diamond district. A total of 44 of the kimberlites have been dated as Late Jurassic–Early Cretaceous (156.7–139.1 Ma; Heaman et al., 2012). Both steeply dipping sheet-like and larger pipe-like kimberlite bodies have been discovered at Chidliak (Pell et al., 2013). The pipe-like bodies commonly contain clastic sedimentary and carbonate xenoliths derived from the paleosurface and incorporated into an open vent structure.

At present, Hall Peninsula lacks Phanerozoic sedimentary cover except for unconsolidated glacial deposits. The closest outcrops of Paleozoic strata on southwestern Baffin Island are approximately 150–280 km west of the Chidliak kimberlite province (Figure 1; Trettin, 1975; Sanford and Grand, 1990, 1998, 2000; Zhang, 2012). Further to the northwest of the Chidliak kimberlite province, the Paleozoic sedimentary rocks are also exposed on the Brodeur Peninsula, Baffin Island (Nentwich and Jones, 1989), northeastern Melville Peninsula (Sanford, 1977; Zhang, 2013) and several small islands in the central Foxe Basin; a nearly complete Paleozoic sedimentary record was recovered in drillcore on the Rowley Island (Figure 1; Trettin, 1975). These Paleozoic sedimentary rocks were deposited

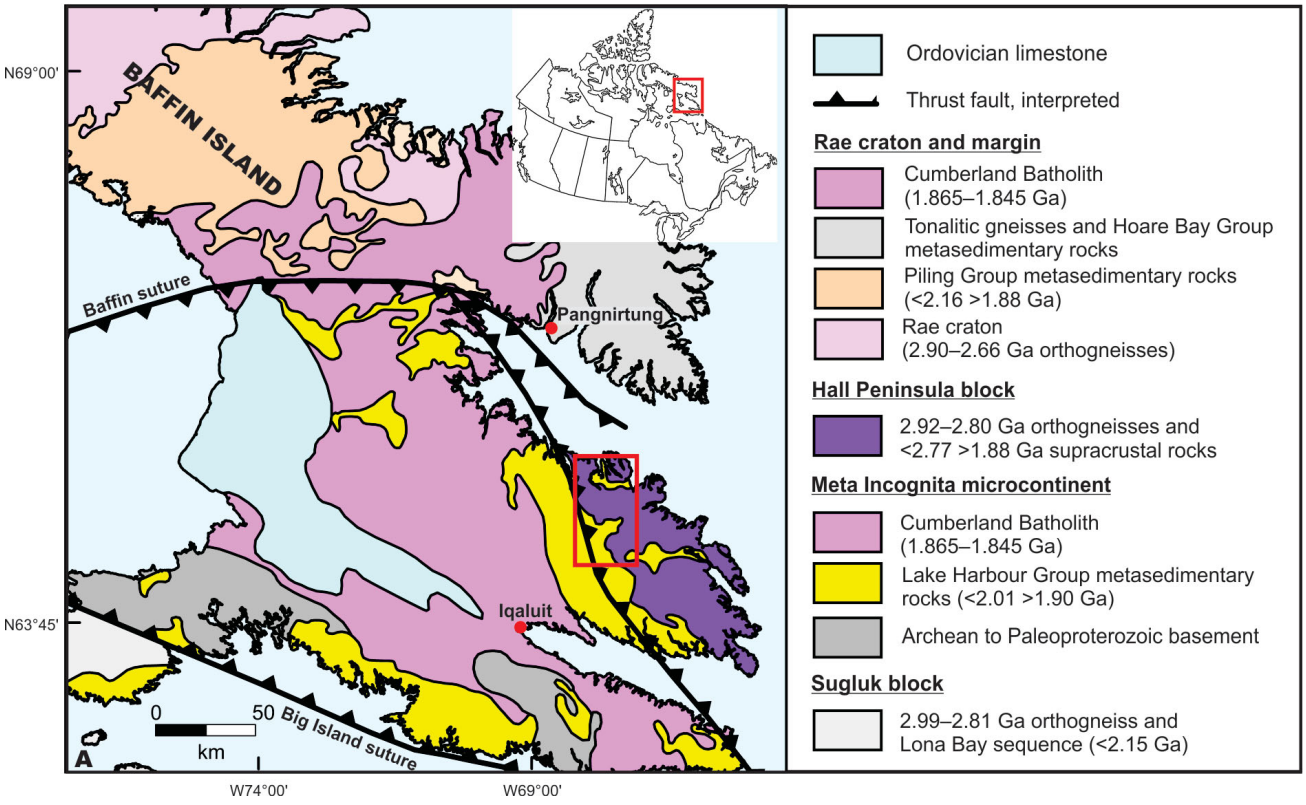

Figure 2: Simplified regional geological map of southern Baffin Island (after St-Onge et al., 2006; Whalen et al., 2010), showing the sample area (red rectangle).

in the Foxe Basin; they were present on Hall Peninsula before the Late Jurassic–Early Cretaceous when the kimberlites were emplaced. The Paleozoic Foxe Basin also included present-day, Phanerozoic-barren Hall Peninsula. These are evidenced by the conodonts discovered from the carbonate xenoliths preserved in the kimberlites on Hall Peninsula (Zhang and Pell, 2013, 2014).

New carbonate xenolith samples and conodonts

Following Zhang and Pell (2013, 2014), a total of 59 additional carbonate xenolith samples were collected from 12 drillholes in 4 kimberlites (CH-06, CH-07, CH-46 and CH-44; Figure 3, Table 1). Most of the samples from drillholes of CH-06 (Table 2), CH-07 (Table 3) and CH-46 (Table 4) are from continuous cores through large carbonate blocks covering a relatively long time interval. Examples include the carbonate xenoliths in CH-46: a xenolith from drillhole CHI-105-DD01 is 17.52 m in a core length of 71.3–88.82 m (Figure 4a), and a xenolith from drillhole CHI-105-DD02 is 9.05 m in a core length of 52.6–61.65 m (Figure 4b). Select portions of the cores from these two drillholes were sampled for processing conodonts (see Table 4 for details). All samples from drillholes in CH-44 (Table 5) represent relatively short intervals of the drillcores, similar to those shown in Figure 4c and d.

Of 59 samples collected and processed, 43 contained conodonts. Nearly 600 identifiable conodont specimens and numerous broken elements were recovered from the 43 conodont-bearing carbonate xenolith samples. Twelve species representing ten genera were identified (see Tables 2–5 for details). They are *Aphelognathus* cf. *A. divergens* Sweet, *Belodina confluens* Sweet, *Culumbodina penna* Sweet, *Drepanoistodus suberectus* (Branson and Mehl), *Pseudobelodina adentata* Sweet, *Panderodus unicostatus* (Branson and Mehl), *P. liratus* Nowlan and Barnes, *P. breviusculous* Barnes, *Periodon grandis* (Ethington), *Plectodina tenuis* (Branson and Mehl), *Protopanderodus liripipus* (Branson and Mehl) and *Walliserodus curvatus* (Branson and Branson). These species have been reported previously from Upper Ordovician outcrops in Foxe Basin area by McCracken (2000) and Zhang (2013) and from carbonate xenoliths on Hall Peninsula by Zhang and Pell (2014). The conodonts recovered from carbonate xenoliths by the present study have CAI values ranging between 4 and 8 (Figure 5, Tables 2–5), which is substantially narrower than those (1.5–8) reported by Zhang and Pell (2014) and Pell et al. (2015).

In the Foxe Basin area, the Upper Ordovician strata are divided into Frobisher Bay, Amadjuak, Akpatok and Foster Bay formations. The conodont species recovered from 12 drillholes mentioned earlier are common in the Amadjuak Formation in the Foxe Basin area (McCracken, 2000; Zhang, 2013); however, neither any typical conodont species that are specifically restricted to the Upper Ordovician Frobisher Bay, Akpatok and Foster Bay formations and Silurian strata, nor any species other than those reported by

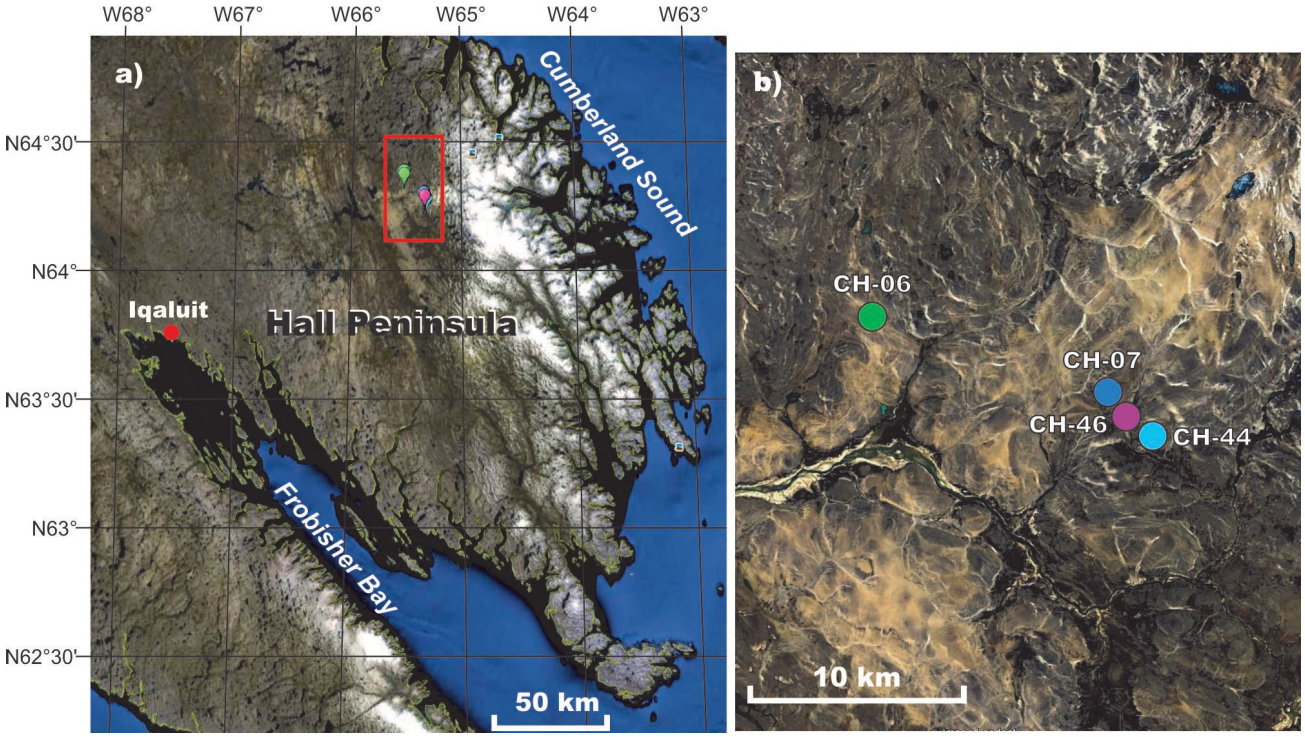

Figure 3:a) Location of four kimberlites highlighted by red rectangle on a Google Maps™ base (Google, 2013); **b)** enlargement of the area highlighted by the red square in a).

Zhang and Pell (2014), have been found from the 12 drillholes reported herein. The new material from the 12 drillholes, therefore, does not provide any new information to emend the Upper Ordovician and lower Silurian stratigraphic framework on Hall Peninsula established by Zhang and Pell (2014).

It is worth stating that two samples, SZ14-050-02 and SZ14-050-06, from drillhole CHI-050-14-DD25 at depths of 114.05–115 m and 119–120 m in kimberlite CH-06 (Table 2), respectively, contain one specimen of *Neogondolella* sp. (Figure 6b) and one specimen of *Neospathodus* sp. (Figure 6d). These conodonts are of late Permian and Early Triassic age. Regionally, there has been no report of marine upper Permian and Lower Triassic deposits in the Foxe Basin area. Whether these conodonts were originally from samples SZ14-050-02 and SZ14-050-06, or resulted from laboratory contamination, needs more investigation. The possibility of laboratory contamination is discussed later in this paper.

Conodont CAI values and thermal history implication

Conodonts are phosphatic marine microfossils of the Cambrian–Triassic; unmetamorphosed conodont elements are transparent, apatitic and contain trace amounts of organic matter that colour them. The conodont colours can be changed with an increase in metamorphic temperature. Eight conodont colours have been recorded, both in the

Table 1: Carbonate xenolith samples collected from 12 drillholes in 4 kimberlite bodies in the Chidliak project area.

Kimberlite	Drillhole	Sampling depth (m)	No. of collected samples	No. of productive samples	Conodont data
CH-06	CHI-050-14-DD25	113.6–140.1	10	6	Table 2
	CHI-050-14-DD26	169.1–169.25	1	0	
	CHI-050-14-DD27	69.2–76.2	2	2	
	CHI-050-14-DD28	87.15–99.5	3	1	
CH-07	CHI-251-14-DD19	81.65–128.13	7	7	Table 3
	CHI-251-14-DD23	156.25–156.5	1	0	
CH-46	CHI-105-14-D01	72.5–88.05	11	11	Table 4
	CHI-105-14-D02	54.2–69.5	7	6	
CH-44	CHI-258-12-DD09	203.95–220.6	8	7	Table 5
	CHI-258-12-DD10	5.78–10.06	3	1	
	CHI-258-12-DD11	63.95–71.82	2	0	
	CHI-258-12-DD12	28.9–179.22	4	2	
Total	**12**		**59**	**43**	

Table 2: Conodont elements recovered from four drillholes in kimberlite CH-06 and their colour alteration index (CAI) values.

Drillhole	CHI-050-14-DD25										CHI-050-14-DD26	CHI-050-14-DD27		CHI-050-14-DD28		
Sample	SZ14-050-01*	SZ14-050-02**	SZ14-050-03	SZ14-050-04	SZ14-050-05	SZ14-050-06**	SZ14-050-07*	SZ14-050-08	SZ14-050-09*	SZ14-050-10*	SZ14-050-11*	SZ14-050-12	SZ14-050-13	SZ14-050-14*	SZ14-050-15	SZ14-050-16*
Sample mass (g)	2010	2159	2269	2520	2456	2264	1777	2205	1700	1742	601	1916	1181	752	2042	1875
Undissolved sample mass (g)	890	596	511	703	540	337	499	832	506	726	0	798	278	203	858	732
Depth (m)	113.6–114.05	114.05–115	115–116	116–116.6	116.6–119	119–120	120–120.4	138.4–139	139–139.7	139.7–140.1	169.1–169.25	69.2–69.7	75.95–76.2	87.15–87.7	98.45–98.65	98.65–99.5
CAI	**?**	**4–5, 6.5**	**6–6.5**	**6**	**6**	**2–3**	**?**	**7**	**?**	**?**	**?**	**7–8**	**6.5**	**?**	**6.5**	**?**
Age	**?**	**?**	**L.O. (?)**			**?**	**?**	**L.O. (?)**	**?**	**?**	**?**	**L.O.**	**L.O. (?)**	**?**	**L.O. (?)**	**?**
Species																
Aphelognathus* cf. *A .divergens												1				
Panderodus unicostatus			3	1	2	1		2				5	1		1	
broken ramiform element		1											1			
***Neogondolella* sp.**		1														
***Neospathodus* sp.**						1										

Note: 1) * and ** represent barren samples and possible contaminated samples, respectively; 2) L.O.: Late Ordovician.

field and laboratory (Epstein et al., 1977; Rejebian et al., 1987), which were numbered 1–8, or called conodont colour alteration index (CAI) 1–8. The conodont CAI values of 1–5 and 6–8 are measures of organic metamorphism to calibrate and substantiate conodont colour alteration in the temperature range of 50 to >300°C in regional metamorphic events (Epstein et al., 1977) and of >300 to >600°C in contact metamorphic events (Rejebian et al., 1987), respectively. Carbonate xenoliths within kimberlites were subjected to contact metamorphism for relatively short times (10^0–10^5 hours); on this basis, CAI values 1–8 are indicative of temperature range of <225 to >780°C in a recent study conducted by Pell et al. (2015).

All conodonts from present-day outcrops of the Upper Ordovician and Silurian strata in Hudson Bay and Foxe Basin areas have CAI 1 (Zhang, 2011, 2013), and some conodonts from deeper parts of the wells in Hudson Bay may have CAI 1.5 (Zhang and Barnes, 2007). The conodont elements recovered from 19 drillholes among 11 Chidliak kimberlites have CAI values ranging from 1.5 to 8 (Zhang and Pell, 2014; Pell et al., 2015). The observations made by Pell et al. (2015) were that CAI values of <4 are found in xenoliths exclusively in volcaniclastic kimberlites (VK); those of 4–7 in xenoliths from VK in VK-only and in mixed infill pipes; and those of 6–8 from apparent coherent kimberlites (ACK).

Kimberlite CH-46

Kimberlite CH-46 has a surface area of <1 ha and is infilled with VK, or strictly speaking, pyroclastic kimberlite (PK). No data from CH-46 had been included in previous studies (Zhang and Pell, 2014; Pell et al., 2015). A total of 17 carbonate xenolith samples were collected from the two closely spaced drillholes, CHI-105-14-DD01 and CHI-105-14-DD02 in kimberlite CH-46 (Figure 3b). The former and the latter yielded an almost continuous carbonate core from 71.3 to 88.82 m and from 52.6 to 61.65 m, respectively.

A similar large carbonate block (8.6 m long core [80.40–89 m] from drillhole CHI-050-11-DD16) had previously been collected, but only two samples from it yielded conodonts with the same CAI value (6.5–7; Zhang and Pell, 2014; Pell et al., 2015), which did not provide enough data for observing CAI value variation within a kimberlite body. The conodonts from the two drillholes of kimberlite CH-46 studied herein exhibit a similar pattern of CAI value variation. The conodonts from middle part of the core have lower CAI values (4 or 4–5) than either end (6–6.5 or 6.5–7), and the highest CAI value of 7 is recorded at, or near, the base of each xenolith core, at 85.85–88.05 m in CHI-105-14-DD01 and 66.98–67.27 m in CHI-105-14-DD02 (Table 4). These two cores were probably from one or two very

Table 3: Conodont elements recovered from two drillholes in kimberlite CH-07 and their colour alteration index (CAI) values.

Drillhole	**CHI-251-14-DD19**							**CHI-251-14-DD23**
Sample	SZ14-251-01	SZ14-251-02	SZ14-251-03	SZ14-251-04	SZ14-251-05	SZ14-251-06	SZ14-251-07	SZ14-251-08*
Sample mass (g)	1182	2338	2470	2199	2244	1796	2554	945
Undissolved sample mass (g)	376	1372	811	430	541	516	530	161
Depth (m)	81.65–81.9	102–103.25	125.5–126.05	126.05–126.55	126.55–127.05	127.05–127.55	127.55–128.13	156.25–156.5
CAI	**4–5**	**5**	**6**	**6**	**6**	**6**	**6–6.5**	**?**
Age	**Late Ordovician**							**?**
Species								
Belodina confluens			1	1				
Culumbodina penna				1			2	
Drepanoistodus suberectus					1		2	
Pseudobelodina adentata							1	
Panderodus unicostatus	1	2	3		4	10	33	
Panderodus liratus							1	
Panderodus breviusculous			2	1			2	
Plectodina tenuis			2	5	9	6	11	
broken ramiform element			1		a few		a lot	

Note: * indicates barren sample.

Table 4: Conodont elements recovered from two drillholes in kimberlite CH-46 and their colour alteration index (CAI) values.

Drillhole	CHI-105-14-DD01											CHI-105-14-DD02					
Sample	SZ14-105-01	SZ14-105-02	SZ14-105-03	SZ14-105-04	SZ14-105-05	SZ14-105-06	SZ14-105-07	SZ14-105-08	SZ14-105-09	SZ14-105-10	SZ14-105-11	SZ14-105-12	SZ14-105-13	SZ14-105-14	SZ14-105-15	SZ14-105-16	SZ14-105-17*
Sample mass (g)	2168	2032	2162	2022	1954	2001	1786	2184	2084	2140	1956	2053	2061	1808	1996	1237	1859
Undissolved sample mass (g)	1061	923	964	865	749	918	723	953	911	839	780	863	705	495	809	94	532
Depth (m)	72.5–73	74.1–74.6	75.6–76.15	77–77.5	78.5–79	80–80.6	81.5–81.95	83–83.52	84.39–84.89	85.85–86.4	87.55–88.05	54.2–54.7	55.7–56.2	57.11–57.61	58.64–59.2	66.98–67.27	69.0–69.5
CAI	**5–6**	**5**	**5–6**	**5–6**	**4–5**	**4–5**	**5–6**	**5–6**	**5–6**	**7**	**6.5–7**	**5–6**	**5–6**	**4**	**5–6**	**7**	**?**
Age	**Late Ordovician**																**?**
Species																	
Belodina confluens			2				2				1	2	1				
Culumbodina penna				1													
Drepanoistodus suberectus		1					1	3	1	1		3	1				
Pseudobelodina adentata		1															
Panderodus unicostatus	7	8	30	16	14	18	27	20	15	14	12	20	14	13	13	6	
Panderodus liratus		1															
Panderodus breviusculous								1									
Periodon grandis							1										
Plectodina tenuis					1								1				
Protopanderodus liripipus									2								
Walliserodus curvatus			1														

Note: * represents barren sample.

large carbonate masses (the one from CHI-105-14-DD01 was greater than 15 m long in one dimension), which was/were enclosed by kimberlite CH-46. The centre of the carbonate mass was not affected by the heat from the kimberlite as much as the edges; the temperature in the centre of the carbonate mass could be 365–610°C, and that near the edge of the carbonate mass could be as high as 850°C, based on Pell et al. (2015). Such pattern of CAI value variation in the two drillholes in kimberlite CH-46 was not previously observed and modelled by Pell et al. (2015); therefore, how the heat from kimberlite travelled and diminished in such huge carbonate xenoliths will be the topic of future studies.

Kimberlites CH-06, CH-07 and CH-44

The carbonate xenoliths and conodonts from kimberlites CH-06, CH-07 and CH-44 (drillholes of CHI-050-11, CHI-251-11 and CHI-258-11) were reported by Zhang and Pell (2014) and Pell et al. (2015). The conodont elements recovered from xenoliths from CH-07, a mixed infill pipe, dominated by VK, have CAI values ranging from 4 to 6, while those from CH-06 and CH-44, which have apparent coherent kimberlite (ACK) infill, vary from 6.5 to 7 and 6.5 to 8, respectively. Most of the conodonts collected from the xenoliths in the additional 10 drillholes in the 3 kimberlites studied herein have similar CAI values (Tables 2–5, Figure 5) to those reported by Zhang and Pell (2014) and Pell et al. (2015), but differ in some aspects.

Figure 4: Examples of carbonate xenolith cores: **a)** continuous carbonate xenolith cores from drillhole CHI105-14-DD01 in kimberlite CH-46, **b)** continuous carbonate xenolith cores from drillhole CHI105-14-DD02 in kimberlite CH-46, **c)** relatively small carbonate xenolith samples from drillhole CHI-050-14-DD25 in kimberlite CH-06, **d)** relatively small carbonate xenolith samples from drillhole CHI-251-14-DD19 in kimberlite CH-07.

Kimberlite CH-06

Kimberlite CH-06 is a 1 ha, mixed infill pipe dominated by ACK, with lesser PK and coherent kimberlite (CK; Nowicki et al., 2016). A conodont CAI of 8 was recorded from sample SZ14-050-12 (Figure 5f) at a depth of 69.2–69.7 m in drillhole CHI-050-14-DD27. This is the highest CAI value encountered at Chidliak and is higher than the maximum CAI value of 7 previously reported by Zhang and Pell (2014) and Pell et al. (2015). This sample may be the closest to recording the actual emplacement temperature of the kimberlite.

Sample SZ14-050-02 from depth of 114.05–115 m in drillhole CHI-050-DD25 contains both a broken unidentifiable ramiform element (Figure 6a) and a Pa element of *Neogondolella* sp. from the late Permian–Early Triassic (Figure 6b). The former has a CAI value of 6.5 and the latter has a value of 4–5. The CAI values of 4 and 6.5 are indicative of temperatures between 365 and 775°C (Pell et al., 2015). The two conodont elements have CAI values of 6.5 and 4–5, but are derived from a <1 m interval of core. It seems unlikely that the conodont elements could have had such large differences in thermal history. Thus, the specimen of *Neogondolella* sp. (Figure 6b), which has an anomalously low CAI value of 4–5 and an anomalous age of late Permian–Early Triassic, may result from contamination in the lab.

Sample SZ14-050-06 from 119 to 120 m in drillhole CHI-050-DD25 from kimberlite CH-6 contains both a compressiform element of *Panderodus unicostatus* (Figure 6c) of Ordovician–Silurian age and a Pa element of *Neospathodus* sp. (Figure 6d) of Early Triassic age, which both have a conodont CAI value of 2–3. Most of the condont-bearing samples collected from CH-6, both in this and previous studies, yield conodonts with CAI values of 6–7, except for SZ14-050-02, as discussed previously. Pell et al. (2015) reported that the conodont CAI values of <4 are found in xenoliths exclusively in VK, but CH-06 is ACK; therefore, the conodonts with such low CAI values in kimberlite CH-06 are also most likely caused by contamination in the lab, especially the unusual age of *Neospathodus* sp. (Figure 6d) in the region. The compressiform element of *P. unicostatus* (Figure 6c) of Ordovician–Silurian age, a common conodont in the region, does not, however, support the argument of lab contamination from the aspect of age, so its origin remains uncertain.

Kimberlite CH-07

Kimberlite CH-07 has a surface area of approximately 1 ha and is infilled by a mix of VK (dominantly PK) and lesser

Table 5: Conodont elements recovered from four drillholes in kimberlite CH-44 and their colour alteration index (CAI) values.

Drillhole	CHI-258-12-DD09								CHI-258-12-DD10			CHI-258-12-DD11		CHI-258-12-DD12			
Sample	SZ14-01-01	SZ14-01-02	SZ14-01-03	SZ14-01-04	SZ14-01-05	SZ14-01-06	SZ14-01-07	SZ14-01-08*	SZ14-01-09	SZ14-01-10*	SZ14-01-11*	SZ14-01-12*	SZ14-01-13*	SZ14-01-14*	SZ14-01-15*	SZ14-01-16	SZ14-01-17
Sample mass (g)	1093	2437	1698	1243	2863	674	6338	454	243.5	946	467	371	594	916	309	690	2762
Undissolved sample mass (g)	748	84	0	51	1200	64	645	27	15	256	0	71	0	435	63	30	238
Depth (m)	203.95–204.25	205.3–205.83	208.1–208.73	210.2–210.5	210.8–211.55	211.9–212.13	216.25–217.65	220.5–220.6	5.78–5.84	8.2–8.5	10.51–10.6	63.95–64.05	71.7–71.82	28.9–29.1	44–44.07	63.5–63.64	178.6–179.22
CAI	6.5	6	6	6	5–6	6–6.5	6	?	6.5–7	?	?	?	?	?	?	7	6–6.5
Age	Late Ordovician							?	L.O.	?	?	?	?	?	?	L.O.	
Species																	
Belodina confluens				1		1	8									3	1
Drepanoistodus suberectus					2		4									6	
Panderodus unicostatus		5	3	5	8	1	36		1							66	1
Panderodus liratus				3												1	
Panderodus breviusculous	1			1												1	
Periodon grandis							11									4	
Plectodina tenuis																2	
Protopanderodus liripipus	1			1			2										
Pseudobelodina adentata		1															
broken ramiform element									3								

Note: 1) * represents barren samples; 2) L.O.: Late Ordovician.

ACK and CK (Nowicki et al., 2016). Seven carbonate xenolith samples were collected from VK at depths of 81.65–128.13 m in vertical drillhole CHI-251-14-DD19 (Table 3). The conodont CAI values from 81.65 to 128.13 m gradually increased from 4 to 6.5 with increasing depth, converting the temperature range from 365 (10^0 hours)–610°C (10^5 hours) to 650 (10^0 hours)–775°C (10^5 hours; Pell et al., 2015). Although the conodont CAI values are directly proportional to the buried depth in regional metamorphism (Harris, 1981), such a small depth difference will not cause any obvious changes in conodont colours. Such a steady change in conodont CAI values could be due to the temperature difference in different parts of the kimberlite, which could result from processes such as the pipe cooling faster near the surface, and slower with increasing depth; heterogeneous temperature distributions in pipe filling deposits; and latent heating of the pyroclastic deposits from below, or some combination thereof.

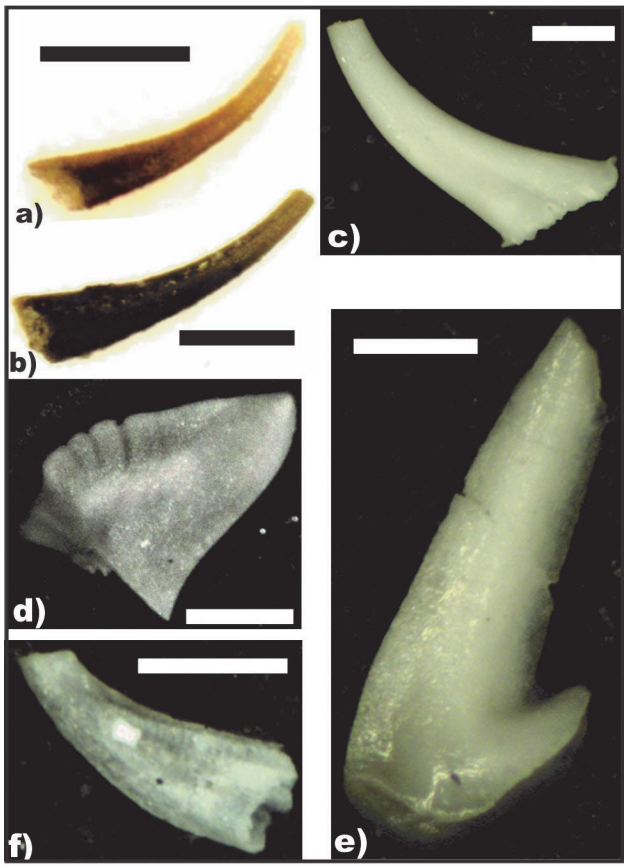

Figure 5: Conodont elements with different colour alteration index (CAI) values recovered from carbonate xenoliths from 12 drillholes in 4 Chidliak kimberlite pipes: **a)** asymmetric graciliform element of *Panderodus unicostatus* (CAI = 4) from sample SZ14-251-01, GSC139098; **b)** asymmetric graciliform element of *P. unicostatus* (CAI = 5) from sample SZ14-251-02, GSC139099; **c)** arcuatiform element of *P. unicostatus* (CAI = 7) from sample SZ14-105-16, GSC139100; **d)** subtriangular element of *Culumbodina penna* (CAI = 6.5) from sample SZ14-251-07, GSC139101; **e)** oistodiform element of *Drepanoistodus suberectus* (CAI = 7) from sample SZ14-105-10, GSC139102; **f)** compressiform element of *P. unicostatus* (CAI = 8) from sample SZ14-050-12, GSC139103 (black and white bars = 0.25 mm). Illustrated specimens are deposited in the National Type Collection of Invertebrate and Plant Fossil, the Geological Survey of Canada, Ottawa; GSC139098–139103 are curation numbers. See Sansom et al. (1994) for descriptive terms of *Panderodus* species and Lindström (1971) for that of *Drepanoistodus species*.

Kimberlite CH-44

Kimberlite CH-44 has a surface area of approximately 0.5 ha and has ACK-dominated infill in the upper 160 m and PK at depth (Nowicki et al., 2016). Zhang and Pell (2014) and Pell et al. (2015) reported five carbonate xenolith samples from four drillholes in kimberlite CH-44, and the conodonts collected from the five samples have CAI values ranging from 6 to 7–8, temperatures typical of ACK.

For this study, a total of 17 carbonate xenolith samples were collected from 4 drillholes in kimberlite CH-44, among which 10 samples contained conodonts. The conodont elements from the 10 samples have CAI values ranging from 5 to 7, indicating that these carbonate xenoliths were heated less (70–100°C) by the kimberlite than those described pre-

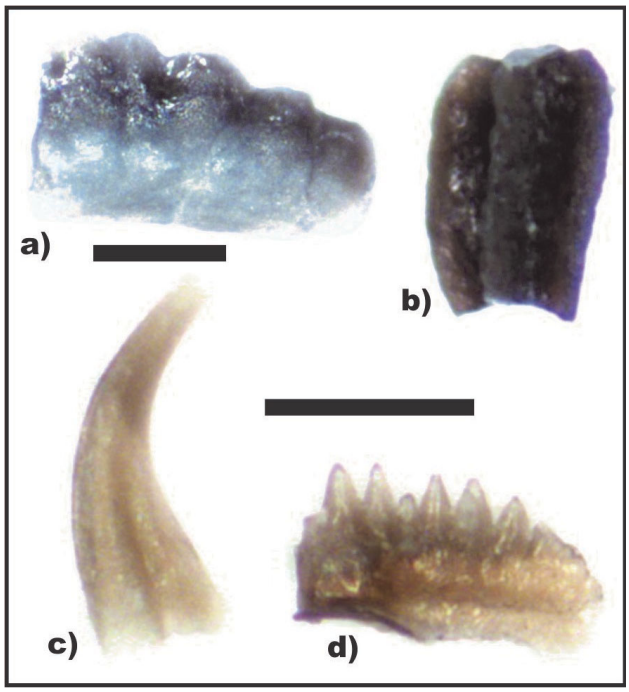

Figure 6: Conodont elements with unusual colours and ages from drillhole CHI-050-14-DD25, kimberlite CH-06: **a)** broken unidentifiable ramiform element (CAI = 6.5) from sample SZ14-050-02, drillhole CHI-050-14-DD25, kimberlite CH-06, GSC139104; **b)** Pa element of *Neogondolella* sp. (CAI = 4–5) from sample SZ14-050-02, drillhole CHI-050-14-DD25, kimberlite CH-06, GSC139105; **c)** compressiform element of *Panderodus unicostatus* (CAI = 2–3) from sample SZ14-050-06, drillhole CHI-050-14-DD25, kimberlite CH-06, GSC139106; **d)** Pa element of *Neospathodus* sp. (CAI = 2–3) from sample SZ14-050-06, drillhole CHI-050-14-DD25, kimberlite CH-06, GSC139107 (black bars = 0.25 mm; shorter bar for a, and longer bar for b, c and d). Illustrated specimens are deposited in the National Type Collection of Invertebrate and Plant Fossil, the Geological Survey of Canada, Ottawa; GSC139104–139107 are curation numbers.

viously; however, 7 out of 17 samples, including all 3 samples from drillhole CHI-258-12-DD11, are barren of conodonts. This could be because the samples did not contain conodonts originally, but could also be because of the high kimberlite emplacement temperatures destroyed the conodonts completely. This possibility is suggested because kimberlite CH-44 is dominated by ACK infill.

Economic and applied considerations

The Paleozoic carbonate xenoliths in the Chidliak kimberlite pipes provide direct evidence for the Paleozoic strata that were eroded from Hall Peninsula (Zhang and Pell, 2013, 2014). They also further the understanding of the kimberlites' emplacement history (Pell et al., 2015). The conodonts recovered from carbonate xenoliths in kimberlites CH-06, CH-07, CH-44 and CH-46 have CAI values ranging from 4 to 8, which provide new insight to kimberlite emplacement process and postemplacement cooling history of these bodies. Thus, the conodonts recovered from carbonate xenoliths and the conodont CAI values provide a reliable and inexpensive tool in reconstructing the previously eroded Paleozoic stratigraphy and estimating the minimum temperature of emplacement of the various types of pipe fills.

Acknowledgments

Thanks to Peregrine Diamonds Ltd. for giving the authors permission to collect xenolith samples and to the Canada-Nunavut Geoscience Office for its continuing financial support for processing the xenolith samples. The Canadian Northern Economic Development Agency's (CanNor) Strategic Investments in Northern Economic Development (SINED) program provided financial support for this work. Special thanks to H. Taylor (Geological Survey of Canada, Vancouver) for processing conodont samples and to K. Russell (The University of British Columbia) for acting as a scientific reviewer.

Natural Resources Canada, Earth Science Sector contribution 20160225

References

Epstein, A.G., Epstein, J.B. and Harris, L.D. 1977: Conodont color alteration – an index to organic metamorphism; US Geological Survey Professional Paper 995.

Google 2013: Google Maps™ satellite image, Chidliak area, Nunavut; Google, image, URL <http://maps.google.ca/maps> [©2013 Google – Imagery, ©2013 TerraMetrics, Map data, June 15, 2013]

Harris, A.G. 1981: Color and alteration: an index to organic metamorphism in conodont elements; *in* Treatise on Invertebrate Paleontology, R.A. Robison (ed.), Part W, Miscellanea Supplement 2, Conodonta, Geological Society of America, Boulder, Colorado, p. W56–W60.

Heaman, L.M., Grütter, H.S., Pell, J., Holmes, P. and Grenon, H. 2012: U-Pb geochronology, Sr- and Nd isotope compositions of groundmass perovskite from the Chidliak and Qilaq kimberlites, Baffin Island, Nunavut; 10th International Kimberlite Conference, Bangalore, Extended Abstract No. 10 IKC-193, CD-ROM.

Lindström, M. 1971: Lower Ordovician conodonts of Europe; *in* Symposium on conodont biostratigraphy, W.C. Sweet and S.M Bergström (ed.), The Geological Society of America Memoir 127, p. 21–61.

Machado, G., Bilodeau, C. and St-Onge, M.R. 2013: Geology, southern part of Hall Peninsula, south Baffin Island, Nunavut; Geological Survey of Canada, Canadian Geoscience Map 135 (preliminary) and Canada-Nunavut Geoscience Office, Open File Map OFM2013-1, scale 1:250 000.

McCracken, A.D. 2000: Middle and Late Ordovician conodonts from the Foxe Lowland of southern Baffin Island, Nunavut; Geological Survey of Canada, Bulletin 557, p. 159–216.

Nentwich, F.W. and Jones, B. 1989: Stratigraphy and sedimentology of Ordovician and Silurian strata, northern Brodeur Peninsula, Baffin Island; Bulletin of Canadian Petroleum Geology, v. 37, p. 428–442.

Nowicki, T., Coopersmith, H. and Pilotto, D. 2016: Mineral resource estimate for the Chidliak project, Baffin Island, Nunavut; URL <https://www.pdiam.com/assets/docs/technical-reports/msc16_006r-mineral-resource-estimate-for-the-chidliak-project_2016-06-16.pdf> [October 2016].

Pell, J., Grütter, H., Neilson, S., Lockhart, G., Dempsey, S. and Grenon, H. 2013: Exploration and discovery of the Chidliak kimberlite province, Baffin Island, Nunavut, Canada's newest diamond district; *in* Proceedings of the 10th International Kimberlite Conference, D.G. Pearson, H.S. Grutter, J.W. Harris, H. O'Brien, N.V.C. Rao and S. Sparks (ed.), Bangalore, India, Journal of the Geological Society India, Special Issue 2, p. 209–227.

Pell, J., Russell, J.K. and Zhang, S. 2015: Kimberlite emplacement temperatures from conodont geothermometry; Earth and Planetary Science Letters, v. 411, p. 131–141.

Rejebian, V.A., Harris, A.G. and Huebner, J.S.1987: Conodont color and textural alteration: an index to regional metamorphism, contact metamorphism, and hydrothermal alteration; Geological Society of America, Bulletin 99, p. 471–479.

Sanford, B.V. 1977: Ordovician rocks of Melville Peninsula, southeastern District of Franklin; Geological Survey of Canada, Bulletin 269, p. 7–21.

Sanford, B.V. and Grant, A.C. 1990: New findings relating to stratigraphy and structure of the Hudson Platform; Geological Survey of Canada, Paper 90-1D, p. 17–30.

Sanford, B.V. and Grant, A.C. 1998: Paleozoic and Mesozoic geology of the Hudson and southeast Arctic Platforms; Geological Survey of Canada, Open File 3595.

Sanford, B.V. and Grant, A.C. 2000: Geological framework of Ordovician system in the southeast Arctic Platform, Nunavut; Geological Survey of Canada, Bulletin 557, p. 13–38.

Sansom, I.J., Armstrong, H.A. and Smith, M.P. 1994: The apparatus architecture of *Panderodus* and its implications for coniform conodont classification; Palaeontology, v. 37, p. 781–799.

Scott, D.J. 1996: Geology of the Hall Peninsula east of Iqaluit, southern Baffin Island; Geological Survey of Canada, Current Research 1996-C, p. 83–91.

Scott, D.J. 1999. U-Pb geochronology of the eastern Hall Peninsula, southern Baffin Island, Canada: a northern link between the Archean of West Greenland and the Paleoproterozoic Torngat Orogen of northern Labrador; Precambrian Research, v. 93, p. 5–26.

Steenkamp, H.M. and St-Onge, M.R. 2014: Overview of the 2013 regional bedrock mapping program on northern Hall Peninsula, Baffin Island, Nunavut; *in* Summary of Activities 2013, Canada-Nunavut Geoscience Office, p. 27–38.

St-Onge, M.R., Jackson, G.D. and Henderson, I. 2006: Geology, Baffin Island (south of 70°N and east of 80°W), Nunavut; Geological Survey of Canada, Open File 4931, 3 sheets, 1 CD-ROM.

Trettin, H.P. 1975: Investigations of lower Paleozoic geology, Foxe Basin, northeastern Melville Peninsula, and parts of northwestern and central Baffin Island; Geological Survey of Canada, Bulletin 251, 177 p.

Whalen, J.B., Wodicka, N., Taylor, B.E. and Jackson, G.D. 2010: Cumberland Batholith, Trans-Hudson Orogen, Canada: petrogenesis and implications for Paleoproterozoic crustal and orogenic processes; Lithos, v. 117, p. 99–119.

Wheeler, J.O., Hoffman, P.F., Card, K.D., Davidson, A., Sanford, B.V., Okulitch, A.V. and Roest, W.R., comp. 1997: Geological Map of Canada; Geological Survey of Canada, Map D1860A.

Zhang, S. 2011: Late Ordovician conodont biostratigraphy and redefinition of the age of oil shale intervals on Southampton Island; Canadian Journal of Earth Sciences, v. 48, p. 619–643.

Zhang, S. 2012: Ordovician stratigraphy and oil shale, southern Baffin Island, Nunavut – preliminary field and post-field data; Geological Survey of Canada, Open File 7199, 26 p.

Zhang, S. 2013: Ordovician conodont biostratigraphy and redefinition of the age of lithostratigraphic units on northeastern Melville Peninsula, Nunavut; Canadian Journal of Earth Sciences, v. 50, p. 808–825.

Zhang, S. and Barnes, C.R. 2007: Late Ordovician–Early Silurian conodont biostratigraphy and thermal maturity, Hudson Bay Basin; Bulletin of Canadian Petroleum Geology, v. 55, p. 179–216.

Zhang, S. and Pell, J. 2013: Study of sedimentary rock xenoliths from kimberlites on Hall Peninsula, Baffin Island, Nunavut; *in* Summary of Activities 2012, Canada-Nunavut Geoscience Office, p. 107–112.

Zhang, S. and Pell, J. 2014: Conodonts recovered from the carbonate xenoliths in the kimberlites confirm the Paleozoic cover on the Hall Peninsula, Nunavut; Canadian Journal of Earth Sciences; v. 51, p. 142–155.

Geochemical, mineralogical and sedimentological results from till, stream and lake sediment and water samples in the Sylvia Grinnell Lake area, Baffin Island, Nunavut

T. Tremblay[1], S. Day[2], J. Shirley[3], K.A. Smith[4] and R. McNeil[2]

[1]*Canada-Nunavut Geoscience Office, Iqaluit, Nunavut, tommy.tremblay@canada.ca*

[2]*Natural Resources Canada, Geological Survey of Canada, Ottawa, Ontario*

[3]*Nunavut Research Institute, Iqaluit, Nunavut*

[4]*Department of Geography, Carleton University, Ottawa, Ontario*

Tremblay, T., Day, S., Shirley, J., Smith, K.A. and McNeil, R. 2016: Geochemical, mineralogical and sedimentological results from till, stream and lake sediment and water samples in the Sylvia Grinnell Lake area, Baffin Island, Nunavut; *in* Summary of Activities 2016, Canada-Nunavut Geoscience Office, p. 13–26.

Abstract

The Sylvia Grinnell Lake area project is a collaborative activity between the Canada-Nunavut Geoscience Office, the Geological Survey of Canada (Geo-mapping for Energy and Minerals program), the Nunavut Research Institute and Carleton University. The study area is located north of Iqaluit, and covers 16 000 km^2 over NTS map areas 25N, 26C and F. The surficial geology results will assist the search for and development of future natural resources, and provide useful input for infrastructure and environmental studies. Samples of till, stream sediment, lake sediment, stream water and lake water were collected during the summer of 2015 and then submitted for mineralogical, geochemical and sedimentological analyses. One of the notable findings was the presence of scheelite ($CaWO_4$) and cassiterite (SnO_2) grains in till and stream sediment, minerals typically related with felsic intrusive rocks. The potential for other commodities is modest to negligible, compared with results from elsewhere in the south Baffin Island area. This work also found that water microbial quality is very good in the study area. The pH values in surface waters measured between 5.0 and 8.0, averaging 6.4.

Résumé

La région du lac Sylvia Grinnell fait l'objet d'un projet de nature collaborative impliquant le Bureau géoscientifique Canada-Nunavut, la Commission géologique du Canada (programme de géocartographie de l'énergie et des minéraux), le Nunavut Research Institute et l'Université Carleton. La zone d'étude est située au nord d'Iqaluit et couvre 16 000 km^2 des régions cartographiques 25N, 26C et F du SNRC. Les résultats des travaux géologiques de surface réalisés devraient d'une part contribuer à rendre plus facile le processus d'exploration et de mise en valeur de ressources naturelles futures et, d'autre part fournir les données nécessaires à la poursuite d'études sur les infrastructures et l'environnement. Des échantillons de till, de sédiments fluviatiles et lacustres et d'eau de lac et de ruisseau ont été recueillis au cours de l'été 2015 en vue d'analyses minéralogiques, géochimiques et sédimentologiques. La présence de grains de scheelite ($CaWO_4$) et de cassitérite (SnO_2) dans le till et les sédiments fluviatiles, soit des minéraux habituellement associés aux roches felsiques intrusives, constitue l'un des résultats d'analyse les plus intéressants obtenus. La probabilité que d'autres substances utiles soient présentes varie de faible à négligeable, du moins lorsque comparée à celle associée aux résultats obtenus ailleurs dans la région sud de l'île de Baffin. Les travaux ont également permis d'établir que la qualité microbienne de l'eau s'avère excellente dans la zone d'étude. La valeur du pH de l'eau superficielle varie entre 5.0 et 8.0, la moyenne se situant à 6.4.

Introduction

The Sylvia Grinnell Lake area project is a collaborative activity between the Canada-Nunavut Geoscience Office, the Geological Survey of Canada (Geo-mapping for Energy and Minerals program), the Nunavut Research Institute and Carleton University. The Canada-Nunavut Geoscience Office (CNGO) has a mandate to provide geoscience knowledge to promote responsible resource exploration and development and responsible infrastructure development in

This publication is also available, free of charge, as colour digital files in Adobe Acrobat® PDF format from the Canada-Nunavut Geoscience Office website: http://cngo.ca/summary-of-activities/2016/.

the territory; this includes gathering baseline information about the geochemistry and mineralogy of surficial sediments. This baseline data will potentially help to lower the financial risks of finding new mineral prospects by the exploration industry. Mineral exploration, geotechnical and aggregate resource studies require accurate surficial geology maps and glaciodynamic interpretations. The collection of baseline information about the geochemistry of soils and water is useful, particularly for environmental studies. Samples of till, stream and lake sediment, and stream and lake water were collected in 2015; this paper presents geochemical, mineralogical and sedimentological data from an area where little or no previous public data exists.

The study area is located north of Iqaluit, and covers 16 000 km^2 over NTS map areas 25N, 26C and F (Figure 1). Currently, the publicly available surficial geology mapping is limited to a national-scale map (1:5 000 000, Fulton, 1995) and detailed mapping of the NTS 25N map area (1:100 000, Hodgson, 2005). The general surficial geology and some of the methodologies are presented in Tremblay et al. (2015).

Regional setting

The study area is located on Baffin Island between extensive lowlands to the west, the Meta Incognita plateau and Frobisher Bay to the south, the Hall Peninsula plateau to the east and a rugged low-lying area, located west of Cumberland Sound, to the north. Within the study area, the Sylvia Grinnell River valley extends southeast at ~100–200 m above sea level (asl), with step-like ridges rising up to the plateaus toward the southwest (Meta Incognita plateau, up to 500–600 m asl; Hodgson, 2005) and north (McKeand River plateau, adjacent to Hall Peninsula plateau, up to 700 m asl). The plateaus are dissected by deep river valleys, and locally display a well-formed, subdendritic drainage pattern. The study area lies within the continuous permafrost zone and local vegetation is typical of the low-arctic tundra (see Tremblay et al., 2015, for detailed descriptions of topography, previous works and glacial geomorphology).

Glacial geology

The geomorphological indicators of glacial erosion are summarized into three glaciodynamic zones in the study area (Figure 1), indicative of the amount of glacial activity (erosion and transport) that took place during the Quaternary period. In warm-based areas, glacial scouring is important, as evident from the presence of numerous small lakes and glacially eroded outcrops. The intermediate cold-based zones are interpreted to be areas where glacial erosion gradually became more marked as evidenced by more lakes and bedrock outcrops, and the sparse appearance of streamlined outcrops and macroforms. In the cold-based zones, the existence of a mix of thick nonglacial regolith, felsenmeer and till would suggest little or no sliding to have occurred at the glacier bed. Coverage by cold-based ice sheets during the Quaternary is indicated by locally abundant glaciofluvial channels and occasional glacial erratics. The dynamic character of the former ice sheet (cold- versus warm-based) can help to understand and outline the nature of glacial transport. On Hall Peninsula, cosmogenic samples (Ross et al., 2015) and mineralogical data (Leblanc-Dumas et al., 2015) emphasize the distinction between till and glacially eroded terrain, and regolith and till mixed with regolith in less glacially eroded terrain (Tremblay et al., 2015).

The glacial ice-flow history of the study area evolved in two main phases (for details of the glacial history see Tremblay et al., 2015). Ice-flow phase 1 involved two important glacial ice outlets that existed during the last glacial maximum (LGM) in Baffin Bay, Frobisher Bay (convergent ice flow to the southeast) and Cumberland Sound (northwest ice flow). During phase 2, as the Hudson Strait ice stream gradually developed and the ice front retreated into Hudson Strait, the west Baffin Island ice flow became increasingly warm-based and westward ice flow developed toward Foxe Basin. In Frobisher Bay, the ice front receded to the Frobisher Bay moraine position ca. 9.0 ka ^{14}C (Blake, 1966), and ice flow switched from a convergent pattern to a divergent pattern. Proglacial lakes were formed as the ice front retreated against the topographic slope, and complete deglaciation of the study area occurred ca. 5.5 ka ^{14}C (Prest, 1969).

Bedrock geology

The bedrock geology of the study area (Weller et al., 2015) is made up of mainly granitoid rocks associated with the middle Paleoproterozoic Cumberland Batholith, which contains screens and enclaves of metasedimentary rocks including quartzite, pelite, marble and greywacke (Lake Harbour and Piling groups affinities). Weller et al. (2015) mention the presence of sulphide-bearing gossans and layered mafic-ultramafic sills that may host sulphide mineralization. The area has been affected by amphibolite-grade metamorphism and deformation associated with the Trans-Hudson Orogen. Diabase dykes (1–20 m thick) of Mesoproterozoic to Neoproterozoic age are mapped in the northern part of the study area. In the southwestern part of the study area, Paleozoic carbonate rocks (limestone, dolomitic limestone and organic-rich black shale) overlie the Paleoproterozoic (Zhang, 2012), and are bounded by either fault zones or unconformities between Ordovician and eroded Paleoproterozoic rocks.

A simplified compilation of geological maps by St-Onge et al. (1999, 2016a–d) is presented in Figure 2. In the southern part of study area, the visible inconsistency of geological units in Figure 2 is due to mapping scale discrepancies between the original maps. The ‘Granite’ unit is principally

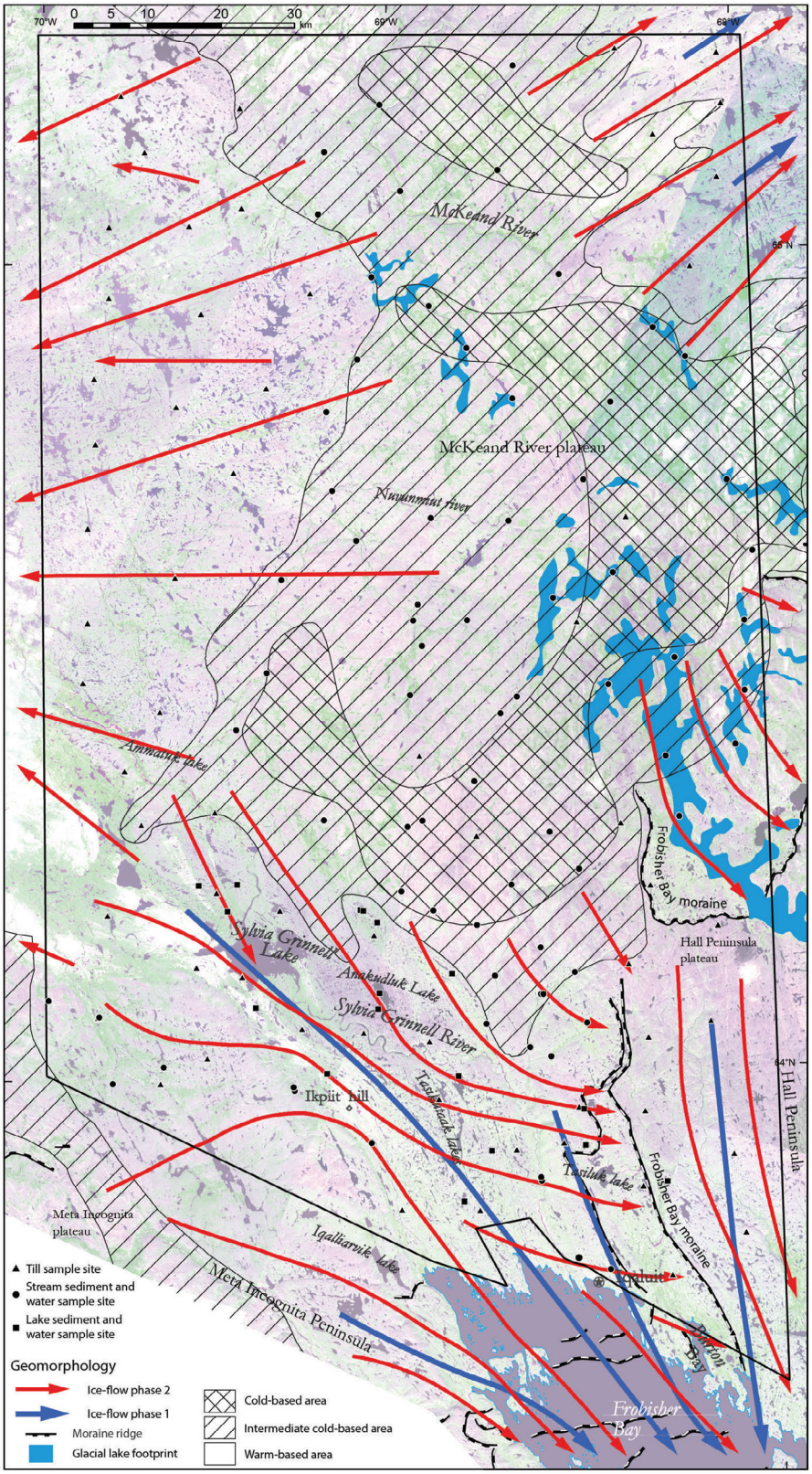

Figure 1: Location map of study area (black outline) and sample sites, Sylvia Grinnell Lake area, Baffin Island, Nunavut. Satellite image in the background is a SPOT multispectral image (GeoBase®, 2015); on this image, green corresponds to vegetation, pink corresponds to boulder diamicton and bedrock, white corresponds to vegetation-poor carbonate material and dark grey corresponds to water. Glaciodynamic indicators, moraines and glacial lakes are also indicated.

composed of monzogranite to granodiorite, with orthopyroxene, hornblende, clinopyroxene, biotite and magnetite. The 'Granite with biotite' unit is principally composed of monzogranite with biotite, hornblende, magnetite and orthopyroxene. The 'Granite with metasedimentary layers' unit is dominated by monzogranite with biotite, garnet, orthopyroxene and abundant inclusions of metasedimentary rock. The 'Metasedimentary rocks' unit is principally composed of Lake Harbour Group rocks that contain metasedimentary rocks (quartzite, psammite, semipelite, pelite [with garnet, sillimanite and biotite], orthoquartzite, marble and calcsilicate rocks) and various igneous rocks (principally garnet-biotite monzogranite, and metaleucodiorite, metagabbro, amphibolite and mafic-ultramafic sills). Diabase dykes and Ordovician carbonate rocks are also present in the area.

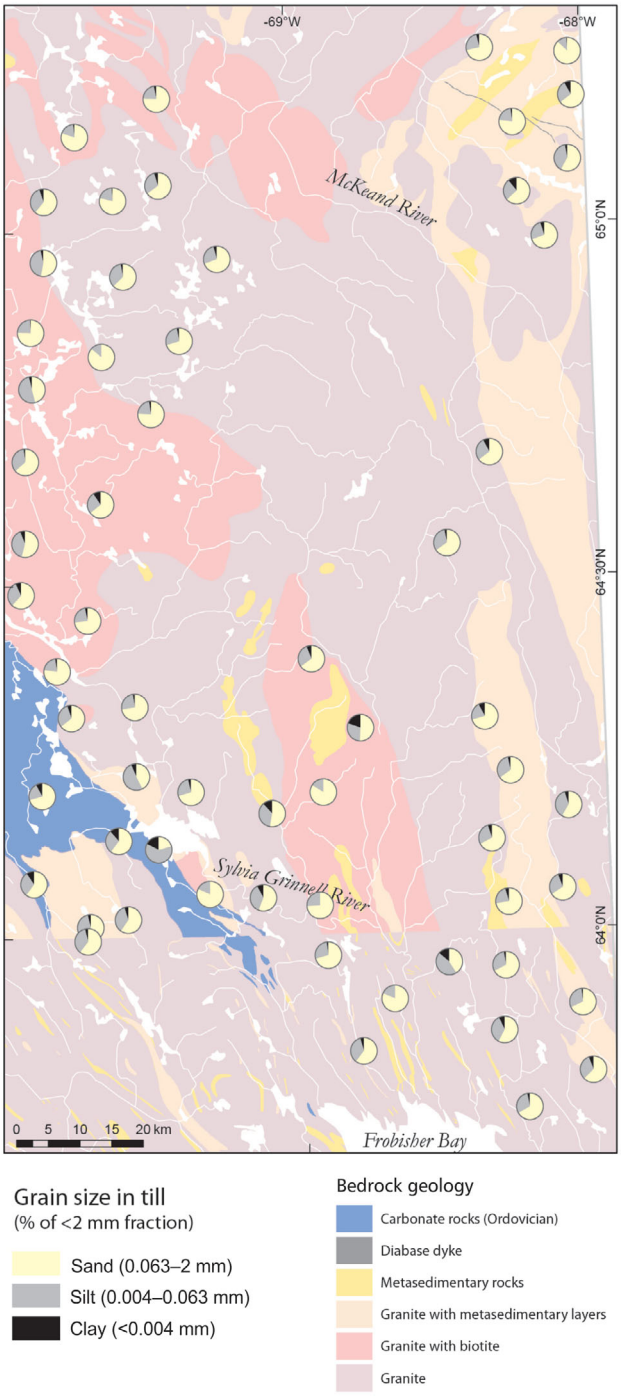

Figure 2: Grain size of till samples, Sylvia Grinnell Lake area, Baffin Island, Nunavut. Background bedrock geology modified from St-Onge et al. (1999, 2016a–d).

Methodology

For the Sylvia Grinnell Lake area survey, samples were collected from multiple surficial media (till, stream sediment, lake sediment, stream water and surface lake water [Table 1]). Certified reference material samples, field duplicate samples and laboratory sample splits were inserted into the sample populations prior to submission for chemical analyses for the purpose of monitoring, evaluating and ensuring data quality. This survey methodology is similar to Utting et al.'s (2008) mixed media survey in the northern Baffin Island region, where till and stream-sediment heavy mineral samples were collected in warm-based and cold-based glaciodynamic zones, respectively. In general, stream sediment and water samples are preferred sampling media when conducting regional drainage geochemical surveys in areas with a regular network of developed streams (Prior et al., 2009). Stream sediment and water samples collected as part of this study followed the Geological Survey of Canada's (GSC) former National Geochemical Reconnaissance (NGR) program's standards for sample collection and analytical techniques (Friske and Hornbrook, 1991). These standards are used to ensure consistent and reliable results regardless of the area, date of the survey or the analytical laboratory used. Field equipment used and samples collected at a typical bulk stream sediment and water site are illustrated in Tremblay et al. (2015, Figure 5). Complete georeferenced results are presented in Tremblay et al. (2016)[5].

Till and stream silt geochemistry and sedimentology

Sixty-three till geochemistry samples (~2 kg) were collected, predominantly in the warm-based glaciodynamic zone, where glacial erosion, transport and depositional processes were most intense (Figure 1). Till samples were processed at the GSC Sedimentology Laboratory (Ottawa, Ontario). Seven stream silt samples were also collected, dried and sieved to obtain the <177 µm fraction and analyzed by the same methods (except grain-size analysis) as the till samples. A portion of the <2 mm sized matrix of

[5] *CNGO Geoscience Data Series GDS2016-001, containing the data or other information sources used to compile this report, is available online to download free of charge at http://cngo.ca/summary-of-activities/2016/.*

Table 1: Number of samples analyzed, per type of material sampled in Sylvia Grinnell Lake area, Baffin Island, Nunavut.

Analysis	Sample type						Total
	Till	Stream sediment	Stream silt	Lake sediment	Stream water	Lake water	
Grain size	63	0	0	0	-	-	63
Munsell colour	63	0	7	16	-	-	86
Carbon content and LOI	0	0	7	14	-	-	21
Carbonate content	63	0	7	14	-	-	84
Geochemistry	63	0	7	16	-	-	86
Heavy mineral fraction	61	74	0	0	-	-	135
Microbial water quality	-	-	-	-	14	0	14
Water geochemistry	-	-	-	-	76	17	93

Abbreviation: LOI, loss-on-ignition.

each till sample was wet-sieved to 63 µm for geochemical analysis. Another <2 mm sized portion was sent for grain-size analysis (except for stream silt samples), inorganic carbon content and loss-on-ignition (LOI; except for till samples), Munsell colour and carbonate content analysis. Lastly, a portion was also saved for archival purposes. The till sample grain-size distribution (sand, silt and clay; Figure 2) was determined by use of a laser particle size analyzer (LECO Corporation's Lecotrac LT-100) in conjunction with sieving or digital image analysis instrumentation (Retsch Technology GmbH's CAMSIZER®) on the <63 µm fraction (see Girard et al., 2004, for details on laboratory protocols). The grain size of fractions between 63 µm and 2 mm was determined by wet sieving. Inorganic carbon content and LOI was measured with the LECO Corporation's LECO® CR412 carbon moisture analyzer. Munsell colour determination was done using X-Rite, Incorporated's SP64 portable sphere spectrophotometer. Carbonate content was analyzed by titration with UIC Inc.'s CM5015 CO_2 Coulometer with CM5230 Acidification Module on the <63 µm fraction, on a (maximum) 2 g sample.

A split of the <63 µm fraction was sent to Bureau Veritas Minerals (Vancouver, British Columbia) for geochemical analysis (see McClenaghan et al., 2013, for laboratory protocols). A 30 g split was digested with aqua regia and analyzed by inductively coupled plasma–mass spectrometry (ICP-MS) for 65 elements, including gold, base metals, platinum and rare-earth elements. Another 2 g split was digested with lithium metaborate/lithium tetraborate fusion and then analyzed by inductively coupled plasma–emission spectrometry (ICP-ES) for 11 major elements and 7 trace elements. Analytical accuracy and precision were monitored by including GSC CANMET-certified standards (TILL-2 and TILL-4) in the sample suites. Quality control samples were inserted into the sample suite at Bureau Veritas Minerals, including laboratory duplicates of samples, blanks, reference standards and analytical duplicates.

Heavy mineral fraction of till and stream sediments

Sixty-one bulk till samples (11 kg average total weight) and 74 bulk stream sediment samples (14 kg average total weight) were collected to provide information on heavy mineral concentrates (HMC), including kimberlite-indicator minerals (KIMs), base-metal sulphides, platinum, gold, gemstones and other minerals of interest. Till samples were collected with a shovel from mudboils between 0 and 40 cm from the surface. Bulk stream sediment samples were wet-sieved onsite to obtain ~14 kg of <2 mm sized material from relatively high-energy, gravel-rich sites.

Samples were sent to Overburden Drilling Management Limited (Nepean, Ontario) for heavy mineral analyses. A standard pre-analysis treatment was applied to all samples, which included initial sieving of pebbles (>2 mm; the 4–8 mm fraction were separated for lithological counting) and pre-concentration of heavy minerals on a shaking table. The gold grains and metallic indicator minerals from a panning concentrate were counted, described and replaced into the same fraction. The heavy mineral pre-concentrate was then submitted for heavy liquid separation (methylene iodide, specific gravity of 3.2) and ferromagnetic separation. The >0.25 mm fraction of nonferromagnetic heavy mineral concentrate (NFHMC) was examined by binocular microscope for the identification of various distinctive mineral species, namely KIMs and metamorphic massive-sulphide–indicator minerals (MMSIMs), which notably include gahnite, red rutile, pyrite, chalcopyrite and arsenopyrite (Averill, 2001). The mineralogical picking was performed on three different size fractions (0.25–0.5 mm, 0.5–1 mm, 1–2 mm) of NFHMC. Scheelite counts were confirmed by ultraviolet (UV) lamping of 1.0–2.0 mm, 0.5–1.0 mm and nonparamagnetic (>1.0 A) 0.25–0.5 mm fractions. Following further preparation, binocular identifications of MMSIMs and KIMs were undertaken and supported in some cases by scanning electron microscope (SEM) analysis.

Four GSC internal blanks (from Bathurst granite grus standard) were inserted for quality control and quality assurance (sample numbers 025N_2015_1001BS, 026C_2015_1021BS, 026C_2015_1041BS, 026F_2015_1074BS; see Plouffe et al., 2013, for laboratory protocols). The four blanks returned expected results, with no KIMs, no gold grains and no MMSIMs, with the exception of trace amounts of goethite. For various minerals of interest, results for bulk stream sediment sample 026C_2015_1020 versus duplicate 026C_2015_1024 show 0 versus 4 pyrite grains, 6 versus 14 coloured spinel grains, trace versus 1% sillimanite, 70 versus 40% orthopyroxene, 7 versus 9 scheelite grains, 0 versus 20 cassiterite grains, 2 versus 4% monazite; the sample and duplicate returned identical results on KIMs (0 grains), goethite (trace) and apatite (trace).

Lake sediment geochemistry and sedimentology

In areas of low to moderate topographic relief and abundant lakes, stream networks are typically poorly developed and generally do not provide a suitable sampling media for a broad regional drainage geochemical survey. However, centre-lake sediment and water samples do provide a suitable medium for regional and higher-density geochemical surveys. Due to the exceptionally cold summer conditions of July 2016, many lakes were frozen and prevented complete sampling, and only 16 lakes, with a surface area of smaller than 5 km^2, were sampled. A torpedo-like grab sampler, routinely used by GSC (see Figure 6 in Tremblay et al., 2015), was used to sample organic-rich lake sediment (gyttja). After sampling, sediment samples were dried to completion (at <40°C) and sieved to obtain the <177 µm fraction, which was analyzed by 1) aqua-regia digestion followed by ICP-MS for 65 elements, and 2) lithium metaborate/lithium tetraborate fusion followed by ICP-ES for 11 major elements and 7 trace elements. Sedimentological analyses (Munsell colour, LOI, carbon and carbonate content; see previous 'Till geochemistry and sedimentology' section) were also performed on the lake sediment samples.

Water geochemistry

Stream and lake water samples were collected at 93 sites at surface (~0.5 m depth). Prior to filling, bottles were triple-rinsed—both in the field and during filtering. Within 24 hours of collection, field samples were passed through a 0.45 µm filter into two separate sets of bottles at the Nunavut Research Institute (NRI) laboratory. Following this, one set of samples was acidified with 0.5 ml of 8 molar ultra-pure nitric acid at the GSC. Chlorine and pH data were determined from the non-acidified set. Trace-element geochemistry analyses using ICP-MS and ICP-ES were undertaken at the GSC's Inorganic Geochemistry Research Laboratory (Ottawa, Ontario). Results are available but being checked for validity and will be published in future papers.

Alkalinity measurements were done at the GSC's Inorganic Geochemistry Research Laboratory (Ottawa, Ontario) using MANTECH Inc.'s PC-Titrate™ system with Titra-Sip™ module. The total alkalinity was measured by potentiometric titration with 0.02 molar sulphuric acid; the software determined the volume of acid required to reach the bicarbonate equivalence point. Alkalinity results are reported as equivalents of $CaCO_3$ in ppm. The pH and conductivity measurements were made using a Fisher Scientific™ accumet™ AR50 dual channel pH/ion/conductivity meter with temperature compensation. The pH measurements were made using Fisher Scientific™ accumet™ liquid-filled polymer body combination electrodes with double junction Ag/AgCl reference (and calibration was done with pH 4.00, 7.00 and 10.00 buffers). Conductivity measurements were done using Fisher Scientific™ accumet™ four-cell conductivity probes with automatic temperature compensation (ATC), with a 1.0 cm cell constant for samples in the 10–2000 microsiemens (µS) per cm range and a 10.0 cm^{-1} cell constant for samples in the 1000–200 000 $\mu S \cdot cm^{-1}$ range. Commercial conductivity standards were used for calibration.

Microbial stream water quality indicators

Concentrations of total coliform and *Escherichia coli* (*E. coli,* a subset of coliforms) were measured in samples of stream surface waters taken at 14 sites visited in the 2015 field season. A sample was taken at each site and duplicates were sampled at 11 sites. These results will extend the Nunavut Research Institute microbial water quality indicators study already in place around Iqaluit (Niaqunguk River [commonly known as Apex river] watershed). Total coliform and *E. coli* concentrations are used worldwide as indicators of the basic microbial quality of surface waters. The bacteria can be detected rapidly, accurately and with relatively minimal cost and effort. For this project, samples were collected in sterile 120 mL plastic bottles containing a minor quantity of sodium thiosulphate. Collection bottles were handled with clean, nitrile, lab gloves to avoid sample contamination. At each site, samples were collected by dipping the sample bottles into the water, just below the surface of the stream sampled. Care was taken to collect samples at a similar depth in an effort to control for variability in the vertical distribution of coliforms in the water column. Following collection, sample bottles were tightly closed and kept as cool as possible for their return to the Nunavut Research Institute lab in Iqaluit.

Upon delivery to the lab, water samples were immediately inoculated with powdered Colilert® reagent (kit from IDEXX Laboratories, Inc.) and incubated for 24 hours at 35°C in heat-sealed disposable 97-well Quanti-Trays®, as per manufacturer's instructions. Total coliform levels were then quantified by enumerating colour change in individual wells of the incubated trays, and *E. coli* levels were quanti-

fied based on ultraviolet-fluorescence of the wells. These well counts were then converted to total organism numbers (with 95% confidence) by reference to the most-probable number charts provided by the manufacturer. The data are reported as most probable number (MPN) of colony-forming units of bacterial cells per 100 ml sample.

Results

Field observations of ice-flow indicators (striae) were compiled and the results were reported in Tremblay et al. (2015, Figure 2). Figure 1 indicates ice-flow direction and glaciodynamic zonation necessary for the interpretation of glacial provenance in surficial sediments. The hydrography of river systems (on all figures) allows the interpretation of stream sediment provenance.

The following section will focus on till (number of samples [n] = 63) and bulk stream sediment samples (n = 74), as well as water samples (n = 93). Geochemistry of lake sediment (n = 16) and stream silt samples (n = 7) will be interpreted in future publications, as well as general Munsell colour, carbon/LOI and carbonate content results. In this paper, all HMC results are reported as normalized to 10 kg (table feed) samples of till and stream sediment.

Till and stream sediment characteristics

Grain-size results from till in the <2 mm fraction (Figure 2) indicate 65% sand (50–70% range; 0.063–2 mm), 30% silt (10–50% range; 0.004–0.063 mm) and 5% clay (1–20% range; <0.004 mm). Larger clay fractions are found near Ordovician limestone outcrops (limestone is easily crushed to silt-size grains compared with granite) and near the McKeand River plateau (in proximity to intermediate cold-based to cold-based zones, where regolith might be found, see Leblanc-Dumas et al., 2015). Grain-size information on the surficial sediments provides geotechnical data, useful in assessing potential ground stability linked with permafrost.

Gold grains results show a maximum of six gold grains in one sample and 42 gold grains total from 25 samples (Figure 3a). The grains are mostly reworked grains (77%), 20% are reshaped and 3% pristine. The till matrix indicates 0.99 ppb average Au, with a maximum of 9.3 ppb (Figure 3b). Highest gold grain counts and the highest Au values (>1.6 ppb) occur in the vicinity of the Sylvia Grinnell River valley. Generally, gold grains in surficial sediments were less abundant in the study area relative to Hall Peninsula to the east (Tremblay and Leblanc-Dumas, 2015).

Results of pyrite grain analysis show a maximum of 370 grains at one site and much lower values at 14 other sites (<20 grains but generally between one and five grains; Figure 4a). Sulphur concentrations in till matrix indicate a maximum of 8 ppm, and 11 samples are over 0.02% (see Tremblay et al., 2016). The highest pyrite grain counts were found close to carbonate rock outcrops. This might be accountable to lower dissolution rates of pyrite in carbonate-rich till relative to carbonate-poor till; or, alternatively, Ordovician carbonate sequences might initially contain pyrite-rich layers. Relatively pyrite-rich biotite granite (±metasedimentary rocks) in the vicinity of Sylvia Grinnell River valley might also account for higher sulphide grain counts in the area.

Chalcopyrite grains are contained in four samples, with a maximum of four grains in one sample (Figure 4a). Till matrix averages 28 ppm Cu, with a maximum of 198 ppm, and five samples are over 90 ppm (Figure 3b). The highest Cu values in the till matrix (>61 ppm) are observed in the vicinity of Sylvia Grinnell River valley and near the metasedimentary outcrops in the northeastern part of the study area. The average Zn value is 78 ppm, with a maximum of 505 ppm, and five samples are over 115 ppm (Tremblay et al., 2016). Gahnite grains, common indicators of the presence of massive sulphides, are present at three sites in the northeastern part of study area (Figure 5a). Chalcopyrite and gahnite grains were more abundant on Hall Peninsula (Tremblay and Leblanc-Dumas, 2015).

Scheelite ($CaWO_4$) grain counts indicate a maximum of 19 grains at one site, and a total of 143 grains were picked from the 47 sites (Figure 5a). Concentrations of W in the till matrix reach a maximum of 1.6 ppm at one site, with five additional sites having concentrations over 0.7 ppm (Figure 5b). Scheelite grains and the highest W values in till matrix are located in the vicinity of the Sylvia Grinnell River valley and slightly to the north.

Cassiterite (SnO_2) grain counts indicate a maximum of 26 grains at one site, and a total of 67 grains were picked from the four sites. The concentration of Sn in till matrix shows a maximum of 1.8 ppm at one site, and four sites have values over 1.3 ppm. Cassiterite grains are located in a pocket 50 km north of Sylvia Grinnell River. The Sn geochemical values are fairly constant all around the study area, and not closely correlated with cassiterite, however, few till matrix geochemistry results were returned from the area where the cassiterite grains were found. Also, it is worth noting that duplicates show poor reproducibility of cassiterite grain results (see 'Heavy mineral fraction of till' methodology section).

Molybdenite grains were found at 13 sites, with two grains maximum from each site (Figure 5a). Arsenopyrite grains are present at three sites, with a highest count of three grains (Figure 5a). Till-matrix geochemical values of Mo indicate a maximum of 5.1 ppm at one site, with five samples over 2.2 ppm (Tremblay et al., 2016). Ruby and sapphirine grains (one each) were found in the study area (Figure 5a); they are generally less abundant than on Hall Peninsula (Tremblay and Leblanc-Dumas, 2015).

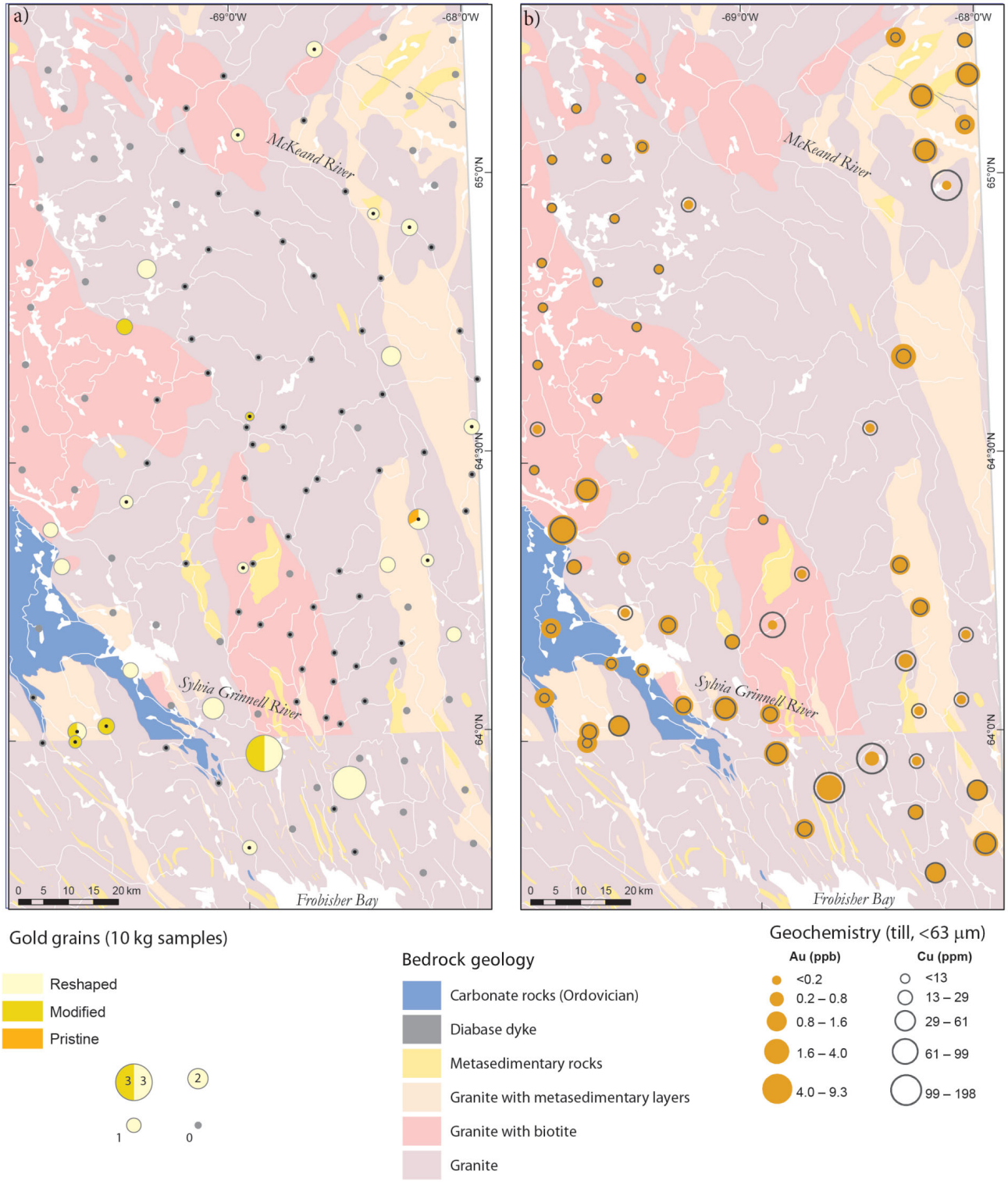

Figure 3: a) Gold grains in heavy mineral fraction of till and stream sediment samples. Black dot indicates stream sediment sample. **b)** Results of geochemical analysis of Au and Cu in till samples, <63 µm size fraction. Background bedrock geology of the Sylvia Grinnell Lake area, Baffin Island, Nunavut, modified from St-Onge et al. (1999, 2016a–d).

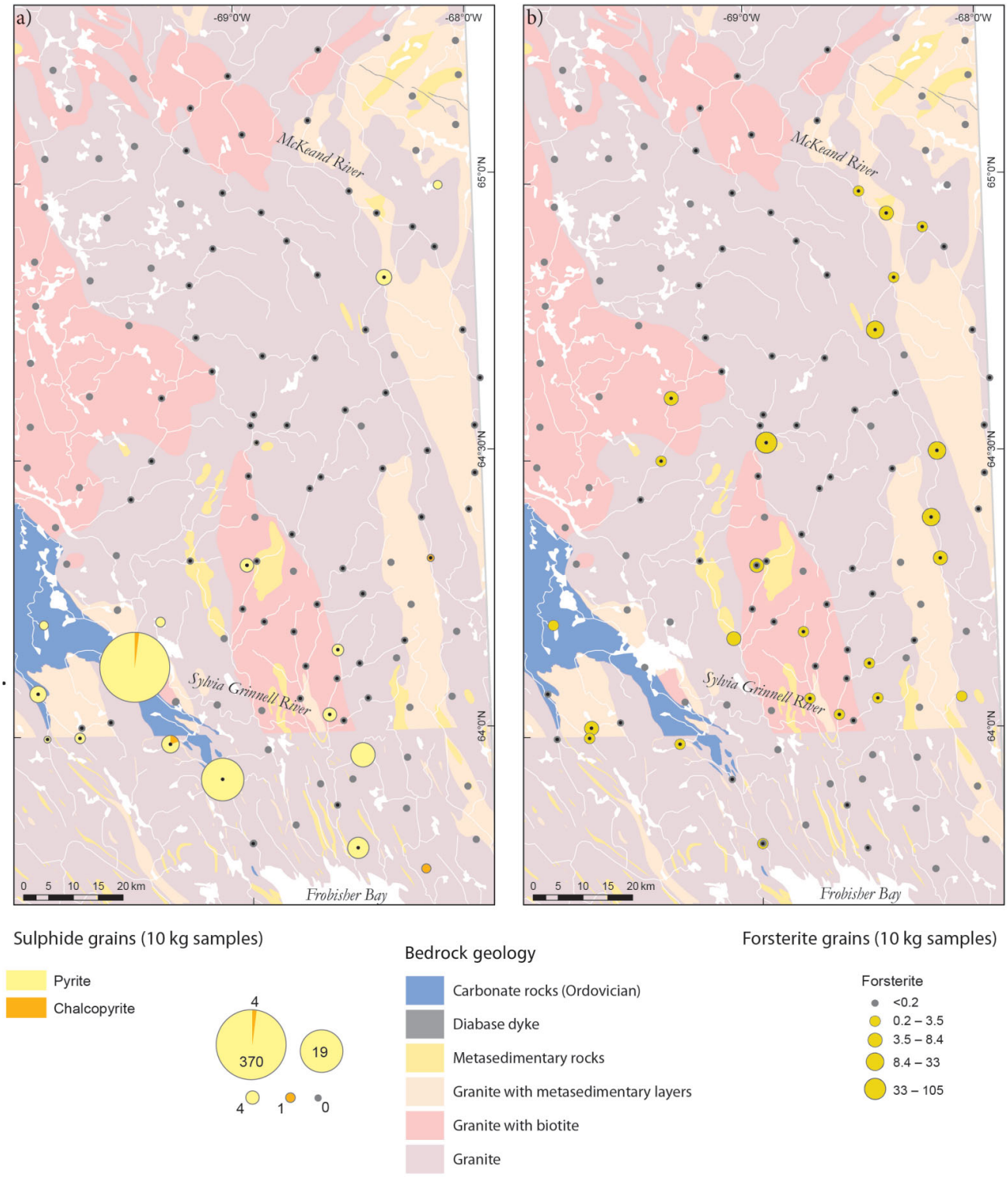

Figure 4: a) Sulphide grains in heavy mineral fraction of till and stream sediment samples. Black dot indicates stream sediment sample. **b)** Forsterite grains in heavy mineral fraction of till and stream sediment samples. Black dot indicates stream sediment sample. Background bedrock geology of the Sylvia Grinnell Lake area, Baffin Island, Nunavut, modified from St-Onge et al. (1999, 2016a–d).

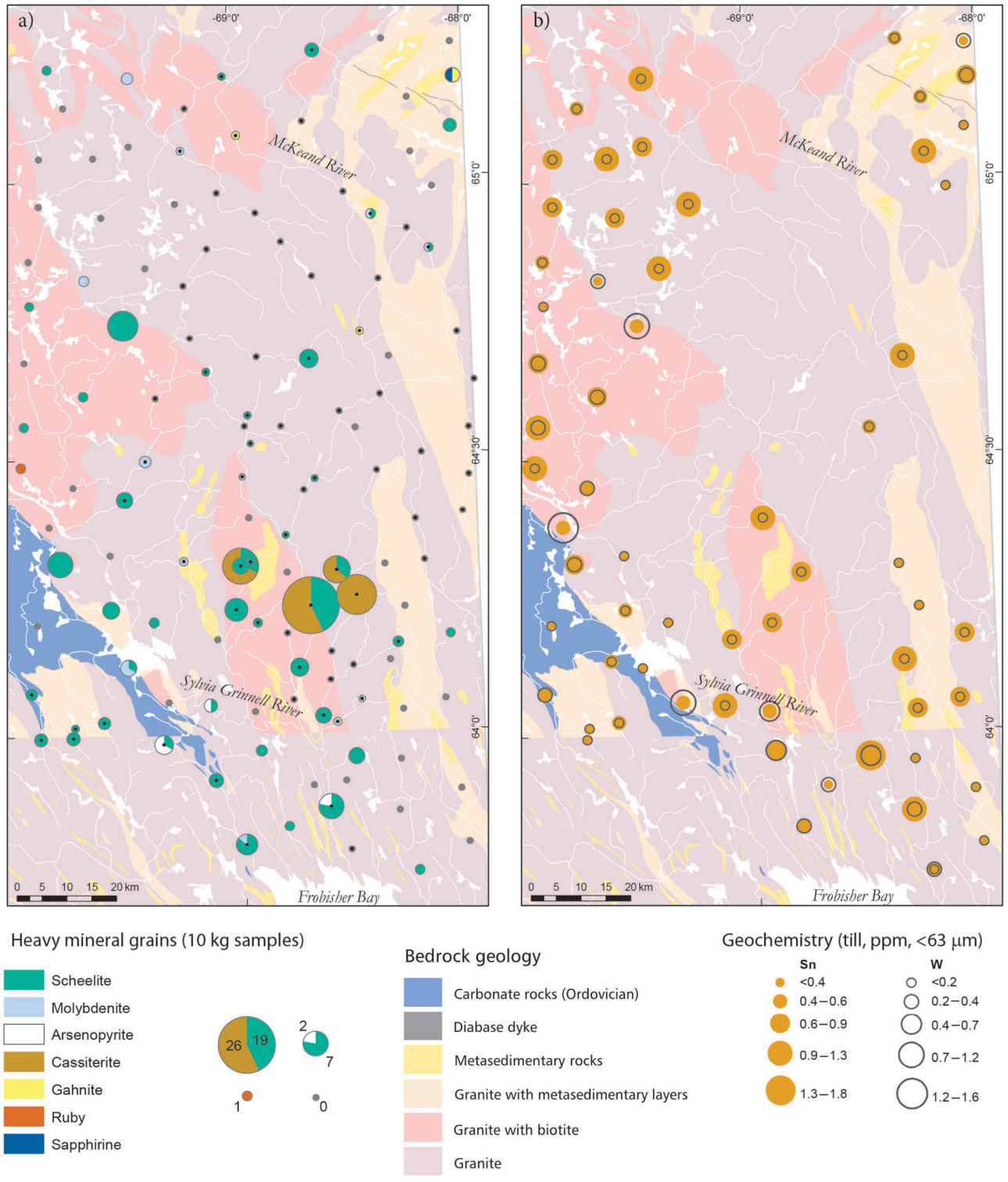

Figure 5: a) Scheelite, molybdenite, arsenopyrite, cassiterite, gahnite, ruby and sapphirine grains in the heavy mineral fraction of till and stream sediment samples. Black dot indicates stream sediment sample. **b)** Results of geochemical analysis of Sn and W in till samples, <63 µm size fraction. Background bedrock geology of the Sylvia Grinnell Lake area, Baffin Island, Nunavut, modified from St-Onge et al. (1999, 2016a–d).

Forsterite grains (n = 262) were found at 24 sites, with a maximum of 105 grains at one site (Figure 4b). Forsterite grains are widespread in the study area, and are especially common in the McKeand River stream sediment samples and in the vicinity of biotite-rich granite. The widespread distribution of forsterite on the plateau, and the absence of other KIMs, suggest that these forsterite are probably not linked with point-source, localized kimberlite rock outcrops in the study area. The origin of forsterite grains in study area is unknown, and is possibly linked with nonkimberlitic intrusive rocks.

Water characteristics

Alkalinity of stream and lake waters show a maximum of 60 ppm, and five samples exceed 20 ppm (Figure 6a). Higher values are found in the vicinity of Sylvia Grinnell River valley (often >2.7 ppm) compared with the rest of study area.

The pH values in surface waters ranged between 5.0 and 8.0, averaging 6.4, with five samples >7.5, and five samples <5.4 (Figure 6a). The highest values were measured in the vicinity of Sylvia Grinnell River valley (frequently >6.5). The values of pH and alkalinity are fairly well correlated (logarithmic regression, R^2=0.72) and apparently result from a mix of a pole of pH of 5–6.5 and alkalinity of 1 ppm, with a pole of pH of 8–8.5 and alkalinity of 60 ppm. The values of pH and alkalinity seem comparable between stream and lake water, based on a few close samples located north of Frobisher Bay. Conductivity and alkalinity are highly correlated (linear regression, R^2=0.99, see Tremblay et al., 2016). Glacial transport (see Figure 1) of carbonate material from Ordovician carbonate outcrops and possibly from minor Lake Harbour Group marble outcrops, and subsequent leaching of the carbonate material into the groundwater, can explain the distribution of relatively high alkalinity and pH water samples in the vicinity of the Sylvia Grinnell River valley. High carbonate content in till matrices and carbonate pebbles in till are found in some samples in the Sylvia Grinnell River valley (see Tremblay et al., 2016); however, it appears that the threshold of detection of carbonate content and carbonate pebbles in till is considerably higher than alkalinity and pH in water.

Total coliform in stream water results average 15 most probable number (MPN) per 100 ml, with a maximum of 80 MPN per 100 ml and a minimum of 0.5 MPN per 100 ml (Figure 6b). Values are lowest in the most elevated part of the plateaus (<8.6 MPN per 100 ml). No *E. Coli* were reported in the water samples. Generally, water microbial quality is very good in the study area.

Economic considerations

The results and interpretation of this surficial geological mapping and sampling program can be used for mineral exploration, development of natural resources and infrastructure, and as an aid to environmental geochemical studies in the study area—around Nunavut's capital city. In this region, where no important economical mineral site has historically been discovered, geochemistry and heavy minerals in surficial sediments were analyzed for different surficial sediment mineral exploration indicators. Minor mineral exploration potential exists for commodities related to felsic intrusive rocks, including W and Sn (up to 19 scheelite and 26 cassiterite grains per 10 kg were found in heavy mineral samples). Analysis of the geochemical and mineralogical data from the surficial sediment samples reveals minor or insignificant potential regional mineral prospect for diamonds, base metals (copper, nickel, zinc), molybdenum, gold (up to six grains per 10 kg were found in heavy mineral samples), other precious metals (silver, platinum, palladium), rare-earth elements and gemstones (one ruby and one sapphirine were found in heavy mineral samples). Environmental and geotechnical studies will benefit from new baseline data on till, stream silt, lake sediment and water (alkalinity, pH and coliforms). The surficial mapping will provide important baseline data for future mineral exploration and possible development in the area, as well as for infrastructure studies (permafrost conditions, granular aggregate sources).

Acknowledgments

The Sylvia Grinnell Lake area project is a collaborative undertaking between the Canada-Nunavut Geoscience Office (CNGO), the Geological Survey of Canada (Geo-mapping for Energy and Minerals program [GEM]), Nunavut Research Institute and Carleton University. Funding has been provided by the Canadian Northern Economic Development Agency (CanNor) under the Strategic Investments in Northern Economic Development program delivered through the Government of Nunavut to CNGO. Polar Continental Shelf Project is thanked for logistical support. Universal Helicopters pilots S. Sande and K. Cashin provided safe and productive flying. Logistical aspects of fieldwork were collaborated on with N. Rayner and M. St-Onge, both from the Geological Survey of Canada and associated with GEM projects. The authors wish to thank Nunavut Research Institute for access to laboratory space and dedicated collaboration with the laboratory staff (J. Peters and students G. Chiasson Poirier and A. Kilabuk). Government of Nunavut, Department of Environment, Fisheries and Sealing division are thanked for sharing summer student M. Kendall with the CNGO during summer 2015. This paper was enhanced by discussions with D. Mate (Polar Knowledge Canada), S. Zhang (CNGO), M. Lamothe (Université du Québec à Montréal), R. Paulen (GSC), L. Ham and C. Gilbert (CNGO). The authors thank M. McCurdy (GSC) for reviewing this paper.

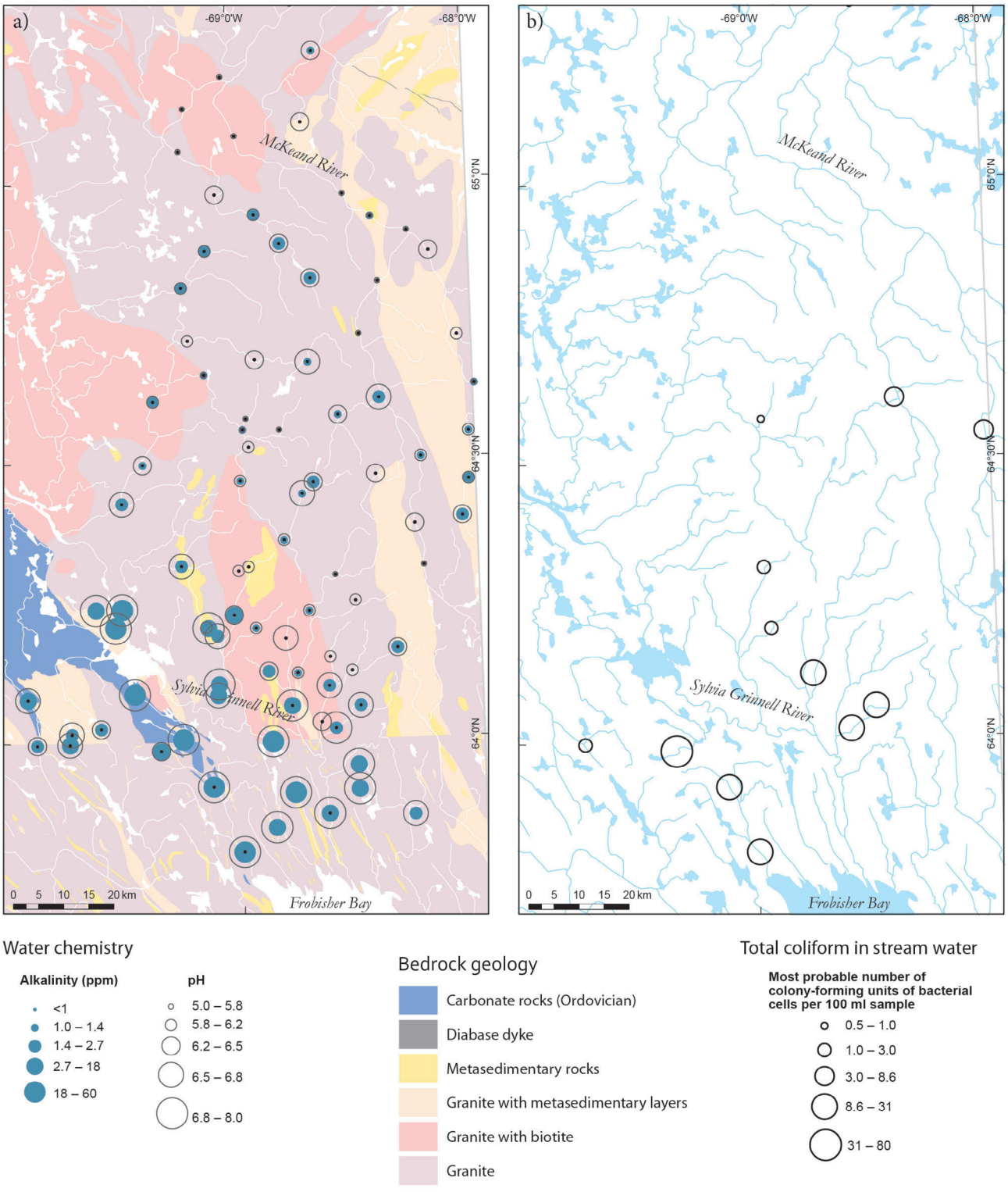

Figure 6: a) Stream and lake water geochemistry (alkalinity, $CaCO_3$ equivalent in ppm) and pH. Black dot indicates stream water sample. **b)** Total coliform in stream water (no *Escherichia coli* were detected in any of the water samples). Background bedrock geology of the Sylvia Grinnell Lake area, Baffin Island, Nunavut, modified from St-Onge et al. (1999, 2016a–d).

Natural Resources Canada, Earth Sciences Sector contribution 20160273

References

Averill, S.A. 2001: The application of heavy indicator mineralogy in mineral exploration with emphasis on base metal indicators in glaciated metamorphic and plutonic terrains; Geological Society of London, Special Publication 185, p. 69–81.

Blake, W.J., Jr. 1966: End moraines and deglaciation chronology in northern Canada with special reference to southern Baffin Island; Geological Survey of Canada, Paper 66–26, 31 p., 1 map, scale 1:2 000 000.

Friske, P.W.B. and Hornbrook, E.H.W. 1991: Canada's National Geochemical Reconnaissance programme; Applied Earth Sciences, Transactions of the Institution of Mining and Metallurgy, Section B, v. 100, p. B47–B56.

Fulton, R.J. 1995: Surficial materials of Canada / Matériaux superficiels du Canada; Geological Survey of Canada, "A" Series Map 1880A, scale 1:5 000 000.

GeoBase® 2015: GeoBase orthoimage 2005–2010; Natural Resources Canada, URL <http://geogratis.gc.ca/api/en/nrcan-rncan/ess-sst/?q=geobase+orthoimage+nunavut+spot&sort-field=relevance> [August 2015].

Girard, I., Klassen, R. and Laframboise, R. 2004: Sedimentology laboratory manual, Terrain Sciences Division; Geological Survey of Canada, Open File 4823, 134 p.

Hodgson, D.A. 2005: Quaternary geology of western Meta Incognita Peninsula and Iqaluit area, Baffin Island, Nunavut; Geological Survey of Canada, Bulletin 582, 74 p., 1 CD-ROM.

Leblanc-Dumas, J., Allard, M. and Tremblay, T. 2015: Characteristics of a preglacial or interglacial regolith preserved under nonerosive ice during the last glacial maximum in central Hall Peninsula, southern Baffin Island, Nunavut; *in* Summary of Activities 2014, Canada-Nunavut Geoscience Office, p. 69–78.

McClenaghan, M.B., Plouffe, A., McMartin, I., Campbell, J.E., Spirito, W.A., Paulen, R.C., Garrett, R.G. and Hall, G.E.M. 2013: Till sampling and geochemical analytical protocols used by the Geological Survey of Canada; Geochemistry: Exploration, Environment, Analysis, v. 13, p. 285–301.

Plouffe, A., McClenaghan, M.B., Paulen, R.C., McMartin, I., Campbell, J.E. and Spirito, W.A. 2013: Processing of unconsolidated glacial sediments for the recovery of indicator minerals: protocols used at the Geological Survey of Canada; Geochemistry: Exploration, Environment, Analysis, v. 13, p. 303–316.

Prest, V.K. 1969: Retreat of Wisconsin and recent ice in North America; Geological Survey of Canada, "A" Series Map 1257A, scale 1:5 000 000.

Prior, G.J., McCurdy, M.W. and Friske, P.W.B. 2009: Stream sediment sampling for kimberlite indicator minerals in the Western Canada Sedimentary Basin: the Buffalo Head Hills survey, north-central Alberta; *in* Application of Till and Stream Sediment Heavy Mineral and Geochemical Methods to Mineral Exploration in Western and Northern Canada, R.C. Paulen and I. McMartin (ed.), Geological Association of Canada, Short Course Notes 18, p. 111–124.

Ross, M., Johnson, C.L., Gosse, J.C., Tremblay, T., Hodder, T.J., Grunsky, E.C. and Pell, J. 2015: Detrital cosmogenic ^{10}Be of till from contrasting landscapes on Hall Peninsula, Baffin Island; Geological Society of America, Abstracts with Programs, v. 47, no. 3, p. 63.

St-Onge, M.R., Scott, D.J. and Wodicka, N. 1999: Geology, Frobisher Bay, Nunavut; Geological Survey of Canada, "A" Series Map 1979A, scale 1:100 000.

St-Onge, M.R., Weller, O.M., Dyck, B.J., Rayner, N.M., Chadwick, T. and Liikane, D. 2016a: Geology, McKeand River (north), Baffin Island, Nunavut; Geological Survey of Canada, Canadian Geoscience Map 259E (preliminary) and Canada-Nunavut Geoscience Office, Open File Map 2016-16E, scale 1:100 000.

St-Onge, M.R., Weller, O.M., Dyck, B.J., Rayner, N.M., Chadwick, T. and Liikane, D. 2016b: Geology, McKeand River (south), Baffin Island, Nunavut; Geological Survey of Canada, Canadian Geoscience Map 260E (preliminary) and Canada-Nunavut Geoscience Office, Open File Map 2016-17E, scale 1:100 000.

St-Onge, M.R., Weller, O.M., Dyck, B.J., Rayner, N.M., Chadwick, T. and Liikane, D. 2016c: Geology, Sylvia Grinnell Lake (north), Baffin Island, Nunavut; Geological Survey of Canada, Canadian Geoscience Map 253E (preliminary) and Canada-Nunavut Geoscience Office, Open File Map 2016-10E, scale 1:100 000.

St-Onge, M.R., Weller, O.M., Dyck, B.J., Rayner, N.M., Chadwick, T. and Liikane, D. 2016d: Geology, Sylvia Grinnell Lake (south), Baffin Island, Nunavut; Geological Survey of Canada, Canadian Geoscience Map 254E (preliminary) and Canada-Nunavut Geoscience Office, Open File Map 2016-11E, scale 1:100 000.

Tremblay, T. and Leblanc-Dumas, J. 2015: Geochemical, mineralogical and sedimentological data for Hall Peninsula, Nunavut; Canada-Nunavut Geoscience Office, Geoscience Data Series GDS2015-003, Microsoft® Excel® files.

Tremblay, T., Day, S., McNeil, R., Smith, K., Richardson, M. and Shirley, J. 2015: Overview of surficial geology mapping and geochemistry in the Sylvia Grinnell Lake area, Baffin Island, Nunavut; *in* Summary of Activities 2015, Canada-Nunavut Geoscience Office, p. 107–120.

Tremblay, T., Day, S., Shirley, J., Smith, K. and McNeil, R. 2016: Data tables accompanying "Geochemical, mineralogical and sedimentological results from till, stream and lake sediment and water samples in the Sylvia Grinnell Lake area, Baffin Island, Nunavut"; Canada-Nunavut Geoscience Office, Geoscience Data Series GDS2016-001, Microsoft® Excel® files, URL <http://cngo.ca/summary-of-activities/2016/>.

Utting, D.J., Little, E.C., Young, M.D., McCurdy, M.W., Dyke, A.S. and Girard, I. 2008: Till, stream-sediment and bedrock analyses, North Baffin Island, Nunavut (NTS 37E, F, G, H and 47E); Geological Survey of Canada, Open File 5742, 1 CD-ROM.

Weller, O.M., Dyck, B.J., St-Onge, M.R., Rayner, N.M. and Tschirhart, V. 2015: Completing the bedrock mapping of southern Baffin Island, Nunavut: plutonic suites and regional stratigraphy; *in* Summary of Activities 2015, Canada-Nunavut Geoscience Office, p. 33–48.

Zhang, S. 2012: Ordovician stratigraphy and petroleum potential of the Hudson Bay and Foxe basins, Nunavut; Geological Survey of Canada, Open File 7199, 25 p.

Overview of bedrock mapping in the northern and western parts of the Tehery Lake–Wager Bay area, western Hudson Bay, Nunavut

H.M. Steenkamp[1], N. Wodicka[2], O.M. Weller[2] and J. Kendrick[3]

[1]*Canada-Nunavut Geoscience Office, Iqaluit, Nunavut, holly.steenkamp@canada.ca*

[2]*Natural Resources Canada, Geological Survey of Canada, Ottawa, Ontario*

[3]*Memorial University, St. John's, Newfoundland*

This work is part of the Tehery-Wager geoscience mapping activity of Natural Resources Canada's (NRCan) Geo-mapping for Energy and Minerals (GEM) program Rae activity, a multidisciplinary and collaborative effort being led by the Geological Survey of Canada and the Canada-Nunavut Geoscience Office (CNGO), with participants from Canadian universities (Dalhousie University, Université du Québec à Montréal, Université Laval and University of New Brunswick). The focus is on targeted bedrock and surficial geology mapping, stream-water and stream- sediment sampling, and other thematic studies, which collectively will increase the level of geological knowledge in this frontier area and allow evaluation of the potential for a variety of commodities, including diamonds and other gemstones, base and precious metals, industrial minerals, carving stone and aggregates. This activity also aims to assist northerners by providing geoscience training to college students, and by ensuring that the new geoscience information is accessible for making land-use decisions in the future.

Steenkamp, H.M., Wodicka, N., Weller, O.M. and Kendrick, J. 2016: Overview of bedrock mapping in the northern and western parts of the Tehery Lake–Wager Bay area, western Hudson Bay, Nunavut; *in* Summary of Activities 2016, Canada-Nunavut Geoscience Office, p. 27–40.

Abstract

Bedrock-geology mapping was conducted in the summer of 2016 in the Tehery Lake–Wager Bay area on the northwestern coast of Hudson Bay, Nunavut, as part of a multiyear, multidisciplinary mapping campaign led by the Geological Survey of Canada, through Phase 2 of the Geo-mapping for Energy and Minerals program (GEM-2), and the Canada-Nunavut Geoscience Office. Fieldwork resulted in the identification and spatial constraint of rock units in the northern and western parts of the study area, which were sampled for geochemical, geochronological and petrographic analysis, as well as to assess their economic potential. Mapping has revealed the presence of a large granulite-facies metamorphic domain in the southern part of the study area; the possibility of two different supracrustal rock sequences; the western continuations of the Chesterfield fault zone and Wager shear zone; and generally high, but locally variable, peak metamorphic conditions across the study area. Further analytical work is required to fully characterize rock units, compare and correlate them with other well-studied units, and determine the geological history and economic potential of the Tehery Lake–Wager Bay area.

Résumé

La cartographie géologique du substratum rocheux dans la région de Tehery Lake–Wager Bay sur la côte nord-ouest de la baie d'Hudson, au Nunavut, a été menée à l'été 2016 dans le cadre d'une campagne de cartographie pluriannuelle et pluridisciplinaire dirigée par la Commission géologique du Canada (programme de géocartographie de l'énergie et des minéraux) et le Bureau géoscientifique Canada-Nunavut. Les travaux de terrain dans les parties nord et ouest de la zone d'étude ont permis l'identification et la contrainte spatiale d'unités lithologiques qui ont été échantillonnées en vue d'analyses géochimiques, géochronologiques et pétrographiques, ainsi que pour évaluer leur potentiel économique. La cartographie a révélé la présence d'un domaine métamorphique au faciès des granulites dans la partie sud de la zone d'étude, la présence possible de deux séquences différentes de roches supracrustales, le prolongement vers le nord-est de la zone de faille de Chesterfield et vers l'ouest de la zone de cisaillement de Wager et des conditions de pic métamorphique généralement élevées mais localement variables dans la zone d'étude. Des travaux analytiques supplémentaires sont nécessaires pour mieux caractériser les unités lithologiques, les comparer et les corréler avec d'autres lithologies bien connues et déterminer l'histoire géologique et le potentiel économique de la région de Tehery Lake–Wager Bay.

This publication is also available, free of charge, as colour digital files in Adobe Acrobat® PDF format from the Canada-Nunavut Geoscience Office website: http://cngo.ca/summary-of-activities/2016/.

Introduction

The Tehery Lake–Wager Bay area, located on the northwestern coast of Hudson Bay (Figure 1), is known to host kimberlite intrusions (Pell and Strickland, 2004), anomalous base- and precious-metal concentrations in till and stream sediments (Jefferson et al., 1991; Day et al., 2013; McMartin et al., 2013), major shear zones (Henderson and Broome, 1990; Panagapko et al., 2003) and significant belts of supracrustal rocks, and yet the region is characterized by limited and outdated geoscience information. A multiyear activity being conducted by the Canada-Nunavut Geoscience Office and the Geological Survey of Canada through the second phase of the Geo-mapping for Energy and Minerals (GEM) program aims to fill in these fundamental geoscience-knowledge gaps (e.g., Lawley et al., 2015; Steenkamp et al., 2015; Wodicka et al., 2015, 2016; this study). The new geoscience information gathered through this activity will specifically support 1) the creation of modern bedrock and surficial-geology maps (1:100 000 Canada Geoscience Maps) for all or parts of eight National Topographic System map areas (NTS 46E, D, 56A, B, C, F, G, H); 2) the establishment of the geological history for the area through identifying, characterizing and analyzing individual rock units and their spatial, temporal and structural relationships (see also Tschirhart et al., 2016); 3) the refinement of glacial and postglacial histories, and re-evaluations of the dispersal and weathering of surficial deposits in the area (see also Byatt et al., 2015; McMartin et al., 2015, 2016; Randour et al., 2016); and 4) the identification of locations and rock units that may have potential for economic materials, such as base and precious metals, gemstones, carving stone, industrial minerals and aggregates.

This paper summarizes the initial bedrock-geology findings from the 2016 field season. Presented here are a simplified bedrock-geology map of the entire study area (Figure 2); lithological, structural and metamorphic descriptions based on field observations of the dominant rock units mapped in the northern and western parts of the study area; and a discussion of the implications of this new mapping and the potential for economic resources in this area.

Regional geological background

Bedrock geology in the Tehery Lake–Wager Bay area was initially mapped at reconnaissance scale (1:1 000 000) by the Geological Survey of Canada (GSC) in the 1950s (Wright, 1955, 1967; Lord and Wright, 1967) and 1960s (Heywood, 1967a, b). The study area comprises Archean to Proterozoic orthogneiss, paragneiss and plutonic rocks belonging to the Rae Province. This region is located north of the Snowbird Tectonic Zone, a significant geophysical lineament that separates the composite Rae-Chesterfield and Hearne cratonic blocks, and records Neoarchean and Paleoproterozoic tectonic events (e.g., Hanmer et al., 1995; Berman, 2007; Martel et al., 2008), the latter of which being a component in the initial assembly of Laurentia at 2.0–1.7 Ga (Hoffman, 1988).

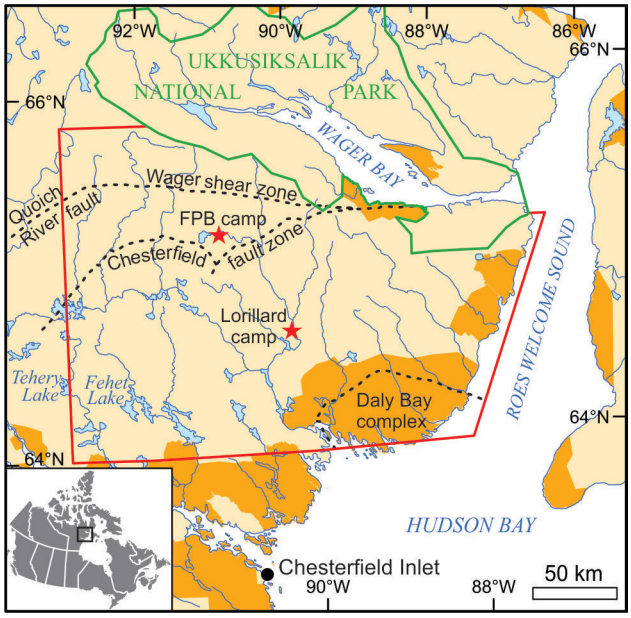

Figure 1: Tehery Lake–Wager Bay study area (outlined in red), northwestern Hudson Bay, in relation to Ukkusiksalik National Park (outlined in green) and Inuit-owned lands (orange polygons). Red stars indicate the locations of the 2016 FPB camp and 2015 Lorillard camp.

The northern part of the study area includes the Wager shear zone, a major, dominantly dextral, strike-slip fault that coincides with a prominent aeromagnetic anomaly extending westward from Wager Bay (Broome, 1990; Henderson and Broome, 1990). Parts of the shear zone were previously mapped along Wager Bay prior to establishment of the Ukkusiksalik National Park (Henderson et al., 1991; Jefferson et al., 1991), and the most recent deformation along the shear zone was dated at <1808 ±2 Ma (Henderson and Roddick, 1990). The Chesterfield fault zone is another significant structure in the northern part of the study area that was previously defined based on a cuspate, folded aeromagnetic anomaly (Panagapko et al., 2003). It is thought to separate amphibolite-facies rocks to the north from amphibolite- to granulite-facies rocks to the south (Schau, 1983).

Panels of supracrustal rocks exist north of the Chesterfield fault zone, and south of, within and north of the Wager shear zone (Henderson et al., 1991; Jefferson et al., 1991; Panagapko et al., 2003). The structural relationships of these panels with respect to the basement orthogneiss, their depositional age and their lithostratigraphic correlations with other known and described supracrustal rock packages in the Rae Province have yet to be determined. The northern part of the study area also hosts three kimberlite

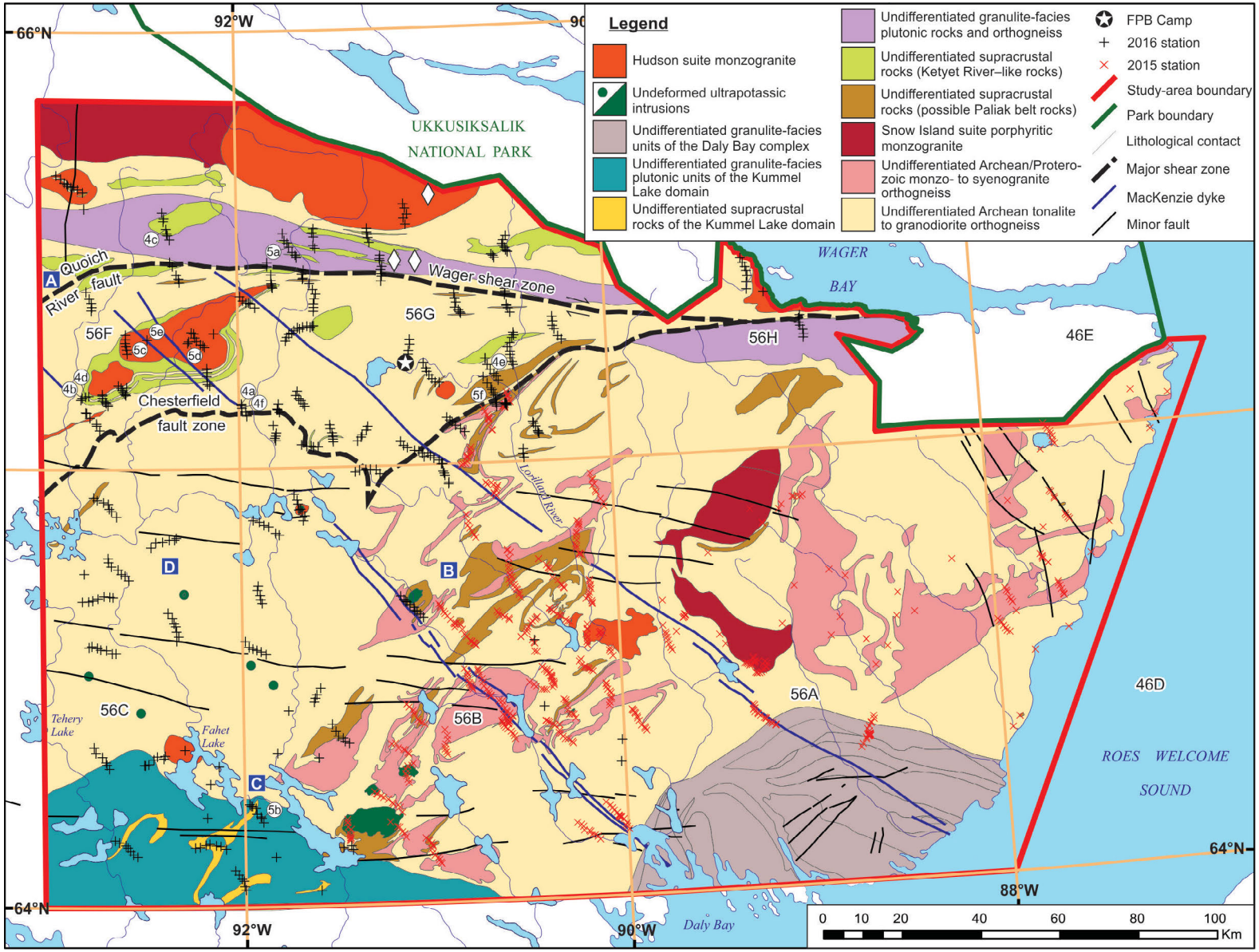

Figure 2: Preliminary bedrock geology of the Tehery Lake–Wager Bay area (after Wodicka et al., 2016), based on observations from the 2015 and 2016 field seasons and aeromagnetic-survey data (see Figure 3). White star in black circle is the location of FPB camp; white diamonds indicate known kimberlite localities; labels in white circles are the locations of photos in Figures 4 and 5; and blue squares are the locations of U-Pb zircon crystallization ages in van Breemen et al. (2007), where A is 2707 ±8 Ma, B is 2701 ±14 Ma, C is 2699 ±11 Ma and D is 2584 ±12 Ma.

occurrences (Figure 2, white diamonds) within the Nanuq property currently held by Peregrine Diamonds Ltd., which were discovered largely through till and stream-sediment sampling, and a high-resolution aeromagnetic survey over the property (Pell and Strickland, 2004).

The west-central part of the study area was previously mapped as mainly undifferentiated Archean orthogneiss (Heywood, 1967a, b; Lord and Wright, 1967). Several small, circular aeromagnetic anomalies in this area were targeted during reconnaissance mapping in 2012 as part of the Geomapping Frontiers' project, conducted within the first GEM program. Most anomalies were identified as ultramafic plugs (Figure 2), likely correlative with Proterozoic ultrapotassic rocks of the Christopher Island formation (Peterson et al., 2002).

The southwestern corner of the study area is just north of the Uvauk complex, which comprises granulite-facies anorthosite–gabbro intrusive rocks (Mills et al., 2007) similar to the Daly Bay complex to the east (Gordon and Heywood, 1987; Gordon, 1988; Hanmer and Williams, 2001) and the Kramanituar complex to the west (Sanborn-Barrie et al., 2001). These complexes, which occur along an east-west trend on the northern side of Chesterfield Inlet, record high-pressure granulite-facies metamorphism and deformation at ca. 1.9 Ga that is likely related to the collision of the Hearne and Rae cratons along the Snowbird Tectonic Zone, but they also contain evidence of Archean tectonic events (Sanborn-Barrie et al., 2001; Mills et al., 2007).

Field observations

Helicopter-supported fieldwork took place between June 27 and July 29, and was based out of FPB camp (Figure 2), a temporary camp built adjacent to the Nanuq property of Peregrine Diamonds Ltd. on the upper Lorillard River. Bedrock-geology mapping, which focused on the northern and western parts of the study area, consisted of daily set-outs of 3–4 teams that traversed 2–12 km routes. Targeted helicopter stops were also planned at sites with anomalous aeromagnetic signatures, with interesting rocks based on archival information, or where few bedrock outcrops are exposed amongst the surficial till. Bedrock samples, structural measurements, digital photographs, and textural and mineralogical observations were collected at a total of 463 stations. The main features of map units present in the northern and western parts of the study area are described in the following subsections.

Archean basement rocks

Much of the northern and western parts of the study area is underlain by biotite±hornblende±titanite±epidote granodiorite to tonalite gneiss (Figure 2, tan map unit) that includes pods, lenses or discontinuous layers of diorite, gabbro, pyroxenite and mafic rocks representing volcanic rocks and/or dykes (e.g., Lawley et al., 2015; Steenkamp et al., 2015). The gneiss is mostly medium grained and displays a moderately to strongly developed compositional layering. It typically contains millimetre- to centimetre-scale biotite±hornblende granitic veins that are transposed parallel to the gneissic fabric (Figure 4a). In general, these rocks resemble much of what exists in the eastern and central parts of the study area (Steenkamp et al., 2015; Wodicka et al., 2015), although more pervasive migmatitic textures are present south of the Chesterfield fault zone.

Rocks with compositions ranging closer to monzogranite or monzonite are also present in the northern and western parts of the study area. In the northwest corner of the area, although outcrop is limited owing to intense glacial weathering and frost heave associated with the Keewatin Ice Divide (e.g., McMartin et al., 2016), deformed K-feldspar–phyric monzogranite may correlate with ca. 2.6 Ga Snow Island suite plutonic rocks found in the east-central part of the area (Steenkamp et al., 2015; Wodicka et al., 2015). However, the poor exposure and complex aeromagnetic signatures (i.e., northern part of NTS 56C; Figure 3) over much of the area make it difficult to separate the monzogranite to monzonite rocks into map units distinct from the widely abundant granodiorite to tonalite gneiss.

Three samples of granodiorite to tonalite gneiss from within the study area were described and dated at ca. 2.7 Ga, and a foliated biotite monzonite at ca. 2.58 Ga (Figure 2), by van Breemen et al. (2007). However, the variability in composition and textures in the orthogneissic rocks suggest that there may be other older and/or younger plutonic phases in the study area than what has already been dated.

Supracrustal rocks

The majority of supracrustal rocks mapped during the 2016 field season are north of the Chesterfield fault zone. At least two different supracrustal sequences are proposed, based on differences in lithological assemblages, degree of partial melting and aeromagnetic signatures. One sequence is characterized by distinct, relative magnetic-low features between the Chesterfield fault zone and Wager shear zone, and north of the Wager shear zone (Figure 2, green map unit; Figure 3; see also Tschirhart et al., 2016), and contains thick units of siliceous metasedimentary rocks. The sequence includes sillimanite±muscovite quartzite interlayered with biotite±garnet±sillimanite psammite, semipelite and minor pelite, with discrete biotite±garnet mafic layers of probable volcanic origin, all of which are locally injected with 2–15 cm thick monzogranitic veins that are oblique or parallel to layering. The white-weathering quartzite (Figure 4b) is typically found at the base of the sequence and is up to 400 m thick, but also occurs as 1–15 m thick layers intercalated with the other metasedimentary rocks. Interlayered psammite, semipelite and pelite vary in thickness and abundance. Sillimanite mats define a mineral foliation, and

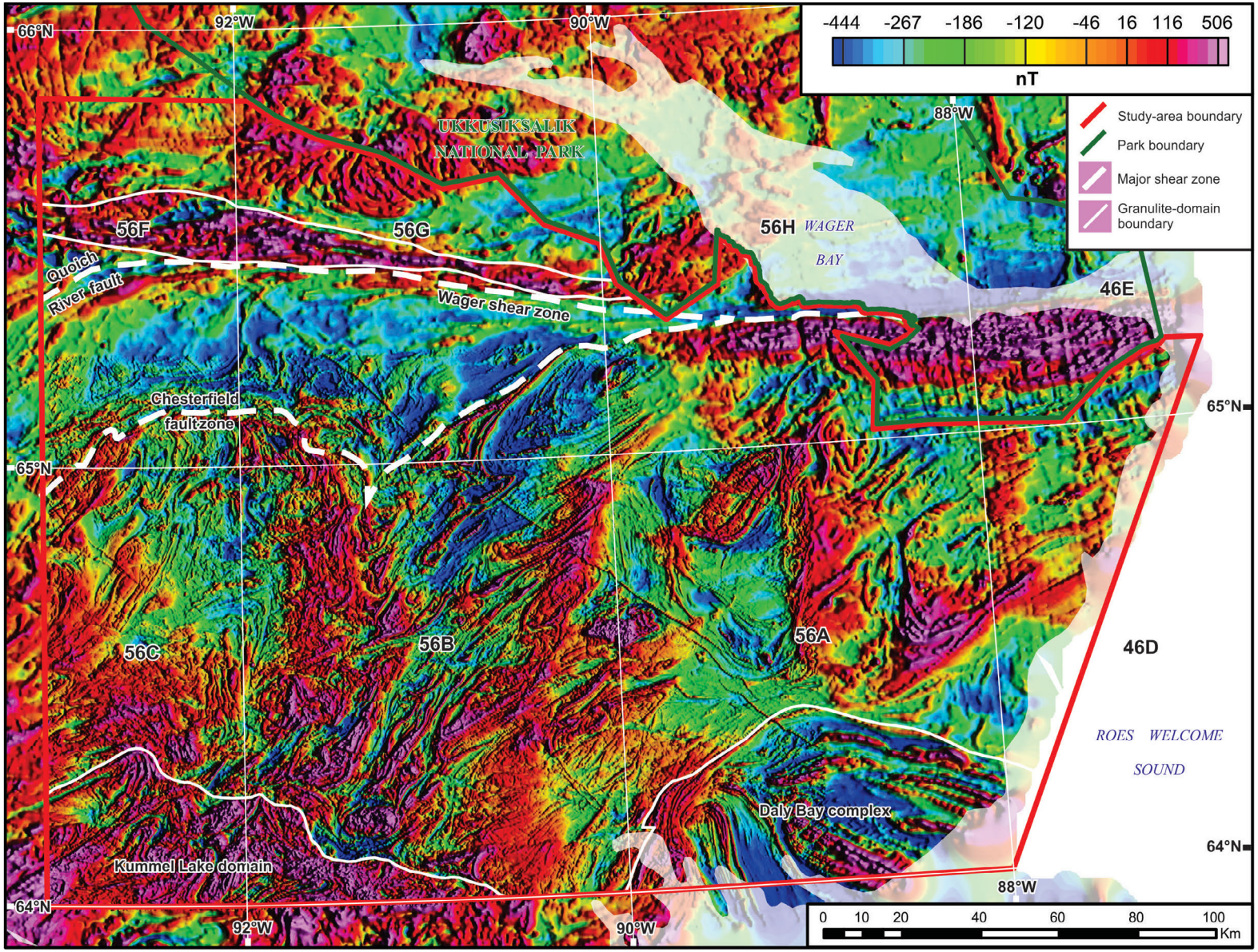

Figure 3: Total-field aeromagnetic anomaly map of the Tehery Lake–Wager Bay area (after Tschirhart et al., 2016), northwestern Hudson Bay, Nunavut, compiled from surveys flown at 800 and 400 m line spacings (Coyle and Kiss, 2012; Natural Resources Canada 2015).

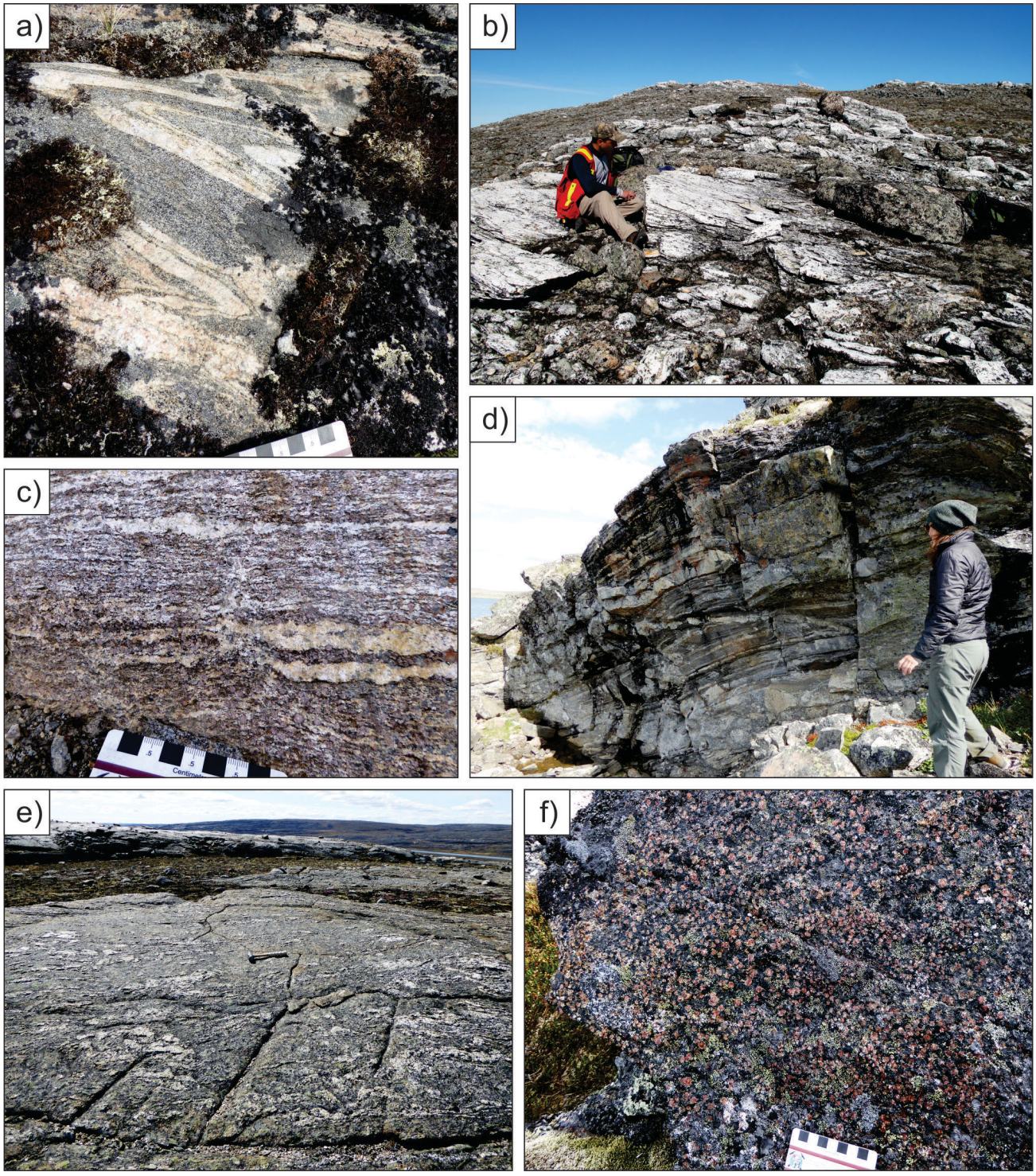

Figure 4: Field photographs of rocks in the Tehery Lake–Wager Bay area: **a)** grey, biotite-bearing granodiorite with injections of white monzogranite that have been transposed parallel to foliation and folded; **b)** thick section of white-weathering, sillimanite+muscovite quartzite in the southwestern nose of a large fold structure in the northwestern part of the study area (NTS area 56F); **c)** leucosome layers and biotite define a foliation in garnet+biotite+sillimanite pelite north of the Wager shear zone; **d)** well-layered mafic rocks of probable volcanic origin in the nose of the large fold structure in the northwestern part of the study area; **e)** migmatitic texture in biotite+sillimanite+leucosome±garnet semipelite mapped within one of the brown supracrustal panels north of the Chesterfield fault zone (hammer for scale is 40 cm long); **f)** red garnet porphyroblasts in a massive mafic rock that surrounds a large ultramafic body located just south of the Chesterfield fault zone.

individual crystals define a lineation parallel to the hinges of large-scale folds. Where present, garnet porphyroblasts are 2–10 mm in diameter and wrapped by biotite and sillimanite (also where present), which define the foliation in these rocks (Figure 4c). The mafic volcanic rocks, which appear to be limited to one or two discrete layers up to 25 m thick (Figure 4d), contain aligned biotite and hornblende, and thin (2–10 mm) quartz-rich layers that together define a well-developed foliation.

The other supracrustal sequence was mapped as discontinuous panels north of the Chesterfield fault (Figure 2, brown map unit). Rocks in this sequence have mostly low magnetic signatures with discrete high bands (Figure 3) and contain more varied rock types that resemble the majority of the supracrustal rocks in the central and eastern parts of the study area (Steenkamp et al., 2015; Wodicka et al., 2015, 2016). Rock types include biotite±garnet psammite–semipelite, garnet+biotite±sillimanite±cordierite pelite, iron formation, garnet-bearing mafic rocks and ultramafic rocks in pods and boudins. The psammite–semipelite is highly recrystallized, with granular, coarse plagioclase and quartz grains, aligned biotite that defines a mineral foliation, and garnet porphyroblasts that are typically <5 mm in diameter. It also contains up to 15 vol. % granitic leucosome present as lenses and discontinuous layers (Figure 4e). Minor pelite is typically associated with the more mafic rocks and contains abundant leucosome layers that define a foliation. The pelite contains garnet porphyroblasts up to 2 cm in diameter, aligned biotite and sillimanite that define a mineral foliation, and local idioblastic cordierite in leucosome layers. The iron formation layers are up to 2 m thick and made up of thinly laminated magnetite and quartz bands with rare coarse-grained garnet and grunerite. The mafic rocks are relatively massive, with garnet porphyroblasts up to 1 cm in diameter (Figure 4f) that are typically rimmed by plagioclase. The mafic rocks are generally associated with ultramafic rocks, including large pods and boudins of pyroxenite or peridotite. These rocks are relatively rare compared with the other units described in this sequence; however, they are very prominent, as they weather positively and have a dark brown to golden brown weathered surface. One peridotite locality north of the Chesterfield fault zone at the western edge of NTS area 56G contains orthopyroxene up to 4 cm long, clinopyroxene, olivine, magnetite and garnet.

Granulite-facies domains

Distinct domains containing granulite-facies plutonic, gneissic and minor supracrustal rocks were mapped in both the northernmost and southernmost parts of the study area, and are associated with strong magnetic-high signatures (Figure 3). In the northern domain, granulite-grade metamorphism is interpreted based on the local presence of orthopyroxene in granodioritic orthogneiss, as well as increased leucosome volumes and migmatitic textures in otherwise typical orthogneiss and supracrustal rocks. These rocks are cut by relatively undeformed, medium- to coarse-grained, monzodiorite to monzogranite plutonic rocks (Figure 2; purple map unit) that contain about 5% biotite, 1% magnetite and rare amphibole, and have distinctive grey, translucent plagioclase grains with white, opaque rims (Figure 5a).

In the southern granulite-facies domain, referred to as the Kummel Lake domain (Wodicka et al., 2016; Figure 2, teal and yellow map units), most orthogneiss and supracrustal rocks have a pervasive, waxy, greenish-brown hue, typical of granulite-facies rocks. Granodioritic to monzogranitic orthogneiss contains the assemblage biotite±hornblende± orthopyroxene±magnetite (Figure 5b). A few metagabbro localities were documented, including a coarse-grained cumulate gabbro and a leucogabbro. Supracrustal rocks (Figure 2; yellow map unit), including minor garnet+clinopyroxene mafic rocks and garnet+biotite pelite, are characterized by magnetic-low anomalies (Figure 3) and are lithologically similar to those present to the south of the Chesterfield fault zone (brown map unit described above; see also Steenkamp et al., 2015; Wodicka et al., 2015, 2016). An undeformed, biotite+magnetite±amphibole monzodiorite to monzogranite plutonic phase, similar to that observed in the northern granulite zone, has also been injected through much of this area, cutting the regional fabrics.

Paleoproterozoic monzogranite and ultrapotassic intrusions

Several large plutonic bodies of mostly undeformed, coarse-grained, biotite±magnetite monzogranite (Figure 2, orange map unit; Figure 5c) were mapped in the northern part of the study area, and one smaller body was identified north of the Kummel Lake granulite domain. The plutons generally have a weak foliation around their margins, defined by aligned biotite, and contain xenoliths of orthogneiss, K-feldspar–phyric monzogranite and quartzite. A large magnetic anomaly north of the Wager shear zone (Figures 2 and 3; NTS area 56G) is also associated with similar biotite+magnetite monzogranite. The core of the plutonic body is undeformed and contains K-feldspar megacrysts up to 3 cm in size. The edge of the pluton has a finer grain size and shows some foliation development defined by aligned biotite grains and deformed feldspar crystals.

Coarse-grained to pegmatitic syenogranite dykes and sill complexes intrude much of the study area, cutting most other rock units and deformational fabrics. These dykes and sills are associated with minor magnetic anomalies in areas dominated by Archean granodiorite to tonalite rocks, and form topographic highs owing to their competent nature. It is believed that these late dykes and sills, and the large plutonic bodies, belong to the 1845–1795 Ma Hudson

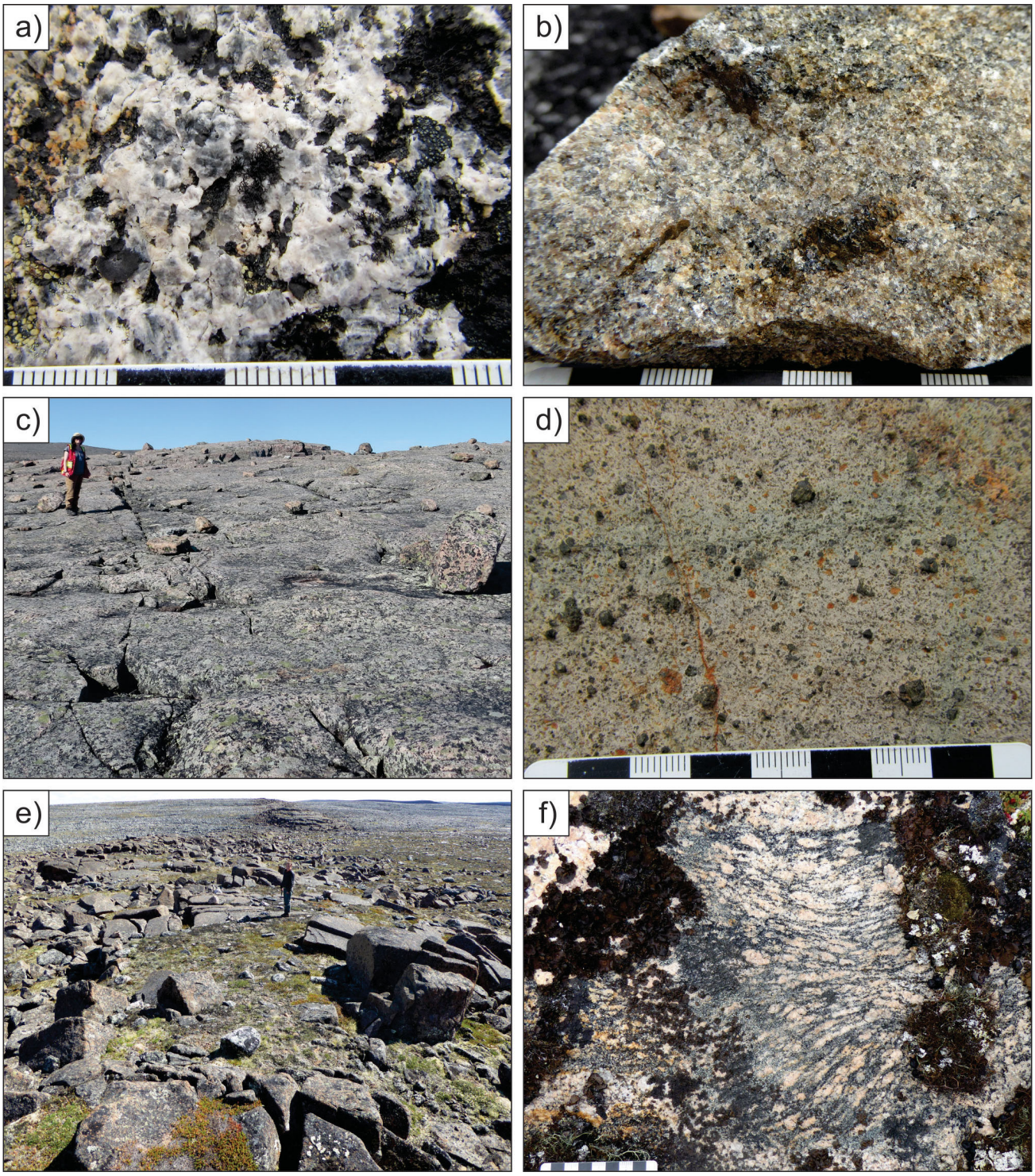

Figure 5: Field photographs of rocks in the Tehery Lake–Wager Bay area: **a)** white-weathering biotite±hornblende monzodiorite spatially associated with the Wager shear zone; plagioclase has grey cores and white rims; **b)** large, brown orthopyroxene grain in granodiorite gneiss found along the Wager shear zone near Wager Bay; **c)** homogeneous, undeformed biotite monzogranite north of the Chesterfield fault zone; **d)** weathered surface of lamprophyre, showing olivine and pyroxene phenocrysts; **e)** blocky, brown-weathering, southeast-trending diabasic dyke cutting through Archean basement orthogneiss in the northwestern corner of the study area (looking southeast); **f)** deformed K-feldspar porphyroclasts in monzogranite consistently found along the northern side of the Chesterfield fault zone.

plutonic suite (Peterson et al., 2002; van Breemen et al., 2005).

Scattered localities with ultrapotassic rocks (Figure 2, dark green unit), including biotite+clinopyroxene syenite, phlogopite clinopyroxenite and biotite+clinopyroxene+olivine lamprophyre (Figure 5d), were documented south of the Wager shear zone and Chesterfield fault zone. These rocks generally correspond to small, circular magnetic-high anomalies, appearing to be plug or stock intrusions. In some places, the ultrapotassic rocks are spatially associated with Hudson plutonic rocks and similarly cut through the older orthogneiss and supracrustal rocks, suggesting that they may be contemporaneous with the emplacement of the Hudson suite.

Mafic dyke swarms

A series of diabasic dykes (Figure 2, thick blue lines) is evident in the aeromagnetic-survey data as continuous, southeast-trending magnetic-high anomalies (Figure 3). They cut all rock types and structural elements, with the exception of relatively younger brittle faults. The dykes are up to 50 m wide, weather dark brown and fracture to form a distinctive blocky pattern (Figure 5e). They typically have a porphyritic texture, with medium-grained, white-weathering plagioclase phenocrysts set in a dark, fine-grained matrix. Based on their orientation, composition, textures and field relationships, these dykes are likely associated with the ca. 1267 Ma MacKenzie dyke swarm (LeCheminant and Heaman, 1989). In the west-central and southwestern parts of the study area, a second set of diabasic dykes trends roughly east-west. These dykes range in thickness from 10 cm to 1.5 m but do not have associated aeromagnetic anomalies, possibly because the aeromagnetic-survey lines were also oriented east-west, effectively hiding the dykes' signatures, or they are simply too thin to resolve, given the scale of the survey.

Regional structure, metamorphism and deformation

The state of strain, orientation of regional fabrics and grade of metamorphism vary considerably across the northern and western parts of the study area. In the west-central part of the area, south of the Chesterfield fault zone, the main foliation (S_m) in the Archean orthogneissic rocks strikes northeast or southwest and dips 25–65°, with mineral and stretching lineations that plunge primarily to the northeast at shallow angles. The foliation is axial planar to dominantly northeast-trending macroscopic folds and is defined mainly by the alignment of biotite±hornblende. The presence of migmatitic textures but continued stability of biotite and absence of orthopyroxene indicate that upper amphibolite–facies conditions prevailed during this deformation event. Evidence for an earlier deformation event comes from the local preservation (e.g., in the hinge zones of major folds) of a foliation oriented at a high angle to the dominant S_m foliation.

The S_m fabrics in the Kummel Lake domain strike northeast or southwest but generally dip more steeply (50–80°) to the southeast or northwest than in the orthogneissic rocks outside the domain. Also, macroscopic northeast-trending folds in the Kummel Lake domain are much better defined than in the neighbouring rocks to the north (Figure 3). As noted in the previous section, the Kummel Lake domain preserves the greatest evidence for granulite-facies peak metamorphism, where orthogneiss contains coarse-grained orthopyroxene, foggy blue quartz and plagioclase with a waxy greenish-brown hue. Pelitic to semipelitic supracrustal rocks, containing the assemblage garnet+biotite±sillimanite, also display a waxy greenish-brown hue and have 10–30 cm wide layers of granitic leucosome that were likely produced through biotite-dehydration reactions. Fine-grained biotite and garnet porphyroblasts up to 5 mm in diameter are concentrated in folded melanosome that defines the S_m fabric. These features suggest that the main deformation fabric and granulite-facies conditions in the Kummel Lake domain were concomitant. Locally, garnet and orthopyroxene porphyroblasts are individually rimmed by biotite, indicating minor retrogression.

The Chesterfield fault zone is characterized by strongly deformed to mylonitic rocks (Figure 5f) that preserve both dextral and sinistral shear-sense indicators. Foliations within and adjacent to the fault zone dip mainly at steep angles to the north-northwest; however, there is a zone approximately 1 km wide where fabrics dip moderately to steeply to the south-southeast. The highly strained rocks contain well-developed stretching lineations that plunge shallowly to the east-northeast or west. Fabrics in the gneissic rocks to the north and south appear to be reoriented close to the fault zone, but the fault zone itself is folded, as suggested by its curved form (Figures 2, 3). Supracrustal rocks along the fault zone generally preserve amphibolite-facies peak mineral assemblages, such as biotite+garnet+sillimanite±leucosome±muscovite in pelite and garnet+hornblende±clinopyroxene in mafic rocks. Evidence of retrogression includes biotite and plagioclase rims on garnet porphyroblasts in pelitic and mafic rocks, respectively, indicative of lower to moderate amphibolite–facies conditions. These retrograde textures are more abundant in rocks along the western part of the Chesterfield fault, while rocks along the eastern part of the fault typically show no or minimal retrogression.

Between the Chesterfield fault zone and Wager shear zone, the foliation fabrics in plutonic and supracrustal rocks vary widely due, in large part, to two phases of folding: an early phase of northeast-trending folds and a later phase of upright, northwest- and southeast-trending folds (Figures 2, 3). These macroscopic folds are broadly similar in orien-

tation and scale to those documented in the southeastern part of the study area (Wodicka et al., 2015). However, as the Wager shear zone is approached from the south, all fabrics are reoriented parallel to this major structure (see also Henderson and Broome, 1990). Pelitic rocks between the two fault zones contain metamorphic mineral assemblages ranging from muscovite+sillimanite+biotite+garnet to biotite+garnet+sillimanite+leucosome. Similarly, mafic rocks within this area contain either biotite+hornblende or a higher grade peak assemblage of clinopyroxene+garnet+hornblende. This could indicate that peak metamorphic conditions varied throughout this area from lower-amphibolite to upper-amphibolite facies, or that the two supracrustal packages preserve distinct mineral assemblages and thus metamorphic histories. In mafic rocks, garnet porphyroblasts are partially to fully pseudomorphed to plagioclase+biotite±hornblende, indicating decompression to lower amphibolite–facies conditions.

Most planar fabrics along the Wager shear zone strike easterly or westerly and have moderate to steep dips (55–85°), whereas linear features are primarily subhorizontal. Highly strained to mylonitized orthogneiss within the shear zone is locally deformed by broad to isoclinal folds, causing reorientation of lineations. Plutonic rocks within and adjacent to the Wager shear zone contain either biotite±hornblende± epidote assemblages or granulite-facies assemblages, as outlined in the previous section. Discontinuous panels of supracrustal rocks contain garnet+biotite+sillimanite+leucosome in pelite. Garnet porphyroblasts show some recrystallization of biotite and plagioclase at their rims that defines strain shadows. These features suggest a complex interplay between deformation and metamorphism along the shear zone.

Discussion and future work

Targeted bedrock mapping and thematic scientific research in the Tehery Lake–Wager Bay study area has led to redefinition and definition of previously known and unknown rock units, respectively. First, the southwestern part of the study area, characterized by the Kummel Lake granulite domain (Figure 2, teal and yellow map units), is thought to be only a part of a much larger, high-pressure, granulite-facies metamorphosed area that would include the Daly Bay, Uvauk and Kramanituar complexes (Gordon, 1988; Hanmer and Williams, 2001; Sanborn-Barrie et al., 2001; Mills et al., 2007). Geochronology and petrography are required to define the timing of protolith formation and the timing, duration and conditions of peak and retrograde metamorphism within the Kummel Lake domain, which in turn will be compared with interpreted histories from the better studied, high-pressure, granulite-grade mafic–anorthosite complexes.

Second, mapping suggests the presence of two distinct supracrustal sequences across the study area: the supracrustal packages either contain an assortment of rock types (pelite, psammite, quartzite, mafic and ultramafic rocks, iron formation, calcsilicate and/or carbonate rocks; Figure 2, brown map unit) or are dominated by siliceous rocks (quartzite, psammite, semipelite, pelite) with minor mafic rocks (Figure 2, green map unit). The latter, silica-dominated supracrustal sequence is tentatively interpreted as correlative with the lower succession of the Paleoproterozoic Ketyet River group documented north of Baker Lake, Nunavut (Rainbird et al., 2010), as previously suggested by Panagapko et al. (2003) and Ferderber et al. (2013). The former, more lithologically varied supracrustal package is similar to the description of the Paliak belt that was mapped near Wager Bay (Jefferson et al., 1991). In both cases, the supracrustal rock sequences in the Tehery Lake–Wager Bay area require detrital geochronology and geochemistry to fingerprint the rock units and enable their comparison with other, better studied sequences outside the study area.

Third, the Chesterfield fault zone, previously defined based on aeromagnetic-anomaly data and metamorphic contrasts, is now better delineated on the basis of the distribution of highly deformed to mylonitic rocks. While most fabrics measured near the Chesterfield fault zone dip to the north, a 1 km wide zone contains south-dipping fabrics. This provides field evidence that is consistent with Spratt et al. (2014), who interpreted a south-dipping fault based on magnetotelluric data, and recent geophysical data collected by Tschirhart et al. (2016). The deformed rocks record at least two major deformational events: one that created the porphyroclastic and lineated textures, and a second that folded and reoriented these fabrics. In-depth structural analysis, petrography and geochronology will be undertaken to fully understand the relative timing and structural relationships of the contrasting fabrics and porphyroclastic textures along and adjacent to the Chesterfield fault zone.

Fourth, mapping has established that the Wager shear zone continues far inland from Wager Bay, as suspected from aeromagnetic-survey data. Similar to the Chesterfield fault zone, rocks within the Wager shear zone appear to record at least two phases of deformation: a high-strain phase that created the mylonitic fabrics and strong lineations, and a second phase that broadly folded and reoriented those structures. It is unclear whether these phases of deformation are related to separate events or were created through progressive deformation during a single event. Additionally, the Wager shear zone has been intruded by younger, dominantly undeformed monzodiorite to diorite, which has obliterated large parts of the shear zone. In the westernmost part of the study area, the shear zone may continue to the southwest to become the Quoich River fault (Figures 2, 3; Schau, 1983; Panagapko et al., 2003), or extend to the

northwest outside the study area toward the Amer mylonite zone (e.g., Broome, 1990). Many samples were collected for geochronology and petrography to constrain the timing, duration and kinematics of deformational events within the Wager shear zone.

Finally, peak metamorphic assemblages are variable across the study area. Detailed petrography and thermodynamic modelling of metamorphic mineral assemblages in pelitic and mafic supracrustal rocks are underway to 1) test whether the two proposed supracrustal sequences record different metamorphic histories, and 2) determine whether the major fault zones are responsible for the juxtaposition of rocks with distinct metamorphic grades.

Economic considerations

Supracrustal panels in the Tehery Lake–Wager Bay area contain rock types that have potential for economic mineralization. For example, gossanous layers were found associated with garnet amphibolite and semipelite in the Ketyet River–like supracrustal rocks, whereas iron formation and ultramafic rocks are concentrated in the supracrustal package that has more variable lithological assemblages. One particular panel of the latter supracrustal package is adjacent to where till and stream-sediment samples containing anomalous concentrations of Au, Cu, Bi and Ag were discovered in 2012 (Day et al., 2013; McMartin et al., 2013). Rock, till and stream-sediment samples were collected from all localities with economic potential to analyze for base and precious-metal concentrations (this study; McMartin et al., 2016).

The Archean basement has previously been explored for its kimberlite potential in the northern part of the study area (Pell and Strickland, 2004). Given the vast expanses of similar Archean crust elsewhere within the study area, there remains potential for existence of other kimberlite occurrences.

Acknowledgments

The authors wish to acknowledge the other field party members who worked tirelessly to complete this mapping project: É. Girard, S. Day, I. McMartin, V. Tschirhart, B. Garrison, L. Lebeau, A. Lion, R. Bayne, I. Randour and M. Roy. Thanks go to D. Guilfoyle for extraordinary meals, T. Evviuk and A. Alooq for monitoring wildlife and maintaining camp infrastructure, D. Willis of Peregrine Diamonds Ltd. for support and co-operation regarding camp logistics, and Discovery Mining Services for building and removing the camp infrastructure. The Polar Continental Shelf Project co-ordinated rotary- and fixed-wing aircraft support (Project 059-16). The authors gratefully acknowledge pilot and engineer E. Polzin and the rest of Prairie Helicopters for providing a safe and enjoyable daily commute in the field, as well as Ookpik Aviation, S.K. Construction and the Baker Lake Lodge for their professional logistics support, expediting and hospitality, respectively.

This project is funded by the Geological Survey of Canada's Geo-mapping for Energy and Minerals program and the Canadian Northern Economic Development Agency's Strategic Investments in Northern Economic Development program. D. Wright, D. Desnoyers, L. Ham, R. Khoun and R. Murphy are thanked for their management and administrative support. K. Clarke assisted with community engagement in Baker Lake, and R. Buenviaje provided pre-field GIS support. This paper benefited from a thorough and thoughtful review by C. Guilmette.

Natural Resources Canada, Earth Science Sector contribution 20160222

References

Berman, R.G., Davis, W.J. and Pehrsson, S. 2007: Collisional Snowbird tectonic zone resurrected: growth of Laurentia during the 1.9 accretionary phase of the Hudsonian orogeny; Geology, v. 35, no. 10, p. 911–914.

Broome, H.J. 1990: Generation and interpretation of geophysical images with examples from the Rae Province, northwestern Canada Shield; Geophysics, v. 55, p. 977–997.

Byatt, J., LaRocque, A., Leblon, B., McMartin, I. and Harris, J. 2015: Mapping of surficial materials south of Wager Bay, southern Nunavut, using RADARSAT-2 C-band dual-polarized and Landsat 8 images, a digital elevation model and slope data: preliminary map and summary of fieldwork; *in* Summary of Activities 2015, Canada-Nunavut Geoscience Office, p. 135–144.

Coyle, M. and Kiss, F. 2012: Residual total magnetic field, aeromagnetic survey of the Tehery Lake area, Nunavut; Geological Survey of Canada, Open Files 7203–7206.

Day, S.J.A., Wodicka, N. and McMartin, I. 2013: Preliminary geochemical, mineralogical and indicator mineral data for heavy mineral concentrates and waters, Lorillard River area, Nunavut (parts of NTS 056 A, B and G); Geological Survey of Canada, Open File 7428, 11 p. doi:10.4095/293113

Ferderber, J., Kellett, D.A., and Wodicka, N. 2013: Exploring the Tehery region: correlating supracrustal sequences using detrital zircon geochronology, Rae Craton, Nunavut; Geological Survey of Canada, Open File 7424. doi:10.4095/292709

Gordon, T.M. 1988: Precambrian geology of the Daly Bay area, District of Keewatin; Geological Survey of Canada, Memoir 422, 21 p.

Hanmer, S. and Williams, M.L. 2001: Targeted fieldwork in the Daly Bay Complex, Hudson Bay, Nunavut; Geological Survey of Canada, Current Research 2001-C15, 24 p. doi:10.4095/212095

Hanmer, S., Williams, M. and Kopf, C. 1995: Striding-Athabasca mylonite zone: implications for the Archean and early Proterozoic tectonics of the western Canadian Shield; Canadian Journal of Earth Sciences, v. 32, p. 178–196.

Henderson, J.R. and Broome, J. 1990: Geometry and kinematics of Wager shear zone interpreted from structural fabrics and magnetic data; Canadian Journal of Earth Sciences, v. 27, p. 590–604.

Henderson, J.R. and Roddick, J.C. 1990: U-Pb age constraint on the Wager shear zone, District of Keewatin, N.W.T.; *in* Radiogenic Age and Isotopic Studies: Report 3, Geological Survey of Canada, Paper 89-2, p. 149–152.

Henderson, J.R., Jefferson, C.W., Henderson, M.N., Coe, K. and Derome, I. 1991: Geology of the region around Wager Bay, District of Keewatin (parts of 46E and 56H); Geological Survey of Canada, Open File 2383, 2 maps at 1:100 000 scale.

Heywood, W.W. 1967a: Geological notes northeastern District of Keewatin and southern Melville Peninsula, District of Franklin, Northwest Territories (parts of 46, 47, 56, 57); Geological Survey of Canada, Paper 66-40, 20 p.

Heywood, W.W. 1967b: Geology of northeastern District of Keewatin and southern Melville Peninsula, Districts of Franklin and Keewatin; Geological Survey of Canada, Open File 1, scale 1:506 880. doi:10.4095/100310

Hoffman, P.F. 1988: United plates of America, birth of a craton – Early Proterozoic assembly and growth of Laurentia; Annual Review of Earth and Planetary Sciences, v. 16, p. 543–603.

Jefferson, C.W., Smith, J.E.M. and Hamilton, S.M. 1991: Preliminary account of the resource assessment study of proposed national park, Wager Bay–Southampton Island areas, District of Keewatin; Geological Survey of Canada, Open File 2351, 47 p. doi:10.4095/131509

Lawley, C.J.M., Steenkamp, H.M. and Wodicka, N. 2015: Portable X-ray fluorescence geochemical results from the Tehery Lake–Wager Bay area, western Hudson Bay, Nunavut; Canada-Nunavut Geoscience Office, Geoscience Data Series 2015-011, Microsoft® Excel® file, URL <http://cngo.ca/cngo-gds/2015-011/>.

LeCheminant, A.N. and Heaman, L.M. 1989: Mackenzie igneous events, Canada: Middle Proterozoic hotspot magmatism associated with ocean opening; Earth and Planetary Science Letters, v. 96, p. 38–48. doi:10.1016/0012-821X(89)90122-2

Lord, C.S. and Wright, G.M. 1967: Geology, southeastern Barren Grounds, District of Keewatin–District of Mackenzie; Geological Survey of Canada, Map 1216A, scale 1:1 000 000. doi:10.4095/108854

Martel, E., van Breemen, O., Berman, R.G. and Pehrsson, S. 2008: Geochronology and tectonometamorphic history of the Snowbird Lake area, Northwest Territories, Canada: new insights into the architecture and significance of the Snowbird tectonic zone; Precambrian Research, v. 161, no. 3–4, p. 201–230.

McMartin, I., Byatt, J., Randour, I. and Day, S.J.A. 2015: Report of 2015 activities for regional surficial mapping, till and stream sediment sampling in the Tehery-Wager GEM 2 Rae Project area; Geological Survey of Canada, Open File 7966, 14 p. doi:10.4095/297440

McMartin, I., Day, S.J.A., Randour, I., Roy, M., Byatt, J., LaRocque, A. and Leblon, B. 2016. Report of 2016 activities for surficial mapping and sampling surveys in the Tehery-Wager GEM-2 Rae Project area; Geological Survey of Canada, Open File 8134, 13 p. doi:10.4095/2993385

McMartin, I., Wodicka, N., Bazor, D. and Boyd, B. 2013: Till composition across the Rae craton south of Wager Bay, Nunavut: results from the Geo-Mapping Frontiers' Tehery–Cape Dobbs project; Geological Survey of Canada, Open File 7417, 31 p. doi:10.4095/293307

Mills, A.J., Berman, R.G., Davis, W.J., Tella, S., Carr, S., Roddick, C. and Hanmer, S. 2007: Thermobarometry and geochronology of the Uvauk complex, a polymetamorphic Neoarchean and Paleoproterozoic segment of the Snowbird tectonic zone, Nunavut, Canada; Canadian Journal of Earth Sciences, v. 44, p. 245-266. doi:10.1139/E06-080

Natural Resources Canada 2015: Canadian aeromagnetic database; Natural Resources Canada, Earth Sciences Sector, Geoscience Data Repository, URL <http://gdr.agg.nrcan.gc.ca/gdrdap/dap/search-eng.php> [April 2015].

Panagapko, D.A., Pehrsson, S., Pilkington, M. and Currie, M. 2003: Geoscience data compilation: Tehery Lake–Wager Bay area, Nunavut (NTS 56 B, C, F, and G), Part 1 – base data themes; Geological Survey of Canada, Open File 1809. doi:10.4095/214767

Pell, J.A. and Strickland, D. 2004: Assessment report on indicator mineral sampling on the Nanuq property, Kivalliq Region, Nunavut, Dunsmuir Ventures Ltd.; Indigenous and Northern Affairs Canada, Assessment Report 084756, 89 p.

Peterson, T.D., van Breemen, O., Sandeman, H. and Cousens, B. 2002: Proterozoic (1.85–1.75 Ga) igneous suites of the western Churchill Province: granitoid and ultrapotassic magmatism in a reworked Archean hinterland; Precambrian Research, v. 119, p. 73–100.

Randour, I., McMartin, I. and Roy, M. 2016: Study of the postglacial marine limit between Wager Bay and Chesterfield Inlet, western Hudson Bay, Nunavut; *in* Summary of Activities 2016, Canada-Nunavut Geoscience Office, p. 51–60.

Sanborn-Barrie, M., Carr, S.D. and Theriault, R. 2001: Geochronological constraints on metamorphism, magmatism and exhumation of deep-crustal rocks of the Kramanituar Complex, with implications for the Paleoproterozoic evolution of the Archean western Churchill Province, Canada; Contributions to Mineralogy and Petrology, v. 141, p. 592–612.

Schau, M. 1983: Geology, Baker Lake, District of Keewatin, map and notes; Geological Survey of Canada, Open File 883, scale 1:250 000.

Spratt, J.E., Skulski, T., Craven, J.A., Jones, A.G., Snyder, D.B. and Kiyan, D. 2014: Magnetotelluric investigations of the lithosphere beneath the central Rae craton, mainland Nunavut, Canada; Journal of Geophysical Research – Solid Earth, v. 119, p. 2415–2439. doi:10.1002/2013JB010221

Steenkamp, H.M., Wodicka, N., Lawley, C.J.M., Peterson, T.D. and Guilmette, C. 2015: Overview of bedrock mapping and results from portable X-ray fluorescence spectrometry in the eastern part of the Tehery Lake–Wager Bay area, western Hudson Bay, Nunavut; *in* Summary of Activities 2015, Canada-Nunavut Geoscience Office, p. 121–134.

Tschirhart, V.L., Wodicka, N. and Steenkamp, H.M. 2016: Shallow crustal structure of the Tehery Lake–Wager Bay area, western Hudson Bay, Nunavut, from potential-field datasets; *in* Summary of Activities 2016, Canada-Nunavut Geoscience Office, p. 41–50.

van Breemen, O., Pehrsson, S. and Peterson, T.D. 2007: Reconnaissance U-Pb SHRIMP geochronology and Sm-Nd isotope analysis from the Tehery-Wager Bay gneiss domain, western Churchill Province, Nunavut; Geological Survey of Canada, Current Research 2007-F2, 15 p.

van Breemen, O., Peterson, T.D. and Sandeman, H.A. 2005: U-Pb zircon geochronology and Nd isotope geochemistry of Proterozoic granitoids in the western Churchill Province: intrusive age pattern and Archean source domains; Canadian Journal of Earth Science, v. 42, p. 339–377.

Wodicka, N., Steenkamp, H.M., Lawley, C.J.M., Peterson, T.D., Guilmette, C., Girard, É. and Buenviaje, R. 2015: Report of activities for the bedrock geology and economic potential of the Tehery-Wager area: GEM-2 Rae Project; Geological Survey of Canada, Open File 7970, 14 p.

Wodicka, N., Steenkamp, H.M., Weller, O.M., Kendrick, J., Tschirhart, V.L., Peterson, T.D. and Girard, É. 2016: Report of 2016 activities for the bedrock geology and economic potential of the Tehery-Wager area: GEM 2 Rae Project; Geological Survey of Canada, Open File 8149, 21 p. doi:10.4095/299392

Wright, G.M. 1955: Geological notes on central District of Keewatin, Northwest Territories; Geological Survey of Canada, Paper 55-17, 21 p.

Wright, G.M. 1967: Geology of the southeastern Barren Grounds, parts of Mackenzie and Keewatin, Operations Keewatin, Baker, Thelon; Geological Survey of Canada, Memoir 350, 91 p.

Shallow crustal structure of the Tehery Lake–Wager Bay area, western Hudson Bay, Nunavut, from potential-field datasets

V.L. Tschirhart[1], N. Wodicka[2] and H.M. Steenkamp[3]

[1]*Natural Resources Canada, Geological Survey of Canada, Ottawa, Ontario, victoria.tschirhart@canada.ca*

[2]*Natural Resources Canada, Geological Survey of Canada, Ottawa, Ontario*

[3]*Canada-Nunavut Geoscience Office, Iqaluit, Nunavut*

This work is part of the Tehery-Wager geoscience mapping activity of Natural Resources Canada's (NRCan) Geo-mapping for Energy and Minerals (GEM) program Rae activity, a multidisciplinary and collaborative effort being led by the Geological Survey of Canada and the Canada-Nunavut Geoscience Office (CNGO), with participants from Canadian universities (Dalhousie University, Université du Québec à Montréal, Université Laval and University of New Brunswick). The focus is on targeted bedrock and surficial geology mapping, stream-water and stream- sediment sampling, and other thematic studies, which collectively will increase the level of geological knowledge in this frontier area and allow evaluation of the potential for a variety of commodities, including diamonds and other gemstones, base and precious metals, industrial minerals, carving stone and aggregates. This activity also aims to assist northerners by providing geoscience training to college students, and by ensuring that the new geoscience information is accessible for making land-use decisions in the future.

Tschirhart, V.L., Wodicka, N. and Steenkamp, H.M. 2016: Shallow crustal structure of the Tehery Lake–Wager Bay area, western Hudson Bay, Nunavut, from potential-field datasets; *in* Summary of Activities 2016, Canada-Nunavut Geoscience Office, p. 41–50.

Abstract

The Tehery-Wager geoscience mapping activity is a multiyear initiative conducted by the Geological Survey of Canada (GSC) and Canada-Nunavut Geoscience Office (CNGO) under the second phase of the Geo-Mapping for Energy and Minerals (GEM-2) program. The second of two field seasons included two ground gravity transects that complement the existing aeromagnetic coverage by providing information on the subsurface geology, and highlight the structure and geometry of the Wager shear zone (WSZ) and Chesterfield fault zone (CFZ). Preliminary processing of gravity data reveals discontinuities in the observed gravity field correlative with these major structures and mapped lithological units. On both gravity transects, the CFZ corresponds to a prominent gravity low and magnetic textural discontinuities. Contrasting potential-field signatures associated with two distinct supracrustal assemblages offer additional insight for remote discrimination. Associations between gravity and magnetic anomalies, physical rock properties and mineral occurrences have the potential to constrain the regional distribution of economically significant horizons.

Résumé

Les travaux de cartographie géoscientifique Tehery–Wager sont une initiative pluriannelle menée conjointement par la Commission géologique du Canada et le Bureau géoscientifique Canada-Nunavut dans le cadre du second volet du programme de géocartographie de l'énergie et des minéraux. Au cours de la deuxième des deux campagnes de terrain prévues, deux transects de levé gravimétrique au sol ont été réalisés; ils viennent s'ajouter à la couverture aéromagnétique déjà disponible et fournissent des renseignements au sujet de la géologie de subsurface, tout en mettant en évidence la structure et les relations géométriques de la zone de cisaillement de Wager et la zone de faille de Chesterfield. Le traitement préliminaire des données du champ gravimétrique observé révèle la présence de discontinuités qui correspondent à ces structures importantes et aux unités lithologiques cartographiées. L'examen des deux transects gravimétriques a permis d'établir que la zone de cisaillement correspond à un creux gravimétrique visible ainsi qu'à des discontinuités texturales liées à des anomalies magnétiques. L'identification de signatures du champ potentiel contrastantes liées à deux assemblages supracrustaux différents fournit d'autres indications venant en aide à la discrimination des structures à distance. L'établissement de liens entre la pesanteur et les anomalies magnétiques, les propriétés physiques des roches et les venues minérales peuvent aider à circonscrire à l'échelle régionale la répartition des horizons d'importance économique.

This publication is also available, free of charge, as colour digital files in Adobe Acrobat® PDF format from the Canada-Nunavut Geoscience Office website: http://cngo.ca/summary-of-activities/2016/.

Introduction

Following reconnaissance work in 2012 to evaluate the potential for future mapping campaigns, the Tehery Lake–Wager Bay area was chosen for investigation during the second phase of the Geo-Mapping for Energy and Minerals (GEM-2 Rae project). The current mapping activity is part of a multiyear initiative involving the Geological Survey of Canada (GSC) and the Canada-Nunavut Geoscience Office (CNGO) to increase the level of geoscience knowledge in the area (e.g., McMartin et al., 2015, 2016; Steenkamp et al., 2015, 2016; Wodicka et al., 2015, 2016). To support the bedrock mapping and compilation efforts, two high-resolution ground gravity transects were conducted within the study area in conjunction with geological mapping and rock sampling. Gravity is easily measured in the field and can be used as a proxy to identify density contrasts in the underlying rocks, whereby an increase in the density of the underlying rock results in an increase in the observed gravity. In this manner, these data provide a noninvasive means of investigating the subsurface distribution of rock packages and allow the interpreter to define shallow crustal structures by modelling gravity signatures.

The purpose of this paper is to describe the acquisition, processing, analysis and preliminary interpretations of gravity data newly collected across two profiles transecting major crustal structures in the Tehery Lake–Wager Bay area. The study area is located in the Kivalliq Region of Nunavut, covering all or parts of eight National Topographic System (NTS) 1:250 000 scale map areas (46D, E, 56A, B, C, D, F, G, H; Figure 1). Helicopter-supported gravity transects were acquired in July 2016 out of the FPB camp. Each day, 8–11 km long segments of the two gravity transects were flown, along which geological observations and samples for rock-property measurements were collected. Future analysis to characterize the density of selected lithological units is planned and will constrain the forward geophysical modelling in conjunction with magnetic-susceptibility datasets.

Regional background

The Tehery Lake–Wager Bay study area (Figure 1) is located in the south-central Rae craton and is underlain predominantly by Archean tonalite to granodiorite orthogneiss (Steenkamp et al., 2015, 2016; Wodicka et al., 2015, 2016). Panels of folded Archean and/or Paleoproterozoic supracrustal rocks overlie the Archean gneissic basement. At least two main packages of supracrustal rocks are recognized in the study area (Figure 1): Paliak-like rocks and Ketyet River–like rocks. Supracrustal panels containing variable proportions of quartzite, psammite, semipelitic to pelitic gneiss, garnetite, iron formation, amphibolite, mafic gneiss, calcsilicate, rare marble and ultramafic bodies may correlate with the Paliak belt, exposed along the western shore of Wager Bay (Jefferson et al., 1991). Supracrustal panels characterized by thick quartzite units interlayered with psammite, semipelite, pelite and amphibolite share many similarities with the Paleoproterozoic Ketyet River group (Rainbird et al., 2010; Steenkamp et al., 2016; Wodicka et al., 2016). Together these rocks were reworked during the Trans-Hudson orogeny (ca. 1.86 Ga; van Breemen et al., 2007) and intruded by 1.83 Ga Hudson suite monzogranite plutons and contemporaneous ultrapotassic intrusions of the Martell syenite.

The northern part of the study area includes the Wager shear zone (WSZ), a 2–5 km wide dextral mylonite zone that parallels the southern shore of Wager Bay (Figure 1; Henderson and Broome, 1990; Panagapko et al., 2003; Steenkamp et al., 2016; Wodicka et al., 2016). The WSZ is associated with linear 200–800 nT magnetic anomalies (Figure 2A) and a collocated regional gravity lineament (Figure 2B), both of which extend more than 100 km to the west toward the Amer mylonite zone (AMZ; Broome, 1990). Broome (1990) attributed the positive magnetic anomaly of the WSZ to abundant magnetite concentrations, possibly formed during granulite-grade metamorphism, with superimposed local variations in magnetite concentrations. The linear gravity anomaly may be due to dense granulite-facies rocks at depth (Broome, 1990). The 1–3 km wide Chesterfield fault zone (CFZ), also located in the northern part of the study area, is interpreted by Panagapko et al. (2003) as the northeastern extension of a major shear zone that separates the Ketyet River group from higher grade gneiss to the south. Subtle magnetic textural contrasts are associated with the CFZ (Figure 2A); however, the regional gravity resolution (Figure 2B) does not permit discrimination of the fault zone.

Geophysical-data collection

During the 2016 field season, ground gravity measurements were taken at 235 stations along two transects in the Tehery Lake–Wager Bay map area (Figures 2A, B). Profile 1 is approximately 62 km long, oriented north-northwest–south-southeast, and profile 2 is 16 km long, oriented north–south. Profile 1 transects the WSZ and CFZ, whereas profile 2 transects only the CFZ.

Gravity at each station was measured with a Scintrex CG-5 AutoGrav™ meter and stations were spaced 300–400 m apart. A local base at FPB camp was tied to base station 93212011 in Baker Lake, Nunavut, and the FPB base was used for daily loop closure. The vertical and horizontal locations of each station were calculated by differential GPS using a Hemisphere S320™ GPS. The GPS data were postprocessed using the Canadian Spatial Reference System Precise Point Positioning (CSRS-PPP) online application. For the most part, preliminary processing results have an elevation accuracy of better than 15 cm. Several errone-

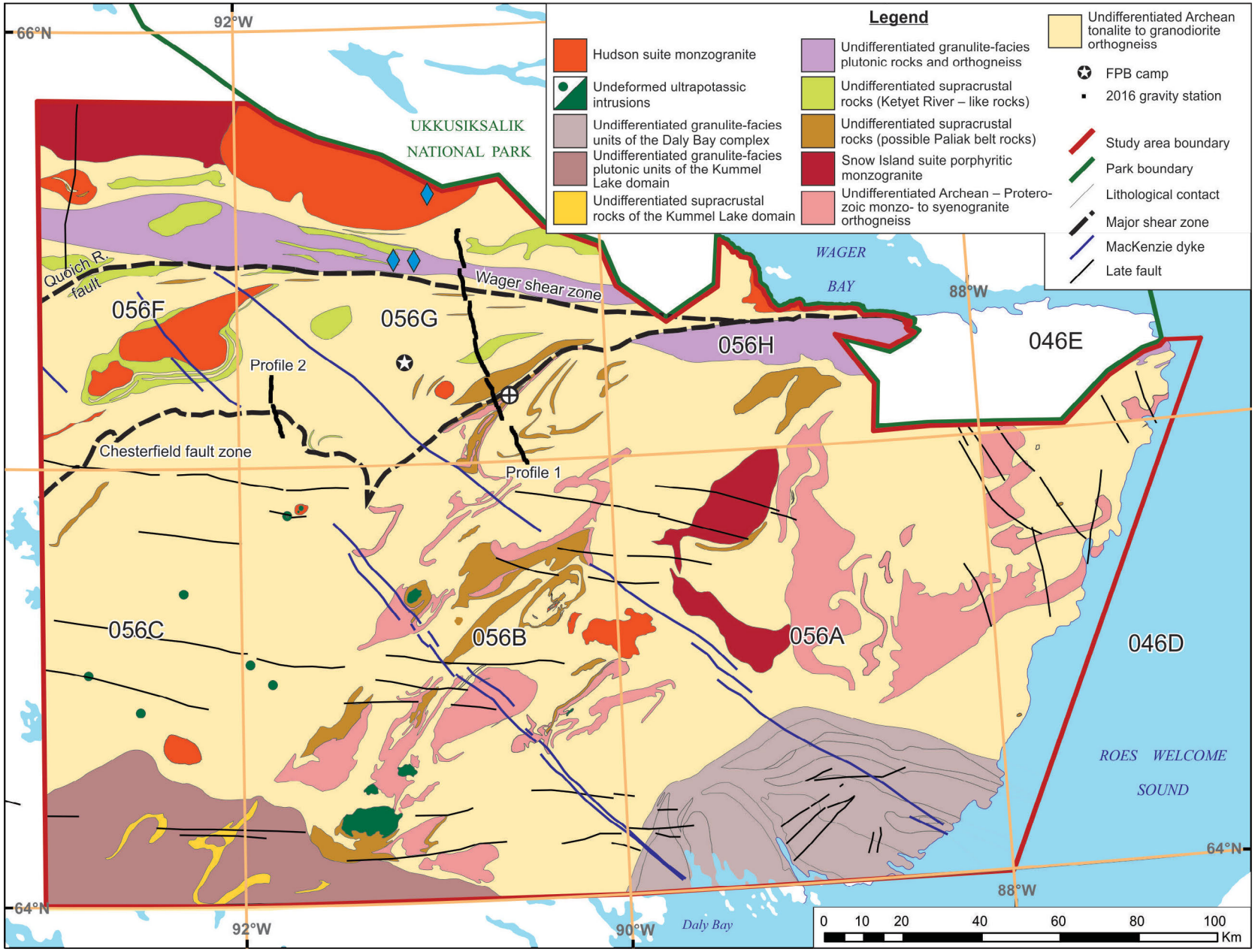

Figure 1: Simplified geology of the Tehery Lake–Wager Bay area, Nunavut (from Wodicka et al., 2016).

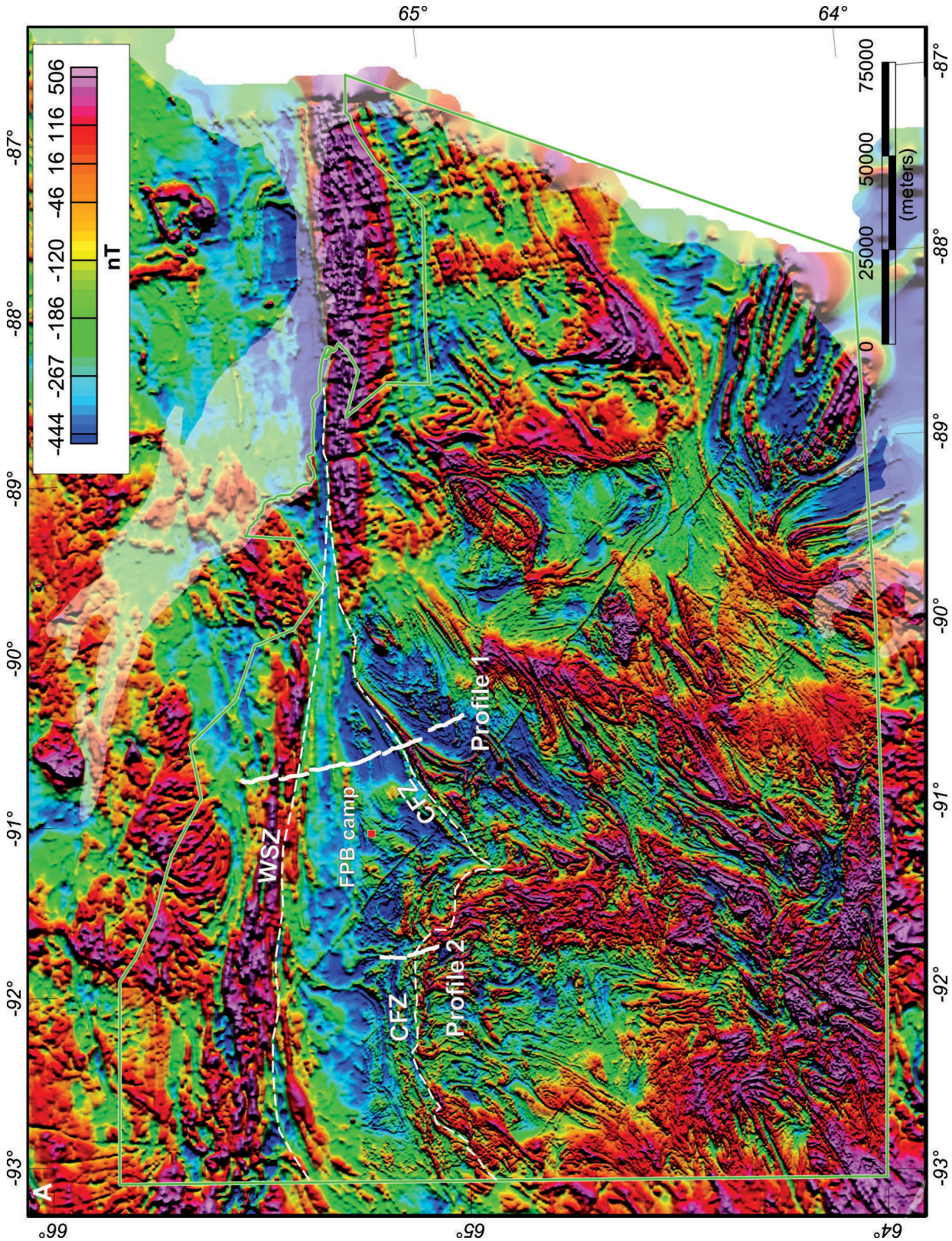
65°
64°
-87°
-88°
-89°
-90°
-91°
-92°
-93°
nT
506
116
16
-46
-120
-186
-267
-444
0
25000
50000
75000
(meters)
WSZ
FPB camp
CFZ
Profile 1
Profile 2
A
66°
65°
64°

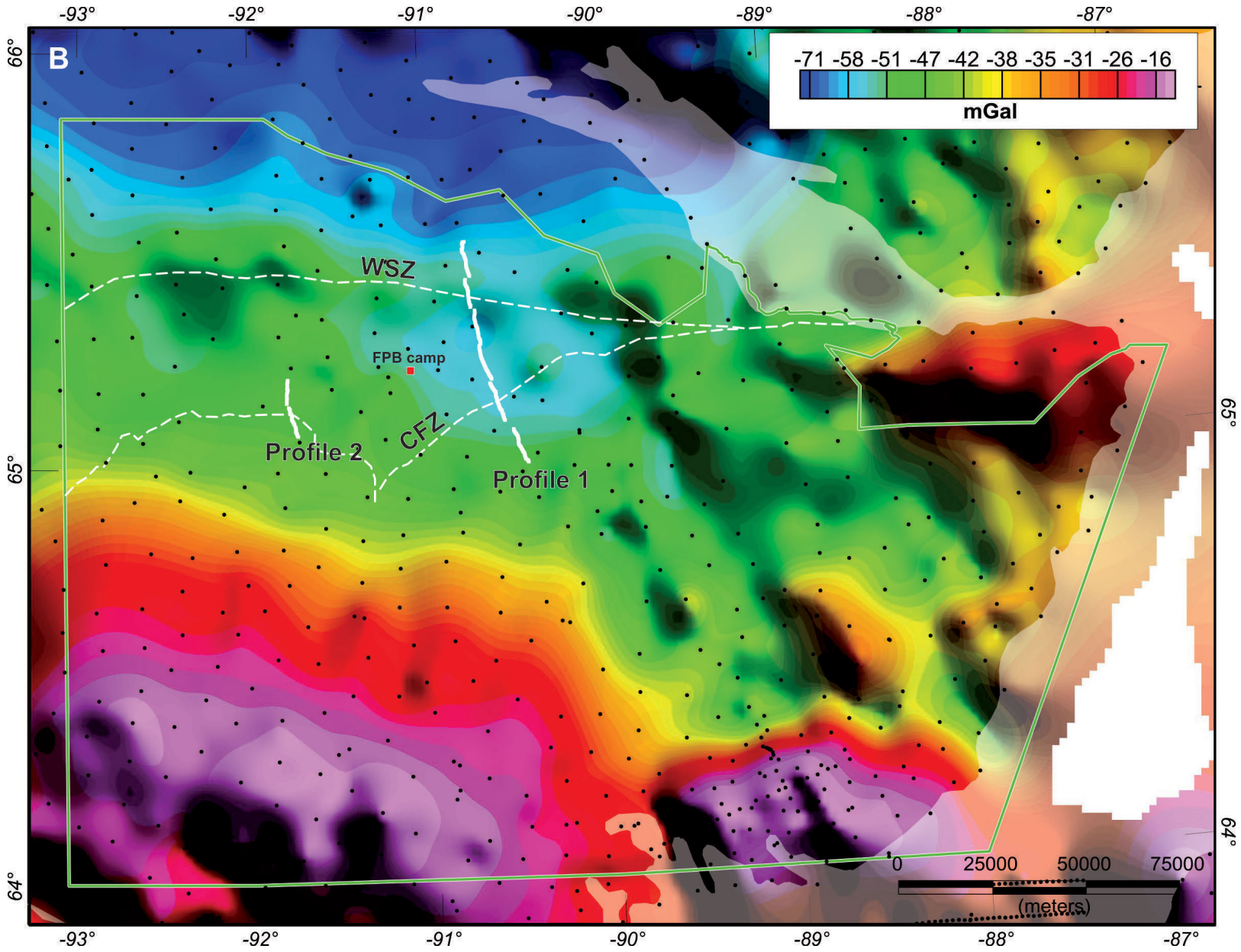

Figure 2: Regional potential-field data for the Tehery Lake–Wager Bay map area: **A)** merged residual total magnetic field; **B)** Bouguer gravity; black dots mark regional gravity stations. Thick white lines denote 2016 gravity transects, green line outlines the study area and dashed white lines denote fault zones.

ous elevation estimates (0.20–0.40 m) impact profile 2; however, they are expected to be resolved through differential postprocessing required for advanced forward modelling. The absolute ground gravity data were further corrected for latitude, instrument drift and Earth's tides, and Free Air and Bouguer corrections were applied (Figure 3). The data were reduced to sea level using a Bouguer slab density of 2.67 g/cm^3. No terrain corrections were made, as the topography of the area is fairly flat.

A regional gravity database for the study area, comprising ground gravity measurements spaced 12–15 km apart, was gridded to 3 km using minimum curvature (Figure 2B). The large station spacing of the regional grid only permits resolution of features greater than 25 km, limiting its resolving power for shallow crustal features. To investigate such structures, values interpolated from the regional gravity grid were subtracted from the detailed profiles to calculate the residual signal. The residual Bouguer data were used in subsequent modelling and interpretation using GeoSoft® GM-SYS gravity and magnetic modelling software.

Magnetic data

The Tehery Lake modern aeromagnetic survey (Coyle and Kiss, 2012) was acquired along east-west flight lines spaced 400 m apart and flown along a smooth draped surface at a height of 150 m. The Tehery Lake survey was merged with regional aeromagnetic data (805 m spacing) available through the Canadian Geoscience Data Repository (http://gdr.agg.nrcan.gc.ca/), to create a comprehensive aeromagnetic map of the study area (Figure 2A). The compilation grid was reduced to pole, and derivative products, including the first vertical derivative, tilt and horizontal gradient, were calculated. Derivative products help to delineate magnetic-lithological units by identifying magnetization contrasts, (i.e., 'source edges') and provide supplementary information for differentiating lithological units during forward modelling. Reduced-to-pole magnetic profiles were extracted along profiles 1 and 2 (Figures 4, 5).

Preliminary interpretation and discussion

Profile 1

Previous interpretations of the crustal structure underlying the study area are restricted to regional magnetotelluric (MT) studies by Spratt et al. (2014). They delineated the CFZ as shallow dipping to the south with a faint crustal MT response over their northwest–southeast transect (Spratt et al., 2014, profile 1), no MT response on their north–south transect (Spratt et al., 2014, profile 2), and no response crossing the WSZ on either transect. Profile 1 from the present study (Figure 4) displays the residual Bouguer gravity (bottom panel) and magnetic (middle panel) anomalies against geology (top panel). Coincident positive gravity and magnetic anomalies (Figure 4, anomaly H1) support the interpretation by Broome (1990), who suggested a dense, magnetic granulite body located beneath the surface north of the WSZ. At surface, the anomalies broadly correspond to extensive magnetite-bearing monzogranite with tonalitic and metasedimentary inclusions, all believed to have been subjected to granulite-facies conditions (Figure 1; Patterson and LeCheminant, 1985; Steenkamp et al., 2016; Wodicka et al., 2016). The CFZ corresponds to the most notable gravity low (L1) on the profile and is located on the northern flanks of coincident gravity (H2) and magnetic (H2) highs. It displays a shallower gradient to the south, suggesting a southward-dipping structure, in agreement with the interpretation of Spratt et al. (2014). However, this contrasts with the variable dips measured along the CFZ at surface (Wodicka et al., 2016). A mapped panel of undifferentiated Paliak-like supracrustal rocks north of the CFZ is associated with subtle magnetic highs (H3, H4) and corresponds to a broad (~7 km) gravity high (H3). These gravity and magnetic signatures suggest that this supracrustal panel is slightly wider than currently mapped (Figure 4, dashed lines). Two panels of Paliak-like supracrustal rocks, >1 km wide, correspond to two-station coincident gravity and magnetic highs (H5, H6). Although their gravity and magnetic responses on the profiles are not as anomalous, the Ketyet River–like supracrustal rocks correspond to a slight magnetic low (L2) and a moderate gravity high (M1) with a northward downslope.

Profile 2

Transecting the CFZ, profile 2 (Figure 5) is oriented over undifferentiated Archean tonalite to granodiorite orthogneiss (Figure 1). The range of gravity anomalies for profile 2 is not very large (~1.5 mGal), indicating that the orthogneiss has a significant degree of homogeneity. The

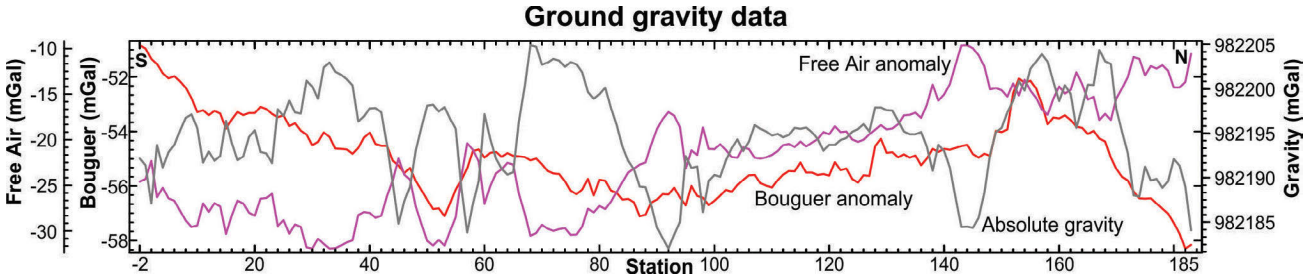

Figure 3: Reduced ground gravity data along profile 1.

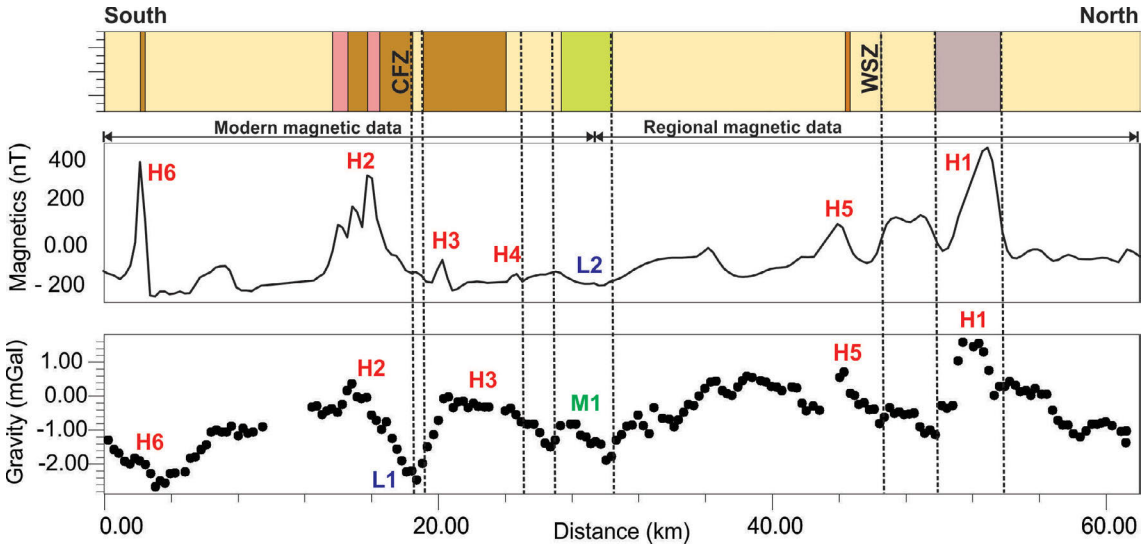

Figure 4: Profile 1 – Top panel shows plan-view geology (without structural data) from Wodicka et al. (2016), the dashed vertical lines indicating potential limits of geological units and major structures, and colours as in Figure 1; black line in the middle panel denotes magnetic field data; black dots in the bottom panel denote residual Bouguer gravity data. Labels as discussed in text.

relatively subtle changes likely relate to compositional variations in the Archean basement. Previous regional geological maps for the Tehery Lake–Wager Bay area (e.g., Panagapko et al., 2003) positioned the CFZ farther north (Figure 5, CFZ-03), where it is situated on a gravity high. Mapping conducted during the 2016 field season led to a reassessment of the location of the CFZ (Figure 5, CFZ-16), based on the distribution of highly strained rocks. The new position adjacent to gravity anomaly L3 suggests a change in density across some kind of geological contact or structure, in this case the CFZ. It is also consistent with the position of the CFZ in the gravity signature in profile 1 (Figure 4, L1), where the fault zone is located at a gravity low with an amplitude of ~1.5 mGal. South of CFZ-16, the gravity anomalies are gently sloping to the south.

Discussion

On both profiles, the CFZ is on (Figure 4, L1) or adjacent to (Figure 5, L3) a gravity low. Wodicka et al. (2016) noted that the CFZ comprises strongly deformed rocks that have subsequently been cut by undeformed coarse-grained monzogranite. Undeformed monzogranite is less dense

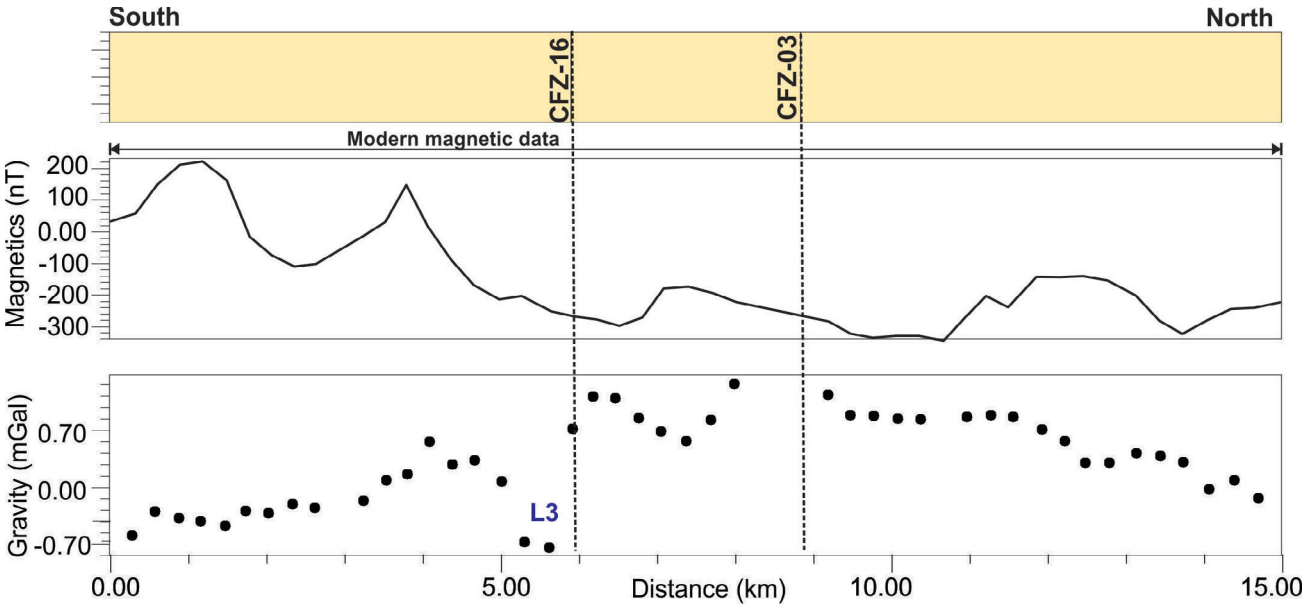

Figure 5: Profile 2 – Top panel shows plan-view geology from Wodicka et al. (2016), the dashed vertical lines indicating the potential limits of the CFZ and colours as in Figure 1; black line in the middle panel denotes magnetic field data; black dots in the bottom panel denote residual Bouguer gravity data. Labels as discussed in text.

than foliated and deformed Archean gneissic rocks and Paleoproterozoic supracrustal rocks; however, these bodies are small at surface and may not be sufficient in volume to produce such gravity lows. The source of the CFZ gravity anomaly is expected to be resolved by rock-property measurements (provided there are sufficient representative samples) that could identify what lithological unit (if present) could generate such an anomaly, or determine if the gravity low cannot be correlated to anything at surface.

North of the WSZ (Figure 4), the (H1) magnetic and gravity anomalies are interpreted to represent granulite-facies rocks (e.g., Broome, 1990; Steenkamp et al., 2016; Wodicka et al., 2016). Potential field anomalies of similar amplitude and wavelength have been modelled by Tschirhart et al. (2016) along the AMZ ~1.5 km below the surface and continuing on beneath the Thelon Basin sedimentary cover. Similar magnetic highs are present over the length of the AMZ and WSZ, suggesting that analogous dense bodies are located at depth. The nature of the dense magnetic bodies along the AMZ is so far unknown.

Profile 1 highlights the different geophysical responses of the Ketyet River–like versus Paliak-like supracrustal belts. The Paliak-like panels have distinct positive gravity and magnetic anomalies associated with them, whereas the Ketyet River–like panel is a magnetic low and moderate gravity high (Figure 4). The Paliak-like panels host more diverse and dense rock types (e.g., iron formation, garnetite), perhaps contributing to their more pronounced geophysical response. Density and magnetic-susceptibility measurements of representative samples aim to further constrain the characteristics of each belt to enable easier interpretation of their presence in the airborne-survey data.

Future studies and economic considerations

In the absence of constraints, geophysical signatures are non-unique, and an infinite number of geological solutions can replicate the observed geophysical response. Detailed forward modelling of gravity and magnetic data will include physical rock-property values (e.g., density and magnetic susceptibility), along with potential remanently magnetized rock units and structural measurements to constrain the geological modelling solution. Remanence may be present where the measured dip of rock bodies can be replicated by the gravity data but not the magnetic data, which introduces additional complications to the modelling process. Furthermore, a wide distribution of rock-property values will help to geophysically characterize selected rock units for a comprehensive understanding of the contribution of individual geological units to the observed gravity and magnetic response, and will assist in regional-mapping efforts.

Within the study area, large-scale structures are prospective for a range of economic mineral deposits. As an example, a Paliak-like supracrustal panel in the immediate hanging-wall of the CFZ is adjacent to anomalous concentrations of Ag, Cu, Bi and Au in surface till (circled black cross in Figure 1; McMartin et al., 2013). A better understanding of the nature and geometry of the CFZ will allow discrimination of its potential to focus base- and/or precious-metal mineralization. North of the western segment of the CFZ (Figure 1), a large synformal structure hosting Ketyet River–like rocks contains several gossanous horizons near folded basement-cover contacts; these horizons are currently being investigated for their economic prospectivity (McMartin et al., 2016; Steenkamp et al., 2016; Wodicka et al., 2016).

Conclusions

The second field season of the Tehery-Wager mapping activity included the acquisition of ground-gravity data to map variations in the density of the underlying rock units. Based on the preliminary analysis of the gravity observations and aeromagnetic data, information related to the geometry of shallow crustal structures is apparent in the geophysical signatures (Figures 4, 5). However, in the absence of physical rock-property constraints, the preliminary interpretations are quite restricted. The WSZ and CFZ flank gravity highs accompanied by coincident magnetic anomalies. The CFZ is accompanied by a gravity low on both profiles. Subtle magnetic and gravity anomalies correspond to mapped panels of supracrustal rocks and highlight distinct differences in the geophysical characteristics of the Ketyet River–like versus Paliak-like supracrustal rocks; the latter apparently have higher magnetization and density, as indicated in the potential-field profiles. It is expected that the geometry of the structures and rock units at depth along these various profiles can be defined in future iterations of this work, following the inclusion of rock-property information as an important constraint.

Acknowledgments

The authors thank E. Girard, A. Lion, B. Garrison and R. Bayne for their GIS support, field assistance and valuable scientific discussion. D. Guilfoyle was responsible for the preparation of many delicious meals. Logistical support was provided by Prairie Helicopters Inc. and Ookpik Aviation Inc. through the Polar Continental Shelf Program (Project 059-16). D. Wright and R. Murphy are thanked for their management and administrative support. This project is funded by the Geological Survey of Canada's Geo-mapping for Energy and Minerals program and the Canadian Northern Economic Development Agency's Strategic Investments in Northern Economic Development program. This paper benefited from a thorough review by M. Thomas.

Natural Resources Canada, Earth Sciences Sector contribution 20160279

References

Broome, J. 1990: Generation and interpretation of geophysical images with examples from the Rae Province, northwestern Canadian Shield; Geophysics, v. 55, p. 977–997.

Coyle, M. and Kiss, F. 2012: Residual total magnetic field, aeromagnetic survey of the Tehery Lake area, Nunavut; Geological Survey of Canada, Open Files 7203–7206.

Henderson, J.R. and Broome, J. 1990: Geometry and kinematics of Wager shear zone interpreted from structural fabrics and magnetic data; Canadian Journal of Earth Sciences, v. 27, p. 590–604.

Jefferson, C.W., Smith, J.E.M. and Hamilton, S.M. 1991: Preliminary account of the resource assessment study of proposed national park, Wager Bay–Southampton Island areas, District of Keewatin; Geological Survey of Canada, Open File 2351, 47 p., doi:10.4095/131509

McMartin, I., Wodicka, N., Bazor, D. and Boyd, B. 2013: Till composition across the Rae craton south of Wager Bay, Nunavut: results from the Geo-mapping Frontiers' Tehery-Cape Dobbs project; Geological Survey of Canada, Open File 7417, 27 p.

McMartin, I., Byatt, J., Randour, I. and Day, S.J.A. 2015: Report of 2015 activities for regional surficial mapping, till and stream sediment sampling in the Tehery-Wager GEM-2 Rae Project area; Geological Survey of Canada, Open File 7966, 14 p. doi:10.4095/297440

McMartin, I., Day, S.J.A., Randour, I., Roy, M., Byatt, J., LaRocque, A. and Leblon, B. 2016. Report of 2016 activities for surficial mapping and sampling surveys in the Tehery-Wager GEM-2 Rae Project area; Geological Survey of Canada, Open File 8134, 13 p. doi:10.4095/299385

Panagapko, D.A., Pehrsson, S., Pilkington, M. and Currie, M. 2003: Geoscience data compilation: Tehery Lake–Wager Bay area, Nunavut (NTS 56 B, C, F, and G), part 1 – base data themes; Geological Survey of Canada, Open File 1809, 1 CD-ROM. doi:10.4095/214767

Patterson, J.G. and LeCheminant, A.N. 1985: A preliminary geological compilation map of the northeastern Barren Grounds, parts of the Districts of Keewatin and Franklin; Geological Survey of Canada, Open File 1138, scale 1:1 000 000. doi:10.4095/129971

Rainbird, R.H., Davis, W.J., Pehrsson, S.J., Wodicka, N., Rayner, N. and Skulski, T. 2010: Early Paleoproterozoic supracrustal assemblages of the Rae domain, Nunavut, Canada: intracratonic basin development during supercontinent break-up and assembly; Precambrian Research, v. 181, p. 167–186.

Spratt, J.E., Skulski, T., Craven, J.A., Jones, A.G., Snyder, D.B. and Kiyan, D. 2014: Magnetotelluric investigations of the lithosphere beneath the central Rae craton, mainland Nunavut, Canada; Journal of Geophysical Research: Solid Earth, v. 119, p. 2415–2439.

Steenkamp, H.M., Wodicka, N., Lawley, C.J.M., Peterson, T.D. and Guilmette, C. 2015: Overview of bedrock mapping and results from portable X-ray fluorescence spectrometry in the eastern part of the Tehery Lake–Wager Bay area, western Hudson Bay, Nunavut; *in* Summary of Activities 2015, Canada-Nunavut Geoscience Office, p. 121–134.

Steenkamp, H.M., Wodicka, N., Weller, O.M. and Kendrick, J. 2016: Overview of bedrock mapping in the Tehery Lake–Wager Bay area, western Hudson Bay, Nunavut; *in* Summary of Activities 2016, Canada-Nunavut Geoscience Office, p. 27–40.

Tschirhart, V., Jefferson, C.W. and Morris, W.A. 2016: Basement geology beneath the northeast Thelon Basin, Nunavut: insights from integrating new gravity, magnetic and geological data; Geophysical Prospecting, doi:10.1111/1365-2478.12430

van Breemen, O., Pehrsson, S. and Peterson, T.D. 2007: Reconnaissance U-Pb SHRIMP geochronology and Sm-Nd isotope analyses from the Tehery-Wager Bay gneiss domain, western Churchill Province, Nunavut; Geological Survey of Canada, Current Research 2007-F2, 15 p.

Wodicka, N., Steenkamp, H.M., Lawley, C.J.M., Peterson, T.D., Guilmette, C., Girard, E. and Buenviaje, R. 2015: Report of activities for the bedrock geology and economic potential of the Tehery-Wager area: GEM-2 Rae Project; Geological Survey of Canada, Open File 7940, 14 p.

Wodicka, N., Steenkamp, H.M., Weller, O.M., Kendrick, J., Tschirhart, V.L., Peterson, T.D. and Girard, É. 2016: Report of 2016 activities for the bedrock geology and economic potential of the Tehery-Wager area – GEM-2 Rae Project; Geological Survey of Canada, Open File 8149, 21 p. doi:10.4095/299392.

Study of the postglacial marine limit between Wager Bay and Chesterfield Inlet, western Hudson Bay, Nunavut

I. Randour[1], I. McMartin[2] and M. Roy[3]

[1]*Département des sciences de la Terre et de l'atmosphère, Université du Québec à Montréal, Montréal, Québec, randour.iyse@courrier.uqam.ca*

[2]*Natural Resources Canada, Geological Survey of Canada, Ottawa, Ontario*

[3]*Département des sciences de la Terre et de l'atmosphère, Université du Québec à Montréal, Montréal, Québec*

This work is part of the Tehery-Wager geoscience mapping activity of Natural Resources Canada's (NRCan) Geo-mapping for Energy and Minerals (GEM) program Rae project, a multidisciplinary and collaborative effort being led by the Geological Survey of Canada and the Canada-Nunavut Geoscience Office (CNGO), with participants from Canadian universities (Dalhousie University, Université du Québec à Montréal, Université Laval and University of New Brunswick). The focus is on targeted bedrock and surficial geology mapping, stream-water and stream- sediment sampling, and other thematic studies, which collectively will increase the level of geological knowledge in this frontier area and allow evaluation of the potential for a variety of commodities, including diamonds and other gemstones, base and precious metals, industrial minerals, carving stone and aggregates. This activity also aims to assist northerners by providing geoscience training to college students, and by ensuring that the new geoscience information is accessible for making land-use decisions in the future.

Randour, I., McMartin, I. and Roy, M. 2016: Study of the postglacial marine limit between Wager Bay and Chesterfield Inlet, western Hudson Bay, Nunavut; *in* Summary of Activities 2016, Canada-Nunavut Geoscience Office, p. 51–60.

Abstract

This paper presents preliminary results of a thematic study on the postglacial marine limit between Wager Bay and Chesterfield Inlet, mainland Nunavut (parts of NTS 46 and 56). The study is part of the surficial geology component of the Tehery-Wager geoscience mapping activity for the Geo-mapping for Energy and Minerals (GEM-2) Rae project area led by the Geological Survey of Canada and the Canada-Nunavut Geoscience Office. The results presented here are compiled from field observations collected in 2015 and 2016.

The geomorphic features used to delineate the postglacial marine limit are derived from distinct raised marine deposits and trimline settings, including boulder beaches, marine terraces, glaciomarine deltas, wave-cut notches in till uplands and wave-washed till surfaces exposing bedrock below. Preliminary mapping and detailed measurement of the maximum marine stand indicate that the limit increases southeastward from 113 to 127 m halfway along Wager Bay (NTS 56H), to 140 m west of Roes Welcome Sound (NTS 46E and 56A) and stays relatively constant at 139–152 m inland toward Tehery Lake (NTS 56B and 56C). Marine shells suitable for radiocarbon (^{14}C) dating are relatively rare in the study area; therefore, bedrock was sampled from wave-washed rock surfaces for cosmogenic nuclide exposure dating at targeted sites along the marine limit to constrain the timing of marine invasion south of Wager Bay.

Résumé

Cet article présente les résultats préliminaires d'une étude sur la limite marine postglaciaire entre la baie Wager et Chesterfield Inlet (parties des feuillets 46 et 56 du SNRC), au Nunavut. Cette étude s'inscrit dans la composante de géologie de surface de l'initiative de cartographie géoscientifique entreprise dans la région Tehery-Wager dans le cadre du projet Rae du programme de géocartographie de l'énergie et des minéraux (GEM-2) dirigé par la Commission géologique du Canada et le Bureau géoscientifique Canada-Nunavut. Les résultats présentés proviennent d'observations de terrain faites en 2015 et 2016.

Les éléments géomorphologiques délimitant l'invasion marine postglaciaire sont représentés par des dépôts marins perchés et des signes d'épaulements, tels que les plages de blocs, les terrasses marines, les deltas glaciomarins, les surcreusements par l'action des vagues dans les buttes de till et les surfaces de roc lessivées. La cartographie préliminaire et les mesures détaillées indiquent que la position maximale occupée par la mer augmente de 113 à 127 m au milieu de la baie Wager (56H) jusqu'à 140 m à l'ouest du détroit de Roes Welcome (46E et 56A du SNRC). Dans l'arrière-pays, la limite marine reste

This publication is also available, free of charge, as colour digital files in Adobe Acrobat® PDF format from the Canada-Nunavut Geoscience Office website: http://cngo.ca/summary-of-activities/2016/.

relativement constante, variant entre 139 et 152 m en direction du lac Tehery (56B et 56C du SNRC). Afin de déterminer aussi précisément que possible le moment auquel eu lieu l'invasion marine dans la région au sud de la baie Wager, des échantillons ont été recueillis à la limite marine. Les coquillages marins pouvant servir à la datation ^{14}C sont relativement rares dans la zone d'étude. Par conséquent, des échantillons de socle prélevés de surfaces rocheuses délavées par l'action des vagues seront analysés au moyen de la méthode de datation par durée d'exposition utilisant des nucléides cosmogéniques.

Introduction

Surficial geology studies and targeted surface sediment sampling were initiated in 2015 south of Wager Bay (Figure 1) as part of a geoscience mapping activity led by the Geological Survey of Canada (GSC) and the Canada-Nunavut Geoscience Office (CNGO) under the GEM-2 Program (see McMartin et al., 2015a, 2016a, b). One of the objectives of the surficial component is to provide a glacial and postglacial history framework required for interpreting the nature and transport history of surficial sediments. Together with bedrock studies (Steenkamp et al., 2015, 2016; Tschirhart et al., 2016; Wodicka et al., 2015, 2016), the work will increase the level of geoscience knowledge, which is needed to help northern communities make informed decisions about their lands, the economy and society.

One of the striking features of the Quaternary geology in the study area is the postglacial marine inundation by the Tyrrell Sea, as shown on the Glacial Map of Canada (1:5 000 000; Prest et al., 1968). At present, the maximum extent of the marine invasion is largely based on reconnaissance-scale mapping with limited ground observations in the study area. Determining more precisely the maximum limit and timing of marine inundation is important for reconstruction of postglacial rebound and crustal deformation, glacial retreat patterns and chronology, and to evaluate the effects of marine processes on sediment composition and redistribution for surface exploration using glacial sediments. Recent mapping south of Brown Lake in NTS 56G (Dredge and McMartin, 2005a, b, 2007), and GEM-1 preliminary mapping initiatives along Roes Welcome Sound in NTS 46D and 56A (Dredge et al., 2013a–c), provided the framework to reconstruct the marine limit for the entire area south of Wager Bay. For this study, detailed field observations and elevation measurements of the marine limit were collected along the southern shores of Wager Bay in NTS 56H, and remapping of the marine limit was completed using all recent and previous maps, as well as new targeted data over the entire region.

To constrain the timing of marine invasion along the northwestern coast of Hudson Bay and to obtain minimum deglaciation ages for the outer part of Chesterfield Inlet and Wager Bay, geochronological samples were collected in the study area. Two marine shell samples collected in NTS 56B were submitted for radiocarbon (^{14}C) dating and six bedrock samples from wave-washed surfaces immediately below the marine limit were collected for cosmogenic nuclide surface exposure dating. Presumably, this latter method has never been used to date a marine limit and this approach may help avoid inaccuracies related to the marine reservoir effects, which can skew ^{14}C dating of shell samples (i.e., McNeely et al., 2006; Ascough et al., 2009). In addition, till samples were collected from frost boils above and below the marine limit as part of a detailed study to document the effects of marine reworking and winnowing on the geochemical composition of till in periglacial environments. This paper provides a summary of the postglacial marine limit mapping, and elevation, chronological and compositional datasets collected during the 2015 and 2016 field seasons.

Location and physiography

The study area lies south of Wager Bay and north of Chesterfield Inlet, in central mainland Nunavut, between latitudes 64–66°N and longitudes 87–93°W (Figures 1, 2) It covers two complete 1:250 000 NTS map areas (56A, 56B) and parts of four more (46E, 46D, 56C, 56H).

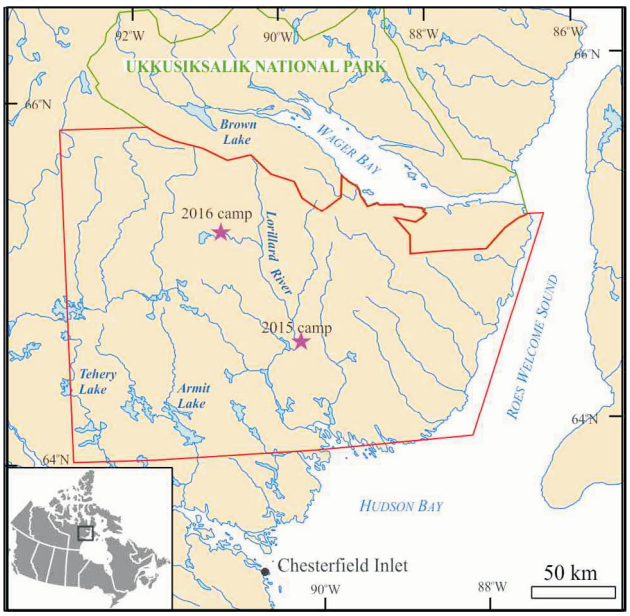

Figure 1: Location of the Tehery-Wager geoscience mapping activity study area (outlined in red) on the western side of Hudson Bay, Nunavut.

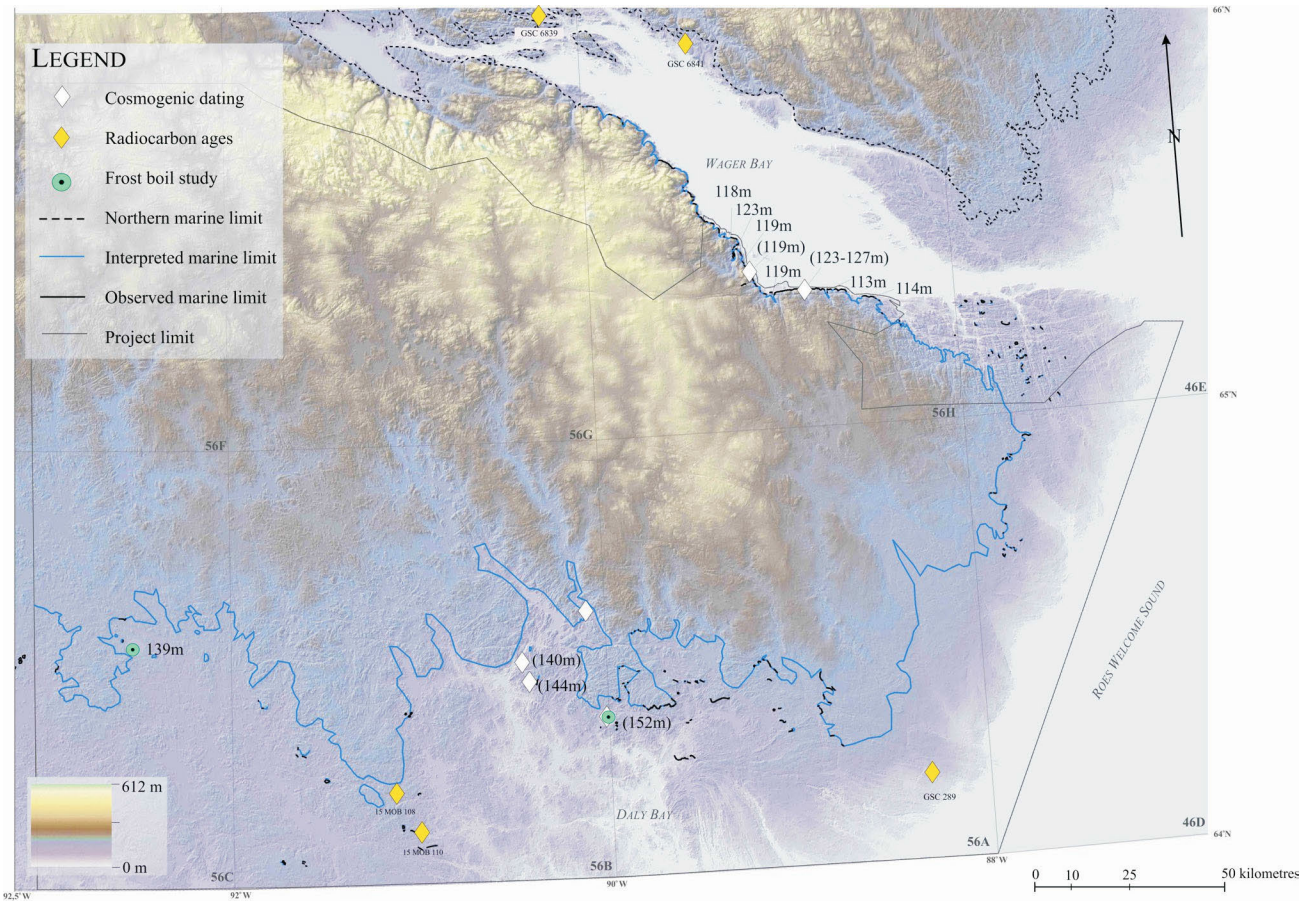

Figure 2: Digital elevation model of the Tehery-Wager geoscience mapping activity study area, derived from Canada digital elevation data (GeoBase®, 2016), based on 1:50 000 National Topographic Data Base digital files showing the postglacial marine limit in the region. Elevation measurements taken in the field and corrected with stationary unit data are indicated in metres. Numbers in parentheses are the noncorrected measurements (see text). The extent of marine limit shown as a dashed line is from Dredge and McMartin (2005b) in NTS 56G and from McMartin et al. (2015b) north of Wager Bay. Locations of samples collected for cosmogenic nuclide surface exposure dating at, or slightly below, the marine limit are also shown. Marine shell samples with radiocarbon ages are samples 15 MOB 108 and 110 from this paper, GSC 289 from Craig (1965) and GSC 6839 and 6841 from Dredge and McMartin (2005b).

Elevations within the area vary from sea level up to 610 m. The area consists of a mixture of coastal lowlands and dissected plateaus. Steep rocky hills rise abruptly from the southern shore of Wager Bay. Two hydrographic basins drain the area toward Hudson Bay: the Wager Bay basin in the extreme north and the Lorillard River basin, which is the dominant drainage basin of the area.

Surficial geological setting and previous work

The study area was covered by Keewatin Sector ice of the Laurentide Ice Sheet during the Late Wisconsinan glaciation (e.g., Dyke and Prest, 1987a). Ice flowed radially from the Keewatin Ice Divide positioned in the uplands, south of Wager Bay, during the last glaciation (i.e., Aylsworth and Shilts, 1989a, b; McMartin and Dredge, 2005).

Numerous streamlined landforms and glacial striations indicate a predominant ice-flow direction toward the southsoutheast and southeast from the ice divide. However, the pattern of glacial retreat is more complex, as shown by relationships between streamlined forms, striations, eskers, subglacial meltwater corridors and proglacial meltwater channels (see McMartin et al., 2015a, 2016b). According to Dyke (2004), deglaciation of the area occurred between 7700 and 6000 ^{14}C yr. BP. During the last glaciation, the weight of the ice sheet depressed the terrestrial crust with respect to today's topographic configuration. Throughout deglaciation, the massive release of meltwater associated with the melting of the ice mass caused a significant rise in sea level, which occurred more rapidly than the glacial isostatic adjustment of the land (postglacial rebound). Consequently, as the ice margin retreated inland toward the northwest, the marine waters inundated the isostatically depressed coast of Hudson Bay. The marine limit is the highest elevation reached by the postglacial sea and thus marks the frontier between submerged lands and those that were never inundated.

The timing of the marine invasion is poorly understood in the study area. Prior to this study, only one ^{14}C date of ~6600 ^{14}C yr. BP on marine shells from a site at an elevation of 126 m was available between Wager Bay and Chesterfield Inlet (GSC-289: corrected age of 6600 ±170 ^{14}C yr. BP; Craig, 1965). Marine shells were found north of Wager Bay (Figure 2) at two sites, in small deltas standing at an elevation of approximately 60 m, well below the postglacial marine limit (Dredge and McMartin, 2005b). The corrected ages for these marine fossils range between 5540 ±60 ^{14}C yr. BP (GSC-6839) and 5690 ±80 ^{14}C yr. BP (GSC-6841). McMartin et al. (2015b) suggested that, northeast of Wager Bay, along the shores of Roes Welcome Sound, the ice had disappeared from Aiviliup tariunga (formerly Repulse Bay) and the northern part of Roes Welcome Sound by ~7000 ^{14}C yr. BP.

Methodology

Marine limit mapping

The marine limit was compiled using a combination of different features from existing surficial geology maps (Aylsworth, 1990a–b; Aylsworth et al., 1990; Dredge et al., 2013a–c) and detailed mapping in progress within NTS 56H south and 46E south. Where the marine limit was not developed and/or identified in previous map areas, elevation measurements from the mapped trimlines were extrapolated from 1:50 000 topographic contour maps (±10 m) and/or directly measured in the field (NTS 56B and 56C). In NTS 56H south, the marine limit was mapped using aerial photographs, a digital elevation model (derived from Canadian digital elevation data based on 1:50 000 National Topographic Data Base digital files), topographic contours (1:50 000) and satellite imagery (SPOT 4 and 5, and Landsat 7 composite, bands 742). In NTS 46E south, mapping in progress was completed using aerial photographs and topographic contours (1:50 000). The marine limit was then approximately traced using these elevation measurements and interpreted positions.

Different types of geomorphic evidence exist for identifying the maximum extent of the marine invasion. The most common features include boulder beaches, perched marine deltas, wave-cut notches in till, wave-washed rock surfaces, raised marine terraces and till remnants on small top-

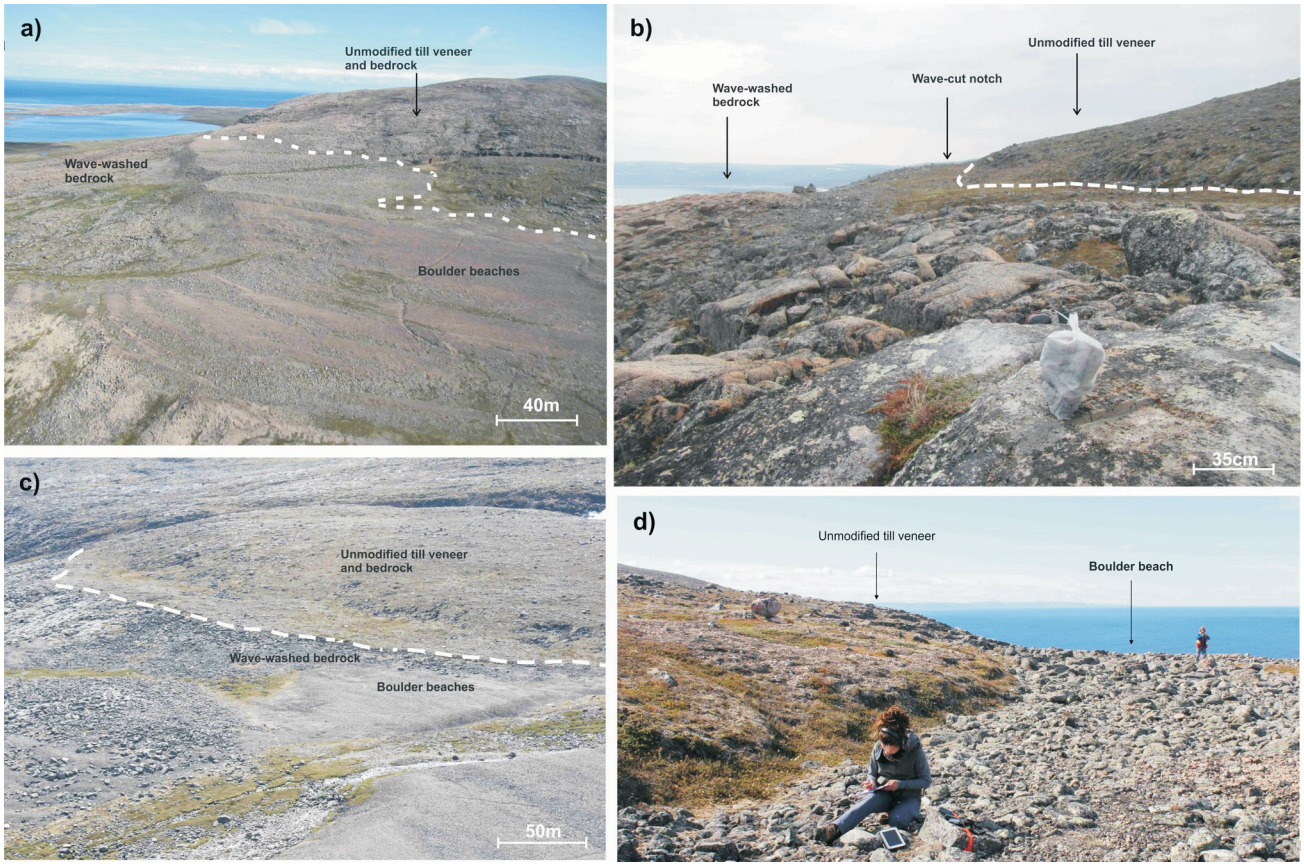

Figure 3: Different features that mark the marine limit (shown with dashed white line) in the Wager Bay–Chesterfield Inlet study area: **a)** perched boulder beaches along Wager Bay in NTS 56H; **b)** wave-cut notch in till veneer and wave-washed, exposed bedrock along Wager Bay; bedrock sample collected in 2015 field season for surface exposure dating using cosmogenic nuclides is shown at the front of the photograph; **c)** perched boulder beaches and wave-washed bedrock surfaces along Wager Bay in NTS 56H; **d)** limit between boulder beaches and unmodified till veneer.

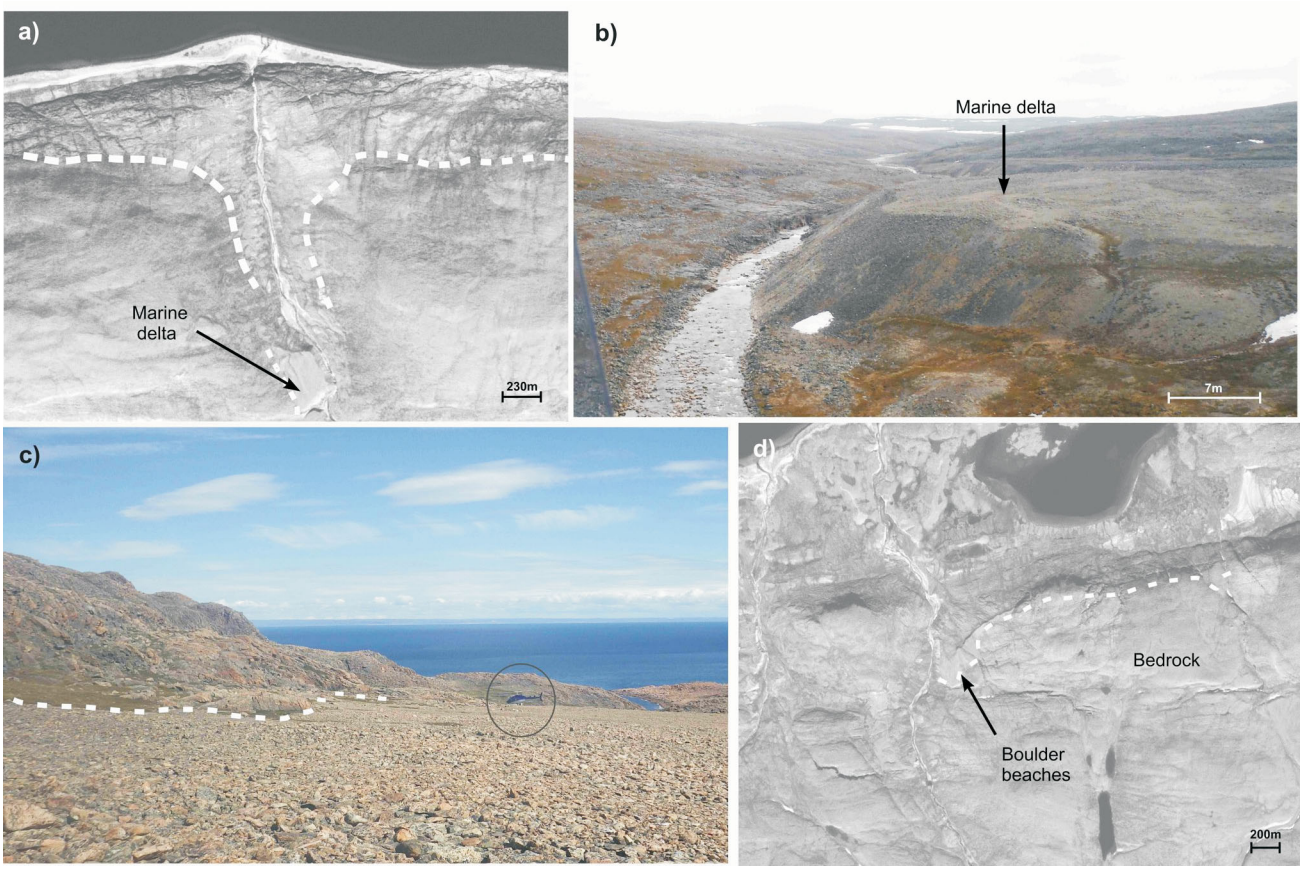

Figure 4: Relationship between marine features in SPOT 4 and 5 satellite imagery, and field observations (dashed white line is the marine limit) in the Wager Bay–Chesterfield Inlet study area: **a)** texture of marine delta is smoother than the surrounding bedrock; **b)** view from a helicopter of flat-topped marine delta shown in 4a; **c)** photograph of boulder beaches in NTS 56H (helicopter for scale); **d)** boulder beaches have a smoother texture and lighter tone than the bedrock on SPOT 4 and 5 imagery.

ographic highs with nearshore-sediment assemblages below and intact till above (Figure 3a–d). In NTS 56H, mainly raised boulder beaches and perched deltas were observed: they show a typical pale grey colour on the airphoto and a less well defined texture than bedrock (Figure 4a–d). Marine limit features represent a time when the marine level was relatively stable for a given period of time.

Elevation measurements

During the 2016 field season, several sites were visited along the coast of Wager Bay to record detailed postglacial marine-limit measurements. These sites were selected based on aerial photographs, satellite imagery (SPOT 4 and 5) and the central location of a nearby National Topographic Data Base bench mark. Six sites were measured at the highest points of selected marine features, mainly boulder beaches.

In order to obtain the highest precision for the detailed measurements, a combination of stationary and mobile devices was used (see Roy et al., 2015). A Track-It™ barometric data logger was placed for the day on a geodesic survey marker (bench mark) with a known elevation near the coast (stationary unit). Several other mobile devices were used at ground-truthing points and calibrated two times a day with the stationary bench mark point. To improve the measures used for calibration, all the instruments, including the data logger, were set relatively close to each other, within a maximum distance of 20 km, and a day with stable (high-pressure) weather was preferentially chosen for the measurements.

The stationary unit data were used to correct the pressure's daily changes, which are related to the elevation as expressed by the ideal gas law. These changes can be large enough to make important differences in the elevation measurements. Data were remotely collected in terms of pressure and temperature and recorded at fixed intervals of 30 seconds during the entire day.

The mobile units included two GPS devices (Garmin GPS-12™ and Oregon® 650t) and one altimeter barometer (Suunto model Escape 203). Elevation data at the selected marine-limit sites were recorded from each mobile unit at intervals of 1 minute during a period of 5 minutes. An average of the three device readings was first done for each minute. The five averages were then corrected if necessary us-

ing the stationary unit records. This adjustment was done by adding or subtracting the difference recorded on the stationary unit from the averages at each recorded time. The corrected data were then averaged to obtain the final elevation at each site. Elevations were recorded to a precision of ~1 m. Moving inland, more than 15 measurements were collected in both NTS 56B and 56C. Due to time constraints associated with field logistics, these measurements were collected using the Garmin GPS-12™ and are considered to be accurate to within ±5 m.

Geochronology

Marine shells were collected at two sites in 2015 near the Connery River northeast of Chesterfield Inlet (McMartin et al., 2015a). The shells were sampled from the surface of frost boils developed in till mixed with marine sediments at 120 and 80 m above sea level. Single shells of *Hiatella arctica* from each of the two sites were analyzed for ^{14}C age determinations at the André E. Lalonde Accelerator Mass Spectrometry Laboratory at the University of Ottawa. Marine shells were not found during the 2016 field season.

In 2015, bedrock from wave-washed surfaces defining trimlines with unmodified till at the marine limit was sampled (McMartin et al., 2015a) for surface exposure dating using cosmogenic nuclides (Dunai and Lifton, 2014; Ivy-Ochs and Briner, 2014). The rock samples were collected using a gas-powered rock saw and a chisel. The ^{10}Be ages will be obtained from quartz grains using standard procedures. Accordingly, bedrock types sampled for this study were rich in quartz, coming from the Hudson suite granite, tonalite to granodiorite orthogneiss and pegmatite intrusions. Two samples were taken directly along Wager Bay, in NTS 56H, and four others were taken further inland, in NTS 56B (Figure 2).

Frost boil sampling

In order to assess the influence of marine processes on till composition, two sites were selected along the marine limit in 2016, one in NTS 56B and one in NTS 56C (Figure 2). The sampling sites were chosen for their well-defined marine limit as identified on airphotos, the presence of thick till above and below the trimline and continuous bedrock

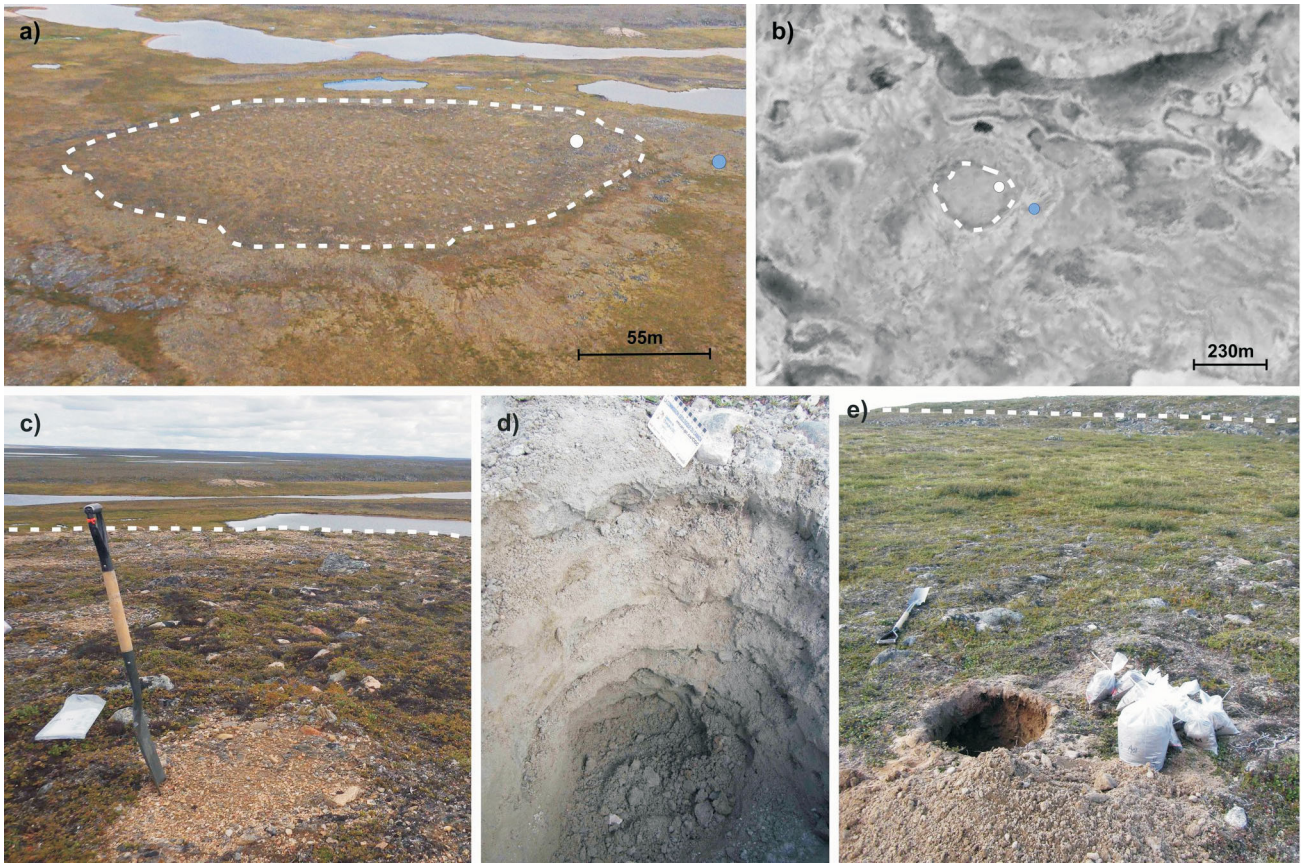

Figure 5: Detailed sampling of frost boils in NTS 56C at sites 16MOB177 and 178 (dashed white line indicates the marine limit) in the Wager Bay–Chesterfield Inlet study area: **a)** white dot represents the sampled frost boil (16MOB177) above the marine limit in part c; blue dot refers to sampled frost boil (16MOB178) under the marine limit shown in part e; **b)** SPOT satellite image of the same 'till island' ~230 m wide; **c)** frost boil-sample site number 16MOB177; **d)** view inside the frost boil after the sampling at site 16MOB178; the samples were collected from a vertical profile at 10–15 cm intervals creating a stratified appearance in the hole wall; **e)** frost boil-sample site number 16MOB178.

units along the trimline (Figure 5a, b). The final selection of the frost boils was done onsite.

At each site, the vertical profiles of paired frost boils were sampled at 10–15 cm intervals down to 95 cm maximum depth; one site was located immediately below the marine limit and the other directly above (Figure 5c–e). An additional large till sample was collected at depth from each hole for precious-metal–grains and indicator-mineral analyses. Five small field duplicate samples were also collected near each frost boil at approximately 40 cm depth to measure the local variability. Geochemical and textural analyses will be performed on the samples to assess how the texture and geochemical composition vary with depth and between sites above and below the marine limit. Till geochemical analytical procedures will follow the protocols used at the Geological Survey of Canada (see Spirito et al., 2011; McMartin et al., 2016b).

Preliminary results

The postglacial limit of marine inundation was mapped, characterized and measured across the study area (Figure 2). Detailed elevation measurements on the highest boulder beaches about halfway along the southern shores of Wager Bay vary from 113 to 127 m asl. The observed marine limit lies at 95 m west of Brown Lake and at 110 m in the inner part of Wager Bay (Dredge and McMartin, 2005b). In the outer, eastern part of the bay within NTS 46E, the elevation of the interpreted marine limit ranges between 120 and 140 m (estimated from 10 m contours). Regionally, the new compilation indicates that the marine limit decreases inland along both shores of Wager Bay (this study; McMartin et al. 2015b). The general inland decrease in the marine-limit elevation suggests that the outer (eastern) part of Wager Bay was deglaciated earlier than the inner (western) part of the Bay. Marine water was prevented from inundating lower lands around Wager Bay by the presence of glacial ice remnants inland and over the western part of the bay.

The limit of the maximum marine stand stays relatively constant at 139–152 m between Roes Welcome Sound (NTS 46E and 56A) and the Armit and Tehery lakes areas (NTS 56B and 56C). The newly defined marine limit is relatively similar to the one presented on the Glacial Map of Canada (Prest et al., 1968). Within the centre of Wager Bay, the elevation remains similar; however, near the boundary between NTS 56H and 46E, the Glacial Map indicates an elevation of 300 feet (92 m), much lower than the new measurement of 114 m. On the western side of NTS 46D, the Glacial Map shows an elevation at 490 feet (149 m), whereas Dredge et al. (2013a) mapped the extent of the marine inundation at a maximum of 140 m.

The location of the marine limit shows that the Tyrrell Sea once occupied a vast area along Hudson Bay, particularly over the coastal lowlands north of Chesterfield Inlet and along Roes Welcome Sound, and a restricted fringe area along the southern abrupt shores of Wager Bay. The character of the marine deposits varies from mainly erosive facies (wave-washed bedrock surfaces and wave-cut notches) along Wager Bay to reworked/depositional facies in the lowlands. Reworked and mixed till with marine sediments are present in areas where the topography is smoother and of lower relief, and where there is greater abundance of glacial/glaciofluvial sediment cover.

The chronology of the local ice retreat remains poorly known in the study area, in part due to the lack of marine shells available for ^{14}C dating. Radiocarbon analysis of the two marine shell samples collected in 2015 provided corrected ages of 6252 ±47 ^{14}C yr. BP (UOC-1674) and 6373 ±43 ^{14}C yr. BP (UOC-1675), using the marine-reservoir correction of 630 years suggested for this area of Hudson Bay (zone 6: Foxe Basin; see McNeely et al., 2006). However, the marine-reservoir effect is poorly defined in the study area with the closest site with pre-bomb marine material available for testing located at Naujaat (formerly Repulse Bay), 250 km to the northeast (i.e., McNeely et al., 2006). Surface exposure dating of wave-washed bedrock surfaces offers a promising avenue. Five samples were selected for cosmogenic nuclide surface exposure dating and results will help constrain the timing of deglaciation and marine inundation. Variations in the elevation of the marine limit will be studied further with respect to local deglacial patterns and the new chronological constraints.

Economic considerations

The determination of the marine limit will help separate first order glacial sediments, which are deposited directly by glacial ice, from second order sediments, which are reworked, in this case by marine processes. First order sediments, such as till, are commonly used in drift prospecting surveys, whereas the complex transport history of the second order sediments makes them more difficult to use for interpreting provenance and mineralized bedrock sources (i.e., McMartin and Campbell, 2009).

The detailed profile sampling in frost boils above and below the marine limit will help assess the impact of marine invasion on till composition in soils affected by cryoturbation. Texture and geochemical composition may be affected by the winnowing and reworking effects of marine waves and currents, and/or diluted by the incorporation of fine-grained marine sediments. The vertical profile sampling at detailed intervals will help measure the variations as a function of depth, an important factor to consider in surface mineral exploration in northern Canada, where systematic till sampling in frost boils is an exploration technique commonly used to find many commodities of economic value.

Acknowledgments

This study is part of a M.Sc. thesis by I. Randour at the Université du Québec à Montréal under the co-supervision of M. Roy and I. McMartin. Funding is provided by grants from the National Sciences and Engineering Research Council and the Quebec Fond de recherche–Nature et technologies to I. Randour, as well as by Natural Resources of Canada through the Research Affiliate Program and the Geo-mapping for Energy and Minerals program, Phase 2 (GEM-2). All the field support and logistics were provided by the Tehery-Wager geoscience mapping activity of the GEM-2 Rae Project led by the Geological Survey of Canada and the Canada-Nunavut Geoscience Office. Special thanks to N. Wodicka and H. Steenkamp for their continued support and for project management. The authors would like to thank É. Girard for GIS support during the field season and D. Guilfoyle for her gorgeous meals at camp. Thanks to J. Campbell for providing a review of the manuscript.

Natural Resources Canada, Earth Sciences Sector contribution number 20160215

References

Ascough, P.L., Cook, G.T. and Dugmore, A.J. 2009: North Atlantic marine ^{14}C reservoir effects: Implications for late-Holocene chronological studies; Quaternary Geochronology, v. 4, no. 3, p. 171–180, doi:10.1016/j.quageo.2008.12.002

Aylsworth, J.M. 1990a: Surficial geology, Armit Lake, District of Keewatin, Northwest Territories; Geological Survey of Canada, Preliminary Map 45-1989, 1:250 000 scale, URL <http://geoscan.nrcan.gc.ca/starweb/geoscan/servlet.starweb?path=geoscan/fulle.web&search1=R=131453> [September 2016], doi:10.4095/131453

Aylsworth, J.M. 1990b: Surficial geology, Tehery Lake, District of Keewatin, Northwest Territories; Geological Survey of Canada, Preliminary Map 46-1989, 1:250 000 scale, URL <http://geoscan.nrcan.gc.ca/starweb/geoscan/servlet.starweb?path=geoscan/fulle.web&search1=R=131454> [September 2016], doi:10.4095/131454

Aylsworth, J.M. and Shilts, W.W. 1989a: Glacial features around the Keewatin ice divide, Northwest Territories; Geological Survey of Canada, Preliminary Map 24-1987, 1:1 000 000 scale, URL <http://geoscan.nrcan.gc.ca/starweb/geoscan/servlet.starweb?path=geoscan/fulle.web&search1=R=126992> [September 2016], doi:10.4095/126992

Aylsworth, J.M. and Shilts, W.W. 1989b: Glacial features around the Keewatin ice divide: districts of Mackenzie and Keewatin; Geological Survey of Canada, Paper, 88-24, p. 1–21.

Aylsworth, J.M., Cunningham, C.M. and Shilts, W.W. 1990: Surficial geology, Schultz Lake, District of Keewatin, Northwest Territories; Geological Survey of Canada, Preliminary Map 43-1989, 1:125 000 scale, URL <http://geoscan.nrcan.gc.ca/starweb/geoscan/servlet.starweb?path=geoscan/fulle.web&search1=R=130943> [September 2016], doi:10.4095/130943

Craig, B.G. 1965: Notes on moraines and radiocarbon dates in northwest Baffin Island, Melville Peninsula, and northeast District of Keewatin; Geological Survey of Canada, Paper, 65-20, p. 1–7, URL <http://geoscan.nrcan.gc.ca/starweb/geoscan/servlet.starweb?path=geoscan/fulle.web&search1=R=100991> [September 2016], doi:10.4095/100991

Dredge, L.A. and McMartin, I. 2005a: Glacial lakes in the Wager Bay area, Kivalliq, Nunavut; Geological Survey of Canada, Current Research 2005-B1, p. 1–7, URL <http://geoscan.nrcan.gc.ca/starweb/geoscan/servlet.starweb?path=geoscan/fulle.web&search1=R=220349> [September 2016], doi:10.4095/220349

Dredge, L.A. and McMartin, I. 2005b: Postglacial marine deposits and marine limit determinations, inner Wager Bay area, Kivalliq region, Nunavut; Geological Survey of Canada, Current Research 2005-B3, p. 1–5, URL <http://geoscan.nrcan.gc.ca/starweb/geoscan/servlet.starweb?path=geoscan/fulle.web&search1=R=220634>, [September 2016], doi:10.4095/220634

Dredge, L.A. and McMartin, I. 2007: Surficial geology, Wager Bay, Nunavut; Geological Survey of Canada, A Series Map 2111A, 1:100 000 scale, URL <http://geoscan.nrcan.gc.ca/starweb/geoscan/servlet.starweb?path=geoscan/fulle.web&search1=R=223218> [September 2016], doi:10.4095/223218

Dredge, L., McMartin, I. and Campbell, J. 2013a: Reconnaissance surficial geology, Daly Bay north, Nunavut, NTS 56-A North; Geological Survey of Canada, Canadian Geoscience Map 147, 1:100 000 scale, URL <http://geoscan.nrcan.gc.ca/starweb/geoscan/servlet.starweb?path=geoscan/fulle.web&search1=R=293046> [September 2016], doi:10.4095/126992

Dredge, L.A., McMartin, I. and Campbell, J. 2013b: Reconnaissance surficial geology, Daly Bay (south) and Cape Fullerton (north), Nunavut, NTS 56-A south and 55-P north; Geological Survey of Canada, Canadian Geoscience Map 146, 1:100 000 scale, URL <http://geoscan.nrcan.gc.ca/starweb/geoscan/servlet.starweb?path=geoscan/fulle.web&search1=R=293045> [September 2016], doi:10.4095/293045

Dredge, L.A., McMartin, I. and Campbell, J.E. 2013c: Reconnaissance surficial geology, Yellow Bluff (west), Nunavut, NTS 46-D west; Geological Survey of Canada, Canadian Geoscience Map 145, 1:100 000 scale, URL <http://geoscan.nrcan.gc.ca/starweb/geoscan/servlet.starweb?path=geoscan/fulle.web&search1=R=293047>[September 2016], doi:10.4095/293047

Dunai, T.J. and Lifton, N.A. 2014: The nuts and bolts of cosmogenic nuclide production; Elements, v. 10, no. 5, p. 347–350, doi:10.2113/gselements.10.5.347

Dyke, A.S. 2004: An outline of North American deglaciation with emphasis on central and northern Canada; Developments in Quaternary Science, v. 2, p. 373–424.

Dyke, A.S. and Prest, V.K. 1987a: Late Wisconsinan and Holocene history of the Laurentide Ice Sheet; Géographie physique et Quaternaire, v. 41, no. 2, p. 237–263.

Dyke, A.S. and Prest, V.K. 1987b: Paleogeography of northern North America, 18 000–5 000 years ago; Geological Survey of Canada, A Series Map 1703A, 1:5 000 000 scale, URL <http://geoscan.nrcan.gc.ca/starweb/geoscan/servlet.starweb?path=geoscan/fulle.web&search1=R=293047> [September 2016], doi:10.4095/133927

GeoBase® 2016: GeoBase raw imagery 2005–2010; Natural Resources Canada, <http://geogratis.gc.ca/api/en/nrcan-

rncan/ess-sst/a1cf5af6-7881-f698-766d-e24fe22a883f.html> [November 2016].

Ivy-Ochs, S. and Briner, J.P. 2014: Dating disappearing ice with cosmogenic nuclides; Elements, v. 10, no. 5, p. 351–356, doi:10.2113/gselements.10.5.351

McMartin, I. and Campbell, J.E. 2009. Near-surface till sampling protocols in shield terrain, with examples from western and northern Canada; *in* Application of Till and Stream Sediment Heavy Mineral and Geochemical Methods to Mineral Exploration in Western and Northern Canada, R.C. Paulen and I. McMartin (ed.), Geological Association of Canada, GAC Short Course Notes 18, p. 75–95.

McMartin, I. and Dredge, L.A., 2005: History of ice flow in the Shultz Lake and Wager Bay areas, Kivalliq Region, Nunavut; Geological Survey of Canada Current Research, 2005-B2, 10 p., URL <http://geoscan.nrcan.gc.ca/starweb/geoscan/servlet.starweb?path=geoscan/fullf.web&search1=R=220376> [September 2016], doi:10.4095/220634

McMartin, I., Byatt, J., Randour, I. and Day, S.J.A. 2015a: Report of 2015 activities for regional surficial mapping, till and stream sediment sampling in the Tehery-Wager GEM 2 Rae Project area; Geological Survey of Canada, Open File 7966, URL <http://geoscan.nrcan.gc.ca/starweb/geoscan/servlet.starweb?path=geoscan/fulle.web&search1=R=297440 > [September 2016], doi:10.4095/297440

McMartin, I., Campbell, J.E., Dredge, L.A., LeCheminant, A.N., McCurdy, M.W. and Scromeda, N. 2015b: Quaternary geology and till composition north of Wager Bay, Nunavut: results from the GEM Wager Bay Surficial Geology Project; Geological Survey of Canada, Open File 7748, URL <http://geoscan.nrcan.gc.ca/starweb/geoscan/servlet.starweb?path=geoscan/fulle.web&search1=R=296419> [September 2016], doi:10.4095/296419

McMartin, I., Day, S.J.A., Randour, I., Roy, M., Byatt, J., LaRocque, A. and Leblon, B. 2016b: Report of 2016 activities for surficial mapping and sampling surveys in the Tehery-Wager GEM-2 Rae Project area; Geological Survey of Canada, Open File 8134, 13 p., doi:10.4095/299385

McMartin, I., Randour, I., Byatt, J., Roy, M., LaRocque, A., Leblon, B., Day, S.J.A., Steenkamp, H.M. and Wodicka, N. 2016a: Overview of surficial geology activities in the Tehery-Wager GEM-2 Rae Project area, Nunavut; Geological Survey of Canada, Scientific Presentation 40, URL <http://geoscan.nrcan.gc.ca/starweb/geoscan/servlet.starweb?path=geoscan/fulle.web&search1=R=297608> [September 2016], doi:10.4095/297608

McNeely, R., Dyke, A.S. and Southon, J.R. 2006: Canadian marine reservoir ages, preliminary data assessment; Geological Survey of Canada, Open File 5049, URL <http://geoscan.nrcan.gc.ca/starweb/geoscan/servlet.starweb> [September 2016], doi:10.4095/221564

Prest, V.K., Grant, D.R. and Rampton, V.N. 1968: Glacial map of Canada; Geological Survey of Canada, A Series Map 1253A, 1:5 000 000 scale, URL <http://geoscan.nrcan.gc.ca/starweb/geoscan/servlet.starweb?path=geoscan/fulle.web&search1=R=108979> [September 2016], doi:10.4095/108979

Roy, M., Veillette, J.J., Daubois, V. and Ménard, M. 2015: Late-stage phases of glacial Lake Ojibway in the central Abitibi region, eastern Canada; Geomorphology, v. 248, p. 14–23, doi:10.1016/j.geomorph.2015.07.026

Spirito, W.A., McClenaghan, M.B., Plouffe, A., McMartin. I., Campbell, J.E., Paulen, R.C., Garrett, R.G. and Hall, G.E.M. 2011: Till sampling and analytical protocols for GEM projects: from field to archive; Geological Survey of Canada, Open File 6850, URL <http://geoscan.nrcan.gc.ca/starweb/geoscan/servlet.starweb?path=geoscan/fulle.web&search1=R=288752> [October 2016], doi:10.4095/288752

Steenkamp, H.M., Wodicka, N., Lawley, C.J.M., Peterson, T.D. and Guilmette, C. 2015: Overview of bedrock mapping and portable X-ray fluorescence spectrometry in the eastern part of the Tehery Lake–Wager Bay area, western Hudson Bay, Nunavut; *in* Summary of Activities 2015, Canada-Nunavut Geoscience Office, p. 121–134.

Steenkamp, H.M., Wodicka, W., Weller, O.M. and Kendrick, J. 2016: Overview of bedrock mapping in the northern and western parts of the Tehery Lake–Wager Bay area, western Hudson Bay, Nunavut; *in* Summary of Activities 2016, Canada-Nunavut Geoscience Office, p. 27–40.

Tschirhart, V.L., Wodicka, N. and Steenkamp, H.M. 2016: Shallow crustal structure of the Tehery Lake–Wager Bay area, western Hudson Bay, Nunavut, from potential field datasets; *in* Summary of Activities 2016, Canada-Nunavut Geoscience Office, p. 41–50.

Wodicka, N., Steenkamp, H.M., Lawley, C.J.M., Peterson, T.D., Guilmette, C., Girard, É. and Buenviaje, R. 2015: Report of activities for the bedrock geology and economic potential of the Tehery-Wager area: GEM-2 Rae Project; Geological Survey of Canada, Open File 7970, URL <http://geoscan.nrcan.gc.ca/starweb/geoscan/servlet.starweb?path=geoscan/fulle.web&search1=R=297294> [September 2016], doi:10.4095/297294

Wodicka, N., Steenkamp, H.M., Weller, O.M., Kendrick, J., Tschirhart, V.L., Peterson, T.D. and Girard, É. 2016: Report of 2016 activities for the bedrock geology and economic potential of the Tehery-Wager area: GEM 2 Rae Project; Geological Survey of Canada, Open File 8149, 21 p., doi:10.4095/299392

Preliminary interpretation of the marine geology of Frobisher Bay, Baffin Island, Nunavut

B.J. Todd[1], J. Shaw[2], D.C. Campbell[2] and D.J. Mate[3]

[1]*Natural Resources Canada, Geological Survey of Canada, Dartmouth, Nova Scotia, brian.todd@canada.ca*

[2]*Natural Resources Canada, Geological Survey of Canada, Dartmouth, Nova Scotia*

[3]*Polar Knowledge Canada, Ottawa, Ontario*

Todd, B.J., Shaw, J., Campbell, D.C. and Mate, D.J. 2016: Preliminary interpretation of the marine geology of Frobisher Bay, Baffin Island, Nunavut; *in* Summary of Activities 2016, Canada-Nunavut Geoscience Office, p. 61–66.

Abstract

The seabed of Frobisher Bay exhibits a complex topography reflecting the predominance of exposed bedrock. Superimposed on the bedrock are landforms created by the flow of grounded ice during the last glacial period. As this ice retreated, glaciomarine sediment was deposited in bedrock troughs and was subsequently overlain by postglacial mud. Areas of the seafloor were impacted by icebergs at the retreating ice margin and by the modern iceberg flux. Slope failures in the seabed sediments are numerous.

Résumé

La topographie complexe du plancher océanique de la baie Frobisher est caractérisée par la présence prépondérante de substratum rocheux exposé. Des formes de terrain superposées au substratum ont été créées par l'écoulement de la glace échouée au cours de la plus récente époque glaciaire. À mesure que la glace reculait, des sédiments glaciomarins ont été mis en place dans des auges creusées dans le substratum, puis recouverts par des boues postglaciaires. Certaines étendues de plancher océanique portent la trace d'icebergs qui se trouvaient à proximité de la marge glaciaire en recul ainsi que du passage de nombreux icebergs contemporains. De nombreuses ruptures de pente ont eu lieu dans les sédiments sur le plancher océanique.

Introduction

Frobisher Bay, Nunavut, a macrotidal inlet of the Labrador Sea in southeastern Baffin Island, is 230 km long and varies in width from 40 km at its southeastern extremity to 20 km at its northwest end (Figure 1a). Potential competing industrial uses of ocean space in Frobisher Bay, coupled with concern for habitat protection, has led to the Canada-Nunavut Geoscience Office and the Geological Survey of Canada, in partnership with Memorial University's Marine Habitat Mapping Group, ArcticNet, and the Government of Nunavut, to undertake a regional seafloor geoscience mapping program. The aim of this work is to provide new knowledge of the seabed geology, geohazards and geological processes to underpin and manage future development in the region (Mate et al., 2015).

Multibeam sonar

As part of the ArcticNet program, the CCGS *Amundsen* surveyed several adjoining swathes along transit lines within Frobisher Bay in 2006, 2007 and 2008 (Bartlett et al., 2006; Hughes Clarke et al., 2015). The vessel was equipped with a Kongsberg Maritime (formerly Simrad, Inc.) EM 302 multibeam sonar system operating at a frequency of 30 kHz. Annually from 2012 to 2015, the RV *Nuliajuk*, operated by the Nunavut Department of Environment, conducted a series of surveys to complement the CCGS *Amundsen* survey coverage (Brucker et al., 2013; Muggah et al., 2013; Hughes Clarke and Renoud, 2014; Hughes Clarke et al., 2015). The RV *Nuliajuk* was equipped with a Kongsberg Maritime EM 2040C system operating at a frequency of 200 kHz with a depth range of up to 300 m.

This publication is also available, free of charge, as colour digital files in Adobe Acrobat® PDF format from the Canada-Nunavut Geoscience Office website: http://cngo.ca/summary-of-activities/2016/.

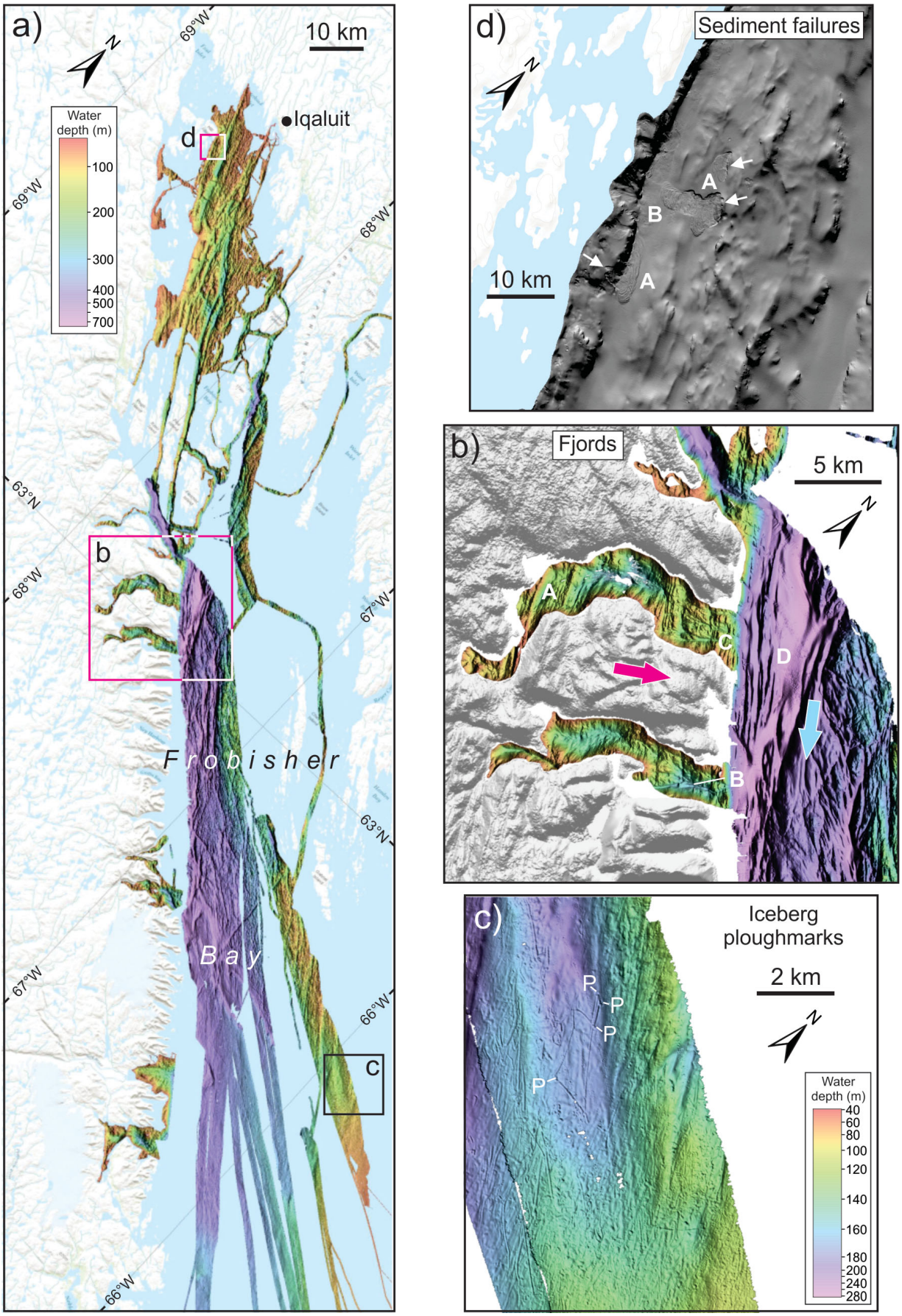
a)
10 km
Water depth (m)
100
200
300
400
500
700
Iqaluit
d
b
c
Frobisher
Bay
69°W
68°W
67°W
66°W
63°N
d)
Sediment failures
A
B
A
10 km
b)
Fjords
5 km
A
C
D
B
c)
Iceberg ploughmarks
2 km
P
P
P
P
Water depth (m)
40
60
80
100
120
140
160
180
200
240
280

Seabed morphology

This region is topographically complex, as a result of

- the strong southeast-trending bedrock structural grain;
- superimposed landforms created by fast-flowing grounded ice, trending at a slight angle to the structural grain;
- glacial landforms transverse to the structural grain, created at former ice margins;
- a drape of glaciomarine sediments deposited by meltwater plumes following ice retreat;
- areas of seafloor impacted by intensive iceberg flux soon after deglaciation;
- areas of seafloor impacted by modern icebergs;
- deposits of postglacial mud and
- submarine slope failures.

Three of these features are highlighted in Figure 1b, c and d.

Bedrock

The strong structural grain is likely imparted by rocks of the Cumberland Batholith (Steenkamp and St-Onge, 2014; St-Onge et al., 2015) that trend south-southeast (Figure 1a, b). Near the head of the bay, the bedrock ridges are shallow to <30 m in places, whereas the troughs attain maximum depths of approximately 260 m. Islands in the map area are separated by narrow troughs. At the southern end of the map area, bedrock topography demonstrates less of the south-southeast structural grain, perhaps indicative of the Lake Harbour Group (Machado et al., 2013). The channels in the south deepen to more than 600 m. Bedrock outcrops are rare on the ridged terrain because a veneer of glaciomarine mud is present.

Streamlined glacial landforms

Flow-parallel glacial landforms are created by moulding of deformable material underneath fast-flowing grounded ice. The glacial landforms occur primarily in the north of the bay, where they are commonly <1 km long and 5 m high, with a streamlined appearance, and are oriented toward the northwest, that is, they cut across the structural grain. Farther south they are longer (commonly 1.5 km), and follow the structural grain. They tend to have bedrock outcrops at the upstream end and taper to the southeast, in the form of crag and tail features. The pattern of the streamlined landforms in the north suggests that there was convergence of grounded ice into a fast flow directed down the bay to the southeast. Where ice flowed northeast from fjords to join the regional southeast flow, medial moraines and eskers are evident (Figure 1b).

Submarine moraines

Submarine moraines are deposits of ice-contact sediment, likely glacial diamicton, formed at ice margins. Two types are present: relatively long and wide moraines, and De Geer moraines. The first type extends transverse to the structural grain and ice-flow direction. They do not extend across the entire width of the bay, however, and exist as series of segments that are 1.5–6 km long and 30–50 m high, characterized by high backscatter strength. They occur either as simple ridges or as ridges with transverse streamlined ridges extending upstream from the former ice margin, along the former ice-flow direction. These transverse moraines formed when grounded ice retreating up the bay halted. The De Geer moraines consist of groups of short ridges of glacial diamicton <1 km in length, with heights of 2–10 m. De Geer moraines may indicate an incremental, perhaps annual, retreat of grounded ice in a north-northwesterly direction.

Glaciomarine sediment

Unconsolidated sediment overlies bedrock and glacial landforms in Frobisher Bay. Stratigraphically lowest is a draped veneer of glaciomarine sediment (likely gravelly sandy mud) derived from meltwater plumes during ice retreat. In troughs, the glaciomarine unit is overlain by postglacial mud.

Postglacial mud and pockmarks

Postglacial mud overlies the glaciomarine sediment and is mainly confined to the south-southeast–trending troughs. It is characterized by a smooth seafloor with little or no relief and high backscatter strength. This unit is derived from the reworking of glacial sediments and, to a lesser degree, from fluvial input. Large numbers of pockmarks are found in several concentrations in the northwestern part of Frobisher Bay. Pockmarks average 150 m in diameter and 2 m in depth. They result from the release of fluids—possibly methane—generated in the postglacial sediments.

Iceberg-impacted terrain

Iceberg-impacted terrain occurs as two classes. In the first class, intensive iceberg pitting is present in the northwest

Figure 1: a) Seabed topographic image of Frobisher Bay based on multibeam sonar mapping. Grid cell size is 10 m. The water depth colour bar is hypsometrically optimized for the water depth range in the image. Locations of parts b, c and d are shown by labelled boxes; **b)** the south coast of Frobisher Bay is characterized by fjords carved by glacial ice flowing through restricted valleys to the northeast (pink arrow), normal to the southeast-trending bedrock structural grain that is clearly defined in the bathymetric data (A); evidence of the direction of ice movement includes medial moraines (B) and eskers (C); the floor of these fjords is at approximately 200 m water depth, perched 500 m above the seafloor of Frobisher Bay (D); ice flowing out of the fjords fed the dominant southeastern ice flow within the bay (blue arrow); **c)** seafloor sediments in outer Frobisher Bay exhibit linear to curvilinear depressions tens of metres in width and kilometres in length; wallow pits are indicated by (P); **d)** this image shows that the uppermost (postglacial) unit has failed in places, creating mass transport landforms (A); the headwall escarpments (white arrows) are several metres high; some slides appear fresh whereas others exhibit subdued relief and their depositional lobes are buried (B; image courtesy of the Ocean Mapping Group, University of New Brunswick).

portion of Frobisher Bay down to depths of approximately 80 m. The pits have a degraded appearance and relief of several metres. This population of iceberg pits likely formed by icebergs originating at the grounded ice margin as it retreated northward. The second class of iceberg impacts occur in the southeastern part of the bay, are fewer in number, fresh-looking, and occur down to 200 m depth. They are mostly pits, although several long iceberg ploughmarks are present (Figure 1c). These ploughmarks were formed by the action of the keels of icebergs dragging through the seabed. Their crosscutting relationships indicate the relative ages of the ploughmarks. One iceberg left a record of abrupt changes in drift direction, associated in places with wallow pits (indicated by P in Figure 1c). This pattern is evidence of repeated groundings of the keel and subsequent drift of the iceberg in response to the driving forces of currents and wind; this process forms an ice-keel turbate (usually reworked glaciomarine sediment that is reworked by the ploughing action of ice keels, and in which the original stratigraphy is disrupted), which is colonized by benthic species after disruption. It is likely that this class of feature is a result of the modern iceberg flux.

Submarine landslides

An unusual feature of the seafloor in inner Frobisher Bay is the large number of submarine landslides (Deering et al., 2015). The slides have emanated from the western margin of the bay and from a ridge to the east, and have flowed in different directions into the intervening basin. They are commonly present on the slopes of the north-northwest–oriented ridges, and are distributed throughout the inner bay, although they are more prevalent on the west side (Figure 1d). A typical slide comprises a steep failure headwall and a low-relief, fan-shaped depositional lobe, commonly with compression ridges normal to the former flow directions. The failure surfaces may be the top of the glaciomarine sediments, and the failed material is the postglacial unit. Although many slides have a fresh appearance, others are subdued, with depositional lobes mantled by postglacial mud. In places, only the erosional chutes are found and depositional zones are completely buried. These observations suggest that failure has been occurring throughout the postglacial period, i.e., since ca. 7 ka BP.

Economic considerations

Seabed mapping is a globally recognized scientific best practice for providing information on which to base decisions about the multiple, potentially competing, uses of ocean space (Todd and Shaw, 2009; Heap and Harris, 2011; Baker and Harris, 2012, Barrie et al., 2014). Prudent management of Frobisher Bay ocean space would consider seabed geology and geohazards in the formulation of development plans that affect its ecosystem and exploitation of its resources. Developments in Frobisher Bay may include new port facilities, fibre-optic cable routes and local fisheries.

Acknowledgments

The majority of the multibeam sonar bathymetric data were collected and processed by the Ocean Mapping Group of the University of New Brunswick under the direction of J.E. Hughes Clarke. The authors thank the captains, crews and scientific staff on board the RV *Nuliajuk* and CCGS *Amundsen* during surveys of the region. J. Kennedy is thanked for co-ordinating data collection on the RV *Nuliajuk*. Financial support for this study was provided by the Canadian Northern Economic Development Agency's (CanNor) Strategic Investments in Northern Economic Development (SINED) program, the Program of Energy Research and Development (PERD) and ArcticNet. The authors thank V. Barrie, Geological Survey of Canada–Pacific, for his helpful review of the manuscript.

Natural Resources Canada, Earth Sciences Section contribution 20160201

References

Baker, E.K. and Harris, P.T. 2012: Habitat mapping and marine management; *in* Seafloor Geomorphology as Benthic Habitat: GeoHab Atlas of Seafloor Geomorphic Features and Benthic Habitats, P.T. Harris and E.K. Baker (ed.), Elsevier Insights, Amsterdam, p. 23–38, doi:10.1016/B978-0-12-385140-6.00002-5.

Barrie, J.V., Todd, B.J., Heap, A.D., Greene, H.G., Cotterill, C., Stewart, H. and Pearce, B. 2014: Geoscience and habitat mapping for marine renewable energy–introduction to the special issue; *in* Geoscience and habitat mapping for marine renewable energy, Continental Shelf Research, J.V. Barrie, B.J. Todd, A.D. Heap, H.G. Greene, C. Cotterill, H. Stewart and B. Pearce (ed.), v. 83, p. 1–2, doi:10.1016/j.csr.2014.03.014.

Bartlett, J., Beaudoin, J., Hughes Clarke, J.E. and Brucker, S. 2006: ArcticNet: the current and future version of its seabed mapping program; *in* Proceedings of the Canadian Hydrographic Conference, Halifax, Nova Scotia, June 6–9, 2006, 15 p.

Brucker, S., Muggah, J., Church, I., Hughes Clarke, J.E., Hamilton, T., Hiroji, A. and Renoud, W. 2013: Hydrographic efficiencies of operating a 19 m research platform in the eastern Canadian Arctic; *in* Proceedings, US Hydrographic Conference, New Orleans, Louisiana, March 25–28, 2013, 21 p., URL <http://ushydro.thsoa.org/hy13/pdf/0328A_06_53.pdf> [November 2016]

Deering, R., Bell, T., Forbes, D.L., Edinger, E. and Campbell, D.C. 2015: Morphology and setting of two submarine slope failures, inner Frobisher Bay, Baffin Island, Nunavut; *in* Poster abstracts, ArcticNet Annual Scientific Meeting, Vancouver, British Columbia, December 7–11, 2015, p. 25.

Heap, A.D. and Harris, P.T. 2011: Geological and biological mapping and characterisation of benthic marine environments–Introduction to the special issue; *in* Geological and biological mapping and characterisation of benthic marine environments, A.D. Heap and P.T. Harris (ed.), Continental Shelf Research, v. 31, no. 2, Supplement, p. S1–S3, doi:10.1016/j.csr.2010.09.015.

Hughes Clarke, J.E., Muggah, J., Renoud, W., Bell, T., Forbes, D.L., Cowan, B. and Kennedy, J. 2015: Reconnaissance sea-

bed mapping around Hall and Cumberland peninsulas, Nunavut: opening up southeastern Baffin Island to nearshore geological investigations; *in* Summary of Activities 2014, Canada-Nunavut Geoscience Office, p. 133–144.

Hughes Clarke, J.E. and Renoud, W. 2014: RV *Nuliajuk* seabed mapping cruise report October 18th to 31st, 2013, Pangnirtung to Iqaluit; Ocean Mapping Group, University of New Brunswick, Fredericton, New Brunswick, URL <http://www.omg.unb.ca/Projects/Nuliajuk_2013/Nu_2013_html/OMG_Nuliajuk_CHS_Leg_2013.html> [November 2013]

Machado, G., Bilodeau, C., Takpanie, R., St-Onge, M.R., Rayner, N.M., Skipton, D.R., From, R.E., MacKay, C.B., Creason C.G. and Braden, Z.M. 2013: Hall Peninsula regional bedrock mapping, Baffin Island, Nunavut: summary of fieldwork; *in* Summary of Activities 2012, Canada-Nunavut Geoscience Office, p. 13–22.

Mate, D.J., Campbell, D.C, Barrie, J.V., Hughes Clarke, J.E., Muggah, J., Bell, T. and Forbes, D.L. 2015: Integrated seabed mapping of Frobisher Bay, southern Baffin Island, Nunavut to support infrastructure development, exploration and natural-hazard assessment; *in* Summary of Activities 2014, Canada-Nunavut Geoscience Office, p. 145–152.

Muggah, J., Hamilton, T., Brucker, S., Renoud, W., Hiroji, A., Church, I. and Hughes Clarke, J.E. 2013: *Nuliajuk* 2012 mapping operations – preliminary results; Ocean Mapping Group, University of New Brunswick, Fredericton, New Brunswick, URL <http://www.omg.unb.ca/Projects/Nuliajuk_2012/Nuliajuk_html_2012/OMG_Nuliajuk_Mapping_2012.html> [November 2012]

Steenkamp, H.M. and St-Onge, M.R. 2014: Overview of the 2013 regional bedrock mapping program on northern Hall Peninsula, Baffin Island, Nunavut; *in* Summary of Activities 2013, Canada-Nunavut Geoscience Office, p. 27–37.

St-Onge, M.R., Rayner, N.M., Steenkamp, H.M. and Skipton, D.R. 2015: Bedrock mapping of eastern Meta Incognita Peninsula, southern Baffin Island, Nunavut; *in* Summary of Activities 2014, Canada-Nunavut Geoscience Office, p. 105–118.

Todd, B.J. and Shaw, J. 2009: International Year of Planet Earth 5: applications of seafloor mapping on the Canadian Atlantic Continental Shelf; Geoscience Canada, v. 36, no. 2, p. 81–94, URL <http://journals.hil.unb.ca/index.php/GC/article/view/12583/13454> [November 2016]

Permafrost studies in the Rankin Inlet and Ennadai Lake areas, southern Nunavut

G.A. Oldenborger[1], O. Bellehumeur-Génier[2], T. Tremblay[3], F. Calmels[4] and A.-M. LeBlanc[2]

[1]*Natural Resources Canada, Geological Survey of Canada, Ottawa, Ontario, greg.oldenborger@canada.ca*

[2]*Natural Resources Canada, Geological Survey of Canada, Ottawa, Ontario*

[3]*Canada-Nunavut Geoscience Office, Iqaluit, Nunavut*

[4]*Yukon Research Centre, Yukon College, Whitehorse, Yukon*

Climate change and warming conditions are occurring in the north. Any decisions concerning land-use planning, infrastructure development or community sustainability are hindered by limited publicly available geoscience information in remote regions. Between 2014 and 2018, CNGO is leading a geoscience compilation project in the Kivalliq Region, along the western coast of Hudson Bay from the Manitoba border to Rankin Inlet (NTS map areas 55D–F, K, L). The objective is to compile all existing aggregate, mineral potential, surficial geology, land cover and permafrost data for this area. Although permafrost and ground ice are important features of the landscape along the western coast of Hudson Bay, there have been few measurements of ground temperature and permafrost studies in the Kivalliq Region of Nunavut. Part of the research activity will involve the development of methods for regional characterization of permafrost conditions by integrating observations from different sources across different scales, from site-based data to remotely sensed data.

Oldenborger, G.A., Bellehumeur-Génier, O., Tremblay, T., Calmels, F. and LeBlanc, A.-M. 2016: Permafrost studies in the Rankin Inlet and Ennadai Lake areas, southern Nunavut; *in* Summary of Activities 2016, Canada-Nunavut Geoscience Office, p. 67–74.

Abstract

The western coast of Hudson Bay in the Kivalliq Region of Nunavut is undergoing significant infrastructure development associated with natural resources and community sustainability. Permafrost and ground ice are important features of this landscape and they can significantly affect land-based infrastructure. Scientific planning operations and fieldwork have been conducted in the Hamlet of Rankin Inlet and over the Kivalliq Region of Nunavut as the preliminary stage in a study to provide permafrost information and an understanding of permafrost conditions for this area. Recent fieldwork involved geomorphological observations, examination of surficial geological materials and site selection for establishment of permafrost and ground temperature monitoring stations. Initial sites in Rankin Inlet and at Ennadai Lake were instrumented with ground temperature and moisture sensors. Additional site locations have been chosen to represent a variety of conditions, including developed and undeveloped land and different geological settings. Field observations will be used for analysis of satellite-based mapping of ground movement and landscape classification, with a major objective of the work being the development of methods for regional permafrost characterization and understanding geological controls on permafrost conditions.

Résumé

La côte ouest de la baie d'Hudson dans la région du Kivalliq, au Nunavut, subit d'importantes transformations au niveau de ses infrastructures en lien avec l'exploitation des ressources naturelles et en vue d'assurer la durabilité des communautés. Le pergélisol et la glace de sol sont des éléments importants du paysage qui peuvent avoir une incidence considérable sur les infrastructures terrestres. La planification d'opérations de recherche scientifique et des travaux de terrain à Rankin Inlet et dans la région du Kivalliq, au Nunavut, ont été entrepris à titre de phase préliminaire d'un projet de recherche visant à fournir de l'information sur le pergélisol et les conditions qui le caractérisent dans la région. Les tâches accomplies au cours des plus récents travaux de terrain impliquaient la réalisation d'observations géomorphologiques, l'examen de matériaux géologiques de surface et la sélection de sites en vue de l'installation de stations de surveillance du pergélisol et de la température au sol. Les premiers sites équipés de capteurs de température et d'humidité du sol ont été installés à Rankin Inlet et au lac Ennadai. L'emplacement de sites supplémentaires s'est fait en fonction de la présence d'une variété de conditions, notamment la présence de terrains mis en valeur et non mis en valeur ou celle de différents contextes géologiques. Les observations de terrain serviront aux fins d'analyse des travaux de cartographie des mouvements de terrain au moyen de la télédétection satellitaire et de classification du paysage. L'objectif principal des recherches est de mettre au point des

This publication is also available, free of charge, as colour digital files in Adobe Acrobat® PDF format from the Canada-Nunavut Geoscience Office website: http://cngo.ca/summary-of-activities/2016/.

méthodes permettant de caractériser le pergélisol à l'échelle régionale et de mieux comprendre l'incidence des contrôles géologiques sur les conditions régissant le pergélisol.

Introduction

The western coast of Hudson Bay in the Kivalliq Region of Nunavut is undergoing significant infrastructure development associated with natural resources and community sustainability. Establishment of a road or power corridor between Manitoba and the Kivalliq Region has been under consideration for several years (Nishi-Khon/SNC-Lavalin Limited, 2007, 2010; Varga, 2014; Rogers, 2015). Permafrost and ground ice are important features of this landscape and they can significantly affect ground stability and infrastructure. Knowledge of permafrost conditions is required to characterize climate change impacts, reduce risks and aid in adaptation solutions for the region. However, there is limited historical or contemporary permafrost data along the western coast of Hudson Bay (Smith and Burgess, 2000). Although ground temperature data are often collected as part of natural resource projects, such as at Agnico Eagle Mines Limited's Meadowbank mine and advanced-stage Meliadine gold project, these data are often site specific and limited in recording period, or are not publicly accessible beyond data released in environmental assessment reports (e.g., Smith et al., 2013). Without fundamental knowledge of past and current permafrost conditions, any response of permafrost or landscape change to climate warming is difficult to establish.

A collaborative activity between the Canada-Nunavut Geoscience Office and the Geological Survey of Canada has been initiated to provide, in part, geoscience information on permafrost and landscape conditions for infrastructure and community development along the western coast of Hudson Bay (Tremblay et al., 2015; LeBlanc et al., 2016; Oldenborger et al., 2016; Short et al., 2016). Objectives of this activity include 1) collection of valuable baseline terrain and permafrost information in the Kivalliq Region of Nunavut, such as surficial geology, land cover, periglacial landforms and ground temperature; 2) development of methods for regional characterization of permafrost conditions by integrating observations from different sources across different scales, from site-based data to remotely sensed data; and 3) understanding permafrost conditions, the relationship to surficial geology and the potential response to infrastructure development and climate warming. Scientific planning operations and fieldwork have been conducted in Rankin Inlet and over the Kivalliq Region as the preliminary stage of research activity. Recent fieldwork involved geomorphological observations, examination of surficial geological materials and site selection for permafrost and ground temperature monitoring stations. Initial sites at Rankin Inlet and Ennadai Lake were instrumented with ground temperature and moisture sensors. Additional site locations have been chosen to represent a variety of conditions, including developed and undeveloped land and different geological settings. The full suite of activities will include sediment sampling, permafrost coring, and measurements of ground temperature, water content and ground movement.

Site-based observations will be used for thermal modelling and the analysis of geophysical and satellite data, which will be used for mapping ground movement and landscape classification. Better understanding of terrain conditions, ground ice occurrence, thaw susceptibility and the processes affecting permafrost will contribute to improved prediction and management of the impacts of permafrost degradation on infrastructure and community welfare in the region.

Study area

Permafrost underlies almost half of Canada's landmass and all of Nunavut (Heginbottom et al., 1995). Rankin Inlet and the western coast of Hudson Bay are within the continuous permafrost zone where 90–100% of the land area is underlain by permafrost (Figure 1). Only the most southwestern portion of the Kivalliq Region is in the extensive discontinuous permafrost zone (Figure 1). Permafrost thickness in the Rankin Inlet region has been estimated to be 200–300 m and active layer thickness may vary from 0.3–4 m depending on local ground conditions (Brown, 1978; Smith and Burgess, 2002; Genivar Inc., 2014). Mean annual ground temperature (MAGT) has been reported as –6.4 to –7.9°C from 4 to 14 m depth (Brown, 1978). Periglacial features, such as ice-wedge polygons and mudboils, have been mapped as part of the surficial geology (McMartin, 2002). Little information exists on ground ice occurrence in the region, although it is likely spatially variable and related to surficial geology and hydrology (e.g., Judge et al., 1991; LeBlanc et al., 2015).

Mean annual air temperature for 1981–2014, calculated using Environment Canada climate station data, is –10.3°C for Rankin Inlet (Environment Canada, 2015). During the same time period, mean annual air temperature has risen by 2.2°C. Similar trends are recorded for Arviat, Chesterfield Inlet and Whale Cove climate stations indicating a regional warming trend (e.g., Tremblay et al., 2015).

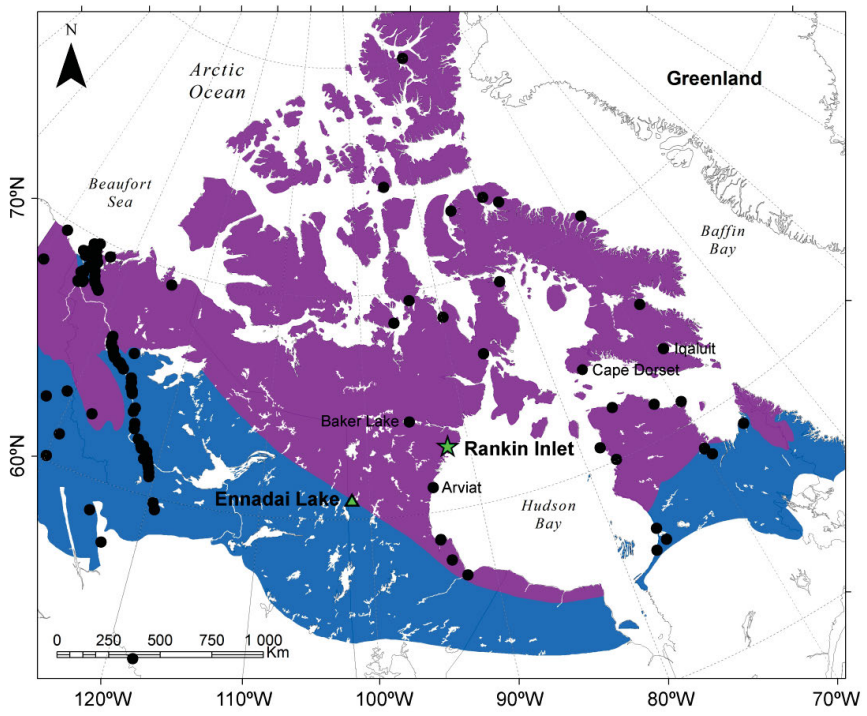

Figure 1: Map of ground temperature monitoring boreholes in the Canadian Permafrost Monitoring Network (black dots, updated from Smith et al., 2010). The Baker Lake site has been inactive since 2008. Purple is the continuous permafrost zone; blue is the discontinuous permafrost zone (extensive and sporadic; after Heginbottom et al., 1995).

Site locations

Field observations were initiated with a general survey of the landscape, taking into consideration available surficial geological mapping (McMartin, 2002) and land-cover mapping (Tremblay et al., 2015). Site visits were planned to cover a representative suite of surficial geological units and land-cover types. Site locations for ground temperature boreholes and permafrost monitoring stations in the region of Rankin Inlet were established after considering the field observations (Figure 2; Table 1) and after in-person consultation with representatives from the Hamlet of Rankin Inlet, the Government of Nunavut and the Kivalliq Inuit Association. Comments were sought from the community, but none have been received to this date beyond those received at previous engagement events (e.g., Oldenborger et al., 2016).

Two ground temperature monitoring sites (RI01, RI02) were chosen to record the thermal regime of the Rankin Inlet area both for developed and undeveloped land-use scenarios. Both sites are on marine-washed till, several metres thick, adjacent to littoral sediments consisting mostly of coarse brown sand raised beaches (McMartin, 2002). Washed till and marine sediments are considered to be representative of large portions of the western coast of Hudson Bay. Sites were chosen to avoid any unusual snow drifting. These boreholes are planned as air-track drillholes that will be completed to bedrock (or 15 m depth). Multi-thermistor cables connected to autonomous data loggers will be deployed in these holes and maintained for future generations.

In addition to permanent ground temperature monitoring borehole sites, five sites were selected for installation of shallow permafrost monitoring stations with permafrost coring and measurements of ground temperature, ground heave, thaw depth and moisture content (RI03–07). At these sites, sensors will be installed using a combination of shallow permafrost coring, water-jet drilling and hand digging of soil pits. Sites were chosen to represent different scenarios of surficial geology to allow investigations of geological controls on permafrost conditions. Sites include a raised beach ridge characterized by large-scale, ice-wedge troughs (RI03), undifferentiated till and nearshore marine sediments characterized by hummocky ground (RI04), nearshore marine sediments with a well-developed ice-wedge polygon network (RI05), littoral and offshore marine sediments (RI06) and transitional till/

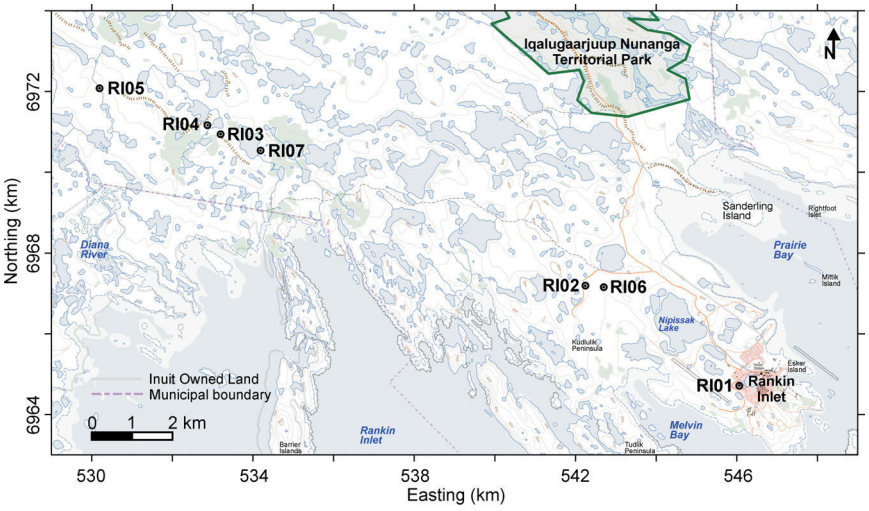

Figure 2: Site locations for permanent ground temperature monitoring stations (RI01, RI02) and shallow permafrost monitoring stations (RI03–07), Rankin Inlet area, southern Nunavut.

Table 1: Anticipated suite of observations for monitoring sites, Rankin Inlet and Ennadai Lake areas, southern Nunavut.

Site	Surficial geology[1]	Deep	Shallow	Coring	Ground temperature	Ground heave	Thaw depth	Moisture content
RI01	Mr/T.M	X			X			
RI02	Mr/T.M	X			X			
RI03	Mr		X	X	X[2]	X	X	X[2]
RI04	T.M		X	X	X	X	X	X
RI05	Mn		X	X	X	X	X	X
RI06	A.M/Mn		X	X	X	X	X	X
RI07	Mr		X	X	X	X	X	X
EL01	GL/Ab		X		X[2]			

[1]Surficial geology according to the Geological Survey of Canada Surficial Data Model (Cocking et al., 2015).

[2]Installed 2016.

Abbreviations: A, alluvial sediments - undifferentiated; Ab, alluvial sediments - blanket; GL, glaciolacustrine sediments - undifferentiated; M, marine sediments - undifferentiated; Mn, marine sediments - littoral and nearshore; Mr, marine sediments - beach; T, glacial sediments - undifferentiated.

nearshore sediments with mudboils (RI07). During site reconnaissance, sediment samples were acquired for grain size and porewater salinity analyses, and landscape/vegetation observations were recorded for verification and training of satellite-based land-cover mapping methods (Tremblay et al., 2015).

Raised beach

Of the five sites selected for shallow permafrost monitoring stations, site RI03 was chosen for the initial installation (Figure 3). Site RI03 is on a raised beach with large-scale ice-wedge troughs that do not connect into a closed polygon network. The site is dry in the summer and the topography slopes gently downhill to an adjacent valley with glaciofluvial fill. Excavation to the thaw depth revealed a thin organic layer, over medium brown eolian sand, over a littoral marine deposit consisting of well-sorted pebbly brown sand with coarse sand layers and shell fragments below 110 cm depth. Thermistors and dielectric (moisture content) sensors were installed side-by-side at the same depths in the excavated pit (Figure 4). Sensors were connected to data loggers on the surface for continuous monitoring. The current sensors will be complemented by permafrost coring and other investigations.

Ennadai Lake

In addition to Rankin Inlet, there is an interest in extending permafrost and landscape characterization to the larger Kivalliq Region. To this end, ground surface observations (from low-level flight) were made from Baker Lake to Ennadai Lake (along the Kazan River) and from Ennadai Lake to Rankin Inlet for further verification and training of satellite-based land-cover mapping methods over a larger area (Tremblay et al., 2015). A ground temperature monitoring borehole was installed at Ennadai Lake to represent the vast inland region of Nunavut, which is lacking in ground temperature data (Figure 1).

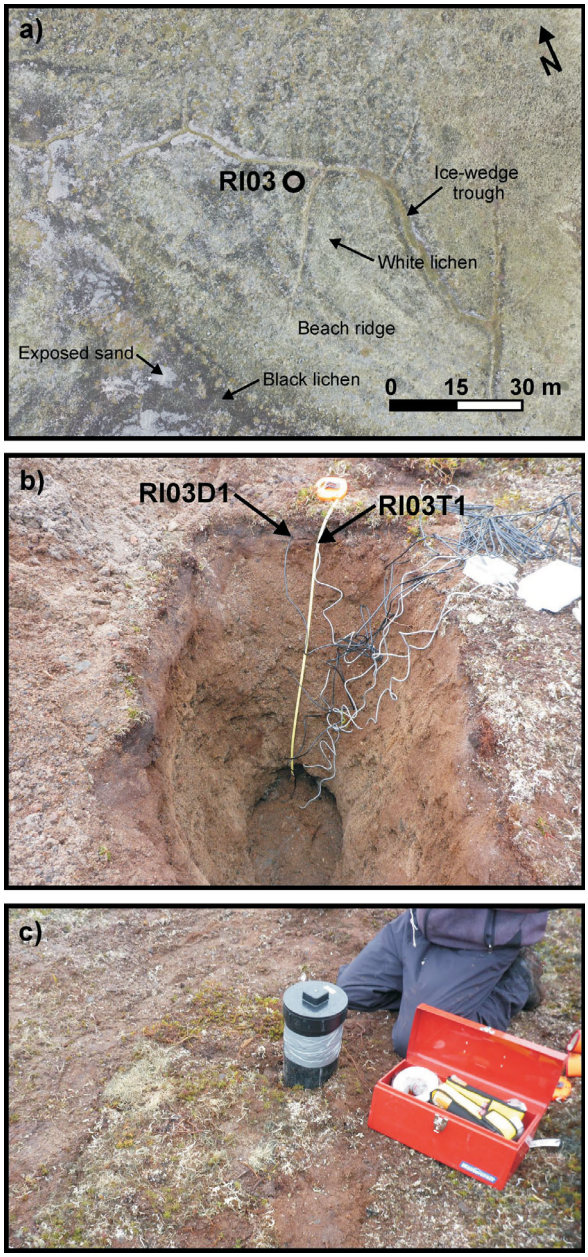

Figure 3: Rankin Inlet site RI03, Rankin Inlet area, southern Nunavut: **a)** aerial photograph of raised beach ridge with ice-wedge troughs; **b)** temperature (RI03T1) and dielectric (RI03D1) sensors installed in a pit excavated to thaw depth; **c)** filled and restored pit with data loggers (connected to sensors) at ground surface.

Site selection at Ennadai Lake was limited to the vicinity of an outpost camp, which is regularly inspected by the Government of Nunavut (Figure 5). The site falls within the extensive discontinuous permafrost zone (Figure 1). Reconnaissance observations indicated three general types of surficial geology in the immediate area: fine-grained clay/silt regions with thaw depths of <70 cm, coarser-grained sandy areas with thaw depths of >150 cm, and peatlands with peat mounds (palsa bogs and peat plateaus) with thaw

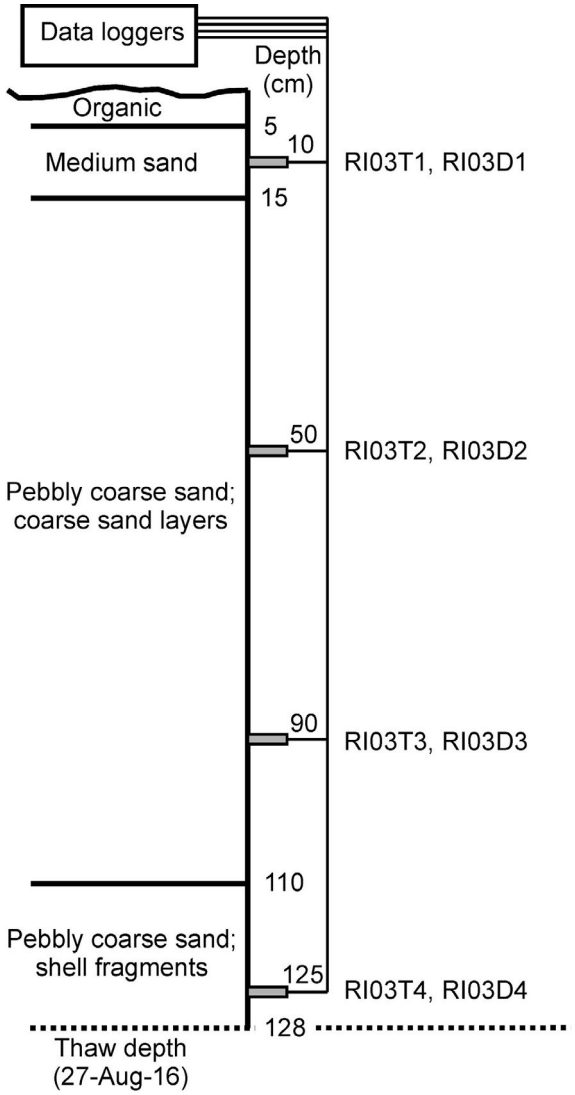

Figure 4: Schematic illustration of the sedimentary section and instrumentation at site RI03, Rankin Inlet area, southern Nunavut (NAD83, UTM Zone 15N, 533198E, 6970943N). Temperature (R103T1–4, Onset® Computer Corporation TMC6-HD) and dielectric (R103D1–4, Decagon Devices, Inc. EC-5) sensors were installed from the surface to the thaw depth, and are connected to data loggers (Onset® HOBO® U12-008 and Decagon Devices, Inc. Em50) on the surface.

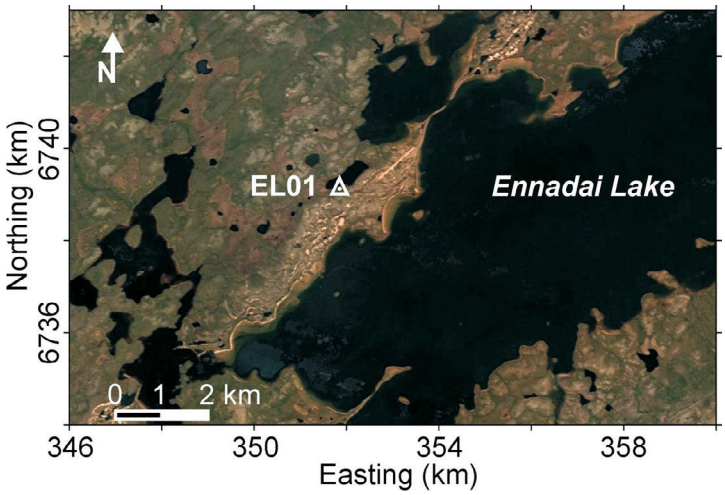

Figure 5: Location of permanent ground temperature monitoring borehole at site EL01 near Ennadai Lake, Kivalliq Region, southern Nunavut.

depths of <70 cm (Figure 6). The clay/silt deposits are interpreted to be glaciolacustrine in nature and associated with the Ennadai glacial lake on the western side of the Keewatin Ice Divide, whereas the sandy deposits are interpreted to be alluvium adjacent to esker sand and gravel (Lee, 1959; Aylsworth, 1986). Permafrost may be absent in thicker outwash material of the esker proper.

The fine-grained sediments were selected as a target for water-jet drilling of a ground temperature monitoring borehole at the forest's edge (Figure 6). A hole was completed to approximately 275 cm at which point, coarse-grained material (pebbly sand, interpreted as glaciofluvial) precluded further drilling. A prebuilt thermistor cable was housed in PVC casing and installed in the hole (Figure 7). The casing was filled with silicone oil and the thermistor cable was connected to a data logger at the surface for continuous monitoring.

Economic considerations

The western coast of Hudson Bay is a region where land-based infrastructure projects could significantly impact the local economy and community welfare. Four coastal communities are located in the region that would be served by the proposed Manitoba–Nunavut road or energy corridor. Permafrost studies provide important knowledge on landscape conditions and ground ice occurrence that may help mitigate risk associated with thaw-sensitive substrate and infrastructure instability. Installation of permanent ground temperature monitoring boreholes that will provide publicly available data will aid the Hamlet of Rankin Inlet in land-use planning both now and in the future. Extension of studies to geophysical- and satellite-based mapping will support methods of regional characterization of permafrost conditions in conjunction with site-specific geotechnical studies to provide geoscience knowledge in support of climate change preparedness and adaptation activities in Canada.

Conclusions

Scientific planning and fieldwork were conducted in Rankin Inlet and over the Kivalliq Region—the initial stage of collecting baseline terrain and permafrost information in data-poor areas of Nunavut. Fieldwork involved examination of surficial geological materials, site selection for permafrost and ground temperature monitoring stations and installation of initial permafrost monitoring equipment.

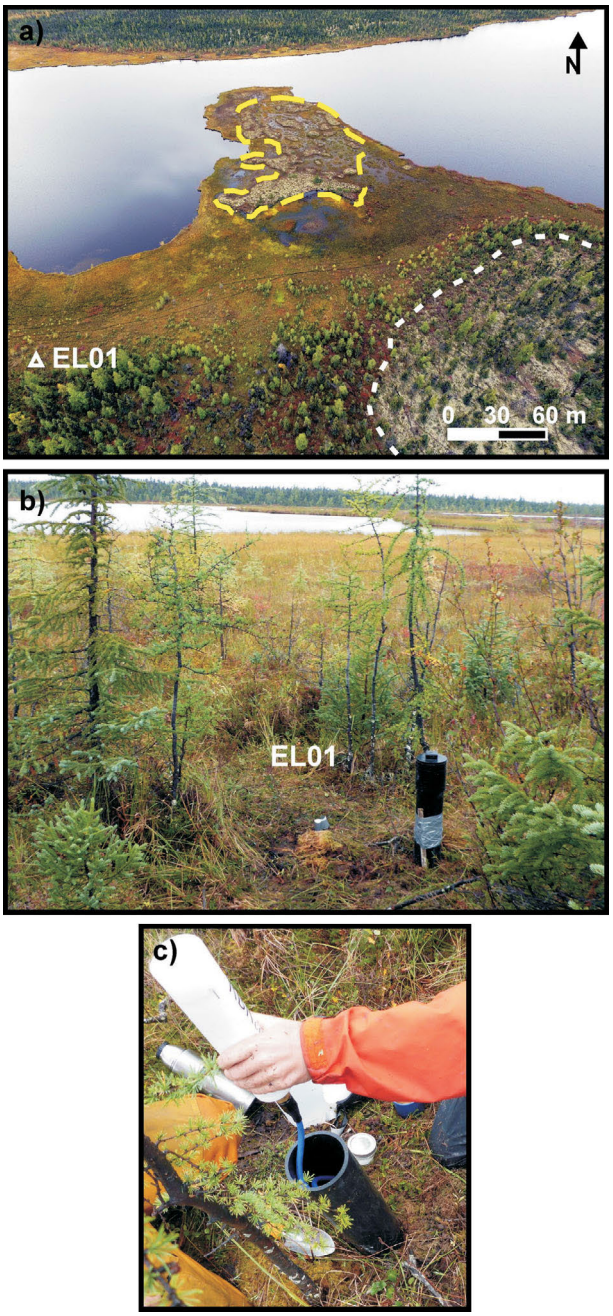

Figure 6: a) Ennadai Lake site EL01 located on glaciolacustrine clayey silt deposits adjacent to a region of peatland with frost mounds (yellow dashed line) and sandy alluvial deposits with deeper thaw depth (white dashed line), Kivalliq Region, southern Nunavut. **b)** Ground temperature monitoring borehole at site EL01. **c)** Multi-thermistor cable connected to data logger at ground surface.

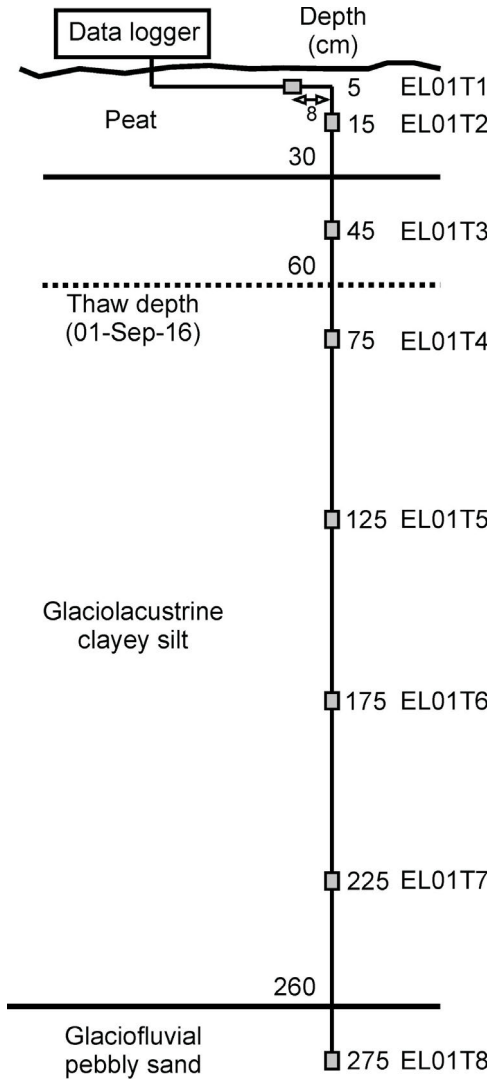

Figure 7: Schematic illustration of the sedimentary section estimated from water-jet drilling, and thermistor depths (EL01T1–8) for ground temperature monitoring borehole at site EL01, Kivalliq Region, southern Nunavut (NAD83, UTM Zone 15N, 351850E, 6739125N). The eight-thermistor cable (YSI Inc. 44033) was installed in polyvinyl chloride (PVC) casing and is connected to a data logger (RBR*concerto*) at ground surface. Thaw depth was obtained by probing.

Ground temperature and moisture content sensors were installed to 1.25 m depth in the active layer near Rankin Inlet, and a multi-thermistor cable was installed to 2.75 m depth in permafrost near Ennadai Lake.

Additional sites were chosen to represent a variety of conditions, including developed and undeveloped land and different geological settings typical of the Rankin Inlet region. These sites will be established in the coming field seasons. The full suite of observations will include sediment sampling, permafrost coring, and measuring ground temperature, thaw depth, water content and ground heave. Results will be used for thermal modelling and analysis of geophysical and satellite data for mapping of ground movement, landscape classification and understanding regional permafrost conditions.

Acknowledgments

This project is funded by the Canadian Northern Economic Development Agency's Strategic Investments in Northern

Economic Development program, the Geological Survey of Canada's Geo-mapping for Energy and Minerals program and ArcticNet. Surficial geology conversion for Rankin Inlet to the Geological Survey of Canada Surficial Data Model was completed by D.E. Kerr. Digital topographic data and Landsat 7 orthoimages were obtained from Natural Resources Canada (http://geogratis.gc.ca), licensed under the Open Government Licence of Canada. Valuable assistance was provided by R. Connelly and J. Case of the Government of Nunavut, Department of Economic Development and Transportation, A. Ymana of the Hamlet of Rankin Inlet, C. Beardsall of the Kivalliq Inuit Association, S. Napier of the Nunavut Arctic College and D. Beamer of the Government of Nunavut, Department of Environment. The thermistor cable at Ennadai Lake was installed in co-operation with Arctic Haven Wilderness Lodge, whose involvement and interest was greatly appreciated. Critical review was provided by W. Sladen.

Natural Resources Canada, Earth Sciences Sector contribution number 20160211

References

Aylsworth, J.M. 1986: Surficial geology, Ennadai Lake, District of Keewatin, Northwest Territories; Geological Survey of Canada, Preliminary Map 5-1985, scale 1:125 000.

Brown, R.J.E. 1978: Influence of climate and terrain on ground temperatures in the continuous permafrost zone of northern Manitoba and Keewatin district, Canada; *in* Proceedings of the Third International Conference on Permafrost, Edmonton, Alberta, July, 1978, p. 15–22.

Cocking, R.B., Deblonde, C., Kerr, D.E., Campbell, J.E., Eagles, S., Everett, D., Huntley, D.H., Inglis, E., Laviolette, A., Parent, M., Plouffe, A., Robertson, L., St-Onge, D.A. and Weatherston, A. 2015: Surficial data model, version 2.1.0: revisions to the science language of the integrated Geological Survey of Canada data model for surficial geology maps; Geological Survey of Canada, Open File 7741, 276 p.

Environment Canada 2015: Canadian climate normals; Environment Canada, <http://climate.weather.gc.ca/climate_normals/index_e.html> [August 2015].

Genivar Inc. 2016: Geotechnical, topographical and environmental assessment for the new arena in Rankin Inlet, NU: final report; *in* Government of Nunavut Request for Proposals, Architectural/Engineering Services — New Arena, Rankin Inlet, Nunavut, Government of Nunavut Department of Community and Government Services, Annex 9.2, 149 p.

Heginbottom, J.A., Dubreuil, M.H. and Harker, P.T. 1995: Canada, Permafrost; National Atlas of Canada, 5th ed., Plate 2.1, MCR 4177.

Judge, A.S., Tucker, C.M., Pilon, J.A. and Moorman, B.J. 1991: Remote sensing of permafrost by ground-penetrating radar at two airports in Arctic Canada; Arctic, v. 44, p. 40–48.

LeBlanc, A.-M., Bellehumeur-Génier, O., Oldenborger, G.A. and Tremblay, T. 2016: Understanding permafrost conditions through integration of local and traditional observations with geoscience data in the vicinity of Rankin Inlet, western Hudson Bay, Nunavut; Canada-Nunavut Geoscience Office, Summary of Activities 2016, p. 75–88.

LeBlanc, A.-M., Oldenborger, G.A., Short, N., Sladen, W.E., Allard, M. and Mathon-Dufour, V. 2015: Ground temperatures and spatial permafrost conditions in Iqaluit, Baffin Island, Nunavut; Canada-Nunavut Geoscience Office, Summary of Activities 2015, p. 161–170.

Lee, H.A. 1959: Surficial geology of southern district of Keewatin and the Keewatin Ice Divide, Northwest Territories; Geological Survey of Canada, Bulletin 51, 42 p.

McMartin, I. 2002: Surficial geology, Rankin Inlet, Nunavut; Geological Survey of Canada, Open File 4116, scale 1:50:000.

Nishi-Khon/SNC-Lavalin Limited 2007: Nunavut-Manitoba route selection study: final report; unpublished report prepared for Kivalliq Inuit Association, 69 p. plus appendices, URL <https://www.gov.mb.ca/mit/transpolicy/tspd/pdf/route_selection_study.pdf> [October 2016].

Nishi-Khon/SNC-Lavalin Limited 2010: Building lasting infrastructure: the case for the Nunavut-Manitoba highway (Nunavut-Manitoba all-weather road business case); unpublished report prepared for Nunavut Department of Economic Development and Transportation and Manitoba Infrastructure and Transportation, 60 p., URL <http://www.gov.nu.ca/sites/default/files/Nunavut_Manitoba_Road_Business_Case.pdf> [October 2016].

Oldenborger, G.A., LeBlanc, A.-M., Bellehumeur-Génier, O., Grosset, C., Holzman, S., Masson, C. and Tremblay, T. 2016: Community workshop on permafrost and landscape change, Rankin Inlet, Nunavut; Geological Survey of Canada, Open File 8057, 31 p.

Rogers, S. 2015: Manitoba–Nunavut hydro link is economically viable: study; Nunatsiaq News, October 6, 2015, URL <http://www.nunatsiaqonline.ca/stories/article/65674manitoba-nunavut_hydro_link_economically_viable_study/> [October 2016].

Short, N., LeBlanc, A.-M. and Bellehumeur-Génier, O. 2016: Seasonal surface displacement derived from DInSAR, Rankin Inlet, Nunavut; Geological Survey of Canada, Canadian Geoscience Map 291 (preliminary), scale 1:35 000.

Smith, S. and Burgess, M.M. 2000: Ground temperature database for northern Canada; Geological Survey of Canada, Open File 3954, 28 p.

Smith, S. and Burgess, M.M. 2002: A digital database of permafrost thickness in Canada; Geological Survey of Canada, Open File 4173, 38 p.

Smith, S.L., Riseborough, D.W., Ednie, M. and Chartrand, J. 2013: A map and summary database of permafrost temperatures in Nunavut, Canada; Geological Survey of Canada, Open File 7393, 20 p.

Smith, S.L., Romanovsky, V.E., Lewkowicz, A.G., Burn, C.R., Allard, M., Clow, G.D., Yoshikawa, K. and Throop, J. 2010: Thermal state of permafrost in North America: a contribution to the international polar year; Permafrost and Periglacial Processes, v. 21, p. 117–135.

Tremblay, T., Kendall, M.S., LeBlanc, A.-M., Short, N., Bellehumeur-Génier, O., Oldenborger, G.A., Budkewitsch, P. and Mate, D.J. 2015: Overview of the surficial geology map compilation, RapidEye land-cover mapping and permafrost studies for infrastructure in the western Hudson Bay area, Nunavut; Canada-Nunavut Geoscience Office, Summary of Activities 2015, p. 145–160.

Varga, P. 2014: GN renews commitment to Manitoba road and hydro link; Nunatsiaq News, November 3, 2014, URL <http://www.nunatsiaqonline.ca/stories/article/65674gn_renews_commitment_to_manitoba_road_and_hydropower_link/> [October 2016].

Understanding permafrost conditions through integration of local and traditional observations with geoscience data in the vicinity of Rankin Inlet, western Hudson Bay, Nunavut

A.-M. LeBlanc[1], O. Bellehumeur-Génier[2], G.A. Oldenborger[2] and T. Tremblay[3]

[1]*Natural Resources Canada, Geological Survey of Canada, Ottawa, Ontario, anne-marie.leblanc@canada.ca*

[2]*Natural Resources Canada, Geological Survey of Canada, Ottawa, Ontario*

[3]*Canada-Nunavut Geoscience Office, Iqaluit, Nunavut*

Climate change and warming conditions are occurring in the north. Any decisions concerning land-use planning, infrastructure development or community sustainability are hindered by limited publicly available geoscience information in remote regions. Between 2014 and 2018, CNGO is leading a geoscience compilation project in the Kivalliq Region, along the western coast of Hudson Bay from the Manitoba border to Rankin Inlet (NTS map areas 55D–F, K, L). The objective is to compile all existing aggregate, mineral potential, surficial geology, land cover and permafrost data for this area. Although permafrost and ground ice are important features of the landscape along the western coast of Hudson Bay, there have been few measurements of ground temperature and permafrost studies in the Kivalliq Region of Nunavut. Part of the research activity will involve the development of methods for regional characterization of permafrost conditions by integrating observations from different sources across different scales, from site-based data to remotely sensed data.

LeBlanc, A.-M., Bellehumeur-Génier, O., Oldenborger, G.A. and Tremblay, T. 2016: Understanding permafrost conditions through integration of local and traditional observations with geoscience data in the vicinity of Rankin Inlet, western Hudson Bay, Nunavut; *in* Summary of Activities 2016, Canada-Nunavut Geoscience Office, p. 75–88.

Abstract

This paper is a follow-up to a mapping workshop held in Rankin Inlet in February 2016 that focused on collecting local and traditional observations on permafrost in the region. A field campaign was held in August 2016 to visit areas of interest identified by the workshop participants. Using a multidisciplinary approach, the workshop and field observations were combined with existing geoscience data to characterize permafrost in the area. Visits to observation sites established at the workshop led to the validation of the occurrence of a number of permafrost-related features or phenomenon that provide important insight into ground conditions and the relationship to the surficial geology of the area. Geoscience data presented in this paper include DInSAR satellite imagery, historic water levels and climate records. The analysis carried out showed that surficial geology units of undifferentiated till and marine sediments along with nearshore marine sediments exhibit the greatest degree of subsidence based on the DInSAR mapping results and thus present a higher potential for containing ground ice. It was determined that all water bodies experience surface area variability, but large (>14000 m^2) and small (>3500 m^2) water bodies exhibit the most numerous occurrences of lake growth.

Résumé

Le présent rapport découle d'un exercice de cartographie qui a eu lieu à Rankin Inlet en février 2016, visant à compiler des observations de savoir traditionnel et local relatives au pergélisol dans la région. Une campagne de terrain, tenue en août 2016, avait pour objectif de visiter les sites correspondant aux observations des participants. Le recours à une approche multidisciplinaire combinant des données géoscientifiques aux données recueillies sur le terrain et pendant l'atelier a fait en sorte que les caractéristiques propres au pergélisol de la région ont pu être établies. Les visites aux sites identifiés par les participants de l'atelier ont permis de valider la présence de multiples caractéristiques de terrain et phénomènes liés au pergélisol. Ces constatations ont fourni d'importantes informations sur les conditions du sol et le lien avec la géologie de surface dans la région. Les données géoscientifiques présentées dans ce rapport incluent des analyses d'imagerie satellite DInSAR, de changements dans la superficie des étendues d'eaux et de données climatiques. Les résultats démontrent que les unités de géologie de surface constituées de till non différencié et de sédiments marins et celles constituées de sédiments marins littoraux sont les plus susceptibles au tassement, ainsi que le démontrent les cartes établies à l'aide des données DInSAR, et pourrait potentiellement renfermer de la glace dans le sol. La superficie de toutes les étendues d'eaux analysées

This publication is also available, free of charge, as colour digital files in Adobe Acrobat® PDF format from the Canada-Nunavut Geoscience Office website: http://cngo.ca/summary-of-activities/2016/.

fait preuve d'un certain degré de variabilité, mais les plus grands (>14000 m^2) et plus petits (>3500 m^2) plans d'eau présentent le plus souvent une tendance à la hausse.

Introduction

Knowledge of ground temperature and permafrost conditions is limited for the western coast of Hudson Bay and the Kivalliq Region of Nunavut (Smith and Burgess, 2000). Infrastructure and community development will require an investment in geoscience information on permafrost to ensure sustainability in the face of climate warming. This paper is a follow-up to a mapping workshop held in Rankin Inlet in February 2016 that focused on collecting local and traditional observations on permafrost in the region (Oldenborger et al., 2016). The majority of landscape observations from the workshop were related to water, slope movement, erosion, ground ice and vegetation. There were observations of water-level changes in rivers, lakes, ponds and streams identified at every mapping session. Subsidence, water pooling and building damage were observed in developed areas of the hamlet. Although there are recognizable signs that the landscape is changing every year, specific changes were most often identified as occurring within the last 5–10 years. This time frame coincides with increased land use and development, including the lengthening and maintenance of access trails.

A field campaign was held in August 2016 to visit areas of interest identified by the workshop participants. Workshop and field observations were combined with additional geoscience data, including surficial geology, DInSAR imagery, satellite images, airphotos, historic water levels and climate records. Analysis of the integrated data allowed limited interpretation of permafrost conditions and a number of land associations to be made with terrain-associated elements, such as surficial geology, hydrology and topography.

Study site

The study area is located in the Kivalliq Region of Nunavut, in the vicinity of Rankin Inlet (Figure 1). The western coast of Hudson Bay lies in the continuous permafrost zone, where 90–100% of the ground surface is underlain by permafrost (Heginbottom et al., 1995). In this region, active-layer thickness is highly variable, ranging from 3 to 400 cm, and permafrost is estimated to be 300–500 m thick (Brown, 1963, 1978; Smith et al., 2005a). Permafrost in the study area often contains high salinity levels ranging from 3.5 to 30 ppt, which can increase the unfrozen water content and thereby decrease the strength of the underlying permafrost (Hivon and Sego, 1993, 1995). The presence of closed and open taliks in the Rankin Inlet area is expected under small yet deep lakes as well as under large and deep lakes, respectively (Golder Associates Ltd., 2014).

The average mean annual air temperature (MAAT) recorded at Rankin Inlet Airport from 1982 to 2012 was –10.3°C (Environment Canada, 2015). During the same time period, MAAT increased by 2°C at an average rate of 0.068°C/year, demonstrating a progressive warming of the climate in the region. The trend in climate warming observed along the western coast of Hudson Bay is similar to that recorded at Arviat, Chesterfield Inlet, Baker Lake and Whale Cove weather stations (Environment Canada, 2015). The landscape is dominated by tundra vegetation, with a winter snow cover in natural terrain that is limited to 25–45 cm and generally windblown (Brown, 1978; Smith et al., 2005a; Throop et al., 2012). Ice-rich permafrost and ground ice are commonly found in marine sediments that have been deposited in low-lying areas. At those locations, numerous periglacial features, such as ice-wedge polygons, patterned ground and mud boils can be found (McMartin, 2002). Recent studies have projected changes to permafrost distribution in Hudson Bay due to increases in the MAAT and loss of sea-ice cover (Gagnon and Gough, 2005a, b; Zhang, 2013; Tam, 2014).

Methodology

Local and traditional observations

Observations of changes to permafrost features and landscape were collected at a participatory mapping workshop held in Rankin Inlet in February 2016. Details of the mapping sessions, data compilation and locations of the observations can be found in Oldenborger et al. (2016). For the purpose of this paper, results of the workshop were sorted into five categories of observations: water-level changes, ground movement and/or ground ice, slope movement, vegetation, and other observations.

To investigate and study the observations made by workshop participants, site visits were performed in August 2016 for all sites that were accessible by foot or a short all-terrain vehicle (ATV) ride. At each site, the area was evaluated in an attempt to match the specific local and/or traditional observation from the workshop with the evidence presented by the surficial geology, permafrost conditions and processes, or landscape change in the vicinity of the original observation.

Geoscience data

Surficial geology

The surficial geology of the region was mapped by Aylsworth et al., (1981) at a scale of 1:250 000 for the western coast of Hudson Bay and by McMartin (2002) at a scale of 1:50 000 for the Rankin Inlet area. Both these maps, re-

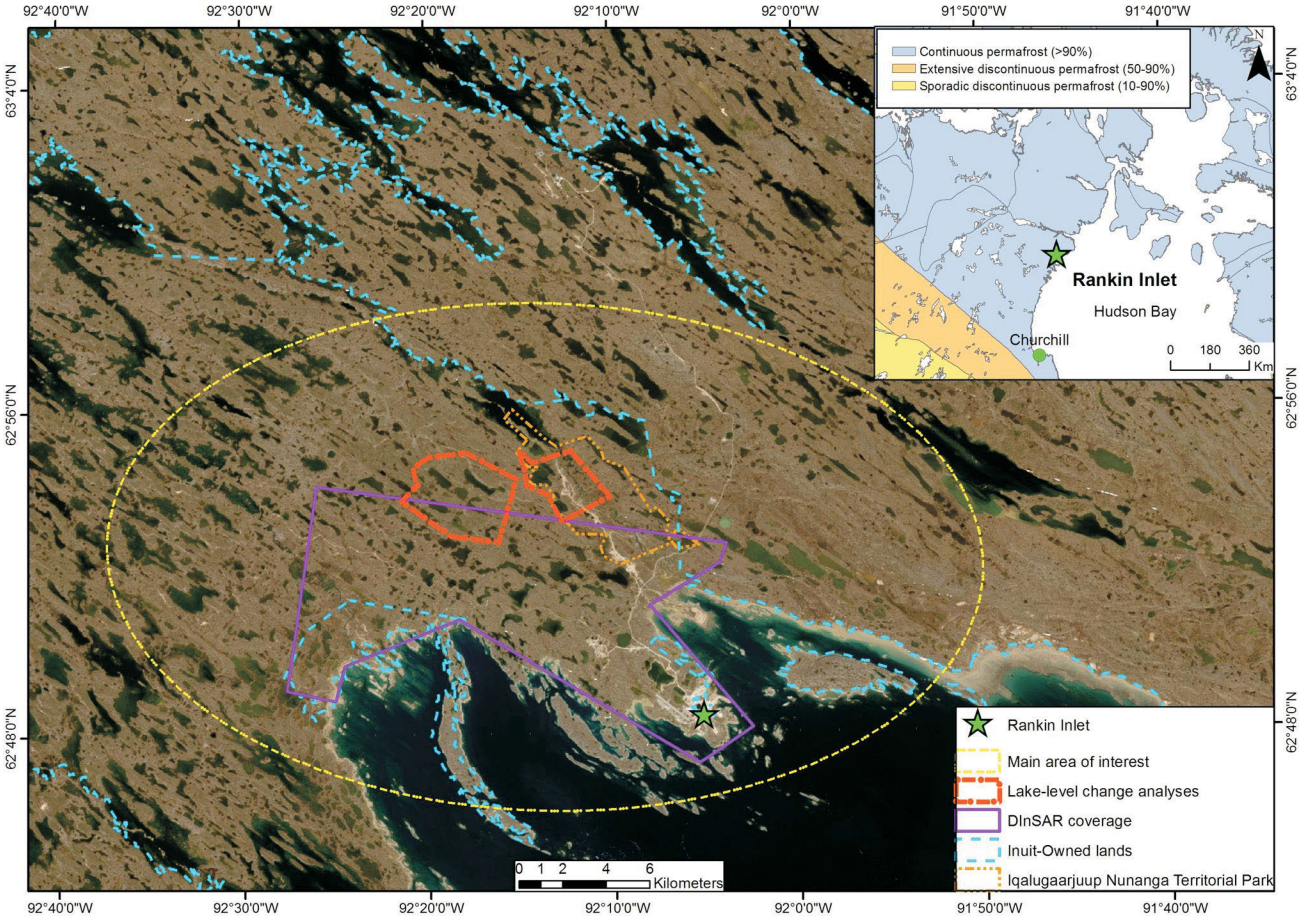

Figure 1: Main area of interest in the Kivalliq Region of Nunavut, covering both the locations of the workshop observations and the zones selected for water-level change analyses. Inset map displays the permafrost zones (after Heginbottom et al., 1995); base map courtesy of the United States Geological Survey (United States Geological Survey, 2016).

cently updated to conform to Surficial Data Model v. 2.1 (Geological Survey of Canada, in press a, b) following the legend from Cocking et al., (2015), were used for this study (Table 1). Landforms, such as retrogressive thaw slumps, solifluction lobes, ice-wedge polygons, palsa-like features and hummocky ground, identified by McMartin (2002) and, to a lesser extent, by Aylsworth et al. (1981), were used for the purpose of comparing them to the local observations made by the workshop participants.

The surficial geology of each workshop observation site was identified by matching observation areas and the surficial maps and visually cross-referencing them. Often, more than one type of surficial geology unit occurred within the observation area. In these cases, the surficial geology was listed in order of importance. In some cases, observation sites fell outside of the area covered by available detailed or regional surficial maps.

DInSAR

Seasonal surface displacement for the area of Rankin Inlet was derived using differential interferometric synthetic aperture radar (DInSAR) data collected in the summer of 2015 (Short et al., 2016), On the DInSAR map, locations where displacement was within the expected range of error (±1.0 cm) represented stable ground; subsidence in the order of 1.0 to 14.0 cm generally represented downward displacement. Other possible causes of apparent downward displacement could be downward movement of a surficial aquifer or sediment erosion. A surface uplift of 1–5 cm represented upward displacement and accounted for only 0.3% of the total coverage of the DInSAR map. Areas of no data resulted from a loss of interferometric signal coherence, which is typically caused by the presence of water, a significant ground-surface disturbance or a relatively smooth surface.

Local observation areas, DInSAR results and surficial geology integrated in a GIS were displayed simultaneously for assessment. Local displacement values derived from DInSAR data were extracted for each observation site. In some cases, observation sites fell outside of the area covered by the DInSAR satellite imagery. Displacement was assessed in conjunction with surficial geology and the expected behaviour of material types (Short et al., 2016).

Table 1: Surficial geology units found in the Kivalliq Region of Nunavut and their descriptions (from Cocking et al., 2015).

Surficial geology units[1]	Description[1]
T	Till undifferentiated
T.M	Undifferentiated till and marine sediments
Tb	Till blanket
Tv	Till veneer
Tr	Ridged moraine
Th	Hummocky till
M	Marine sediments undifferentiated
Mr	Beach sediments
Md	Deltaic sediments
Mi	Intertidal sediments
Mn	Nearshore sediments
A	Alluvial sediments undifferentiated
A.M	Undifferentiated alluvial and marine sediments
GF	Glaciofluvial sediments
GF2	Subaqueous outwash fan sediments
GFh	Hummocky sediments
GFc	Ice-contact sediments
O	Organic
R	Bedrock undifferentiated
R2	Igneous bedrock, plutonic

[1]Surficial geology units and description from Cocking et al. (2015)

Lake-size analysis

Lake-size comparison was performed in a GIS using historical airphotos and satellite imagery in combination with climate data. Two areas of interest were selected based on the likelihood that thermokarst would be present (as indicated by the surficial geology, geomorphological evidence and lake density), the airphoto spatial and/or temporal coverage, and the satellite imagery spatial coverage. Thermokarst results from the combination of processes that alter the landscape following the melting of ground ice, which can cause lake expansion or lake drainage (van Everdingen, 2005; Kokelj and Jorgenson, 2013). The two main areas of interest were located within and west of the Iqalugaarjuup Nunanga Territorial Park (Figure 1), and were chosen prior to the community mapping exercise.

Airphotos were orthorectified on National Topographic System maps prior to analysis with a root-mean–square error varying between 0.4 m and 3 m. The airphotos used in these analyses were taken in July and August 1954, 1965, 1969, 1975, 1986 and 1992. The satellite images, taken in June and July, consisted of a WorldView-2 image from 2014 and DigitalGlobe Inc. imagery from 2005 available in Google Earth Pro™. Lakeshore limits were digitized manually for each year for which data were available, with an estimated human error factor of ±10 m^2 from the actual shoreline, resulting in estimation errors that are likely on the order of tens of square metres. For small regions, manual interpretation and mapping of water bodies on time series of rectified aerial photographs and recent high-resolution imagery have proven to be more reliable than semi-automatic remote-sensing techniques (Kokelj and Jorgenson, 2013).

Compiled results were then assessed against a control year (1954) and the differences calculated. These were then rounded to the nearest 10 m^2 to account for human error and to be expressed as a percentage for ease of comparison. Lakes were divided into three categories according to their size: large (>14000 m^2), medium (>3000 m^2) and small (<3000 m^2).

Climate analysis

A climate database was created from meteorological data collected from 1981, when the record began, to 2014 (Environment Canada, 2015), to assess whether lake-size differences were due to seasonal precipitation trends or to thermokarst expansion. For airphoto and satellite images taken after 1981, the average total precipitation was calculated for the two months prior to the date the image was taken to assess precipitation anomalies for these specific times. The values for snow depth days were also calculated to compare snow-cover behaviour (Table 2).

Table 2: Summary of climate data for 1986, 1992, 2005 and 2014 recorded at the Environment Canada (Environment Canada, 2015) weather station in Rankin Inlet, Nunavut.

Photo date	Historical average total precipitation (mm)[1]	Total precipitation (mm)[2]	Snow depth days (cm/d)[3]	Total rainfall (mm)[4]	Total snowfall (cm)[4]	Total precipitation (mm)[4]	Conditions[5]
09/08/1986	52	58	6492	186	185	356	wet
24/07/1992	61	19	9101	140	127	265	wet
29/08/2005	91	54	6157	155	305	460	dry
21/06/2014	40	22	7916	152	92	244	dry

[1]Represents the average of the total precipitation for the two months prior to the date the photo was taken from 1981 to 2015

[2]Represents the total precipitation for the two months prior to the date the photo was taken

[3]Snow depth days values for the winter season preceding the picture date (hydrological year: October to August)

[4]Calendar year annual value for the date the photo was taken

[5]Assumed groundwater conditions for the picture varying from dry to wet

Results

Water-level changes

Of the 56 workshop observation locations identified, 17 were related to water-level changes (Figure 2a), and more precisely to low water levels occurring within the last 5–10 years (Table 3). Lakes associated with this type of observation are commonly found on undifferentiated till and marine sediments (T.M; Table 1; Cocking et al., 2015) and glaciofluvial sediments (GFc, GFh, GF2), whereas rivers flow over alluvial sediments (A). Less than half of these observation sites overlap with DInSAR-derived values of surface displacement at the river or lakeshore; results vary between stable terrain and downward displacements of up to 10 cm. Stable terrain is associated with GFc, GFh, GF2, marine beach sediments (Mr) and T.M, when bedrock (R) is found in the vicinity. Highest displacements are associated with T.M, and occasionally marine nearshore sediments (Mn) and GFh with GFh.T. The origin of DInSAR-identified displacement close to a water body is difficult to assess due to surface aquifer movement and sediment erosion, which cause signal incoherence in the DInSAR results.

As indicated in Table 3, among the observations of low water levels, three were associated with large lakes (Nipissak [11[4]], Qamanaarjuk [also known as Little Meliadine; 21–22] and Meliadine [25]) and five with small lakes or ponds (Sandy lake [13] and ponds west of it [14], Sanderling Island [35], as well as east and southwest of Rankin Inlet [41 and 54]). Analysis of low water levels excluded lakes affected by human activity, such as Williamson lake (10; see Table 3) and other lakes that were drained for construction purposes.

Lake-size analysis with respect to meteorological data showed that there was no obvious continuous trend from 1954 to 2014 with the exception of large lakes (Figure 3). Small and medium lakes showed more variability than large lakes, although small lakes peaked in 1986 and thereafter remained higher than the control year. In contrast, workshop observations noted that small and large lakes had decreased in size (low water levels) over the last ten years. Except for 1975, there was a general trend toward an increase in large lake size from 1954 to 2014. However, the number of large lakes considered in the analysis was smaller compared to that of medium and small lakes.

Nipissak Lake (11; see Table 3), which is the potable-water reserve for Rankin Inlet, was not included in the lake-size analysis, but results by Budkewitsch et al. (2011) updated to 2014 using DigitalGlobe Inc. WorldView imagery indicate that the surface of the lake has decreased by 18% between 2005 and 2014, whereas it was stable between 1972 and 2005. First Landing lake, northwest of Nipissak Lake, has remained more or less the same between 1972 and 2009 with a slight increase (2%) in surface size between 2005 and 2009, followed by a decrease of 1% in 2014 (Budkewitsch et al., 2011). Climate data suggest that the conditions were relatively wet in the summers of 1986 and 1992, and relatively dry in summer 2005 and spring 2014 (Table 2).

Ground movement and ground ice

Subsidence, ground ice and muddy conditions accounted for 16 of the observations (Table 4; Figures 2b–e). The most common surficial unit on which these observations were found was T.M. This unit was often associated with the highest displacement values in the observation areas. Remaining observations were associated with surficial units such as Mn and till blanket (Tb), which also exhibit high displacement. One observation of ground movement (Rankin Inlet area 8; Table 4) was associated with Mr, which are typically stable. Within the Hamlet of Rankin Inlet, more than half of the observation areas occurred in regions identified as stable by the DInSAR data. This apparent lack of association between observed ground movement and DInSAR displacement values may be related to modification of surface conditions by addition of fill material (e.g., roads and gravel pads), which results in higher stability compared to natural conditions in typically unstable terrain (Short et al., 2016).

Observations of ice-wedge polygons collected at the workshop were associated with marine nearshore sediments (Mn) and, to a lesser extent, with Mr, undifferentiated till (T), T.M and Tb. Ice-wedge polygons were also mapped by McMartin (2002) at the same two areas as those identified by workshop participants (Table 4). Other observations of ground ice by workshop participants were notably associated with glaciofluvial sediments (GF). In addition to Mn, McMartin (2002) identified Mr, glaciofluvial sediments (GF), organic cover (O) and T.M as supporting ice-wedge polygons. On site visits, no ground ice was identified at the locations identified by the participants, but landforms such as palsas and erosion of river banks and/or at lakeshores were observed.

Slope movement

Landslides (slope movement; Figures 2f–h), identified by participants are presented in Table 5, although many observations fell outside of the mapped area (7 of the 11 observations) and DInSAR coverage (10 of the 11 observations). Two of the three landslides identified by participants were mapped by McMartin (2002) as gelifluction lobes occurring in T and in T.M, and gelifluction lobes were observed during field visits on various types of surficial units. The third landslide in the Rankin Inlet area (16) occurred within A. Inactive active-layer detachment scars were also ob-

[4]*Numbers in brackets refer to the location of observations in Oldenborger et al. (2016).*

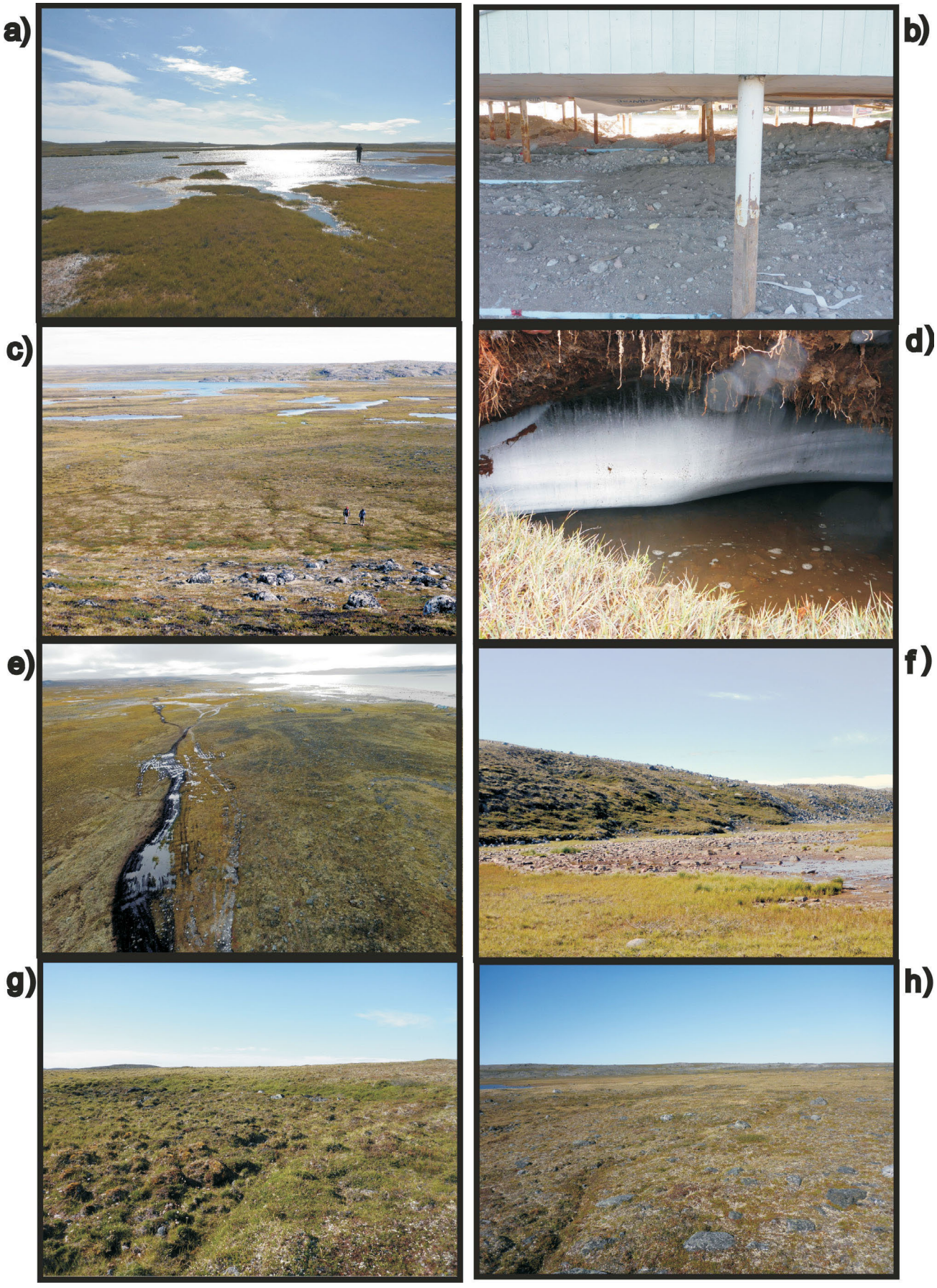
a)
b)
c)
d)
e)
f)
g)
h)

Table 3: Observations of water-level changes by participants in the Rankin Inlet workshop, and associated geoscience data.

Locations[1]	Observations	Surficial geology[2]	DInSAR results[3]
Josephine River (1)	Low water level causing fish death	n/a	n/a
Josephine River (2)	Low water level; river bank erosion	n/a	n/a
Rankin Inlet area 6 (5)	Historical lakes within the Hamlet limits; drained prior to infrastructure construction	T.M, Mn, A.M	Between stable and displacements of -6 cm
Rankin Inlet, Williamson lake area (10)	Lake size reduced	T.M	Eastern side of the lake is mostly stable (in T.M with bedrock outcrop in the vicinity), western side of the lake has displacements between -2.5 and -7 cm (in T.M)
Nipissak Lake (11)	Low water levels in recent years	T.M, GFh.T, Mr	Surrounding areas of the lake are stable stable (in GFh.T and Mr) or have displacements of up to -10 cm (in T.M and GFh.T)
Sandy lake (13)	Low water levels in Sandy lake, especially during the last five years; past shorelines exposed; adjacent esker stable	GFc	n/a, but should be stable according to close displacement values in GFc
Rankin Inlet, Sandy lake area (14)	Ponds west of Sandy lake are drying out	Mn, T.M, GF2, Tv	Displacements between -1 to -10 cm (highest displacements at the contact of Mn and T.M)
Qamanaarjuk[4] (21)	Increased exposure of island; water level decrease	GFc	n/a
Qamanaarjuk[4] (22)	River coursing earlier in spring	GFh	n/a
Meliadine Lake (25)	Low water level	n/a	n/a
Diana River (27)	Low water level in the last five years; adjacent creek now dry	A, Tr	n/a
Diana River (30)	low water level in recent years; still areas of strong current and deep water	A, T.M	Surrounding areas of the river fall between stable and displacements of -10 cm
Barrier Islands (33)	Low seawater level; more land exposed in the last ten years	T.M, R	n/a
Sanderling Island (35)	Low water level in ponds; dryer conditions in last 30 years; mud cracks	Mi, GFc, Mr	n/a
(East) Rankin Inlet (41)	Lakeshore erosion, shrinking ponds, increased snow thickness, change of predominant wind to the northeast	n/a	n/a
Southwest of Rankin Inlet (54)	Low water level	Tb, Mr, A[5]	n/a
Southwest of Rankin Inlet (55)	Low water level in ponds; dryer conditions in last ten years	n/a	n/a

[1]Numbers in parentheses refer to the location of observations in Oldenborer et al. (2016)
[2]Geological Survey of Canada (in press a)
[3]Short et al. (2016); negative values correspond to downward displacements
[4]Also known as Little Meliadine lake
[5]Geological Survey of Canada (in press b)
Abbreviation: n/a, not available

served at locations identified by the participants (Figures 2g, h).

Vegetation

Two types of observations related to vegetation were noted by workshop participants (Table 6): vegetation has changed from green to brown (decrease in vegetation productivity) and willow height has increased (increase in vegetation productivity). The change in vegetation colour east of Rankin Inlet (37) spans a wide range of surficial geology units; the northern sector is dominated by T.M, whereas the southern sector is mainly Mr and R. At the location of increased willow height west of Rankin Inlet (51), the surficial geology is also variable, but consists mainly of till and bedrock units (T.R). In both areas, the highest displacements are often associated with T.M and Mn, whereas stable terrain includes Mr and R units.

Figure 2: Field photographs from various workshop observation sites near Rankin Inlet and Iqaluit: **a)** possible pond expansion through active thermokarst processes on marine sediments; **b)** shifting of pile structure at the Taparti Centre in the hamlet; **c)** ice-wedge polygon network; **d)** frost blister in the Niaqunguk River watershed near Iqaluit; **e)** ponding water and erosion of an ATV track; **f)** gelifluction lobes on the side of an esker; **g)** active-layer detachment scar with regrown vegetation near Qamanaarjuk (also known as Little Meliadine lake); **h)** active-layer detachment scar with regrown vegetation near the Char River.

Other observations

Half of the observations in the 'other' category was related to water bodies: flooding, water temperature and winter

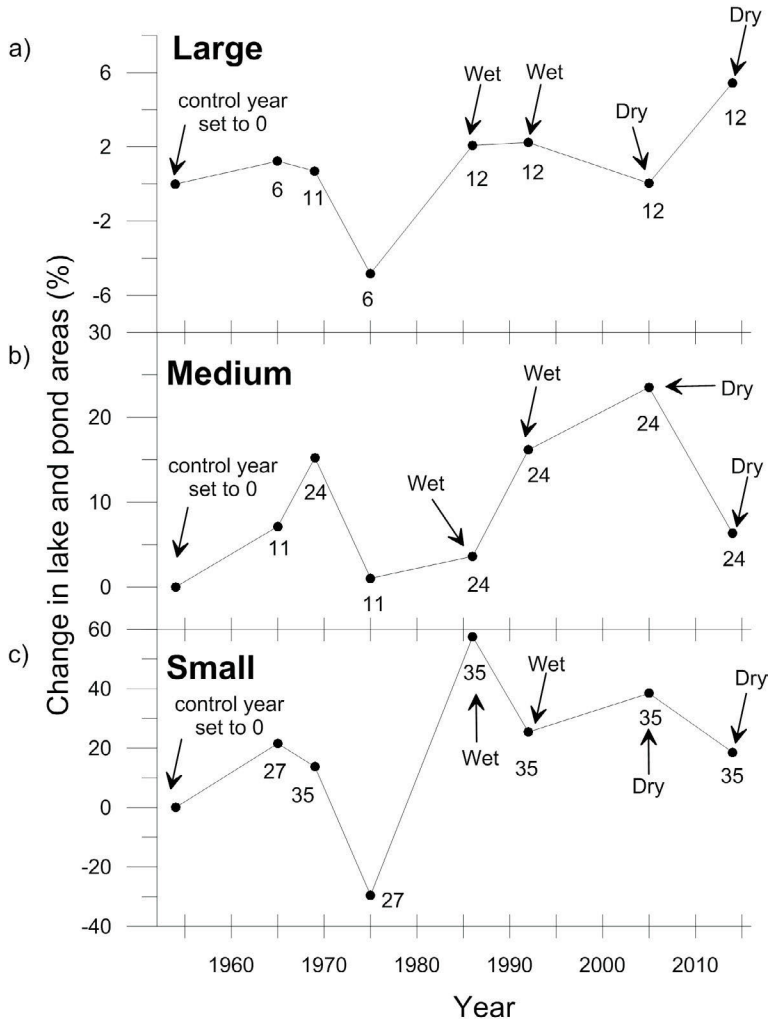

Figure 3: Percentage change in surface area from 1954 to 2014 for **a)** large, **b)** medium and **c)** small lakes. The number below the data point represents sample size. Wet and dry annotations refer to analysis in Table 2 of climate data recorded at the weather station at Rankin Inlet, southern Nunavut.

conditions (Table 7). First Landing lake (12), an alternative potable-water source for Rankin Inlet, covers primarily T.M, whereas rivers (Meliadine [17–18], Diana [28–29] and Char [32]) flow mainly over A. Other observations reported include the presence of the water table near the surface in the aggregate quarry, warming of a historical food cache, road damage by flooding and perennial snow (Table 7). Surficial geology at these locations is variable. Available displacement data over the region show that stable terrain is often associated with R and Mr and higher displacements with T.M and Mn, which correlation is commonly observed between surficial geology and displacement.

Discussion

Shoreline changes may be due to anthropogenic alteration of water levels or drainage patterns, changes in the precipitation regime or active thermokarst processes. Based on lake-size analysis, large lakes displayed the clearest pattern of expansion from 1954 to 2014. Medium lakes showed variability with a general low water level in the last decade. Small lakes showed oscillations of water levels with a high plateau in the late 1980s, followed by a rapid drop in the last decade. The latter two patterns agreed with local observations of low water levels in the recent past and the recognition that changes are annual (Oldenborger et al., 2016). The variation of small and medium lake areas according to whether the year was wet or dry suggested that their dynamics may be driven by precipitation conditions over the last decade. Low water levels could also have resulted from external factors, such as melting of ice-wedge networks in the surrounding ground and the formation of drainage pathways (Kokelj and Jorgenson, 2013).The increase in surface area observed for the large lakes was inconsistent with both local observations and the climatic trend of dry conditions. This may be a reflection of the small number of large lakes included in the analysis, a lower sensitivity of large lakes to annual precipitation events and/or a bias on the part of on-

the-ground observers to notice changes in smaller lakes. The shoreline error introduced by manual digitization also has a greater effect on the analysis of small lakes in comparison to large lakes and could influence the results.

Anthropogenic effects are important in the case of Nipissak Lake, for which the volume reductions prior to 2014 were attributed to inefficient water use and increased water demand from a growing community (FSC Architects and Engineers, 2010; Budkewitsch et al., 2011). In contrast, nearby First Landing lake was more or less stable, showing only a slight increase in surface size in recent years (Budkewitsch et al., 2011). Some large lakes such as Nipissak, First Landing and Qamanaarjuk (also known as Little Meliadine) are deep enough (6.9, 17.6 and <8 m, re-

Table 4: Observations of ground movement and ground ice by participants in the Rankin Inlet workshop.

Locations[1]	Observations	Surficial geology[2]	DInSAR results[3]
Rankin Inlet area 5 (3)	Buildings need levelling to adjust to ground movement	T.M, Mr	Most of the buildings are in an area that falls between stable and displacements of up to -2.5 cm (in Mr, T.M). Small areas of displacements between -2.5 and -4 cm under buildings (in T.M)
Rankin Inlet area 6 (4)	Ground movement causing the houses to shift shortly after construction (during the last five years)	T.M, Mn, Mr, A.M	Most of the area falls between stable and -1 to -2 cm (in Mr, T.M, Mn), but some areas have displacements up to -6 cm (in T.M and Mn) and up to -8 cm (in A.M, undeveloped area)
Rankin Inlet (cemetery) (6)	Subsidence of graves in the cemetary in the last 10-15 years	Mi	Most of the cemetery is stable, small areas of displacements between -1 and -2.5 cm
Rankin Inlet (8)	Shifting of residential pile structure	Mr	Half of the area is stable, the second half is showing displacement between -2.5 and -6 cm (some infrastructures are located in this area)
Rankin Inlet (9)	Ground movement causing damage to municipal pipe system	T.M, R	Most of the area is stable (in R, T.M), small areas of displacements between -1 to -4 cm (in T.M)
Iqalugaarjuup Nunanga Territorial Park (15)	Numerous ice-wedge polygons; stable	Mn	Most of the displacements between -4 to -10 cm with some areas showing less than -4 cm. One particular polygon has displacements between -6 and -10 cm at its centre. Cohence lost in the general area
Qamanaarjuk[4] (19)	Exposed visible ice in the ground	T.M, Tb, T, R	n/a
Qamanaarjuk[4] (20)	Ground ice exposed along creeks	T.M, T	n/a
Qamanaarjuk[4] (24)	Relocation of ATV trail from northern to southern side of the lake due to muddy conditions in the last 10-15 years	Tb, T.M, Th, GFh	n/a
Barrier Islands (34)	Exposed visible ice	R	n/a
(East) Rankin Inlet (38)	The land has become muddy during recent years	n/a	n/a
(East) Rankin Inlet (39)	Exposed visible ice in mounds surrounded by sediment	T.M, Mr, Mi, Mn, R, R.Mr, A.M	n/a
(Northeast) Rankin Inlet (47)	Increased difficulty travelling overland by ATV	n/a	n/a
Caribou valley and west of Rankin Inlet (50)	Ice-wedge polygons; change in drainage following construction of access trail	T.M, Mr, Mn, Tb	Area falls between stable (in Mr) and displacements up to -8 cm (in Mn, Tb, T.M). Ice-wedge polygons are located in Mn with some areas with displacement of -8 cm
(Southwest) Rankin Inlet (52)	Ground subsidence along ATV trail; furrows filled with rocks need to be re-filled as rocks sink	Mr, Tb, GFc (north) and T.M, A.M (south)	The northern site falls between stable (in Mr, GFc) and displacements up to -4 cm (in Tb). Data n/a for the southern site
Southwest of Rankin Inlet (56)	Exposed visible ice with soil cover; feature dimensions are roughly 1.8 m by 2.4 m by 0.6 m high	R, Tb, GFc, Mr, A, Tr[5]	n/a

[1]Numbers in parenthesis refer to the location of observations in Oldenborer et al. (2016)

[2]Geological Survey of Canada (in press a)

[3]Short et al. (2016) / negative values correspond to downward displacements

[4]Also known as Little Meliadine lake

[5]Geological Survey of Canada (in press b)

Abbreviation: n/a, not available

Table 5: Observations of slope movement by participants in the Rankin Inlet workshop.

Locations[1]	Observations	Surficial geology[2]	DInSAR results[3]
Rankin Inlet area (esker) (16)	Landslide	A	Displacements between -1 and -4 cm
Qamanaarjuk[4] (23)	Landslide; mud	T	n/a
Meliadine Lake area (26)	Landslide	n/a	n/a
Thompson Island (36)	Landslide; wet gentle slope	n/a	n/a
(East) Rankin Inlet (42)	Landslide	n/a	n/a
(East) Rankin Inlet (43)	Lanslide; exposed visible ice	n/a	n/a
(East) Rankin Inlet (44)	Landslide	n/a	n/a
(East) Rankin Inlet (45)	Landslide; muddy area	n/a	n/a
(East) Rankin Inlet (46)	Slope movement	T.M	n/a
(Northeast) Rankin Inlet (49)	Landslide, muddy area and ice-wedge polygons	n/a	n/a
Southwest of Rankin Inlet (53)	Landslide	Tb, GFc, Mr, A[5]	n/a

[1]Numbers in parenthesis refer to the location of observations in Oldenborer et al. (2016)

[2]Geological Survey of Canada (in press a)

[3]Short et al. (2016) / negative values correspond to downward displacements

[4]Also known as Little Meliadine lake

[5]Geological Survey of Canada (in press b)

Abbreviation: n/a, not available

spectively; Budkewitsch et al., 2011) to maintain taliks that can contribute to lateral lake expansion (Jorgenson et al., 2010) and subsequently to lake drainage (Smith at al., 2005b). Field observations along lakeshores suggested that pond and/or lake expansion does exist in the vicinity of Rankin Inlet but is most likely a rare phenomenon (Figure 2a).

Many observations of low water levels are also located on the coast or on islands along the coast. Relative sea level is falling in the region at a rate of approximately 6.4 mm/year due to crustal uplift that is outpacing sea-level rise (Allard et al., 2014). A falling relative sea level combined with active beach-production processes could account for observations of low water levels close to the sea and in rivers and connecting ponds.

Open water throughout the winter along with bubbles present at the lake surface have been reported by workshop participants at First Landing lake, which has a maximum depth of 17.6 m (Budkewitsch et al., 2011). In particular situations, methane emissions (bubbles) from an unfrozen lake bottom to the surface can prevent ice formation (e.g., Boereboom et al., 2012); however, methane emissions are typically released from lake sediments containing a significant amount of organic material. First Landing lake is surrounded by T.M, which could contain a small amount of organic material at its surface, but this might not be sufficient to explain the open water and bubbles in winter time.

Ground subsidence observations could be linked to active-layer thickening and thaw settlement due to the recent climate warming. Although the DInSAR results only refer to data from one summer, they can be used to infer permafrost

Table 6: Observations of vegetation change by participants in the Rankin Inlet workshop.

Locations[1]	Observations	Surficial geology[2]	DInSAR results[3]
(East) Rankin Inlet (37)	The summer vegetation has changed colour from green to brown making it harder to predict change of season	T.M, Tv, Mr, Mn, Mi, R, R.Mr, Tb, A.M (western sector); data n/a for the eastern sector	For most of the area n/a. The small portion with data (western sector) falls between stable (in Mr, Tv, and some areas of T.M) and displacements of -9 cm (in Mn)
(West) Rankin Inlet (51)	Increase in willow height from 0.3 m in the past to 1.2 m currently	T.M, R, Tv, R.Mr, R.T, Tb, A.M, Mr	Area falls between stable (in R, R.MR, Mr) and displacements up to -8 cm (in T.M, Tb, R.T, Tv, A.M)

[1]Numbers in parenthesis refer to the location of observations in Oldenborer et al. (2016)

[2]Geological Survey of Canada (in press a)

[3]Short et al. (2016) / negative values correspond to downward displacements

Abbreviation: n/a, not available

Table 7: Other observations by participants in the Rankin Inlet workshop.

Locations[1]	Observations	Surficial geology[2]	DInSAR results[3]
Rankin Inlet (quarry) (7)	Aggregate quarry: coarse gravel underlain by fine sand; water table 2 m below ground surface, level with top of sand	Mr, R.Mr, R, Tv	Most of the area is stable (in R, R.Mr and Mr) with an area of displacement between -2.5 and -6 cm (in Tv)
First Landing lake (12)	The lake is not totally frozen during winter and there are bubbles present at the lake surface in the open water	T.M (also surrounded by Mi, Mn, Mr, R)	Area falls between stable (in R, Mr and Mi) and displacements up to -10 cm (in T.M and Mn)
Meliadine River (17)	Unusal ice build-up on the river during winter months that raised the surface up to 3.7 m; occurred only twice in the last 30 years, both times in the last 5 years	A, Md, T.M, GFf2, Tv	Data n/a for the northern part of the Meliadine River. On the shore and islands of the river, southern part and Meladine River mouth, displacements are mostly beetween -2.5 and -6 cm with localized areas of -9 and -10 cm
Meliadine River (18)	Warmer water temperature	A, Md, T.M, GFf2, Tv	For the northern part of the Meliadine River. On the shore and islands of the river, southern part and Meladine River mouth, displacements are mostly beetween -2.5 and -6 cm with localized areas of -9 and -10 cm
Diana River (28)	At least one event of flowing water on top of river ice in winter months that flooded an important area adjacent to the river	A, Tr, T.M, Mn, Tb	n/a
Diana River (29)	Historical food-cache site not cold enough since the last 7-8 years	A, Tr, Tb, T.M	n/a
Rankin Inlet area - Diana River access road (31)	Access road to Diane river washed away during summer 2015	T.M, Mr	The access road is mostly stable with some areas of displacements between -1 and -7 cm. In surrounding terrain, falls between stable (in Mr) and displacements up to -8 cm (in T.M)
Char River (32)	Bridge damaged by flooding	A, Mn, Mr, GFh, Mi	Most of the area surrounding the river is stable. Some areas have displacements between -1 and -7 cm (in A)
(East) Rankin Inlet (40)	Perennial snow	T.M, Mr, Mi, Mn, R, R.Mr, A.M	n/a
(Northeast) Rankin Inlet (48)	Shrinking of perennial snow patch	n/a	n/a

[1]Numbers in parenthesis refer to the location of observations in Oldenborer et al. (2016)
[2]Geological Survey of Canada (in press a)
[3]Short et al. (2016) / negative values correspond to downward displacements
Abbreviation: n/a, not available

conditions when combined with information on the surficial geology and the ground conditions; they therefore constitute an effective tool in identifying potential ice-rich and thaw-sensitive terrain (Short et al., 2014). However, ground movement can also be the result of frost heave, especially when dealing with piles and municipal pipes, yet problematic infrastructures observed during field visits were not associated with high DInSAR displacement values (Figure 2b).

Besides ice-wedge polygons (Figure 2c), no other observations of ground ice were made during site visits. The workshop observations of ground ice were located at creeks or lakes and the workshop descriptions were consistent with frost blisters (Figure 2d). Frost blisters are not perennial features and this might explain why no ground ice was encountered during field visits. Erosion and water ponding along ATV tracks was observed in the field associated with a surficial layer of fine-grained (marine) sediment in low-lying areas (Figure 2e). The amount of traffic on those trails is unknown, but the general degradation of the path and the surficial material might suggest a disturbance of the active layer causing deeper summer thaw.

Slope movements observed during the site visits were attributed to active-layer detachments, gelifluction lobes and frost-creep slopes (Figure 2f–h). The active-layer detachment scars were identified downslope of an esker in fine-grained sediment underlain by till or by a river bank adjacent to the esker, on low-lying slopes. They are now covered by vegetation and are evidence of past disturbance in the active-layer thickness and drainage (Figure 2g, h). Gelifluction and frost-creep slopes were observed on a large variety of surficial units, from tills to marine deposits,

and are probably still active. The active-layer detachment scars could also be the product of a thermal disequilibrium at the surface of the permafrost that might have caused deeper thaw of the active layer. Therefore, it is possible that these events were triggered in a similar time period that might have coincided with the onset of climate warming in the eastern Arctic.

An increase in tundra greenness (increase in vegetation productivity) in Canada's high-latitude regions and Alaska has been observed for the last three decades (1984–2012) using remote-sensing data (Ju and Masek, 2016). However, tundra 'browning' (decrease in vegetation productivity) has been reported for the past 2–4 years throughout the Arctic (Epstein et al., 2015). This recent observation seems to corroborate the workshop observations regarding change in vegetation colour. Remote-sensing data show that the decrease in seasonal greenness (browning) is greatest in the far northern Canadian Arctic Archipelago and is less pronounced in the Rankin Inlet area (Epstein et al., 2015). However, localized greening was also observed by workshop participants (increase of willow height), although no precise time frame for this greening has been determined (Table 6). Willow height could be associated with long-term tundra greening prior to 2011 or it could indicate a disparity between local field observations and satellite remote-sensing data (Epstein et al., 2015). In general, vegetation change shown on remote-sensing products can result from climatic or nonclimatic related factors, such as changes in open water in the summer, summer air temperature, snow cover, freeze-thaw events or impacts from wildfires, drained lakes and industrial infrastructure (Epstein et al., 2015). Topography, glacial history and soil conditions have also been reported as environmental factors that need to be taken into account when considering the issue of greenness change (Ju and Masek, 2016).

Economic considerations

Permafrost is an important factor in infrastructure development, planning and maintenance in Canada's North. Few permafrost maps and monitoring stations cover the study area. Therefore, the development of a collective understanding of permafrost characteristics and past and present dynamics for the vicinity of Rankin Inlet is important for decision makers and local inhabitants. An all-weather road that would connect the four coastal communities of the Kivalliq Region to the national road system in Manitoba has been proposed and a better knowledge of ground-ice content proxies along the western coast of Hudson Bay would be of great importance for the development of such infrastructure. Better knowledge of permafrost characteristics in the region would also provide vital information regarding future behaviour of the ground in the context of a warming climate, which will enable local communities to prepare resilience plans for infrastructure and prevent possible ground hazards.

Conclusions

The majority of the sites identified by the workshop participants in the vicinity of Rankin Inlet were visited in August 2016. During those visits, thermokarst ponds, gelifluction lobes, frost-creep slopes, shifting of pile structures in urban areas, increased wetness on ATV tracks and active-layer detachment scars were identified. No active or recent permafrost related landslides were observed and the active-layer detachment scars were the only evidence of slope movement identified. This could attest to a period of high activity in the area that might have disturbed the thermal regime of permafrost and affected an ice-rich layer near the frost table; however, further investigation is required to assess the timing of events. None of the participants' ground-ice observations were noted during the field visits, but the environmental settings at the locations displayed a favourable environment for the development of ice blisters, which are a nonperennial ice-rich feature.

The juxtaposition of geoscience data and traditional and/or local knowledge has proven useful in initiating permafrost studies in the area of Rankin Inlet. Regardless of the type of observations, the study revealed that surficial units of T.M and Mn are of particular interest for permafrost characterization due to their wide distribution in the region, their recurring association with workshop observations of ground ice and ground movement, and their association with high DInSAR displacement values. Lakes in the study area have shown oscillations in the size of their surface area, probably linked to precipitations patterns. Although, the lake-size analyses revealed an increasing trend in small and large lakes that is asynchronous with the recent yearly precipitation patterns, this trend might coincide with the start of climate warming in the eastern Arctic in the 1990s. Further investigation will be required to validate many of the hypotheses put forth herein and to clearly establish links between local and traditional observations and permafrost conditions.

Acknowledgments

The authors would like to thank all the workshop participants who generously shared their knowledge and observations of the land. Assistance from the Rankin Inlet Hamlet office, the Kivalliq Inuit Association, the Hunter and Trappers Association of Rankin Inlet, the Nunavut Arctic College and the Government of Nunavut was much appreciated. The authors also thank D. Kerr of the Geological Survey of Canada, who provided up-to-date surficial geology maps for the region. This research is a partnership between the Geological Survey of Canada and the Canada-Nunavut Geoscience Office. The authors also want to ac-

knowledge critical reviewers P. Morse and L. Ham for their constructive comments on the paper.

Financial support for this project was provided by the Geomapping for Energy and Minerals program, Phase 2 (GEM-2) of the Geological Survey of Canada and the Strategic Investments in Northen Economic Development (SINED) program delivered by the Canadian Northern Economic Development Agency (CanNor).

Natural Resources Canada, Earth Sciences Sector contribution number 20160210

References

Allard, M., Manson, G.K. and Mate, D.J. 2014: Reconnaissance assessment of landscape hazards and potential impacts of future climate change in Whale Cove, southern Nunavut; *in* Summary of Activities 2013, Canada-Nunavut Geoscience Office, p. 171–182.

Aylsworth, J.M., Boydell, A.N. and Shilts, W.W. 1981: Surficial geology, Tavani, District of Keewatin, Northwest Territories; Geological Survey of Canada, Preliminary Map 9-1980; scale 1: 125 000, doi:10.4095/109695

Boereboom, T., Depoorter, M., Coppens, S. and Tison J.-L. 2012: Gas properties of winter lake ice in northern Sweden: implication for carbon gas release; Biogeosciences, v. 9, p. 827–838.

Brown, R.J.E. 1963: Relation between mean annual air and ground temperatures in the permafrost region of Canada; *in* Proceedings of the Permafrost International Conference, Lafayette, Indiana, November 1963, p. 241–246.

Brown, R.J.E. 1978: Influence of climate and terrain on ground temperatures in the continuous permafrost zone of northern Manitoba and Keewatin district, Canada; *in* Proceedings of the Third International Conference on Permafrost, Edmonton, Alberta, July 1978, v. 1, p. 15–21.

Budkewitsch, P., Prévost, C., Pavlic, G. and Pregitzer, M. 2011: Description of water depth survey datasets from Rankin Inlet, Nunavut; Geological Survey of Canada, Open file 6751, 47 p., doi: 10.4095/288667

Carey, K.L. 1973. Icings developed from surface water and ground water; Engineer Research and Development Centre, Cold Regions Science and Engineering Laboratory, Monograph 3-D3.

Cocking, R.B., Deblonde, C., Kerr, D.E., Campbell, J.E., Eagles, S., Everett, D., Huntley, D.H., Inglis, E., Laviolette, A., Parent, M., Plouffe, A., Robertson, L., St-Onge, D.A. and Weatherston, A. 2015: Surficial Data Model, version 2.1.0: revisions to the science language of the integrated Geological Survey of Canada data model for surficial geology maps; Geological Survey of Canada, Open File 7741, 276 .

Environment Canada 2015: Canadian climate normals; Environment Canada, URL <http://climate.weather.gc.ca/climate_normals/index_e.html> [November 2016].

Epstein, H.E., Bhatt, U.S., Raynolds, M.K, Walker, D.A., Bieniek, P.A., Tucker, C.J., Pinzon, J., Myers-Smith, I.H., Forbes, B.C., Macias-Fauria, M., Boelman, N.T. and Sweet, S.K. 2015: Tundra greenness; *in* Arctic Report Card: Update for 2015, National Oceanic and Atmospheric Administration, URL < http://arctic.noaa.gov/Report-Card/Report-Card-2015/ArtMID/5037/ArticleID/221> [November 2016].

FSC Architects and Engineers (FSC) 2010: Water supply capacity, consumption and conservation study, Rankin Inlet, NU; prepared for the Government of Nunavut, Department of Community and Government Services, FSC Project 2009-1310.

Gagnon, A. and Gough, W.A. 2005a: Trends in the dates of ice freeze-up and breakup over Hudson Bay, Canada; Arctic, v. 58, no. 4, p. 370–382.

Gagnon, A. and Gough, W.A. 2005b: Climate change scenarios for the Hudson Bay region: an intermodel comparison; Climate Change, v. 69, p. 269–297.

Geological Survey of Canada, in press a: Surficial geology, Rankin Inlet, Nunavut, NTS 55-K/16; Geological Survey of Canada, Canadian Geoscience Map 68 (preliminary, Surficial Data Model v2.1 conversion of Open File 4116), scale 1:50 000.

Geological Survey of Canada, in press b: Reconnaissance surficial geology, Tavani, Nunavut, NTS 55-K: Geological Survey of Canada, Canadian Geoscience Map 244 (preliminary, Surficial Data Model v2.1 conversion of Map 9-1980), scale 1:125 000.

Golder Associates Ltd. 2014: Meliadine Environmental Impact Statement (FEIS)–Meliadine Gold Project, Nunavut; Golder Associates Ltd., Report Number Doc 288-1314280007.

Heginbottom, J.A., Dubreuil, M.A. and Harker, P.T. 1995: Canada: Permafrost; National Atlas of Canada, Fifth Edition, Natural Resources Canada, MCR 4177.

Hivon, E.G. and Sego, D.C. 1993: Distribution of saline permafrost in the Northwest Territories, Canada; Canadian Geotechnical Journal, v. 30, p. 506–514.

Hivon, E.G. and Sego, D.C. 1995: Strength of frozen saline soils; Canadian Geotechnical Journal, v. 32, p. 336–354.

Jorgenson, M.T., Romanovsky, V., Harden, J., Shur, Y., O`Donnel, J., Schuur, A.G.E., Kanevskiy, M. and Marchenko, S. 2010: Resilience and vulnerability of permafrost to climate change; Canadian Journal of Forest Research, v. 40, p. 1219–1236.

Ju, J. and Masek, J.G. 2016: The vegetation greenness trend in Canada and US Alaska from 1984–2012 Landsat data; Remote Sensing of Environment, v. 176, p. 1–16.

Kokelj S.V. and Jorgenson, M.T. 2013: Advances in thermokarst research; Permafrost and Periglacial Processes, v. 24, p. 108–119.

McMartin, I. 2002: Surficial geology, Rankin Inlet, Nunavut; Geological Survey of Canada, Open File 4116, scale 1:50 000, doi: 10.4095/213219.

Oldenborger, G.A., LeBlanc, A-M., Bellehumeur-Génier, O., Grosset, C., Holzman, S., Masson, C. and Tremblay, T. 2016: Community workshop on permafrost and landscape change, Rankin Inlet, Nunavut; Geological Survey of Canada, Open File 8057, 31 p., doi: 10.4095/298806

Short, N., LeBlanc, A.-M. and Bellehumeur-Génier, O., 2016: Seasonal surface displacement derived from DInSAR, Rankin Inlet, Nunavut; Geological Survey of Canada, Canadian Geoscience Map 291 (preliminary), scale 1:50 000, doi:10.4095/298815

Short, N., LeBlanc, A.-M., Sladen, W., Mathon-Dufour, V., Oldenborger, G. and Brisco, B. 2014: RADARSAT-2 DInSAR for ground displacement in permafrost terrain, validation from Iqaluit Airport, Baffin Island, Canada; Remote

Sensing of Environment. V. 141, p. 40–51, doi: 10.1016/j.rse.2013.10.016

Smith, S. and Burgess, M.M. 2000: Ground temperature database for northern Canada; Geological Survey of Canada, Open File 3954, 28 p., doi: 10.4095/211804

Smith, S.L., Burgess, M.M., Riseborough, D. and Nixon, F.M. 2005a: Recent trends from Canadian permafrost thermal monitoring network sites; Permafrost and Periglacial Processes, v. 16, p. 19–30.

Smith, L.C, Sheng, Y., MacDonald, G.M. and Hinzman, L.D. 2005b: Disappearing arctic lakes; Science, v. 308, p. 1429, doi: 10.1126/science.1108142

Tam, A. 2014: The impacts of climate change on potential permafrost distributions from the subarctic to the high arctic regions in Canada; Ph.D. thesis, University of Toronto, Toronto, Ontario, 168 p., URL <http://hdl.handle.net/1807/68103> [November 2015].

Throop, J., Lewkowicz, A.G. and Smith, S.L. 2012: Climate and ground temperature relations at sites across the continuous and discontinuous permafrost zones, northern Canada; Canadian Journal of Earth Sciences, v. 49, p. 865–876.

United States Geological Survey 2016: Landsat 8, downloaded via USGS EarthExplorer, imagery date 2016/07/09, WRS path 032, row 16.

van Everdingen, R.O (ed.) 2005 (revised edition): Multi-language glossary of permafrost and related ground-ice terms; International Permafrost Association, URL <http://globalcryospherewatch.org/reference/glossary_docs/Glossary_of_Permafrost_and_Ground-Ice_IPA_2005.pdf> [November 2016].

Zhang, Y. 2013: Spatio-temporal features of permafrost thaw projected from long-term high-resolution modeling for a region in the Hudson Bay Lowlands in Canada; Journal of Geophysical Research, v. 118, p. 542–552.

Preliminary findings on snow accumulation in the Niaqunguk River watershed near Iqaluit, Baffin Island, Nunavut

K.A. Smith[1]

[1]*Department of Geography and Environmental Studies, Carleton University, Ottawa, Ontario, keegan.smith@carleton.ca*

This work is part of the Carleton University–led Partnership for Integrated Hydrological and Water Quality Monitoring, Research and Training in the Niaqunguk River Watershed, Iqaluit, Nunavut, a Polar Knowledge Canada–supported integrated collaboration with Nunavut Research Institute, Université du Québec à Montréal, Queen's University and Nunavut Arctic College. The research is also supported through an ArcticNet initiative, Water Security and Quality in a Changing Arctic. The shared objective of these programs is to improve knowledge in the area of arctic snow hydrology and its cascading influences on freshwater resource supply and aquatic ecosystems in the Niaqunguk River watershed, and is being developed for long-term sustainability and capacity building with local residents.

Smith, K.A. 2016: Preliminary findings on snow accumulation in the Niaqunguk River watershed near Iqaluit, Baffin Island, Nunavut; *in* Summary of Activities 2016, Canada-Nunavut Geoscience Office, p. 89–104.

Abstract

Snow is the predominant input to arctic hydrological systems, and the spring melt is the most hydrologically important time of the year. Predicting timing and volume of meltwater arrival is therefore of great importance to hydrological modelling and water management and requires the estimation of the snow water equivalent storage in the landscape at the time of melt. Estimation is complicated by redistribution of snow by wind and by a lack of spatially distributed measurements. In this study, extensive field surveys of snow water equivalent were conducted to characterize the snow distribution in the Niaqunguk River (commonly known as Apex river) watershed, near Iqaluit, Nunavut. The mean snow water equivalent storage was 24 ±3 cm (number of samples = 193) for the whole watershed in 2016. Segmenting this sample by terrain type showed shallow accumulation on the ridges and broad valley floors, which form most of the landscape, and deep drifts on mainly steep slopes. As part of this project, a meteorological tower was established north of Iqaluit to monitor basic weather variables through the winter. In 2017, this tower will be equipped with an open-path eddy covariance system for direct measurement of the latent heat flux. This work contributes to the hydrological characterization of the Niaqunguk River, identified by the City of Iqaluit as a secondary water supply. Ongoing work will focus on incorporation of micrometeorological observations for full water balance accounting within the watershed, including sublimation and evaporation rates over the spring snowmelt period. This will make fundamental contributions to the understanding of snow and landscape hydrology in southern Baffin Island.

Résumé

La neige est la composante prédominante des systèmes hydrologiques de l'Arctique et la fonte au moment du dégel printanier, la période la plus importante de l'année au sens hydrologique. Il est donc très important de pouvoir prévoir aussi bien le volume que le moment où l'eau de fonte se manifestera aux fins de modélisation hydrologique et de gestion des ressources hydriques; pour ce faire, il s'agit d'estimer la capacité de stockage d'équivalent eau-neige du paysage au moment de la fonte. Cette évaluation est rendue d'autant plus difficile que la neige est remaniée par le vent et que trop peu de mesures réparties spatialement sont disponibles. Dans le cadre de la présente étude, des levés de grande envergure ont été réalisés dans le bassin hydrographique de la rivière Niaqunguk (communément appelée Apex), près d'Iqaluit, au Nunavut, afin d'y caractériser la répartition de la neige. La moyenne de stockage d'équivalent eau-neige pour l'ensemble du bassin hydrographique était de 24 ±3 cm (nombre d'échantillons = 193) en 2016. En segmentant l'échantillon en fonction du type de terrain, il est possible de voir de faibles accumulations de neige sur les crêtes et les fonds de vallée plus larges, ce qui constitue la majorité du paysage, mais aussi d'épaisses congères sur les pentes escarpées. Une étape du projet a vu l'installation d'une tour météorologique au nord d'Iqaluit, laquelle a pour fonction de suivre les variables climatiques au cours de l'hiver. Cette tour sera équipée en 2017 d'un système de covariance des turbulences en circuit ouvert permettant la mesure directe du flux de chaleur latente. Ces travaux contribuent ainsi à la caractérisation hydrologique de la rivière Niaqunguk, que la ville d'Iqaluit a désigné à titre de source d'eau complémentaire. Des travaux en cours verront à incorpor-

This publication is also available, free of charge, as colour digital files in Adobe Acrobat® PDF format from the Canada-Nunavut Geoscience Office website: http://cngo.ca/summary-of-activities/2016/.

er les observations de nature micrométéorologiques de façon à obtenir un portrait exact du bilan hydrique au sein du bassin hydrographique, tenant compte des taux d'évaporation et de sublimation au cours de la période de fonte lors du dégel printanier. Il s'agit d'une contribution fondamentale à l'état des connaissances portant sur l'interaction de la neige et de l'hydrologie du paysage dans le sud de l'île de Baffin.

Introduction

Arctic hydrology in brief

Arctic rivers show extreme seasonality in their flow behaviour, relative to similar watercourses in the south, and exhibit strongly nival (snowmelt-dominated) flow regimes, with peak discharges during snowmelt and reduced summer/autumn base flows. Smaller rivers may dry up or freeze-up completely in winter, whereas large rivers (e.g., Sylvia Grinnell River on southern Baffin Island) flow under the ice through the winter (Williams and Smith, 1989). This strong seasonality is coupled to arctic atmospheric conditions—water is stored as ice and snow for months during the long, cold winters and the prolonged cold leads to the formation of permafrost in the subsurface.

The presence of permafrost gives arctic rivers their 'flashy' characteristics, as permafrost acts as a largely impermeable aquitard, preventing connection of surface water to deep groundwater. The top of the permafrost table also presents a limit to infiltrating water. Since the active layer thickens through the summer, infiltration capacity increases as the warm season continues, and percolation to an increasingly lower water table reduces the responsiveness of rivers to inputs (Dingman, 1973; Church, 1974). Rivers underlain by continuous permafrost show higher peaks and lower base flows relative to those underlain by discontinuous or sporadic permafrost (Newbury, 1974).

The active layer is still frozen at the time of snowmelt, preventing infiltration of meltwater. This causes a rapid initial response in streamflow. As snowmelt continues and patches of bare ground open, active layer thaw begins, allowing some infiltration and gently moderating the streamflow response. However, this also decreases ground albedo, increasing absorbance of shortwave radiation and resulting in increased melt energy (Woo, 2012). Thus, predicting the quantity and timing of peak discharge in an arctic river is a complex function of the meteorological variables affecting the melt rate, the responsiveness of the watershed to meltwater inputs and, most importantly, the antecedent water storage in snow at the end of winter. Unfortunately, snow water storage in the landscape is a difficult variable to quantify because of the spatial variability resulting from redistribution by wind, and the inability of standard measuring techniques to accurately represent it.

Snow distribution

Snow's low density and high aerodynamic resistance allow it to be entrained by wind during snowfall events, so snow distribution on the ground is initially determined by differential accumulation at snowfall. McKay and Gray (1981) observed that this process is determined by terrain characteristics and vegetation at 0.1–10 km scales, and by obstructions on the ground at smaller scales. Although this is generally true, open landscapes with limited vegetation, such as the Canadian Prairies or eastern Arctic, tend to be more strongly affected by redistribution of snow after falling (Pomeroy et al., 2002), with either interception at the surface or sublimation being the ultimate fate of entrained particles.

Snow transport by wind is described in detail by Pomeroy and Gray (1995). Three mechanisms prevail: creep, saltation and turbulent suspension. Creep is the movement of particles, which are too heavy to be lifted en masse, by rolling action—commonly seen in the Arctic as advancing snow dunes. Creep typically occurs over poorly consolidated snow cover during periods of light winds, but is not typically the dominant transport mechanism.

When wind speeds exceed a threshold velocity (which varies, dependent mainly on the roughness of the snow surface and the strength of bonds between surface snow particles), saltation begins; particles are dislodged from the snow surface and move abruptly upward, then they are carried a distance downwind and re-impact the surface, dislodging other particles. Saltation is the dominant mode of transport in many cases, with most mass moving within a few centimetres of the snow surface.

If saltation can continue long enough, small particles may move from the upper saltating layer into turbulent suspension, moving at a horizontal velocity approximating that of the air. Due to their large exposed surface area, suspended particles are prone to an extremely high rate of sublimation during periods of available energy, for example, on clear sunny days (Pomeroy, 1988). This sublimation returns their water equivalent to the atmosphere. In the western Arctic, wind transport has been found to result in snow accumulations ranging from 54 to 419% of measured snowfall (Pomeroy et al., 1999).

A variety of measurement techniques exist for monitoring snow (Pomeroy and Gray, 1995; Lundberg et al., 2008), with point measurements ranging in simplicity from moni-

toring snow accumulation around a stick, to catching snowfall in a recording gauge, to monitoring the attenuation of passive gamma radiation from the ground to measure snow water equivalent (SWE). Areal measurements also vary widely in approach, with ground-based measurements (such as snow courses), ground-penetrating radar and airborne- or satellite-based remote sensing. Work by Budkewitsch et al. (2011, 2012) indicates some promise in the use of RADARSAT-2 data for snow depth monitoring near Clyde River, Nunavut, but satellite results are rarely applicable at the small watershed scale. Each technique has associated advantages and challenges, which are outside the scope of this work. Choice of technique is usually determined by budget, labour-intensiveness and repeatability of measurement.

Environment and Climate Change Canada monitors weather variables at the climate station situated at Iqaluit International Airport. At this location, point-based measurements are made of snow depth on the ground and a snowfall gauge is used to make point-based measurements of precipitation. Snow accumulation measurements are only representative of the terrain type that they are situated in, with exposed sites potentially losing upward of 50% of snow to wind action (Pomeroy and Li, 2000). Similarly, snowfall gauges require careful shielding and wind-bias compensation to reduce the effect of wind, as wind undercatch rates as high as 75% have been reported for arctic tundra by Liston and Sturm (2004). Both snow measurements are conducted in a wind-exposed valley at Iqaluit airport, where the problems associated with their measurements are greatest.

Ground-based, spatially extensive field measurements may comprise one of the best estimates for end-of-winter snow accumulation and are commonly used for ground-truthing remote-sensing data during short-term research projects (e.g., Rees et al., 2013). In long-term monitoring, they have typically been avoided because they are very labour intensive. Their use in this project is made possible through the partnership between Carleton University (CU), Nunavut Research Institute (NRI) and Nunavut Arctic College (NAC). The college provided local student support and other logistical resources allowing the study area to be covered at a reasonably dense sample spacing over a relatively short period. One anticipated outcome of this work is an efficient sampling approach that will minimize the fieldwork required for future surveys.

Regional setting

This study is being carried out in the Niaqunguk River (commonly known as Apex river) watershed (NRW), a small (58 km^2) watershed, originating in the hills north of Iqaluit and draining into Frobisher Bay at the nearby neighbourhood of Apex (Figure 1). The river's flow regime is nival, with a significant discharge peak during spring melt. The base-flow period through summer and fall is generally low flow, but exhibits occasional large rainfall peaks (such as the late July 2016 rainfall and flooding event [Zerehi, 2016]). There is no flow during the winter (Environment and Climate Change Canada, 2016a).

The watershed is situated in the continuous permafrost zone, on the Precambrian shield. The topography ranges from rugged to rolling hills arranged in parallel ridges running to the northwest. The surficial material is primarily thin glacial till with granite/granitoid rock outcrops (Blackadar, 1967; St-Onge et al., 1999; Hodgson, 2005; Allard et al., 2012; Tremblay et al., 2015). Frequent boulder fields and isolated glaciofluvial or lacustrine deposits (Squires, 1984) are also evident. Vegetation is extremely low lying and consists of tundra grasses, dwarf shrubs and forbs, considered typical for the region. This low vegetation provides very little interception to blowing snow, unlike arctic shrub tundra or taiga landscapes.

Annual precipitation is 404 mm, with 57% received as snow, mostly from October to May (though precipitation type has not been reported at the Iqaluit airport climate station since 1997), with 97% of daily snow accumulation rates below 9.5 mm, though extreme daily snowfalls up to 32 cm have been recorded in the 1981–2010 climate normals (Environment and Climate Change Canada, 2016a). Rainfall predominates from June to September, when average daily air temperatures rise above 0°C.

Prevailing winds are funneled northwest or southeast between the mountainous areas of the Hall and Meta Incognita peninsulas (to the north and south, respectively), which is channeled in the NRW by the northwest-trending ridges that dominate the topography. Average annual wind speeds are 15.7 $km \cdot h^{-1}$, though winter storms can bring gusts well over 100 $km \cdot h^{-1}$ (Environment and Climate Change Canada, 2016a). These storms originate primarily over Hudson Bay to the south, over the Arctic Ocean to the northwest, or from the eastern seaboard of North America (Gascon et al., 2010). Frequent blowing snow events during these storms pose considerable logistical challenges and hazards for eastern Arctic communities (Gordon et al., 2010), and redistribute snow from exposed to sheltered areas. This results in substantial snow depth variability before spring melt (Figure 2a), which contributes to the development of a patchy snow cover during melt (Figure 2b).

Review of Niaqunguk River hydrological studies

Past scientific interest in the NRW has been limited. A Water Survey of Canada gauge has been recording stage (water level) near the river's mouth at Apex since 1973 (Environment and Climate Change Canada, 2016b, record gap from 1997 to 2006), and a geochemical characterization of the watershed was conducted by Obradovic and Sklash (1986) and repeated by Kjikjerkovska (2016), but little other hydrological information is available. In recent years, there

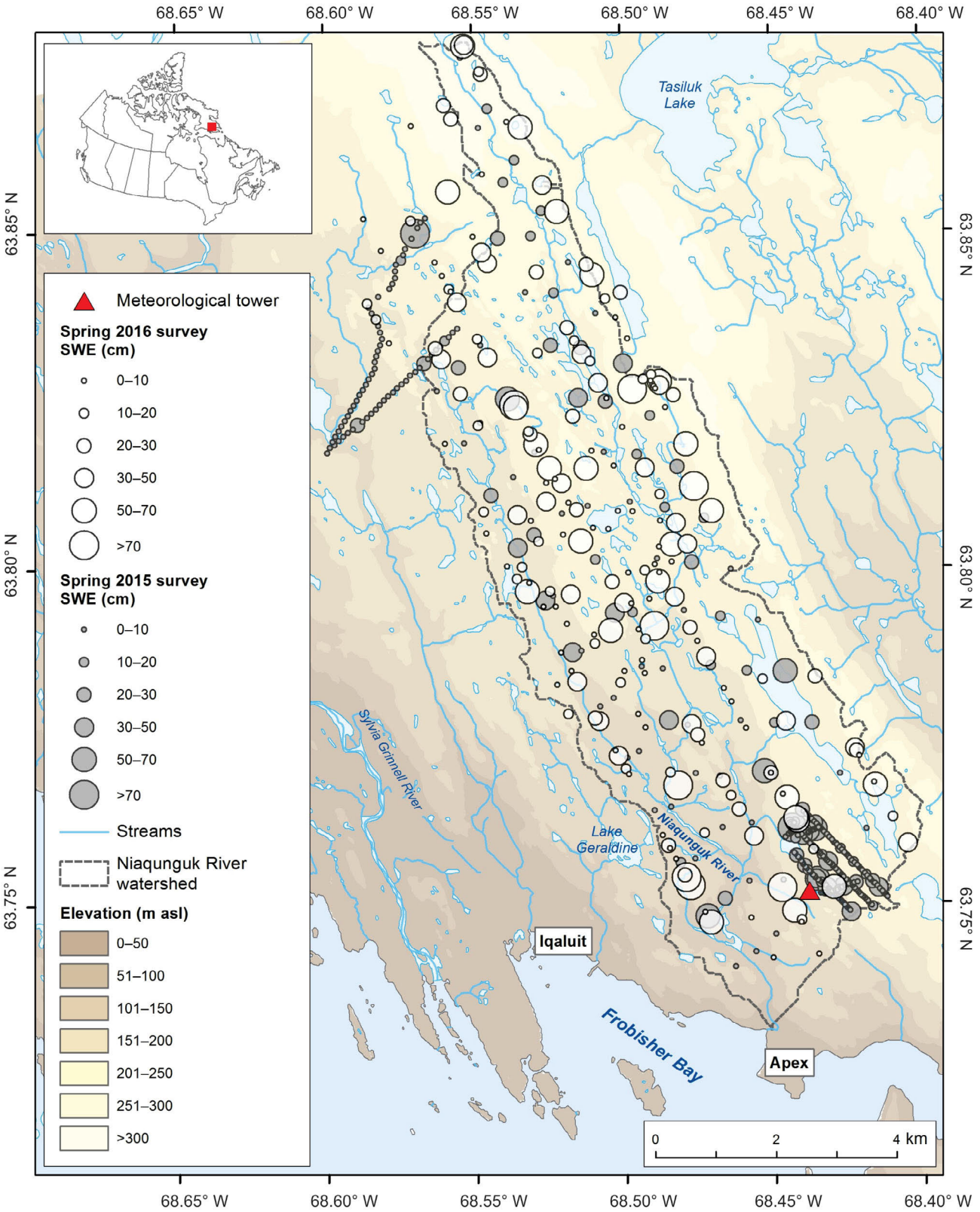

Figure 1: Locations of snow survey points from the spring of 2015 and 2016 and the Carleton University/Nunavut Research Institute meteorological tower, Niaqunguk River watershed, southern Baffin Island, Nunavut. Snow water equivalent (SWE) measured in the field in 2015 and 2016 corresponds to the maximum snow accumulation on the ground for that snow year, just before the onset of spring melt. The digital elevation model (derived from WorldView-1 stereo optical data) for this map was provided by Canada Centre for Remote Sensing, Natural Resources Canada (NRCan). Shoreline and watercourse shapefiles were drawn from NRCan's CanVec dataset (Natural Resources Canada, 2015). Map created using ArcGIS 10.4 (Esri, 2016).

Figure 2: Different areas of the Niaqunguk River watershed, southern Baffin Island, Nunavut, showing **a)** the relatively continuous snow cover before melt, April 17, 2015, compared to **b)** the patchy snow cover during melt, June 12, 2015. Note in photo 2a that many exposed ridges have been completely scoured of snow by winter winds.

has been renewed interest in the Niaqunguk River as a secondary water supply for the rapidly growing City of Iqaluit (Sims and Allard, 2014) to augment the current supply from Lake Geraldine (Golder and Associates Ltd., 2014). The City of Iqaluit classified the watershed as a protected area (FoTenn Consultants Inc., 2010), and several subsequent studies on the hydrology of the NRW have been conducted to support source water planning efforts.

Snowmelt is the largest contributor to the annual streamflow of the Niaqunguk River, delivered in a short-lived pulse during spring melt. The continuous permafrost underlying the NRW prevents significant annual infiltration, and the shallow frost table in the active layer during spring melt further limits snowmelt infiltration. Recent work by Thiel (2016) identified partial overland flow along the soil–vegetation interface during snowmelt, determined using the concentration and composition of dissolved organic carbon (DOC). The DOC concentration decreased after peak discharge, simultaneous with a compositional change away from a dominance of humic compounds derived from vegetative material. The associated increasing dominance of protein-like molecules, typically generated in the water by microbial action, suggests a switch from surface to subsurface pathways after peak discharge, and an increasing importance of lake water or groundwater to the total stream discharge.

During the summer base-flow period, an increase in specific conductance (Obradovic and Sklash, 1986; Chiasson-Poirier, 2016) and total dissolved solids (Rusk, 2016) indicate increased groundwater contributions. Since the isotopic signals of lake water and groundwater were not well resolved in the two isotope studies conducted in NRW to date (Obradovic and Sklash, 1986; Kjikjerkovska, 2016), the exact contribution of lake water to annual streamflow is not known. Richardson and Shirley (in press) determined that thorough mixing of snowmelt and soil water occurred before streams entered lakes in the NRW, but the mixing between this streamflow and the lake water column was limited. This suggests that stored lake water does not become an important component of river flow until after snowmelt has concluded.

Despite the recognition by past researchers of the importance of snowmelt for providing peak discharge and comprising the largest overall source of water to the NRW annually, there have been no systematic snow cover observations reported, and no effort to quantify the end-of-winter snow water storage at a landscape scale. Improvements to precipitation measurement by Environment and Climate Change Canada at the Iqaluit airport 'supersite' (Mariani et al., 2016) will allow for increased confidence in estimates of snowfall depths, but must be matched by field data, due to the strong wind-driven redistribution typical to arctic tundra. This redistribution results in a spatially heterogeneous snow cover, complicating prediction of water storage and melt dynamics from point measurements.

The work described here partners researchers from Carleton University with staff and students from the NRI and NAC Environmental Technology Program (ETP) to fill this gap in hydrological knowledge. A community-based water quality monitoring campaign has been conducted by the NRI in the NRW since 2009 (Shirley, 2014) and long-term monitoring work at Tasiluk Lake (commonly known as Crazy lake) has been conducted by ETP students for over a decade (Dyck, 2007). During the project described in this paper, the ETP students learned snow hydrology monitoring techniques and applied them while working in the field with the author. The students are exceptionally knowledgeable of the complex terrain in the NRW, well trained in environmental science, with particular focus on local conditions, and skilled snowmobile operators; these attributes make them an essential part of data collection for this project, especially in more remote areas of the watershed. A sustainable program of annual snow surveying is in development, which will engage future cohorts of ETP students

and enhance capacity for field data collection to monitor trends in the end-of-winter snowpack.

Methodology

Snow surveying

Extensive snow surveys were conducted in the NRW in April–May of 2015 and 2016 (see Figure 1 for sampling locations) by CU researchers, NRI staff and ETP students (Figure 3). Travel in the field was by snowmobile, with sampling stops at predetermined locations. At each location, a SWE sample was taken using a Geo Scientific Ltd. Federal snow sampler and weighed on a sling scale, providing a measurement of snow depth and density. When the cores were weighed, they were sheltered from the wind as much as possible to prevent jittering of the scale, which could cause erroneous readings. Calibration of the snow scale in the NRI lab at the end of the 2016 season confirmed that the scale's readings were linear along its measurement range (R^2 = 0.999). Several supporting depth measurements were taken at random locations within 2–3 m of each core using a Snowmetrics depth probe, to characterize the site-scale variability in snow depth. This variability was expressed in terms of both a standard deviation (SD) and a coefficient of variation (CV, a unitless standardization of SD divided by mean).

The sampling strategy differed between the two years. Since 2015 was an exploratory analysis, locations were visited systematically (every 1 km) along seven transects running northwest-southeast in the NRW. Two additional areas were surveyed at a much closer spacing (30–100 m), with a SWE core being measured at approximately one out of five sampling sites; only depth was measured at the remainder of the sites to save time. These areas were lake catchments, one situated to the north of the NRW and the other in the southern end of the NRW (see Figure 1). Variography of the closely spaced samples indicated an autocorrelation range of approximately 80 m, giving a minimum range between future samples (Figure 4; variography was performed using the R spatial statistics package geoR [Ribeiro and Diggle, 2001]).

Figure 3: Nunavut Arctic College Environmental Technology Program student S. Noble-Nowdluk weighs a snow water equivalent (SWE) core during the 2016 snow survey, Niaqunguk River watershed, southern Baffin Island, Nunavut.

The 2016 sampling strategy was modified accordingly. A terrain-based model predicting snow accumulation was created in

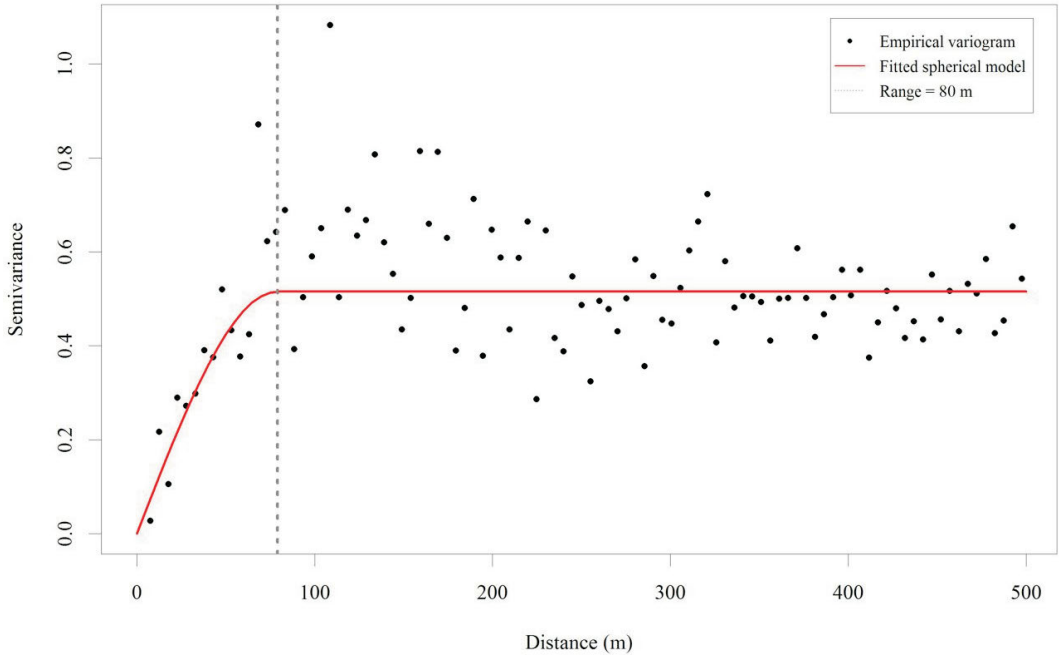

Figure 4: Variogram from the 2015 data, indicating the 80 m autocorrelation range identified in the snow surveying work, Niaqunguk River watershed, southern Baffin Island, Nunavut.

2015–2016, and used to stratify the NRW by terrain unit. Six transects were planned, again running northwest-southeast to take advantage of faster travel time along river valley floors. Points were then randomly generated along these transects, with a minimum spacing of 100 m, stratified by the terrain units identified in the model. Opportunistic random sampling, stratified by terrain unit, was conducted during the last days of surveying, to maximize survey coverage before the melt.

Carleton University/Nunavut Research Institute meteorological tower

To facilitate measurement and modelling of the snowpack energy balance, and to provide local weather monitoring data for the lower Niaqunguk River watershed, an automated meteorological tower was set up with the help of ETP students (Figure 5) at latitude 63.752°N, longitude 68.437°W, in April 2015 (see Figure 1 for location).

The meteorological tower was augmented in October 2015 with the addition of automated melt collectors (Figure 6a, b), and in spring 2016 with solar panels, additional sensors and communication devices (Figure 7a, b). In its present configuration, the tower averages meteorological data on 15 min intervals, takes a high-resolution photograph of the nearby valley daily, and transmits all data and photographs via cellular modem weekly.

The tower will provide winter wind data to drive blowing snow models, and to drive energy balance models by collecting air temperature, humidity, wind speed (and direction) and net radiative data through the year. Rainfall data is also collected from May through October. In 2017, the tower will be upgraded with an open-path eddy covariance system to measure the latent heat fluxes of snow sublimation and water evaporation. A summary of the measurements currently taken at the tower, including the sensors used, their instrumental accuracies and the measurement periods throughout the year, are presented in Table 1.

Aside from installation and maintenance of the meteorological equipment, the author also monitored melt in snow pits during the spring of both 2015 and 2016. These data will be used to validate the snow ablation model being developed. During this work in May 2016, two new snowfalls occurred, allowing density sampling of the newly fallen snow.

Figure 5: Nunavut Arctic College Environmental Technology Program students A. Pedersen and P. Aqqaq taking measurements at the Carleton University/Nunavut Research Institute meteorological tower in April 2015, Niaqunguk River watershed, southern Baffin Island, Nunavut.

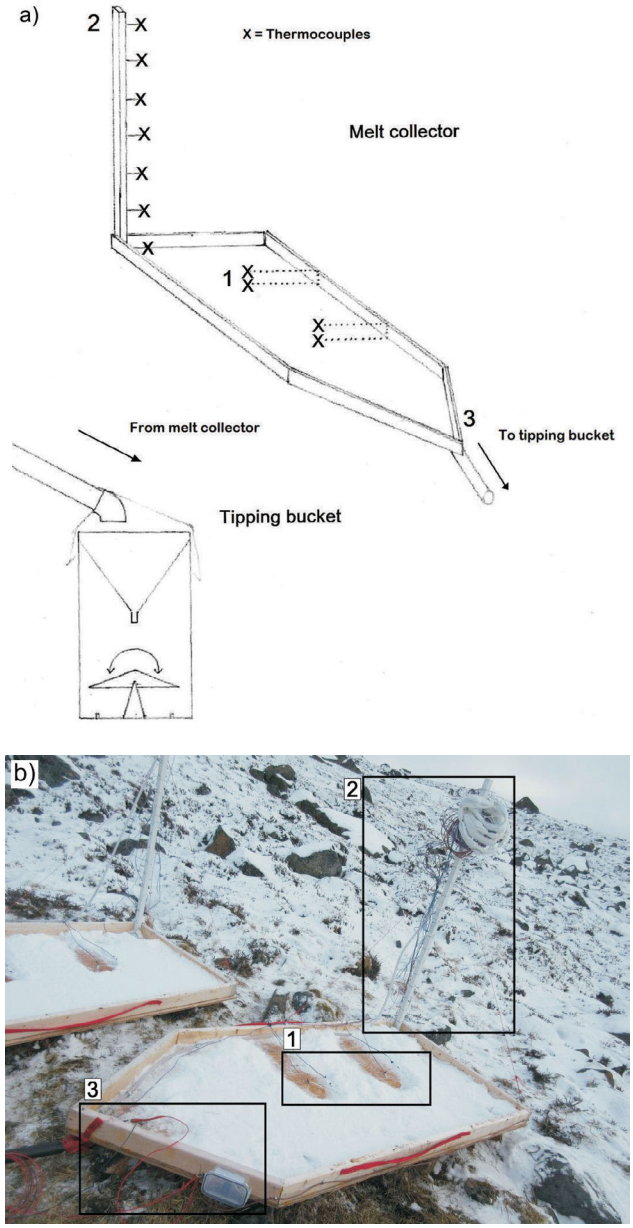

Figure 6: Carleton University/Nunavut Research Institute automated snowmelt collector, Niaqunguk River watershed, southern Baffin Island, Nunavut: **a)** schematic view of collector and **b)** photo of collector, taken in October 2016. Instruments are 1) basal thermocouples, 2) ablation stake with mounted thermocouple array and 3) drain heater with control system.

Snow distribution: spatial and statistical analysis

Terrain analysis was conducted in System for Automated Geoscientific Analyses (SAGA), an open-source, cross-platform GIS application designed for geoscientific analyses (Conrad et al., 2015). A variety of terrain variables were computed from a digital elevation model (DEM; derived from WorldView-1 stereo optical data and provided by the Canada Centre for Remote Sensing, Natural Resources Canada) in an effort to determine which terrain variables were correlated to snow accumulation. Due to the complex interplay of terrain and wind in determining snow distribution, no single variable provided a relationship robust enough for reliable prediction of snow accumulation.

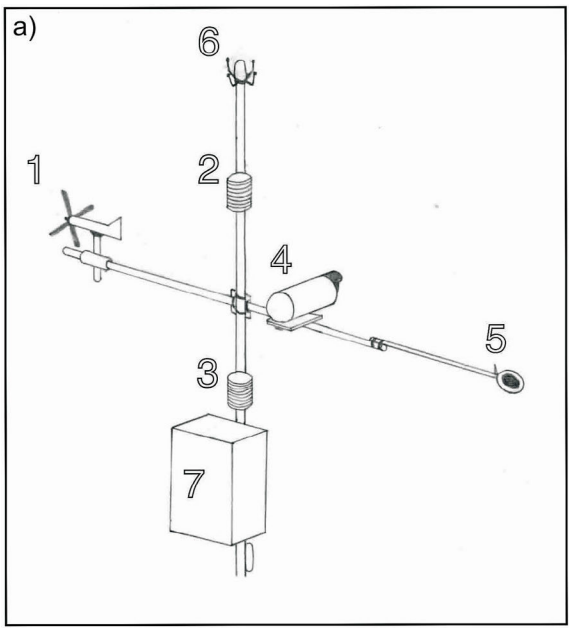

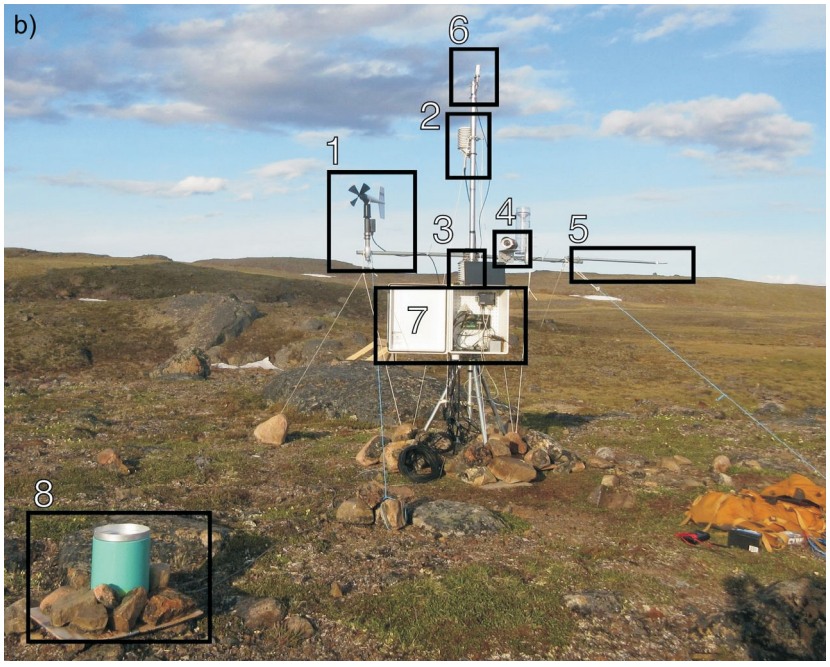

Figure 7: Carleton University/Nunavut Research Institute meteorological tower, Niaqunguk River watershed, southern Baffin Island, Nunavut: **a)** schematic view of tower and **b)** photo of tower, taken in July 2016. Instruments are 1) R.M. Young Company Model 05103 wind monitor, 2) Vaisala HMP35C temperature and relative humidity probe, 3) Rotronic Instrument Corp. HC2-S3-L temperature and humidity probe, 4) Campbell Scientific Canada CC5MPX digital camera, 5) Kipp & Zonen USA Inc. NR Lite net radiometer, 6) Sierra Wireless® AirLink® Raven RV50 4G LTE gateway with cellular modem antenna, 7) weatherproof enclosure containing the Campbell Scientific Inc. CR1000 measurement and control data logger, 8) Geo Scientific Limited Jarek tipping bucket rain gauge.

An alternative approach was tested using k-means clustering (Forgy, 1965; MacQueen, 1967) to delineate terrain units. The technique of k-means clustering is one of the fundamental methods of data classification by automated machine learning, where a multivariate dataset is divided into unique, definitive groupings (called clusters) based on similar values in the independent variables. Terrain clusters were defined based on hillslope gradient, aspect, curvature, a topographic openness index and a normalized height index. The initial result was four terrain clusters, which corresponded roughly to hilltops/ridges, valley floors, hill midslopes and hill toe-slopes.

The SWE data was then segmented by terrain cluster and differences between clusters were tested using a one-way analysis of variance (ANOVA), which indicated that the two slope classes were sufficiently similar to warrant merging them into a single class. The distribution of the resulting three terrain classes in the NRW is shown in Figure 8. The ANOVA tests for difference in means between multiple groups using an F-test, and as such is an extension of the classic two-group t-test (Fisher, 1970). Even though the test indicates whether a difference exists, a post-hoc test is required to determine the statistical nature of each difference. A Tukey test allows for pairwise comparison of group means, with an associated confidence (Tukey, 1949). Statistical analyses were performed using the R statistical programming language (R Development Core Team, 2013).

Results

Snow accumulation differed substantially between the two years (Table 2). The full-survey mean watershed SWE for 2015 was 14 ±1 cm (number of samples [n] = 152), with a mean watershed snow density of 330 ±14 kg·m^{-3} (n = 152), and mean watershed snow depth of 39 ±4 cm (n = 392). The full-survey mean watershed SWE for 2016 was 24 ±3 cm (n = 193), with a mean watershed snow

Table 1: Parameters measured at the Carleton University/Nunavut Research Institute meteorological tower, Niaqunguk River watershed, southern Baffin Island, Nunavut. All parameters are scanned every 5 s and averaged over 15 min, unless otherwise specified.

Parameter	Instrument	Accuracy	Measurement period
Wind speed ($m \cdot s^{-1}$) and direction (°) at 2 m height	Model 05103 wind monitor[1,2]	Speed: ±0.3 $m \cdot s^{-1}$ Direction: ±3°	Full year
Air temperature (°C) and relative humidity (%) at 1.5 m height	HMP35C temperature and relative humidity probe[3] with Model 41003-2 10-plate radiation shield[2]	T_A: ±0.4°C RH: ±2% if RH <90% ±3% if RH >90%	
Air temperature (°C) and relative humidity (%) at 2.5 m height	H2C-S3-L temperature and humidity probe[4] with Model 41003-2 10-plate radiation shield[2]	T_A: ±0.1°C RH: ±0.8%	
Net radiation ($W \cdot m^{-2}$)	NR Lite net radiometer[5]	±30 $W \cdot m^{-2}$	
Rainfall (mm)	Jarek tipping bucket (0.5 mm tip)[6]	±2% at 25.4 $mm \cdot h^{-1}$	May to October
Barometric pressure (kPa)	HOBO® water level logger (Model U20-001-04)[7]	±0.3% FS (i.e., ±0.435 kPa)	
Snowpack temperature (°C)	Type "E" thermocouples (wire[8]), referenced to Model 109 temperature probe[9]	±1.38°C (theoretical) ±0.158°C (observed)	May to end of snowmelt (typically mid-June)
Snowmelt (mm)	Jarek tipping bucket (1 mm tip)[6]	±2% at 25.4 $mm \cdot h^{-1}$	
Landscape image (noon)	CC5MPXWD digital camera with lens defroster[9]	2592 by 1944 pixels	October to May, daily

[1]Wind monitor's lower wind speed threshold is 1.0 $m \cdot s^{-1}$. Wind speed is reported as a 15 min average, along with a 15 min minimum and maximum (gust). Wind direction is reported as a 15 min vector average, with a standard deviation provided.
[2]R.M. Young Company
[3]Vaisala
[4]Rotronic Instrument Corp.
[5]Kipp & Zonen USA Inc.
[6]Geo Scientific Limited
[7]Onset® Computer Corporation
[8]dba Omega Environmental
[9]Campbell Scientific Canada
Abbreviations: FS, full scale; Pa, pascal; RH, relative humidity; T_A, air temperature; W, watt.

density of 460 ±16 $kg \cdot m^{-3}$ (n = 193), and mean watershed snow depth of 57 ±8 cm (n = 193). The supporting site depth measurements also differed substantially; the 2015 data had a mean site SD of 20 cm, whereas the mean site CV was 0.46. In comparison, 2016 showed less site-scale variability, with a mean site SD of 11 cm and a mean site CV of 0.35. New snowfalls observed in May 2016 had densities of 174 $kg \cdot m^{-3}$ on May 21 and 67 $kg \cdot m^{-3}$ on May 22.

The terrain model applied to the 2016 data showed clear differences between the snow accumulations within the three terrain units identified (Figure 9; Table 3). The sample populations of SWE on each terrain unit were found to be significantly different by one-way ANOVA (F-test score = 25.21, significance value [p] = 1.9×10^{-10}) with a subsequent Tukey post-hoc multiple comparisons test, which confirmed that each of the three clusters was distinct (all p values <0.005). Ridges accumulated the least, with a mean SWE storage of 11 ±3 cm, whereas valley floors stored 27 ±5 cm mean SWE on average, which is similar to the overall mean value. Each of these terrain units comprises approximately 40% of the landscape. Drifts mainly occurred on slopes, with a mean SWE of 39 ±8 cm, though this unit occupied only approximately 20% of the landscape. With landscape weighting, it was determined that concentrated sampling in drift zones on slopes and on valley floors would help reduce the overall error in the SWE estimate derived from the 2016 survey.

Discussion

The 2016 survey showed a near-doubling of snow water storage relative to 2015, despite snow accumulation only

increasing by 50% on average. Observations by the author were that windswept areas appeared similar in the two years, but that drift areas in 2016 were deeper and denser due to increased wind compaction and ice layer presence. This was exemplified particularly well in gullies, where similar depositional patterns were apparent between both years, but larger drift features were found in 2016 (Figure 10a, b).

Consultation with community members made it clear that 2016 was a deep snow year, with an uncharacteristically high frequency of late-season blizzards. These blizzards are clearly evident in the Iqaluit airport weather record and caused almost half of the end-of-winter snow accumulation (Figure 11). These blizzards led to the formation of multiple ice layers in the snowpack in 2016, which increased the overall density and hardness of the pack. Unfortunately, this created challenges for sampling in some locations as the Federal snow sampler could only be pushed into the snowpack if significant force was used. This is undesirable for several reasons: 1) it is labour intensive, 2) it puts high stress on the sampling equipment, risking damage, and 3) it reduces accuracy by compacting snow inside the core barrel. At several locations, multiple cores were taken until one was acquired without applying large amounts of force, whereas some locations were abandoned entirely due to heavy ice layer formation. Because such ice layers were most often encountered at deep drift sites, this introduces bias to any unstratified SWE estimates, favouring shallower locations. This provides further justification for the stratification approach taken here, though it also

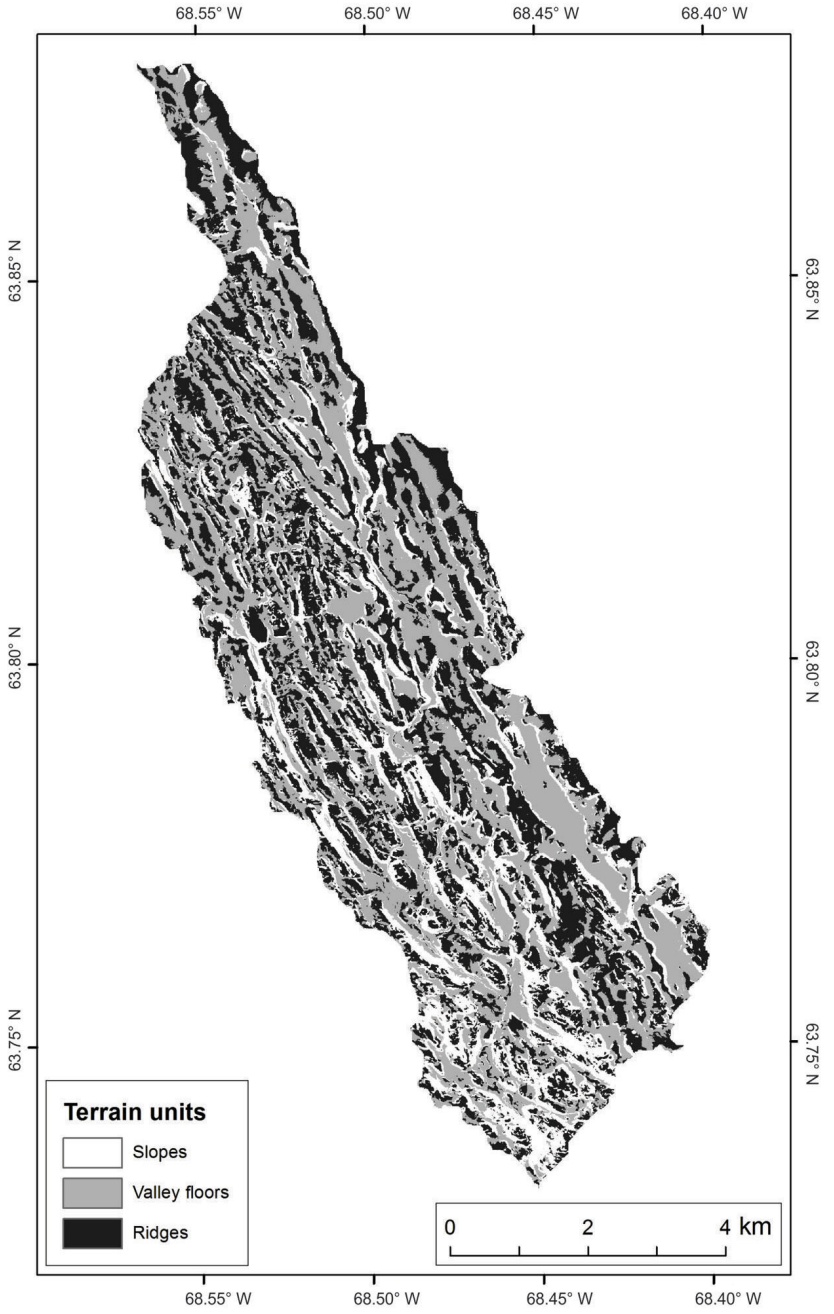

Figure 8: Distribution of the three terrain clusters in the Niaqunguk River watershed, southern Baffin Island, Nunavut. Snow accumulation was found to be greatest on the slopes class (white) and lowest on the ridges class (black).

Table 2: Summary statistics for the 2015 and 2016 snow surveys, Niaqunguk River watershed, southern Baffin Island, Nunavut. Site depth refers to the supporting depth measurements taken within 2–3 m of each snow water equivalent (SWE) core.

Year	Mean SWE (cm)	Mean density ($kg \cdot m^{-3}$)	Mean depth (cm)	Site depth SD (cm)	Site depth CV
2015 (SWE n=152, depth n=392)	14 ±1	330 ±14	39 ±4	20	0.46
2016 (n=193)	24 ±3	460 ±16	57 ±8	11	0.35

Abbreviations: CV, coefficient of variation; n, number of samples; SD, standard deviation.

Table 3: Summary statistics for the 2016 clustered data, indicating the snow storage depth and areal coverage of each terrain unit identified within the Niaqunguk River watershed, southern Baffin Island, Nunavut. Compare the cluster results to the full-survey mean in Table 2.

Terrain unit	Mean SWE (cm)	Landscape area (%)	Contribution to overall error (%)
Ridges	11 ±3	41.4	27
Valley floors	27 ±5	39.2	41
Slopes	39 ±8	19.4	32
Overall	23 ±5	100	-

Abbreviation: SWE, snow water equivalent

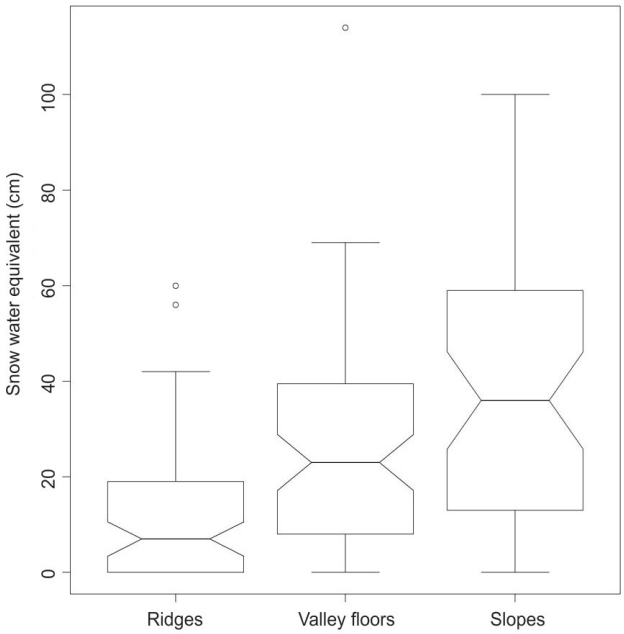

Figure 9: Boxplots showing the 2016 clustered data for the Niaqunguk River watershed, southern Baffin Island, Nunavut). Notches indicate the 95% confidence interval around the median value.

underscores the importance of operator experience and training in performing snow surveys.

The supporting measurements suggested that site-scale (<2–3 m) variability in snow depth was higher in 2015 than 2016. This may be due to the smoothing effect of a deeper snowfall, which has the potential to overcome small-scale accumulation forms that occur in rough terrain (Figure 12). These forms were commonly observed during the 2015 surveys, but were generally less prevalent in 2016. This may also be a sampling artefact, however, as the sampling protocol was less strict regarding the distance for support measurements in 2015. A larger footprint has greater potential to pick up on terrain-driven mesoscale variability, rather than the intended roughness-driven microscale variability (McKay and Gray, 1981). For example, supporting depth measurements taken within 2 m of a ridge peak will likely show similar shallow depths, whereas measurements taken within 5 m of the same point could capture both the shallow ridgetop accumulation and the edge of the deep lee slope accumulation.

Terrain clustering showed intuitive, physically oriented relationships to snow accumulation. Higher exposed areas on ridges and hilltops accumulated the least snow, as these areas are prone to scouring by wind. Steeper slopes accumulated the greatest amount of snow, which is commonly observed in arctic landscapes. This may correspond to deposition on lee slopes of hills or on the sides of narrow gullies and stream valleys, which tend to accumulate large drifts (Figure 10a, b). Further work will be needed to refine these relationships and apply them to additional years of snow survey data.

The snowfall densities observed in May 2016 differed from one snowfall event to another, likely resulting from different meteorological conditions, which altered crystal morphologies and liquid water content. Typical densities for North American winter snowfall range from 50–100 $kg \cdot m^{-3}$ (Pomeroy and Gray, 1995). On May 21, 2016, the measured snowfall density of 174 $kg \cdot m^{-3}$ was surprisingly high. It was associated with a mean air temperature of –0.6°C (close to the freezing point) suggesting a potential for high liquid content, resulting in an increased overall density. Crystal morphology consisted mainly of plates and needles, forms which have few delicate processes and thus settle quickly on the ground (McClung and Schaerer, 2006). Comparatively, on May 22, 2016, a density measurement of 67 $kg \cdot m^{-3}$ corresponds more closely to the range reported by Pomeroy and Gray (1995). The snow that day was composed mainly of stellar dendrites and plates (low density crystals corresponding to the classic snowflake). This snow compacts over a longer period on the ground as delicate processes are broken during settling. Mean temperature on that day was –1.8°C, suggesting a moderate liquid water content in the snow. Anecdotally, the snowfall felt drier on the skin that day.

Further work

Work is ongoing to fine-tune the terrain-based snow accumulation model, and to compare those results to results from a blowing snow model driven by data from Iqaluit airport and the CU/NRI meteorological tower. Improved models will help to develop more accurate sampling schemes, to maximize accuracy and efficiency in the field. Efforts continue through this partnership project to build the capacity at NRI and NAC to monitor snow hydrology, with sustained interest in the project from a number of students and recent ETP graduates. Training students in sampling techniques can benefit other research projects, both in

Figure 10: The same location in the Niaqunguk River watershed (southern Baffin Island, Nunavut) in **a)** April 2015 and **b)** April 2016 (taken at different angles). Note the large drift blocking the entrance to the gully in 2016, which was not present to a significant extent in 2015.

the NRW (e.g., NRI microbial monitoring campaign [Shirley, 2014]) and further afield in the territory.

Work is also being conducted to prepare a snow ablation model to quantify spring sublimation and evaporative loss. This will be enhanced by the addition of an open-path eddy covariance system to the CU/NRI meteorological tower in 2017. This sophisticated equipment allows for direct measurement of the movements of water vapour in the near-surface boundary layer at high frequency, and should significantly improve the understanding of surface–atmospheric exchanges during snowmelt. This, in turn, will improve modelling of fluxes of water and atmospheric contaminants in the arctic environment (Richardson and Shirley, in press).

Economic considerations

This joint work between Carleton University, Nunavut Research Institute and the Nunavut Arctic College Environmental Technology Program has generated useful knowledge on spatial distribution of snow water equivalent, as well as an ongoing meteorological record, within the Niaqunguk River watershed. The results can be employed in hydrological analyses and modelling, supporting hydrological and geochemical studies in the area. As the Niaqunguk River has been identified as a secondary water supply for the City of Iqaluit, municipal engineers have an interest in continuing field research efforts to monitor and predict annual water resource availability. The results of this study can inform the planning of such efforts. As baseline data on snow distribution and hydrology are limited in the eastern Arctic, this work represents an important

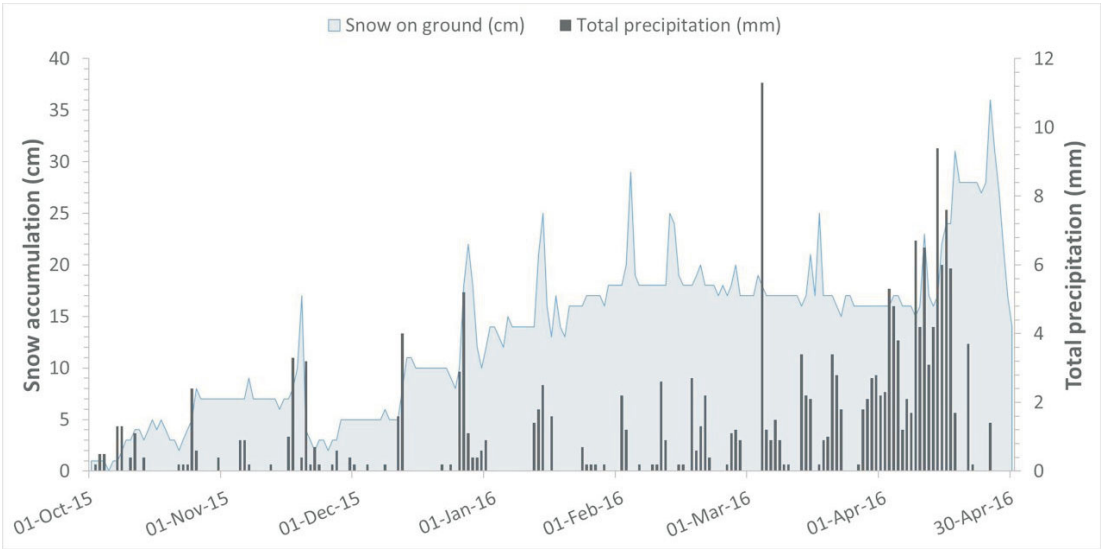

Figure 11: Snowfall water equivalent (measured as total precipitation, dark grey bars) and snow accumulation depth on the ground (blue area) measured at Iqaluit International Airport (southern Baffin Island, Nunavut) for the 2015–2016 snow year. Note the large number of precipitation events in March and April 2016, with a near-doubling of snow accumulation in April. High storm-wind speeds may have prevented accumulation during many of the events in March, and these winds, together with rapid densification of snow crystals through settling, likely account for the rapid drop in snow depth on the ground after each accumulation event.

Figure 12: Snow features, called sastrugi or uqalurait (in Inuktitut), form from snow accumulation and erosion downwind of sharp surface nonconformities (in this case, boulders at a rough site in a valley bottom, near Iqaluit, southern Baffin Island, Nunavut). These forms can strongly influence site-scale snow depth variability, but can be smoothed out by deeper snow accumulations. Because they indicate the direction of the prevailing wind, uqalurait are traditionally used as navigation aids on the land (R. Qitsualik, pers. comm., 2016).

contribution to the scientific record. Several ETP students gained valuable training and employment as research technicians in support of the project.

Acknowledgments

The author gratefully acknowledges the helpful suggestions of reviewers from the Canada-Nunavut Geoscience Office. The work detailed here is part of the author's graduate thesis work, and the author is grateful to M. Richardson (Carleton University) for academic supervision and fieldwork support, and to J. Shirley (Nunavut Research Institute) for supervision and support in Iqaluit (both M. Richardson and J. Shirley also provided helpful critical reviews of this manuscript). Nunavut Research Institute summer students J. Peters, J. Allen and A. Bychok are thanked for their contributions to fieldwork and laboratory analyses. Nunavut Arctic College Environmental Technology Program instructors J. Carpenter and D. Martin, and ETP students P. Aqqaq, R. Hinanik, A. Kilabuk, K. Lindell, T. Lee, S. Noble-Nowdluk, N. Panniuq, A. Pedersen and D. Taukie have all been instrumental in fieldwork and logistics in 2015 and 2016. The digital elevation model employed in terrain analyses conducted for this work was provided by N. Short at Canada Centre for Remote Sensing, Natural Resources Canada. At Carleton University, E. Humphries, M. Treberg and D. Mueller are thanked for technical advice on the design and setup of meteorological instrumentation. This work has been conducted as a part of projects that have received funding from the National Sciences and Engineering Research Council of Canada, Indigenous and Northern Affairs Canada's Northern Contaminants Program, ArcticNet Inc., Polar Knowledge Canada and the Northern Scientific Training Program.

References

Allard, M., Doyon, J., Mathon-Dufour, V., LeBlanc, A.-M., L'Hérault, E., Mate, D., Oldenborger, G.A. and Sladen, W.E. 2012: Surficial geology, Iqaluit, Nunavut; Geological Survey of Canada, Canadian Geoscience Map 64 (preliminary version), 1:15 000, doi:10.4095/289503

Blackadar, R.G. 1967: Geological reconnaissance, southern Baffin Island, District of Franklin; Geological Survey of Canada, Paper no. 66-47, 39 p. plus 3 maps, scale 1:506 880.

Budkewitsch, P., Prévost, C., Pavlic, G. and Pregitzer, M. 2011: Watershed mapping and monitoring for northern community impact assessment – Clyde River, Nunavut; Geological Survey of Canada, Open File 6620, 63 p., doi:10.4095/288034

Budkewitsch, P., Prévost, C., Pavlic, G., Pregitzer, M., Zhang, Y., Sauvé, P., Lavergne, J.C. and Mate, D. 2012: Arctic infrastructure (Nunavut): geomatics information to support monitoring and mapping of freshwater supplies in northern communities; *in* Climate Change Geoscience Program: 2006-2011 Program Final Report, A.N. Rencz (ed.), Geological Survey of Canada, Open File 6879, p. 132–137, doi:10.4095/290156

Chiasson-Poirier, G. 2016: Identification and characterisation of subsurface flow contributions to surface water during the baseflow recession of a small Arctic River; B.Sc. honours thesis, Université de Montréal, Montréal, Quebec, 39 p.

Church, M. 1974: Hydrology and permafrost with reference to northern North America; *in* Permafrost Hydrology: Proceedings of the Workshop Seminar, 1974, Canadian National Committee for the International Hydrological Decade, Environment Canada, p. 7–20.

Conrad, O., Bechtel, B., Bock, M., Dietrich, H., Fischer, E., Gerlitz, L., Wehberg, J., Wichmann, V. and Böhner, J. 2015: System for Automated Geoscientific Analyses (SAGA) v. 2.1.4; Geoscientific Model Development, v. 8, p. 1991–2007, doi:10.5194/gmd-8-1991-2015

Dingman, S.L. 1973: Effects of permafrost on stream flow characteristics in the discontinuous permafrost zone of central Alaska; *in* North American Contribution Permafrost Second International Conference, July 13–28, 1973, Yukutsk, USSR, National Academy of Sciences, p. 447–453.

Dyck, M. 2007: Community monitoring of environmental change: college-based limnological studies at Crazy Lake (Tasirluk), Nunavut; Arctic, v. 60, no. 1, p. 55–61.

Environment and Climate Change Canada 2016a: Canadian climate normals 1981–2010; Environment and Climate Change Canada, URL <http://climate.weather.gc.ca/climate_normals/index_e.html> [October 2016].

Environment and Climate Change Canada 2016b: Water Survey of Canada; Environment and Climate Change Canada, URL <https://www.ec.gc.ca/rhc-wsc/> [October 2016].

Esri 2016: ArcGIS Desktop: release 10.4; software, Esri, Redlands, California [September 2016].

Fisher, R. 1970: Statistical Methods for Research Workers (14th edition); Oliver & Boyd, Edinburgh, United Kingdom, 378 p.

FoTenn Consultants Inc. 2010: City of Iqaluit General Plan: By-law 703; prepared for City of Iqaluit Planning and Lands Department, Nunavut, 95 p.

Forgy, E. 1965: Cluster analysis of multivariate data: efficiency versus interpretability of classifications; Biometrics, v. 21, p. 768–769.

Gascon, G., Stewart, R. and Hension, W. 2010: Major cold-season precipitation events at Iqaluit, Nunavut; Arctic, v. 63, no. 3, p. 327–337.

Golder Associates Ltd. 2014: Lake Geraldine Water Balance Assessment; unpublished report prepared for City of Iqaluit, Nunavut, 88 p.

Gordon, M., Biswas, S., Taylor, P., Hanesiak, J., Albarran-Melzer, M. and Fargey, S. 2010: Measurements of drifting and blowing snow at Iqaluit, Nunavut, Canada, during the STAR project; Atmosphere-Ocean, v. 48, no. 2, p. 81–100.

Hodgson, D. 2005: Quaternary geology of western Meta Incognita peninsula and Iqaluit area, Baffin Island, Nunavut; Geological Survey of Canada, Bulletin No. 582, 74 p.

Kjikjerkovska, E. 2016: Long-term hydroclimatic change and interannual variability in water sources, Apex River (Iqaluit), Baffin Island, Nunavut; M.Sc. thesis, Queen's University, Kingston, Ontario, 107 p.

Liston, G. and Sturm, M. 2004: The role of winter sublimation in the Arctic moisture budget; Nordic Hydrology, v. 35, no. 4, p. 325–334.

Lundberg, A., Granlund, N. and Gustaffson, D. 2008: "Ground truth" snow measurements – review of operational and new measurement methods for Sweden, Norway, and Finland; *in* Proceedings of 65th Eastern Snow Conference, Fairlee, Vermont, May 28–30, 2008, p. 215–237.

MacQueen, J. 1967: Some methods for classification and analysis of multivariate observations; *in* Proceedings of the Fifth Berkeley Symposium on Mathematical Statistics and Probability, Volume 1: Statistics, L.M. Le Cam and J. Neyman (ed.), University of California Press, June 21–July 18, 1965 and December 27, 1965–January 7, 1966, Berkley, California, p. 281–297

Mariani, Z., Dehghan, A., Gascon, G., Joe, P., Strawbridge, K., Burrows, W. and Melo, S. 2016: Iqaluit calibration/validation supersite for meteorological satellites; *in* Living Planet Symposium 2016 Conference Proceedings, European Space Agency, May 9–13, 2016, Prague, Czech Republic, SP-740, p. 528.

McClung, D. and Schaerer, P. 2006: The Avalanche Handbook; The Mountaineers Books, Seattle, Washington, 338 p.

McKay, G. and Gray, D. 1981: The distribution of snowcover; *in* Handbook of Snow: Principles, Processes, Management and Use, D.M. Gray and D.H. Male (ed.), Pergamon Press, Toronto, p. 153–190.

Natural Resources Canada 2015: CanVec; Natural Resources Canada, topographic reference digital product, URL <http://geogratis.gc.ca/api/en/nrcan-rncan/ess-sst/23387971-b6d3-4ded-a40b-c8e832b4ea08.html> [October 2015].

Newbury, R. 1974: River hydrology in permafrost areas; *in* Permafrost Hydrology: Proceedings of the Workshop Seminar, 1974, Canadian National Committee for the International Hydrological Decade, Environment Canada, p. 31–37.

Obradovic, M. and Sklash, M. 1986: An isotopic and geochemical study of snowmelt runoff in a small Arctic watershed; Hydrological Processes, v. 1, p. 15–30.

Pomeroy, J. 1988: Wind transport of snow; Ph.D. thesis, University of Saskatchewan, Saskatoon, Saskatchewan, 226 p.

Pomeroy, J. and Gray, D. 1995: Snow accumulation, relocation and management; National Hydrology Research Institute, Environment Canada, NHRI Science Report No. 7, 144 p.

Pomeroy, J. and Li, L. 2000: Prairie and arctic areal snow cover mass balance using a blowing snow model; Journal of Geophysical Research, v. 105, no. D21, p. 26619–26634.

Pomeroy, J., Gray, D., Hedstrom, N. and Janowicz, J. 2002: Prediction of seasonal snow accumulation in cold climate forests; Hydrological Processes, v. 16, p. 3543–3558.

Pomeroy, J., Hedstrom, N. and Parviainen, J. 1999: The snow mass balance of Wolf Creek, Yukon: effects of snow sublimation and redistribution; *in* Wolf Creek Research Basin - Hydrology, Ecology, and Environment, J. Pomeroy and R.J. Granger (ed.), Environment Canada, National Water Research Institute, NWRI Contribution No. 99-326, p. 15–30.

R Development Core Team 2013: R: a language and environment for statistical computing; software development tools, R Foundation for Statistical Computing, Vienna, Austria, URL <http://www.R-project.org/> [September 2013].

Rees, A., English, M., Derksen, C., Toose, P. and Silis, A. 2013: Observations of late winter Canadian tundra snow cover properties; Hydrological Processes, v. 28, no. 12, p. 3962–3977.

Ribeiro, P. and Diggle, P. 2001: geoR: a package for geostatistical analysis; R-NEWS, v. 1, no. 2, p. 15–18.

Richardson, M. and Shirley, J. in press: Metal loading and retention in Arctic tundra lakes during spring runoff; Indigenous and Northern Affairs Canada, Northern Contaminants Program Synopsis Report, 11 p.

Rusk, B. 2016: Characterization of the geochemical processes and importance of subsurface water input at the confluence of the Apex River in Iqaluit, NU; B.Sc. honours thesis, Queen's University, Kingston, Ontario, 37 p.

Shirley, J. 2014: Microbial water quality in Apex River from 2009 to 2012: insights from community based monitoring; Arctic Change 2014, Oral Presentation Abstracts, December 8–12, 2014, Ottawa, Ontario, ArcticNet, p. 168–169.

Sims, J. and Allard, B. 2014: City of Iqaluit Supplementary Water Supply Study; unpublished report prepared for the City of Iqaluit, Nunavut, 95 p.

Squires, C. 1984: The late Foxe deglaciation of the Burton Bay area, southeastern Baffin Island, N.W.T.; M.A. thesis, Windsor University, Windsor, Ontario, 115 p.

St-Onge, M., Scott, D. and Wodicka, N. 1999: Geology, Frobisher Bay, Nunavut; Geological Survey of Canada, "A" Series Map 1979A, scale 1:100 000.

Thiel, G. 2016: Investigating seasonal hydrology and its relationship with microbiological indicators in the Apex River watershed (Iqaluit, Nunavut); B.Sc. honours thesis, Queen's University, Kingston, Ontario, 57 p.

Tremblay, T., Day, S., McNeil, R., Smith, K., Richardson, M. and Shirley, J. 2015: Overview of surficial geology mapping and geochemistry in the Sylvia Grinnell Lake area, Baffin Island, Nunavut; *in* Summary of Activities 2015, Canada-Nunavut Geoscience Office, p. 107–120.

Tukey, J. 1949: Comparing individual means in the analysis of variance; Biometrics, v. 5, no. 2, p. 99–114.

Williams, P.J. and Smith, M.W. 1989: The Frozen Earth. Fundamentals of Geocryology; Cambridge University Press, Cambridge, United Kingdom, p. 202–236.

Woo, M. 2012: Permafrost Hydrology; Springer-Verlag, Berlin, Germany, 519 p.

Zerehi, S.S. 2016: Iqaluit rain 'just won't stop', causes flooding in parts of city; CBC News: North, July 22, 2016, URL <http://www.cbc.ca/news/canada/north/iqaluit-rainfall-causes-flooding-1.3690953> [October 2016].

Methodological approach to characterize flow paths and water sources during the active-layer thaw period, Niaqunguk River watershed, Iqaluit, Baffin Island, Nunavut

G. Chiasson-Poirier[1], J. Franssen[2], D. Fortier[2], A. Prince[2], T. Tremblay[3], M. Lafrenière[4], J. Shirley[5] and S. Lamoureux[4]

[1]*Department of Geography, Université de Montréal, Montreal, Quebec, gabriel.chiasson-poirier@umontreal.ca*

[2]*Department of Geography, Université de Montréal, Montreal, Quebec*

[3]*Canada-Nunavut Geoscience Office, Iqaluit, Nunavut*

[4]*Department of Geography, Queen's University, Kingston, Ontario*

[5]*Nunavut Research Institute, Iqaluit, Nunavut*

This work is part of the Carleton University–led Partnership for Integrated Hydrological and Water Quality Monitoring, Research and Training in the Niaqunguk River Watershed, Iqaluit, Nunavut, a Polar Knowledge Canada–supported integrated collaboration with Nunavut Research Institute, Université du Québec à Montréal, Queen's University and Nunavut Arctic College. The research is also supported through an ArcticNet initiative, Water Security and Quality in a Changing Arctic. The shared objective of these programs is to improve knowledge in the area of arctic snow hydrology and its cascading influences on freshwater resource supply and aquatic ecosystems in the Niaqunguk River watershed, and is being developed for long-term sustainability and capacity building with local residents.

Chiasson-Poirier, G., Franssen, J., Fortier, D., Prince, A., Tremblay, T., Lafrenière, M., Shirley, J. and Lamoureux, S. 2016: Methodological approach to characterize flow paths and water sources during the active-layer thaw period, Niaqunguk River watershed, Iqaluit, Baffin Island, Nunavut; *in* Summary of Activities 2016, Canada-Nunavut Geoscience Office, p. 105–120.

Abstract

In its 2010 General Plan, the City of Iqaluit identified the Niaqunguk River as a supplemental potable-water source. Knowledge about subsurface flows, one of the major sources of water for rivers during the baseflow period, is still limited in permafrost environments. Groundwater flow paths and their connections with surface water remain difficult to predict due to the dynamic state of the active layer in the surrounding alluvial plain and under the river bed. This paper presents a detailed methodology that aims to address the gap in knowledge about the interaction between subsurface flow and active-layer thaw. During the 2016 summer thaw period, water levels were continuously recorded in 28 piezometers installed across a hillslope-stream toposequence. By carefully analyzing piezometer water levels in response to rainfall inputs, it was possible to identify preferential routing and storage of water across the hillslope, and to determine how the hydrological dynamics of the study site responded to, or were associated with, the spatial-variable evolution of the frost-table topography. To determine the proportion of different water sources contributing to flows, a total of 148 water samples were collected from groundwater wells, streamflow, lake water and rainfall for chemical analysis (i.e., electrical conductivity, stable isotopes in water and dissolved organic carbon). End-member mixing analysis will be used to confirm the proportion of groundwater and other sources (e.g., precipitation, surface runoff) contributing to streamflow. The results of this research will be used to assess the relative importance of subsurface flow to Arctic river systems and to determine how anticipated climate-related changes are likely to impact these systems.

Résumé

Dans son Plan général qui a paru en 2010, la communauté d'Iqaluit désignait la rivière Niaqunguk en tant que source d'eau potable complémentaire. L'état des connaissances au sujet de l'écoulement souterrain de l'eau, soit une des principales sources d'eau pour les rivières pendant la période de débit de base, est faible en ce qui a trait aux milieux touchés par le pergélisol. Les voies d'écoulement de l'eau souterraine et leurs rapports avec l'eau superficielle sont difficiles à prévoir en raison de la nature dynamique de la couche active dans la plaine alluviale environnante et sous le lit de la rivière. La présente étude décrit en détail les méthodes utilisées en vue de combler les lacunes au niveau de l'état des connaissances au sujet de l'interaction entre l'écoulement souterrain et le dégel de la couche active. Au cours de la période de dégel de l'été 2016, les

This publication is also available, free of charge, as colour digital files in Adobe Acrobat® PDF format from the Canada-Nunavut Geoscience Office website: http://cngo.ca/summary-of-activities/2016/.

niveaux d'eau ont été enregistrés en continu au moyen d'un réseau de 28 piézomètres installé à travers une toposéquence située dans un ruisseau sur une pente de colline. Une analyse détaillée des niveaux d'eau enregistrés suite aux précipitations a permis d'identifier la voie empruntée de préférence par l'eau et les aires de stockage le long de la pente, ainsi que la façon dont la dynamique de l'hydrologie de la région à l'étude réagissait, ou tout au moins était associée, à l'évolution de la variable spatiale de la topographie de la table de gel-dégel. Afin de définir la proportion des sources d'eau distinctes contribuant à l'écoulement, 148 échantillons ont été recueillis provenant de puits d'eau souterraine, de ruisseaux, de lacs et de précipitations aux fins d'analyses chimiques (conductance spécifique, isotopes stables en solution aqueuse et carbone organique dissous). Le recours à l'analyse de mélange de membres extrêmes permettra de confirmer la proportion d'eau provenant de sources souterraines ou d'autres sources (par ex. les précipitations et l'écoulement superficiel) qui contribue à l'écoulement fluvial. Les résultats acquis permettront en outre d'évaluer l'importance relative de l'écoulement de l'eau souterraine dans les systèmes fluviaux arctiques et de déterminer dans quelle mesure les changements prévus liés au climat sont susceptibles d'avoir une incidence sur ces systèmes.

Introduction

Surface waters are abundant in the Arctic landscape, but transportation constraints and critical low flow during summer complicate the management of water resources (White et al., 2007). In response to population growth and the inadequacy of the current water source (Lake Geraldine), the City of Iqaluit has identified the Niaqunguk (commonly known as Apex) River as a supplementary water source (City of Iqaluit, 2010). In 2015, an extensive period of low flow (<1 m^3/s), from the end of July to the end of August, underlined the need to better understand the water sources and flow dynamics at work in the Niaqunguk River watershed to ensure sustainable management of the river. This research project, which involved Queen's University, Carleton University, the Université de Montréal and the Nunavut Research Institute, aims to improve understanding of both the quality and quantity of water in the Niaqunguk River watershed.

In the context of a warming climate, it has been suggested that groundwater pathways and contributions to surface water will increase due to permafrost degradation (Connon et al., 2014). However, groundwater fluxes and their contribution to surface water remain difficult to predict due to uncertainties about the temporal variation of thaw depths (i.e., frost-table depths). As the frost table in Arctic environments acts as an impermeable boundary, frost-table depth is a key factor influencing how water is routed from hillslope recharge areas to lakes and streams (Semenova et al., 2013). Although studies using sophisticated instruments and elaborate field-research design have been conducted to understand the role of bedrock topography on groundwater flow in southern watersheds (Rodhe and Siebert, 2011; van Meerveld, 2015), relatively little research on Arctic groundwater dynamics has taken place during the first decade of the 2000s (Woo et al., 2008). Furthermore, most of the recent research investigating shallow groundwater-flow processes in permafrost environments has been model based and the results of that research need to be confirmed by field-based inquiry (Bring et al, 2016). A few studies (e.g., Quinton and Marsh, 1998; Carey and Woo, 2002) have demonstrated that microtopography, the ground freeze-thaw cycle, and the properties of soil and surficial deposits can significantly influence subsurface drainage on Arctic hillslopes. Others have addressed the relationship between water storage and variable active-layer thawing (Quinton et al., 2005; Wright et al., 2009). Improved knowledge of active-layer dynamics is key to a better understanding of hydrological processes at work in permafrost landscapes (Bring et al., 2016). In a pioneering study, Woo and Steer (1983) examined the variation of subsurface flow patterns and active-layer thaw depths on two hillslopes near Resolute, Nunavut. The authors observed a change in runoff flow patterns due to an increase in the active-layer thawing depth, and thus water-storage capacity, which highlighted the need for a better understanding of the interaction between these two processes. No subsequent field-based study seems to have employed a similar methodology to investigate the relationship between subsurface flow patterns and active-layer thawing dynamics. Characterizing the relationship between these two subsurface processes is essential to acquiring the fundamental knowledge needed to develop models that can predict active-layer thawing dynamics. Approaches that combine detailed spatiotemporal characterization of subsurface flow patterns with chemical analysis to track variable water sources will lead to a better understanding of flow-path development and hydrological connectivity during the active-layer thawing period (Woo et al., 2008). This knowledge is essential to predict the way in which climate change and alterations to permafrost will impact the hydrology of Arctic rivers.

As part of this research, instruments were installed on a hillslope-stream toposequence, where subsurface flow is constrained by the presence of the frost table; this stream is a tributary of the Niaqunguk River. The purpose of the study was to provide a detailed characterization of the patterns of water flow and storage at this site during the active-layer thaw period in order to assess how different thaw depths and soil characteristics influence hydrological connectivity across the hillslope-stream toposequence and to

investigate the influence of hydrological processes on the evolution of frost-table depths during the summer thawing period. This knowledge will help to determine the relative importance of subsurface-flow contribution to Arctic river systems and the impacts of climate-related changes. Four specific research objectives were identified

- track the flow and storage of suprapermafrost groundwater across and within a hillslope consisting of glaciofluvial and organic deposits during the active-layer thawing period;
- characterize the physical processes governing the routing of shallow groundwater and the influence of this subsurface flow on active-layer development;
- assess the relative importance of different water sources (rain, groundwater, lake, overland flow) contributing to the flow of a tributary stream at the foot of the studied hillslope; and
- theorize on the role of distinct hydrogeomorphic features in controlling surface and subsurface runoff into the Niaqunguk River watershed.

Study site

The Niaqunguk River is a fourth-order stream located northeast of the City of Iqaluit (latitude 63°45'N, longitude 68°33'W) and draining an area of 58 km^2. The hydrological network comprises three main tributaries with a fourth-order segment downstream of their confluence. Elevations range between sea level at the river outlet in the neighbourhood of Apex and 360 m at the headwaters. The topography of the watershed is characterized by longitudinal bedrock hills trending northwest that have been smoothed by glacial erosion. An end moraine forms the eastern border of the watershed and a wide variety of Quaternary deposits (e.g., till blanket and veneer, glaciofluvial deposits, boulder fields) are found throughout the watershed (Hodgson, 2005). Figure 1a shows the distribution of surficial deposits in the southern half of the watershed (T. Tremblay, unpublished data, 2016), which is situated in the continuous permafrost zone where the active layer is on average 1.35 m thick under natural ground. Streamflow season typically begins in May and ends in October. Based on data from 1973 to 2010, total mean precipitation for the months of July and August is 52 and 70 mm, respectively, whereas the mean annual total is 404 mm, with snow accounting for 57% (Environment Canada, 2016). Total precipitation for the months of October 2015 to September 2016 was 495 mm and mean precipitation for July and August was 132 and 57 mm, respectively. The 2016 thawing season began on April 26 and the thawing index on September 31 was 703 degree-days C.

The field study was undertaken predominantly in a subwatershed (0.41 km^2) centrally located within the Niaqunguk River watershed, approximately 6 km north of the City of Iqaluit. Figure 1b shows the topography and hydrological network of the subwatershed, as well as the location of the piezometer installation, the water sample sites and the flow- or water-level–monitoring stations. The stream draining this subwatershed discharges into the middle branch of the Niaqunguk River. This site is located outside of the area covered by the 1:15 000 surficial geology map of Iqaluit (Allard et al., 2012) and a detailed surficial geology map (T. Tremblay, unpublished data, 2016) of the study site. The most recently published surficial geology map of this area (Hodgson, 2003) is a small-scale map (1:100 000) that identifies till blanket as the only surficial deposit type within this subwatershed. A larger scale map of the surficial geology of the area will be presented in this study. This study site was chosen because the surficial geology of this subwatershed is representative of the surficial geology of the Niaqunguk watershed. To characterize subsurface flow-path dynamics at this site over the thawing season, a network of piezometers was installed at the foot of a convergent (bowl-shaped) hillslope. The hillslope is almost entirely (~90%) covered by organic material of varying thickness, with turf hummocks found predominantly in the upslope area (often covering boulder deposits). Turf hummocks consist of an accumulation of organic material covered by living vegetation (van Everdingen, 1998). The size of the turf hummocks within the hillslope study site varies from small (<20 cm wide by <20 cm high) to large (~1 m wide by ~50 cm high).

Methodology

Water-table monitoring

A total of 38 piezometers were installed in the hillslope study site on July 8, 2016 (Figure 2a); they were placed from the foot of the hillslope (at the streambank) to 60 m upslope and were distributed across an area ~30 m wide. Water levels were recorded continuously in 28 piezometers; manual water level measurement were conducted in 5 piezometers and 5 piezometers were used for water sampling. During piezometer installation, terrain features were taken into account such that piezometers were not placed directly in turf hummocks, in which it was assumed that groundwater could not be stored due to the high hydraulic conductivity of the organic material (peat; Quinton et al., 2008). The piezometer installation was designed to help characterize the groundwater-flow direction in the mineral deposits below the surface organic layer. Where the water table comes in contact with the surface organic layer (which has a higher hydraulic conductivity), flow patterns may change and be concentrated in overland flow channels or preferential flow paths between turf hummocks, which are more influenced by local surface topography than by the characteristics of the underlying mineral deposits. However, spot water-level measurements were conducted under 14 turf hummocks seven times throughout the summer to

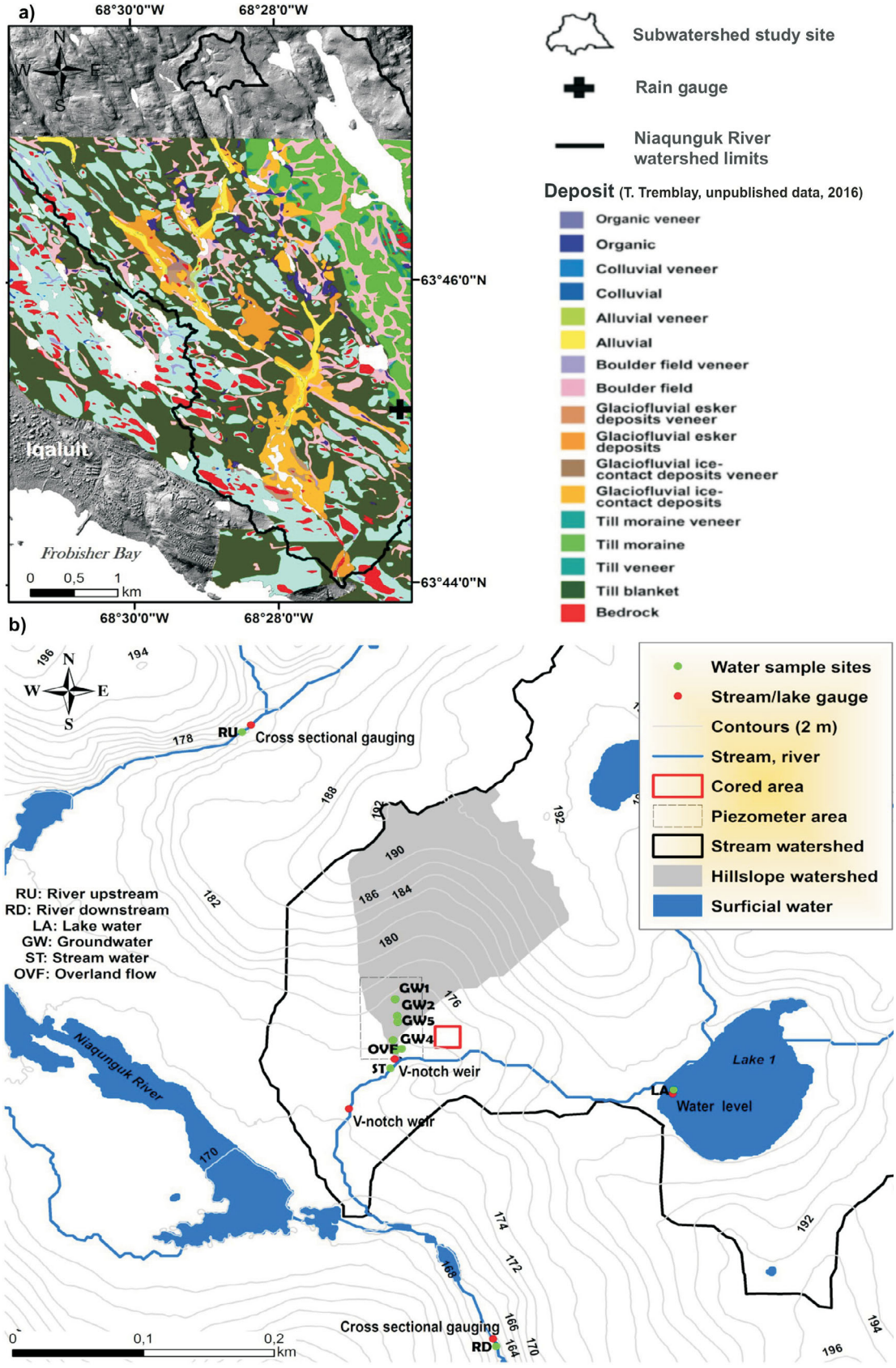

Figure 1: Location of the study area in the Niaqunguk River watershed, showing **a)** the surficial geology of the southern portion of the watershed (T. Tremblay, unpublished data, 2016); **b)** the topography and hydrological network surrounding the hillslope study site, and the location of the different measurement and sampling sites.

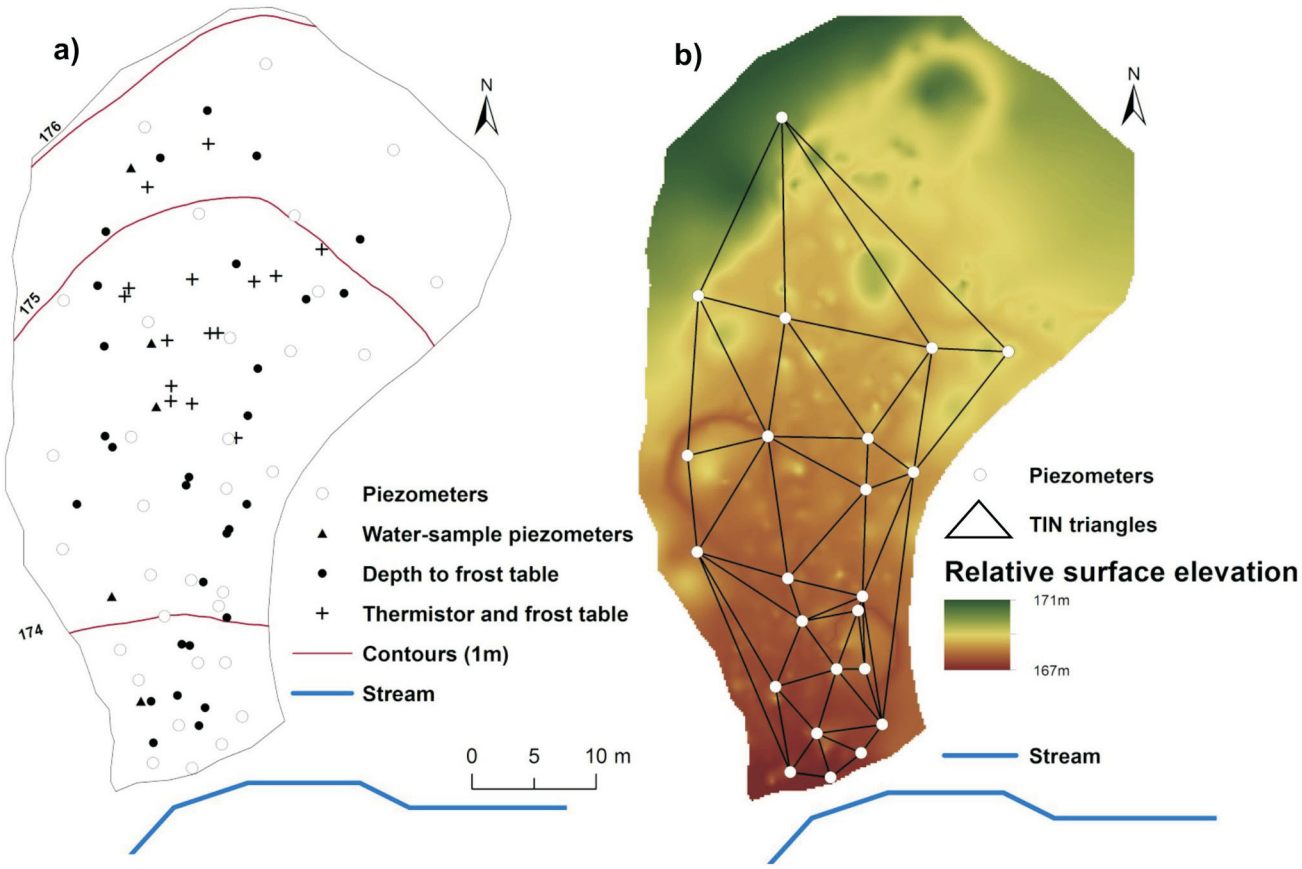

Figure 2: Schematic illustration of the studied hillslope in the Niaqunguk River watershed, showing **a)** the location of the 38 piezometers, thermistor and frost-table measurements; **b)** the triangulated irregular network (TIN) used for analysis of the surface topography, the groundwater levels and the frost-table depths; surface topography (1 m) is derived from a Topo to Raster tool for ArcGIS 10.2 (Esri, 2013) interpolation of 1000 elevation values measured using a total station. The sampling method was based on the characterization of slope break and microtopography (i.e., turf hummocks, boulder).

verify that the water table was not locally influenced by the microtopography of the turf hummocks.

Piezometers were constructed of schedule 80 polyvinyl chloride (PVC) tubing (3.7 cm in diameter) cut to lengths of 1 or 1.5 m. A solid PVC drive point was fitted to the bottom of each PVC tube. Each piezometer had a screen length of 14 cm at the bottom end of the tube and 20 holes of 1 cm in diameter were pierced through the walls of the tube. A Nitex® nylon 50 µm mesh was fitted to the interior of the screened section to prevent the infiltration of fine sediment into the piezometer.

A small hand auger was used to install the piezometers, which would be advanced weekly with a hammer to the depth of the frost table until they penetrated no further. Each time the piezometers were repositioned, the vertical hydraulic head directly above the frost table and the depth of the active layer were measured. The relatively high density of piezometers across the downslope portion of the instrumented hillslope (one piezometer per 16 m^2) and across the entire hillslope (one piezometer per 34 m^2) is comparable to previous studies that investigated variation of groundwater-flow directions on hillslopes (Rodhe and Siebert, 2011; van Meerveld, 2015). The piezometers were installed in such a way as to help determine the influence of surficial and frost-table microtopography on groundwater-flow patterns at the hillslope scale. The triangle surface tool of the ArcGIS 3D Analyst module (Esri, 2010) was used to generate a triangulated irregular network (TIN) to interpret the water levels between three adjacent piezometers and to derive flow directions based on the slope surfaces of the triangles. Figure 2b shows the TIN triangles formed between piezometers.

Groundwater levels in 28 piezometers were measured at 20 min intervals using vented-pressure sensors installed at the bottom of each piezometer. Readings from each pressure sensor were recorded using either a CR1000 or CR10 datalogger manufactured by Campbell Scientific. Additionally, the water level in each piezometer was routinely measured with an electronic water-level dipper with a measurement accuracy of ±1 mm (Figure 3).

The water-level sensors were built using a model MPXV5100GC6U 1 cm micropressure transducer manu-

factured by NXP that was fitted with three 22-gauge copper wires to route the power supply and allow communication with the dataloggers. The pressure transducers were each fitted with a flexible tube 3.2 mm (1/8 in.) in diameter that was vented to atmosphere to establish the difference between air and water pressure at the sensor. The venting tubes were connected to desiccant reservoirs to prevent condensation within the vent tube that would negatively

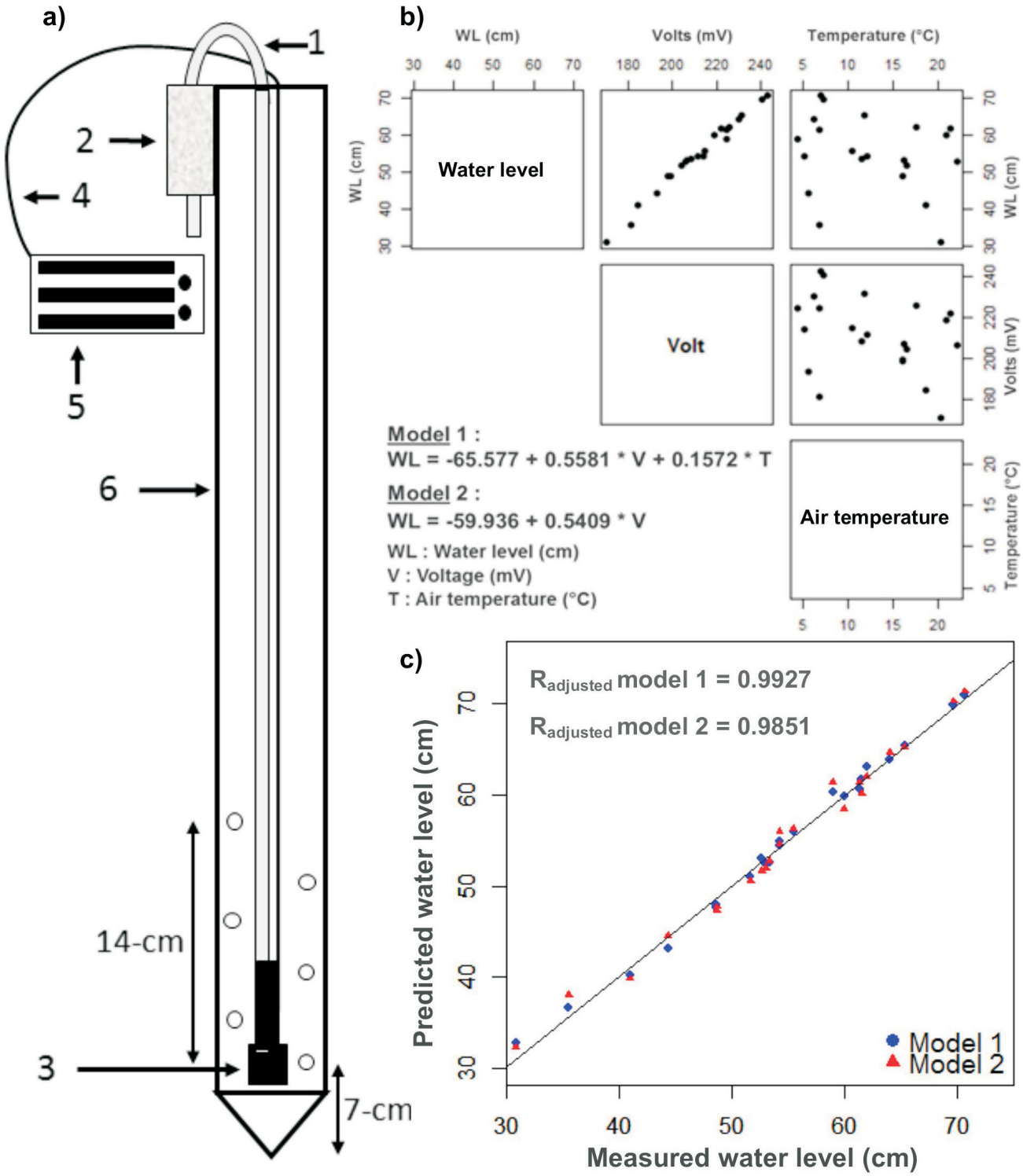

Figure 3: a) Schematic illustration of a groundwater-level measurement setup, in which is shown the venting tube (1), the desiccant reservoir (2), the pressure sensor (3), the copper cable (4), the data logger (5), and the piezometer (6). **b)** Graphs representing the relation between water level–outputted voltage, voltage–temperature and water level–temperature, respectively, and **c)** an example of the multiple-regression model used to predict water level.

impact sensor function. The laboratory tested accuracy of the sensors at 25°C was ±3 mm of water level over a range of 0 to 0.7 m.

The relation between the voltage output of the sensor and the water pressure at the sensor, and the relationship between the water pressure and the water level in the piezometer are both linear. A linear relationship also exists between the air temperature and the cable resistivity. Outputted voltage from the pressure transducer is temperature compensated, but the relationship between air temperature and cable resistivity needs to be accounted for to convert the voltage recorded by the loggers to an accurate measure of water level within the piezometer. To associate a given water level in the piezometer to a given voltage output of the sensor, approximately 20 water-level measurements were recorded with the electronic water-level dipper in each piezometer and a multiple-regression analysis was performed to account for voltage and temperature as descriptive variables to derived water level. The resulting equation is

$$h = a + (b_1 * V) + (b_2 * T)$$

where h is the water level, V is the voltage recorded at the logger, T is the air temperature and a, b_1 and b_2 represent the constant factors acquired from the regression for every sensor.

To evaluate the horizontal hydraulic conductivity over the hillslope, falling-head tests were performed in each piezometer on August 21, 2016. Water levels during the tests were recorded every 10 seconds for the first three hours and every 20 minutes thereafter, if the water level hadn't reached the initial level within the first three hours. These measurements will be used to examine the influence of surface and frost-table topography, and the physical properties of the subsurface (i.e., soil type, hydraulic conductivity) on subsurface flow patterns, as well as to examine how subsurface flow patterns may have evolved during the active-layer thaw period.

Active-layer depth and deposits properties

Various techniques were used to establish frost-table depths across the hillslope during the active-layer thaw period. The depth of the frost table was measured using a graduated metal rod that was pushed into the soil until it would penetrate no further. Thaw depths were also measured at each piezometer throughout the summer. Figure 2a illustrates frost-table–depth measurement stations (n = 29). To complement these measurements, additional stations were located in the centre of the TIN triangles (i.e., points roughly equidistant from the nearest three piezometers). As the instrumented hillslope is characterized by heterogeneous organic cover, frost-table measurements were also made in turf hummocks or dry organic deposits (n = 15), areas with thin organic material cover (n = 8) and inter-hummock preferential flow paths (n = 21). These additional measurement points provided insight into the influence of these surface features on thawing depths.

Thermistors were installed 5 cm below the surface of turf hummocks (n = 7) and bare ground inter-hummock flow paths (n = 8) to assess the influence of air-heat conduction on the thawing depths in areas with different surficial characteristics. By comparing the probed thaw depths to temperature-modelled thaw depths at thermistor locations, the influence of air temperature and flow accumulation on the extent of the active-layer thawing can also be compared. Soil temperature and frost-depth probe measurements at thermistor locations were undertaken from July 20 to August 26.

Using a handheld concrete core drill, five soil cores were extracted at depths below the frost table on August 3. Two of these coring sites were located in turf hummocks and the remaining three, in inter-hummock channels. The coring was conducted adjacent to the hillslope study area (Figure 1b) so as not to interfere with the routing of flow in the study site. However, saturation conditions, vegetation, deposits and slopes at the coring locations were comparable to the adjacent locations on the instrumented hillslope.

Overland flow, stream discharge and meteorological measurements

To establish the relative contribution of surface and subsurface flow from the instrumented hillslope to the stream in the study site and the relative contribution of the stream to the Niaqunguk River, the discharge or water level at five locations in the subwatershed area was monitored (Figure 1b). A v-notch weir was installed in the stream downstream of the hillslope and gauging sites were established on the main channel of the Niaqunguk River upstream and downstream of the confluence with the tributary stream draining the subwatershed (Figure 1b). At each of these sites, water levels were monitored continuously from July 4 to August 26. Using data loggers manufactured by Onset (model HOBO® U20), Global Water (model WL16) and Solinst Canada Ltd., water levels were recorded every 15 minutes in the lake situated 100 m upstream of the instrumented hillslope (Figure 1b). During the final two weeks of the study period (August 14–26), a second v-notch weir was installed at the foot of the hillslope to quantify overland flow.

Other data collected included rainfall data measured using a tipping-bucket rain gauge (Figure 1a) located ~3 km south of the instrumented hillslope (M. Richardson and K. Smith, unpublished data, 2016) and meteorological data (e.g., daily precipitation, temperature; Environment and Climate Change Canada, 2016) available from the Iqaluit Airport meteorological station operated by Environment

Canada. The air temperature and relative light intensity at the instrumented hillslope were measured and logged at 20 min intervals using an Onset HOBO® temperature data logger placed in a vented radiation shield, and an Onset HOBO® Pendant temperature/light data logger placed horizontally on a raised platform.

River, stream, lake and groundwater sampling

From July 7 to August 26, water samples were collected for chemical analysis at ten locations in the study area (Figure 1b). On the hillslope, five groundwater sampling iezometers were installed in inter-hummock channels (n = 3) and in hummocks (n = 2), and pushed downward to the depth of frost table throughout the summer. Water in the piezometers was sampled using a bailer sampler. An instream sampling location was situated immediately downstream of the hillslope. Water samples were also collected in the Niaqunguk River at both the upstream and downstream gauging sites and from the lake identified as Lake 1 located along the subwatershed stream just upstream of the hillslope. Samples of overland flow at the foot of the hillslope were also collected during the last two weeks of August, when the overland-flow contribution was monitored at the second v-notch weir. These samples will be analyzed for electrical conductivity, stable isotopes ($ä^{18}O$ and $ä^{2}H$) and dissolved organic carbon. End-member mixing analysis will be used to determine the proportion of each different water source (e.g., precipitation, runoff and groundwater) contributing to flow to each location in the study site during the thaw season.

Deposit delineation

Terrain surveys were conducted to characterize the spatial distribution of surficial deposits and hydrogeomorphic terrain features within the subwatershed study site and at various locations throughout the southern half of the Niaqunguk River watershed. In the area shown on Figure 1a, field mapping with a handheld GPS device was used to verify the delineation of detailed surficial geology units northeast of Iqaluit derived from high-definition satellite images and DEM interpretation (T. Tremblay, unpublished data, 2016). Pedons were used to characterize the stratigraphy and grain-size characteristics of the deposits. These vertical sections were also used to confirm the accuracy of frost-table depth measurements obtained with probing instruments. Within the subwatershed study site, specific attention was given to delineating the surface-water network and locating the interface between different deposit types. Deposit delineation is essential as it will not only provide information on the spatial organization of the deposit units within the watershed but also help in assessing the structural hydrological connectivity, which will show how different contiguous deposit types can be linked together and affect the course of water in the watershed.

Subwatershed-scale flow-accumulation modelling

To investigate surface-water flow paths within the subwatershed, a flow-accumulation model based on a DEM at 1 m resolution was generated using the Arc Hydro tools for ArcGIS 10.2 (Djokic et al., 2011). The DEM was derived from WorldView-1 satellite imagery (Short et al., 2013). To generate the flow-direction model, the deterministic eight-node (D8) algorithm was used, based on DEM grid-elevation values ranging from 150 to 240 m in the subwatershed area. This grid was then used to produce the surface-flow accumulation network. A first iteration of the model was based only on topography, followed by a second run of the model that involved a 1 m lowering of the spatial resolution of the DEM elevation values to account for the well-drained boulder deposits. This second iteration of the model was undertaken to better reflect the hydrological influence of the well-drained boulder fields within the study area.

Results and discussion

Evolution of groundwater flow

The instrumented hillslope was snow free for the entire period of the study, although there was snow on the relatively steep north-facing slope located on the streambank opposite the hillslope study site. There were eight rainfall events during the study period; total precipitation for each event ranged from 1.2 to 80.5 mm. The total amount of precipitation during the month of July was 132 mm, greater than twice the mean monthly rainfall/precipitation for July as recorded over the last 20 years at Iqaluit Airport (5 km southeast of the study site; Environment and Climate Change Canada, 2016). Up to 80% of the hillslope remained saturated during the last two weeks of July and during rainfall events, overland flow was observed in the central portion of the hillslope. During a rain-free period that occurred between July 28 and August 10, no overland flow was observed. A heavy rainfall event toward the end of August resaturated the hillslope and overland flow was also observed at approximately the same location where it had been observed earlier in the season.

The hillslope piezometer network equipped with pressure transducers specifically designed by the authors for this study provided a continuous record of water levels in 23 piezometers over the course of the study period (July 8 to August 26, 2016). Preliminary analysis indicates that water levels in the piezometers ranged from 3 to 105 cm above the frost table, which represents a saturation of 1 to 100% of the fractional active-layer thickness. Positive hydraulic-head values relative to ground surface were also observed at multiple locations across the hillslope during the summer. Based only on the spot water-level measurements (n = 20) collected from the piezometers located on the hillslope, the highest average hydraulic head (+2.9 cm) occurred on

July 23, one day after the most important rainfall event (80 mm) of the summer. The lowest average hydraulic head (-6.9 cm) on the hillslope was observed on August 5, no doubt due to the fact that only very small rainfall events (<1 mm) occurred between July 27 and August 5. An interpolation of the relative elevations of the water-level measurements in the piezometers compared to the ground surface of the hillslope shows that on July 23 (Figure 4a) positive hydraulic-head values were present on almost all the hillslope, except small areas mid-slope and downslope (see paler shades of blue). Hydraulic head values on August 5 (Figure 4b) were significantly lower and were negative or below ground surface (bgs) in all the piezometers. On July 23, higher gradients were observed in piezometers 4, 6, 10, 11 and 19, which were located close to an overland flow that formed in the middle of the hillslope during important rainfall events (>30 mm) on July 13–18 and 21–22, and on August 22–25. Hydraulic heads observed on August 5 suggest that subsurface flow was concentrated in the middle of the hillslope, where higher relative water levels were observed.

Piezometer water levels in response to rainfall inputs will be analyzed in detail to determine not only if there was preferential routing and storage of water across the hillslope, but also how the hydrological dynamics of the study site responded to, or were associated with, the spatial-variable evolution of the frost-table (i.e., frost-table topography) at this site (see below). Of the 38 piezometers installed, 28 were equipped with pressure transducers, of which 23 (80%) remained functional throughout the entire study period. Given the relatively modest cost (~$40) of the components required to build the sensor relative to that of a comparable, commercially available water-level sensor (~$500), a modified version will be used in subsequent studies. Sensor failure was attributed to inadequate sealing of the sensor housing and malfunction was due to water penetration; future versions will be constructed using a higher quality sealant. In addition, pairing the sensors with wireless technology to eliminate some of the drawbacks (e.g., temperature influence on wire resistivity, placement constraints due to wire lengths) associated with direct wiring of the sensors to a datalogger could prove useful.

Active-layer, deposits and subsurface-flow relations

Measurements of frost-table depth made throughout the study period revealed that the extent of frost-table lowering varied substantially across the hillslope. The median frost-table depth on July 8, 2016 was 37 cm (range of 24 to 53 cm) bgs, whereas the median frost-table depth on August 24, 2016 was 81 cm (range of 54 to 126 cm) bgs. A model of frost-table topography derived from the interpola-

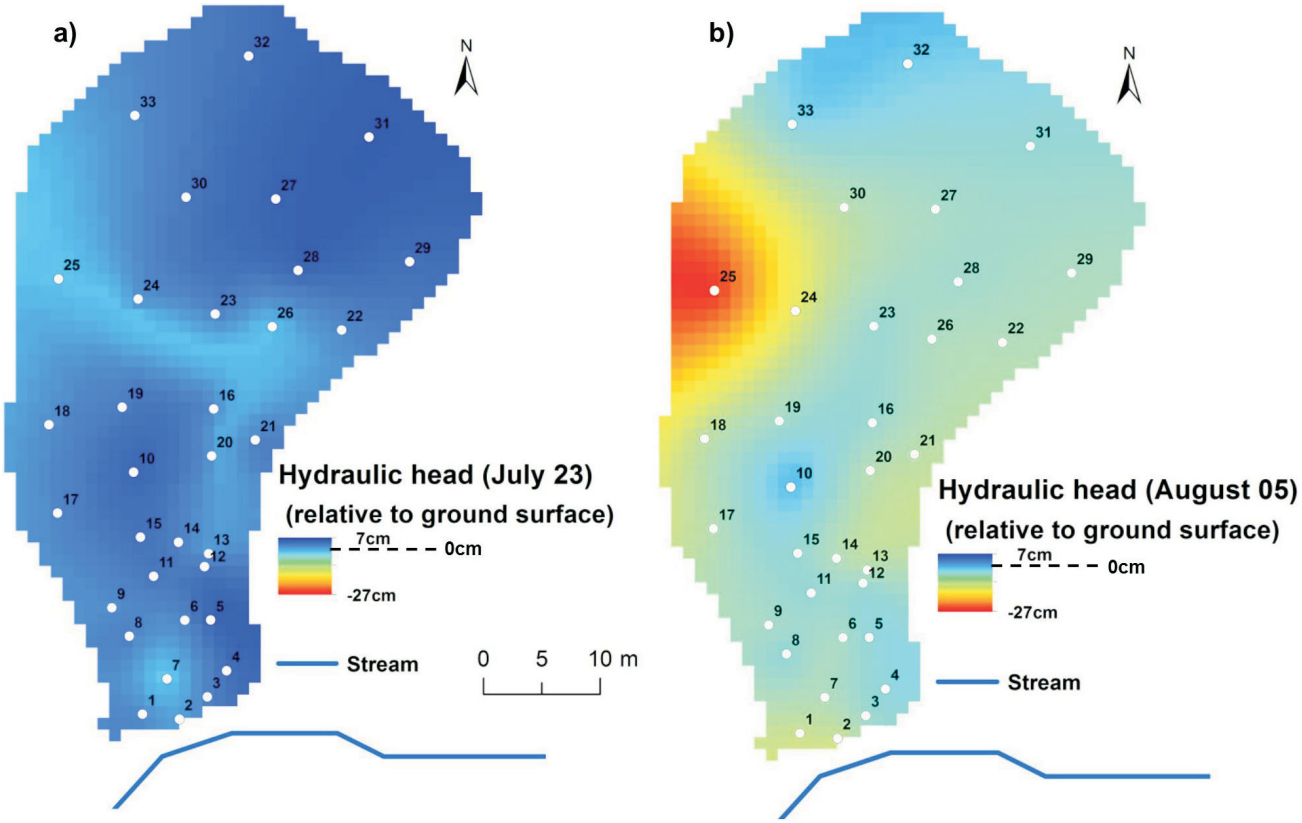

Figure 4: Interpolation using ArcGIS 10.2 (Esri, 2013) of the hydraulic head relative to ground surface, based on punctual water-level measurements taken in the Niaqunguk River watershed study-site piezometers (33) on **a)** July 23 and **b)** August 5.

tion of the depth to frost-table measurements at the piezometer locations using the Topo to Raster tool for ArcGIS 10.2 for these two dates is shown on Figure 5a and b. Frost-table topography was generally more subdued at the beginning of the study period (early thaw period) then at the end of August, when it is close to maximum thaw depth (Quinton et al., 2005). For both dates, the observations indicate that the active layer was deeper on the western side and the upper portion of the hillslope; an accentuated deepening was observed in these locations by late August. The active layer also remained shallower in two isolated areas downslope and upslope throughout the study period. The western side of the hillslope, where the deepest thawing was observed (August 24), was also associated to lower hydraulic head than the middle and eastern part of the hillslope (Figure 4a, b). The upper part of the deepest active-layer area corresponded to the origin of the overland flow path on the hillslope, where it was centrally located and extended continuously to the foot of the slope and into the stream. The relatively small downslope area where the active layer remained shallow was characterized by the accumulation of organic material, which could possibly make the overland-flow path divert toward the east from the middle of the hillslope at this height.

Cores samples collected under an inter-hummock channel downslope (active-layer depth of 93 cm), a hummock mid-slope (active-layer depth of 82 cm), an inter-hummock channel mid-slope (active layer depth of 77 cm) and a hummock upslope (active-layer depth of 62 cm) on August 25 revealed that the surficial layer of the soil contained a high proportion (90%) of organic matter and vegetation. Core samples further revealed that organic matter accumulation under hummocks was much thicker (15–18 cm) compared to inter-hummock areas of the hillslope (2–3 cm). Beneath the surface organic cover, within the mineral deposit, a progressive decrease in the amount of organic material content was observed, transitioning to a mineral deposit with minor organic debris close to the frost table. Core analysis revealed that the subsurface of the hillslope is mainly characterized by fine-grained sand to silt.

Preliminary analysis of the samples recovered from the area adjacent to the studied hillslope suggests that an ice-rich transient layer is not present below the hillslope active layer; core characteristics are summarized in Table 1. Visual analysis of the cores showed that grain size varies from coarse-grained sand to silt, but appears to be predominantly fine-grained sand. At the time of coring, frozen organic de-

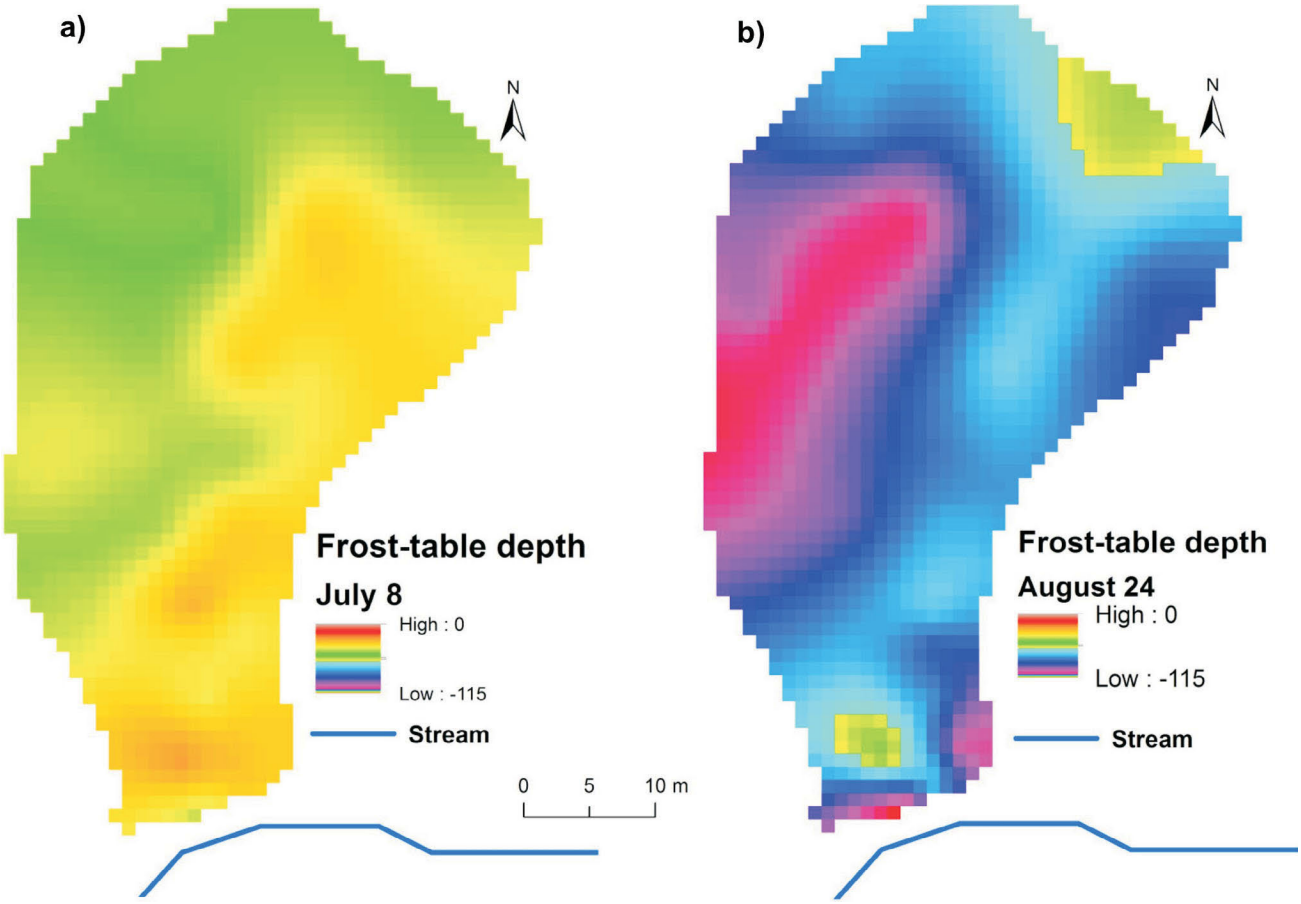

Figure 5: Interpolation using ArcGIS 10.2 (Esri, 2013) of the frost-table depths based only on the measured thawing depths at the Niaqunguk River watershed piezometer locations on **a)** July 8 and **b)** August 24.

Table 1: Characteristics of the cores of frozen material sampled under turf hummocks and the inter-hummock channel adjacent to the studied hillslope in the Niaqunguk River watershed.

Core	Surface type	Active-layer depth (cm)	Coring depth (cm)	Total coring depth (cm)	Gravimetric ice content (%g/g)
1.1.1	Inter-hummock	56	29	113.5	0.23
1.1.2			7		0.18
1.2			21.5		0.23
2.1	Hummock	69	18	106	0.15
2.2			19		0.22
3.1	Inter-hummock	63	15	95	0.17
4.1	Inter-hummock	69	14	96	0.18
5.1	Hummock	57	18	98.5	0.32
5.2.1			9.5		0.22
5.2.2			14		0.21

posits were only observed under the turf hummock (core no. 5), between 57 and 84.5 cm bgs; other cores mainly consisted of mineral deposits. Gravimetric ice-content analysis showed that the proportion of ice-content in the cores was consistent with porosity values of fine-grained sand (i.e., 0.25–0.50; Sliger, 2015).

Subwatershed surface-water flow

The flow-accumulation model presented in Figure 6a is based on the topographic flow-direction D8 algorithm of the Arc Hydro tool (Djokic et al., 2011) applied to a 1 m DEM (Short et al., 2013). The model confirmed that surface flow paths in the watershed are driven by factors other than surface topography. The first iteration of the model based only on the surficial topography directed the flow to the lower cell of the neighborhood (n = 8). This model identified a southwestern drift of the flow paths at the outlet of the Lake 1 located in the middle portion of the watershed, which doesn't correspond to the observed and mapped trajectory of the flow. This lack of accuracy can be attributed to the well-drained boulder field at the lake outlet; because the abundant pore space offers a high-velocity flow path for the water, the elevation values of this unit cannot be used for hydrological modelling (Figure 6a). The second iteration of the model, which involved a slight lowering (1 m) of the DEM pixel elevation values associated with well-drained boulder areas, better reflected the real trajectory of channelized surface-water flows from the previously iden-

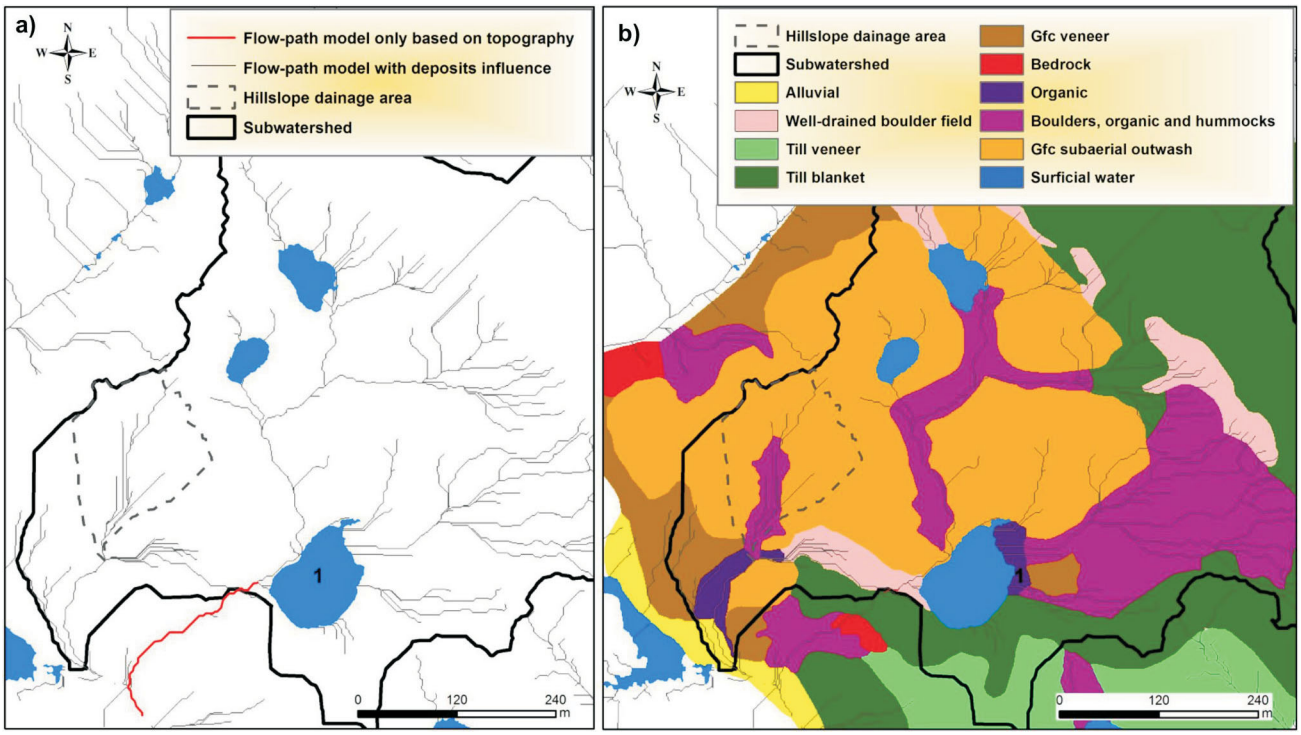

Figure 6: Map of the hillslope study site in the Niaqunguk River watershed, showing **a)** the flow-accumulation models based on topography only and taking into account the influence of surficial deposits; **b)** the surficial geological deposit types within the subwatershed. The number 1 was assigned to the lake upstream of the monitored hillslope. Abbreviation: Gfc, glaciofluvial deposit in contact with ice.

tified lake outlet that flow toward the northwest. More investigations are required to better characterize the depth of boulder-field units that have little or no matrix material to provide a better estimation of the actual elevation values that should be used in a topography-based hydrological model. The flow-accumulation area identified in the second model also shows that flow accumulations correspond to the second category of boulder-field units (boulders, organic material and hummocks), which is subject to reduced flow velocity compared to well-drained boulder areas (Figure 6a). Advanced characterization of the surficial geological units based on their hydrological characteristics should allow for a much better understanding of the influence of these units on hydrological processes within the Niaqunguk River watershed.

Deposit characterization

Nine different surficial geological deposit types were identified within the study site subwatershed (Figure 6b). The dominant deposit types within the subwatershed were till blanket (1–10 m thick; 38%), glaciofluvial sediments (22%) and boulders covered with organic material and a few turf hummocks (11%). The most recent surficial geology map of the area identified this area as 100% till blanket (Hodgson, 2003). The northwestern part of the subwatershed is dominated by glaciofluvial deposits consisting of sand and gravel, and morphologically similar to the perched deltas identified elsewhere in the Niaqunguk River watershed (e.g., Hodgson, 2005). A thick deposit of till mantles the eastern portion (0.24 km^2) of the watershed. This deposit is associated with a terminal moraine identified in Hodgson (2005) and Allard et al. (2012), and which delineates the entire eastern extremity of the Niaqunguk River watershed. Till veneer <1 m thick is present over a rolling bedrock ridge in the southern portion of the subwatershed. The instrumented hillslope is located in a boulder field covered with organic deposits and turf hummocks, and situated within a glaciofluvial deposit unit (Figure 6b).

In areas with relatively moderate to high gradients (5–10°), the boulder deposits are generally well drained (Figure 7a). Although vegetation can be seen, no accumulation of organic matter fills the void spaces between boulders, thus leaving abundant interconnected pore spaces (i.e., preferential flow paths). Well-drained boulder deposits can be distinguished from glaciofluvial or till units by the absence of finer matrix material between the boulders. The other class of boulder field (i.e., boulders with organic deposits and hummocks) is associated with lower slope gradients, pore spaces that contain mineral and organic material, and is an important flow-accumulation area. The presence of boulders is evident but there is also an accumulation of mineral and organic material between or over the boulders. The presence of turf hummocks and saturated organic matter are other features that often characterize this unit (Figure 7a).

Deposit characterization and importance of further investigation

The presence of permafrost significantly influences the routing and storage of water by reducing the infiltration rate and soil water-storage capacity, and by altering the surface and subsurface drainage patterns during the summertime flow period (Connon et al., 2014). Differential thaw depths within the active layer can be expected throughout the Niaqunguk River watershed due in part to the mosaic of distinct surficial geology deposit types that covers the watershed. Ground truthing of the detailed surficial geology mapping conducted during the 2015–2016 field season (T. Tremblay, unpublished data, 2016) generally confirmed the delineation of deposit types based on high-definition satellite images and DEM-derived interpretation (Figure 7b).

Field observations indicated that the glaciofluvial deposits within the study site with relatively small flow-accumulation areas are often characterized by dry surficial conditions with a deeper active layer than deposits covered with thick organic material or vegetation. Till is a dominant unit in the watershed and, in areas where the till cover is shallow (till veneer), water storage is likely to be limited; however, overland flow should be an important source of water during heavy rainfall events (Figure 7b). Where thick till cover is present, subsurface flow should be concentrated in water tracks, which form in places with significant upslope accumulation areas (Figure 7a). Deeper thaw below water tracks is likely to enhance flow-accumulation processes, as shown by the higher wetness conditions that prevail in water tracks compared to adjacent areas (McNamara et al., 1998).

In low-lying areas of the watershed, where flows are concentrated, accumulations of organic deposits were often found (Figure 7a). These deposits exercise a distinct control on subsurface flows. The slow rate of decomposition in the Arctic leads to an accumulation and a compaction of the organic matter at the interface with the mineral layer; consequently, the hydraulic conductivity exponentially decreases with depth (Quinton, 2008). Previous studies indicated that when the water table comes in contact with the surficial layer (e.g., -0.1 m bgs) of an organic deposit, subsurface-flow velocities can be significant (10–1000 m/d; Carey and Woo, 2002). These deposits, which can contain an ice-rich transient layer between the permafrost and the active layer, are likely to be characterized by a shallower active layer that limits subsurface flow to the surficial organic layer (Figure 7b). Where this ice-rich transient layer forms, the ice must melt before the thawing front can advance to a lower depth and thus the latent heat consumed in this process is dependent on the amount of ground ice

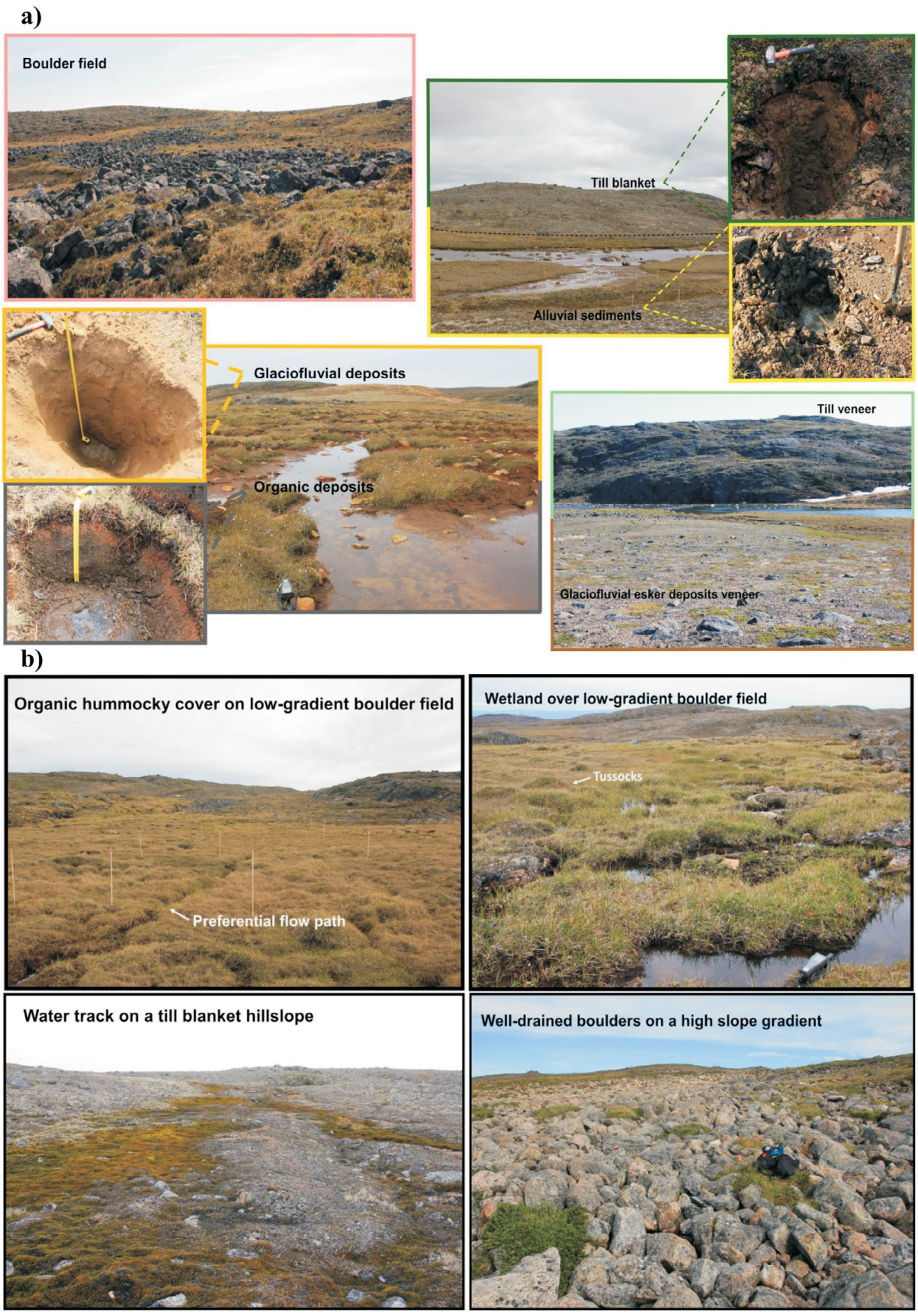

Figure 7: Examples in the Niaqunguk River watershed of **a)** delineation and characterization of surficial deposit types and **b)** additional mapped hydromorphic features.

(Woo, 2012). As previously suggested, glaciofluvial boulder fields are likely to have an important influence on the patterns and rates of groundwater discharge into surface waters.

Economic considerations

Preliminary results of this study highlight the importance of developing an improved understanding of the role of surficial geology deposit types and hydrogeomorphic unit types (e.g., hummocky organic cover, water track) in controlling surface and subsurface runoff in the Niaqunguk River watershed. The lack of high-resolution surficial deposit maps for this area limits the ability to understand hydrological dynamics at the watershed scale. This type of detailed knowledge is necessary to assess the relative importance of subsurface flows into Arctic river systems and to determine how climate-related changes are likely to impact these systems. As part of an ongoing collaborative research project investigating the environmental controls on runoff into the Niaqunguk River, this research should also contribute to improved decision making regarding the use of the Niaqunguk River as a potential source of potable water for the City of Iqaluit.

Conclusions

This study presented a detailed methodological approach for characterizing hillslope-scale hydrological dynamics during the active-layer thaw season. It involved the continuous measurement of groundwater levels using an instrumented piezometer network in combination with routine monitoring of the active-layer depths across the instrumented-hillslope study site. This type of approach has seemingly never been implemented at this spatiotemporal resolution in an Arctic environment. The resulting high-resolution mapping of surficial deposits conducted at the subwatershed scale highlights the need for detailed knowledge about the hydrogeomorphic and hydrogeological characteristics of the landscape to better understand how water is routed from hillslope recharge areas to the Niaqunguk River and its tributaries.

Acknowledgments

Research support for this study was provided by the Nunavut Research Institute, Additional logistical support was provided by the Canada-Nunavut Geoscience Office. The authors thank G. Oldenborger and O. Bellehumeur-Génier for their invaluable advice regarding the preparation of this manuscript. This project involved an intense amount of fieldwork that would not have been possible without the invaluable assistance provided by L.-G. Pouliot, E. Harbec, K. Smith, M. Demers-Lemay, A. Bychok, M. Bakaic, J. Allen, S. Masina and V. Watson. This work was supported by an ArcticNet Networks of Centres of Excellence of Canada program grant to M. Lafrenière, S. Lamoureux and J. Franssen, and by a grant to G. Chiasson-Poirier from the Northern Scientific Training Program, administered by Polar Knowledge Canada.

Natural Resources Canada, Earth Sciences Sector contribution 20160223

References

Allard, M., Doyon, J., Mathon-Dufour, V. LeBlanc, A. M., L'Hérault, E., Mate, D., Oldenborger, G.A. and Sladen, W.E. 2012: Surficial geology, Iqaluit, Nunavut; Geological Survey of Canada, Canadian geoscience Map 64 (preliminary version), scale 1:15 000

Bring, A., Fedorova, I., Dibike, Y., Hinzman, L., Mård, J., Mernild, S. H., Prowse, T., Semenova, O., Stuefer, S.L. and Woo, M.-K. (2016): Arctic terrestrial hydrology: a synthesis of processes, regional effects, and research challenges; Journal of Geophysical Research: Biogeosciences, v. 121, no. 3, p. 621–649, doi:10.1002/2015JG003131

Carey, S. and Woo, M. 2002: Hydrogeomorphic relations among soil pipes, flow pathways, and soil detachments within a permafrost hillslope; Physical Geography, v. 23, no. 2, p. 95–114, doi:10.2747/0272-3646.23.2.95

City of Iqaluit 2010: Iqaluit General Plan; Planning and Lands Department, City of Iqaluit, No. By-law 703, p. 90.

Connon, R. F., Quinton, W. L., Craig, J. R. and Hayashi, M. 2014: Changing hydrologic connectivity due to permafrost thaw in the lower Liard River valley, NWT, Canada; Hydrological Processes, v. 28, no. 14, p. 4163–4178, doi:10.1002/hyp.10206

Djokic, D., Ye, Z. and Dartiguenave, C. 2011: Arc Hydro tools overview, version 2.0; software, Esri Water Resources Team, Redlands, California, URL <http://downloads.esri.com/blogs/hydro/ah2/arc_hydro_tools_2_0_overview.pdf> [October 2016].

Environment and Climate Change Canada 2016: Canadian climate normals; Environment Canada, URL <http://climate.weather.gc.ca/climate_normals/index_e.html> [March 2016].

Esri 2010: 3D Analyst extension for ArcGIS for Desktop; software, Esri, Redlands, California.

Esri 2013: Topo to Raster tool for ArcGIS for Desktop, release 10.2; software, Esri, Redlands, California.

Hodgson, D. A. 2003: Surficial geology, Frobisher Bay, Baffin Island, Nunavut; Geological Survey of Canada, Map 2042A, scale 1:100 000, 1 CD-ROM, doi:10.4095/214808

Hodgson, D. A. 2005: Quaternary geology of western Meta Incognita Peninsula and Iqaluit area, Baffin Island, Nunavut; Geological Survey of Canada, Bulletin 582, 74 p., 1 CD-ROM.

Ladino, L.A. and Rondon, S. H. 2015: Resistance of copper wire as a function of temperature; Physics Education, v. , no. 1, p. 42–44, doi:0031-9120/15/010042+4$33.00

McNamara, J. P., Douglas, L. and Hinzman, L. D. 1998: An analysis of streamflow hydrology in the Kuparuk River Basin, Arctic Alaska: a nested watershed approach; Journal of Hydrology, v. 206, p. 39–57, doi:10.1016/S0022-1694(98)00083-3

Quinton, W. L. and Marsh, P. 1998: The Influence of mineral earth hummocks on subsurface drainage in the continuous perma-

frost zone; Permafrost and Periglacial Processes, v. 9, p. 213–228, doi:CCC 1045±6740/98/030213

Quinton, W. L., Hayashi, M. and Carey, S. K. 2008: Peat hydraulic conductivity in cold regions and its relation to pore size and geometry; Hydrological Processes, v. 22, no. 15, p. 2829–2837, doi:10.1002/hyp.7027

Quinton, W. L., Shirazi, T., Carey, S. K. and Pomeroy, J. W. 2005: Soil water storage and active-layer development in a sub-alpine tundra hillslope, southern Yukon Territory, Canada; Permafrost and Periglacial Processes, v. 16, no. 4, p. 369–382, doi:10.1002/ppp.543

Rodhe, A. and Seibert, J. 2011: Groundwater dynamics in a till hillslope: flow directions, gradients and delay; Hydrological Processes, v. 25, no. 12, p. 1899–1909, doi:10.1002/hyp.7946

Semenova, O., Lebedeva, L. and Vinogradov, Y. 2013: Simulation of subsurface heat and water dynamics, and runoff generation in mountainous permafrost conditions, in the Upper Kolyma River basin, Russia; Hydrogeology Journal, v. 21, no. 1, p. 107–119, doi:10.1007/s10040-012-0936-1

Short, N., LeBlanc, A.-M., Sladen, W. and Brisco, B. 2013: RADARSAT-2 InSAR for monitoring permafrost environments: Pangnirtung and Iqaluit; IEEE Radar Conference (RadarCon13), April 29–May 3, 2013, Ottawa, Ontario, doi:10.1109/RADAR.2013.6585954

Sliger, M. 2015: Structure et évolution du pergélisol depuis le Pléistocène Tardif, Beaver Creek, Yukon; M.Sc. thesis, Université de Montréal, Montreal, p. 156.

van Everdingen, R.O. (ed.) 1998: Multi-language glossary of permafrost and related ground-ice terms; International Permafrost Association, Terminology Working Group, p. 222.

van Meerveld, H. J., Seibert, J. and Peters, N. E. 2015: Hillslope-riparian-stream connectivity and flow directions at the Panola Mountain Research Watershed; Hydrological Processes, v. 29, no. 16, p. 3556–3574, doi:10.1002/hyp.10508

White, D. M., Gerlach, C., Loring, P.A., Tidwell, A. C. and Chambers, M. C. 2007: Food and water security in a changing Arctic climate; Environmental Research Letters, v. 2, no. 4, 4 p., doi:10.1088/1748-9326/2/4/045018

Woo, M. 2012: Permafrost Hydrology; Springer, Heidelberg, Germany, 564 p.

Woo, M. and Steer, P. 1983: Slope hydrology as influenced by thawing of the active layer, Resolute, NWT; Canadian Journal of Earth Sciences, v. 20, no. 6, p. 978–986

Woo, M.-K., Kane, D. L., Carey, S. K. and Yang, D. 2008: Progress in permafrost hydrology in the new millennium; Permafrost and Periglacial Processes, v. 19, no. 2, p. 237–254, doi:10.1002/ppp.61

Wright, N., Hayashi, M. and Quinton, W. L. 2009: Spatial and temporal variations in active layer thawing and their implication on runoff generation in peat-covered permafrost terrain; Water Resources Research, v. 45, no. 5, W05414, doi:10.1029/2008WR006880

Geological mapping and petrogenesis of carving stone in the Belcher Islands, Nunavut

H.M. Steenkamp[1], L. Timlick[2], R.A. Elgin[3] and M. Akavak[3]

[1]*Canada-Nunavut Geoscience Office, Iqaluit, Nunavut, holly.steenkamp@canada.ca*
[2]*Department of Geological Sciences, University of Manitoba, Winnipeg, Manitoba*
[3]*Lands and Resources Department, Qikiqtani Inuit Association, Iqaluit, Nunavut*

Steenkamp, H.M., Timlick, L., Elgin, R.A. and Akavak, M. 2016: Geological mapping and petrogenesis of carving stone in the Belcher Islands, Nunavut; *in* Summary of Activities 2016, Canada-Nunavut Geoscience Office, p. 121–130.

Abstract

Soft stone suitable for carving is a highly sought-after resource in Nunavut. The Qikiqtani Inuit Association (QIA) has developed a program to assess carving stone reserves, site accessibility, and quarry safety, management and development in their jurisdiction. A team of geologists from the QIA, Canada-Nunavut Geoscience Office and University of Manitoba visited four carving stone sites on the Belcher Islands to conduct land surveying, geological mapping and petrogenetic evaluations of the rock being extracted as raw carving stone by local quarriers and carvers.

The carving stone at these sites is interpreted to comprise dolostone in sedimentary strata of the Costello and McLeary formations that have been intruded by diabasic to gabbroic rocks of the Haig suite and are locally contact metamorphosed. Within these areas, the dolostone beds are metamorphosed to a softer, more easily carved rock, likely due to the growth of fine-grained talc and other metamorphic minerals. Other locations in the Belcher Islands where dolomitic sedimentary strata are cut by Haig intrusive rocks also have the potential to host undiscovered carving stone reserves.

Résumé

La pierre tendre se prêtant à la sculpture est une ressource fort recherchée au Nunavut. La Qikiqtani Inuit Association (QIA) a mis en place un programme d'évaluation des réserves de pierre à sculpter, d'accessibilité aux sites et de pratiques de sécurité, de gestion et de mise en valeur des carrières au sein de leur territoire. Une équipe formée de géologues issus de la QIA, du Bureau géoscientifique Canada-Nunavut et de l'Université du Manitoba a visité quatre emplacements de pierre à sculpter dans les îles Belcher afin d'y mener des travaux de levé, de cartographie géologique et d'évaluation pétrogénétique de la roche extraite sous forme de pierre à sculpter à l'état brut par les exploitants de carrières et les sculpteurs.

Les géologues décrivent la pierre à sculpter à ces endroits comme étant de la dolomie gisant dans des strates sédimentaires des formations de Costello et de McLeary, lesquelles sont pénétrées par des roches de la suite de Haig dont la composition varie de diabasique à gabbroïque et qui ont subi par endroits les effets du métamorphisme de contact. À ces endroits, les couches de dolomie ont été métamorphisées et sont formées de roches plus tendres, et ainsi plus faciles à sculpter; ce phénomène est attribuable à la croissance de talc à grain fin et d'autres minéraux métamorphiques. D'autres endroits dans les îles Belcher où des roches intrusives de la suite de Haig recoupent les couches sédimentaires formées de dolomie pourraient également receler des réserves encore non découvertes de pierre à sculpter.

Introduction

Soft stone suitable for decorative carving is a resource of special significance in Nunavut. Under Section 19 of the Nunavut Land Claims Agreement, an almost unrestricted access to carving stone is guaranteed for Inuit peoples, providing a supply of raw stone to a growing industry of artisan carvers (Government of Canada, 1993). Under the guidance of the Government of Nunavut's Department of Economic Development and Transportation (EDT), an intergovernmental document called *Ukkusiksaqtarvik, The Place Where We Find Stone: Carving Stone Action Plan*

This publication is also available, free of charge, as colour digital files in Adobe Acrobat® PDF format from the Canada-Nunavut Geoscience Office website: http://cngo.ca/summary-of-activities/2016/.

(Nunavut Department of Economic Development and Transportation, 2007) was created. This document highlights the importance of carving stone as a commodity in the territory, and encourages improvement for access to quality carving stone across Nunavut by strengthening traditional quarrying methods and facilitating intercommunity distribution.

The first step in *Ukkusiksaqtarvik* was to identify, locate and estimate resources at known, traditional and relatively new carving stone localities. This was accomplished during approximately five years of community consultation and site visits by the EDT's Nunavut Carving Stone Deposit Evaluation Project (NCSDEP; Beauregard et al., 2013; Beauregard and Ell, 2014, 2015). Although the NCSDEP identified hundreds of potential sites across the territory and concluded that sufficient good- to excellent-quality carving stone exists to supply the territory's needs for hundreds of years, the challenges associated with co-ordinating the distribution of raw materials to communities and carvers have yet to be addressed.

In recognition of the economic and cultural importance of carving stone in Nunavut and the logistical challenges associated with implementation of the next steps of *Ukkusiksaqtarvik*, the Qikiqtani Inuit Association (QIA) launched their own evaluation project in the summer of 2016. The project targets the largest carving stone deposits on Inuit Owned Lands in the Qikiqtaaluk Region, and provides the necessary expertise to evaluate and assess resources at each site. It builds on the results of the NCSDEP, implementing its recommendations and addressing regional issues with regards to quarry development and the economic feasibility of community-led expansions. The project will include quantifying the lifespan of sites based on surface and subsurface deposits, and evaluating the work required to make deposits accessible and free from dangers such as rock falls, flooding or wall collapse. The conclusion of this work will provide critical information for understanding long-term resource availability in the region, which is necessary for further implementation of the *Ukkusiksaqtarvik*, and will ultimately enable local Inuit to utilize their resources in a commercially viable and responsible manner.

Sites targeted by the QIA for resource and development assessment require geological mapping and interpretation, land surveying and site-accessibility evaluations. Geophysical surveys (i.e., magnetic-anomaly mapping), prospecting and/or satellite-imagery analysis may also aid in the full evaluation of resource viability at these sites. The top-priority sites include Kangiqsukutaaq (Korok Inlet, near Cape Dorset), Tatsituya and Tatsitui Tiniiniya (Aberdeen Bay, near Kimmirut), Opingivik Island (near Pangnirtung), Qullisajaniavvik (near Sanikiluaq) and the Koonark deposit at Mary River (near Pond Inlet). Detailed geological mapping has already been conducted at the Kangiqsukutaaq (Steenkamp et al., 2014) and Opingivik (Steenkamp et al., 2015) sites.

On September 11–14, the Canada-Nunavut Geoscience Office, the QIA and a research student from the University of Manitoba visited four carving stone localities near Sanikiluaq (Figure 1a; Beauregard and Ell, 2015) to conduct detailed geological mapping and further the QIA's carving stone resource assessment project. This paper provides a detailed geological description and map for the Qullisajaniavvik carving stone site, herein referred to as the community quarry (CQ in Figure 1b), as well as an abandoned quarry site (Aqituniavvik; AQ in Figure 1b) and two other carving stone occurrences near Salty Bill Hill, referred to as SBH1 and SBH2 (Figure 1b), on Tukarak Island. The authors present a geological interpretation for the petrogenesis of soft, easily carved stone at these sites, and highlight the geological elements required for future prospecting of similar carving stone resources.

Geological background and site histories

The geology of the Belcher Islands was mapped at a 1:125 000 scale and described in detail by Jackson (2013). The islands are underlain by the Proterozoic (ca. 1.96–1.87 Ga) Belcher Group, comprising dominantly shallow-marine carbonate and siliciclastic strata interrupted by volcanic flows and associated volcaniclastic rocks. Jackson (2013) summarized the depositional history of the Belcher Group in three major stages:

1) Steady, dominantly carbonate sedimentation occurred in a stable continental-shelf environment during marine transgression.
2) Abrupt emplacement of volcanic flows and minor associated volcaniclastic and fluvial sedimentary rocks was followed by a return to marine sedimentation in a less stable continental-shelf environment. Sedimentation included local iron formation, greywacke, mudstone, siltstone and carbonate rocks.
3) A second phase of abrupt volcanism included emplacement of regionally extensive basalt flows and intrusion of diabase–gabbro sills in pre-existing strata. Volcanism was followed by a thick succession of mostly deep-water turbidites that shallowed upward into more proximal, coarse-grained, nearshore-marine and terrestrial strata.

The Belcher Group was regionally folded and weakly metamorphosed (sub-greenschist facies), likely due to continental-collision events associated with the 1.85–1.83 Ga Trans-Hudson orogeny (Hoffman, 1989; Corrigan et al., 2009). The islands are included in the Reindeer Zone, in the upper-plate Churchill Province north of the orogenic front. The impact of the Trans-Hudson deformation is highlighted by the uniquely folded and interconnected geography of the Belcher Islands.

During the Pleistocene, the Belcher Islands were completely covered by ice, and they are still rebounding at a rate of a few centimetres per year. It is likely that the islands were completely inundated by the sea when the ice retreated, based on the presence of beach deposits atop the highest hills on Tukarak Island (Jackson, 2013).

The four carving stone sites visited during this study (Figure 1b) were previously visited by Beauregard and Ell (2015), who completed carving stone quality assessments and preliminary resource-reserve calculations. The community quarry, established in the 1970s, provides good- to excellent-quality, grey, dark green and black carving stone that can be extracted as blocks up to 1 m across and 40 cm thick and is soft enough to carve by hand. The stone is traditionally quarried using the plugger-and-feather method, and excavated with a hammer and chisel or pry bar before being transported approximately 50 km by snowmobile or motorboat to the hamlet of Sanikiluaq. The community quarry contains an estimated 30 000 tonnes of carving stone reserves, making it the second largest deposit in Nunavut (Beauregard and Ell, 2015).

The abandoned quarry yields a desirable light green stone, yet this is viewed by traditional carvers as lower quality than the stone from the community quarry. An area within this site was abandoned in the late 1990s when rocks from the outcrop above the quarry slid down to partially cover the quarry access, raising concerns about the integrity of the remaining overhanging outcrop. The abandoned quarry site is estimated to have 1000 tonnes of carving stone reserves, as the desired horizon of carving stone continues along strike to the north of the blocked quarry access (Beauregard and Ell, 2015).

The two occurrences of carving stone near Salty Bill Hill have not been traditionally quarried, as they are farther inland and would require development of an ATV route to transport stone to the shore. However, they are estimated to each hold <100 tonnes of good-quality carving stone (Beauregard and Ell, 2015).

Field observations

Community quarry (Qullisajaniavvik)

The community quarry area is underlain by steeply west-dipping sedimentary rocks of the Costello Formation that

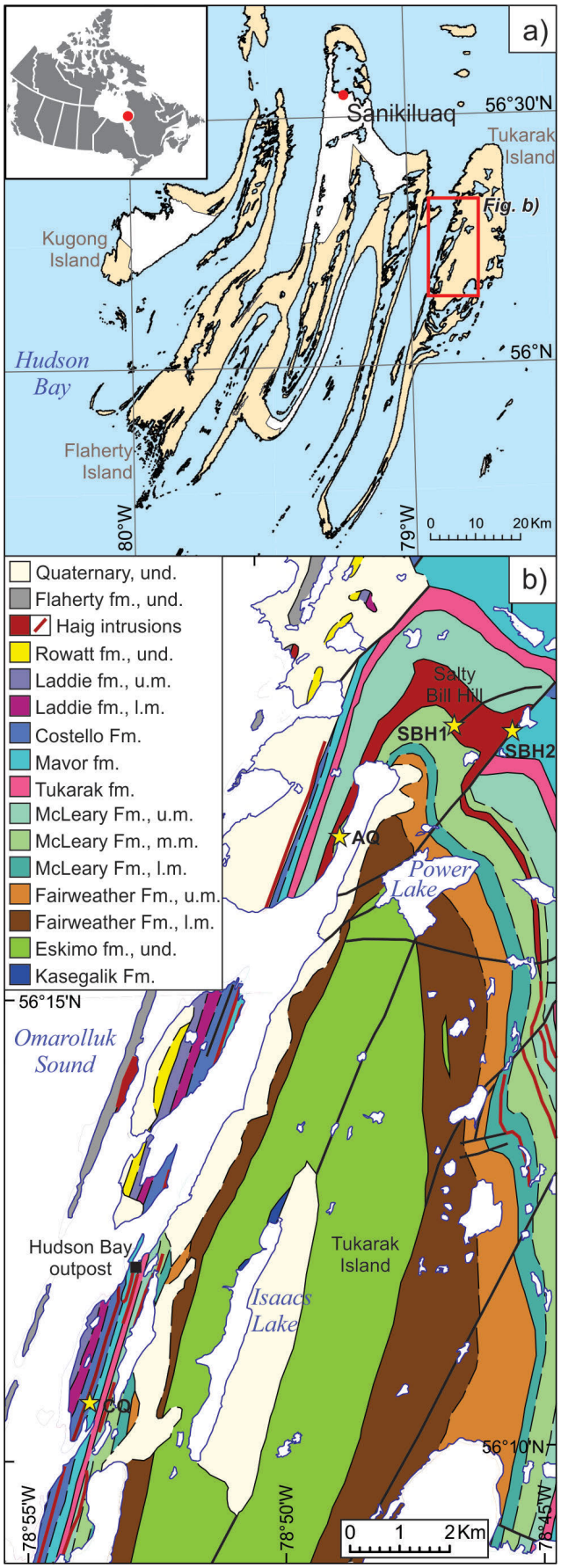

Figure 1: a) Location of the Belcher Islands in eastern Hudson Bay (Inuit-owned land in yellow) and location of study area (red box) in relation to Sanikiluaq. **b)** Geology of the study area (adapted after Jackson, 2013) and locations of the community quarry (CQ), abandoned quarry (AQ) and carving stone occurrences near Salty Bill Hill (SBH1 and SBH2), indicated by yellow stars. Thick black lines represent minor faults. Thin, continuous black lines represent observed geological contacts, and thin, dashed black lines represent interpreted geological contacts. Abbreviations: Fm./fm., Formation/formation; l.m., lower member; m.m., middle member; u.m., upper member; und., undivided.

are injected by a diabasic to porphyritic gabbro of the Haig intrusive suite (Figure 2). Along the tideline of the small bay in the southern part of the map area, the basal member of the Costello Formation is well exposed and contains thinly laminated, dark grey shale. This is in conformable contact with interbedded orange-weathering, fine-grained dolostone and grey-weathering, thin (<4 cm) mudstone (Figure 3a) that dominate the Costello Formation in this area. The dolostone exhibits wavy and low-angle crosslamination, and is medium grey on fresh surfaces. The mudstone exhibits low-relief, asymmetric ripple crosslamination and is dark grey to black on fresh surfaces. Dolostone beds are locally boudinaged, likely an effect of dewatering processes operating during regional compaction and diagenesis.

At the southern end of the map area, the Haig gabbro intrudes the Costello Formation parallel to bedding as a sill. The sill thickens to the north, near the active quarry sites, and locally crosscuts the sedimentary bedding at oblique angles. The interior parts of the Haig intrusion have a porphyritic texture, with individual phenocrysts and agglomerations of plagioclase in a black aphanitic matrix. West of the active quarry area, where the sill is thickest, plagioclase grains appear to have dark cores (Figure 3b), which could be due to compositional zoning (suggesting two-stage crystallization from compositionally different magmas) or be a different mineral phase (possibly clinopyroxene) that acted as nucleation sites for later plagioclase crystallization.

Along the intrusive contact, the gabbro has 10–20 cm thick, aphanitic chilled margins that are regularly fractured perpendicular to the contact. The fractured margin segments appear to be subsequently rotated 10–20°, possibly by continued internal flow of magma during injection. Locally, the rotated margin segments of the gabbro have been slightly offset. Where this occurs, the dolostone and mudstone layers are ductilely deformed and appear to infill the offset spaces (Figure 3c), suggesting that the displacement may have occurred during later regional deformation. The interlayered dolostone and mudstone of the Costello Formation, both stratigraphically below and above the Haig intrusion (to the east and west, respectively), is contact metamorphosed adjacent to the contact surface. The width of the contact aureole appears to correlate with the thickness of the intrusion, ranging from 20–50 cm where the sill is 3–5 m thick in the southern part of the map area, up to 30 m in the community quarry area where the sill is thickest.

The contact-metamorphosed dolostone and mudstone have a bleached grey-white appearance on weathered surfaces

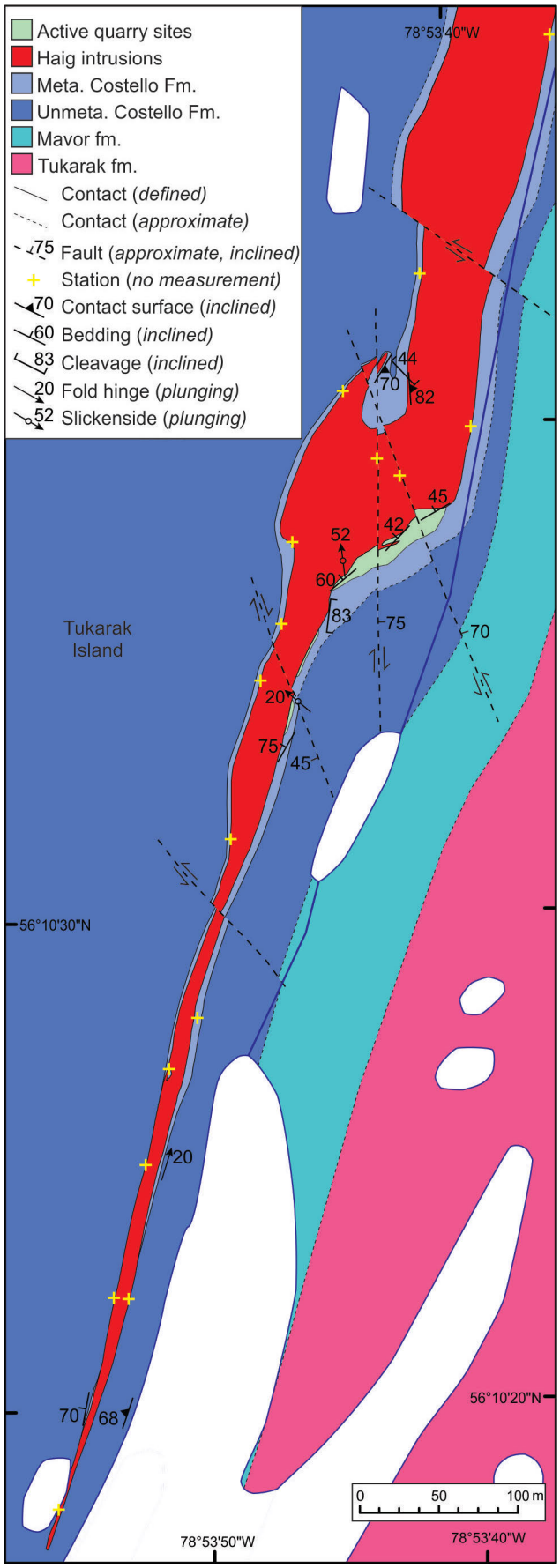

Figure 2: Geology of the community quarry area on Tukarak Island, Belcher Islands. Abbreviations: Fm./fm., Formation/formation; meta., metamorphosed; unmeta., unmetamorphosed.

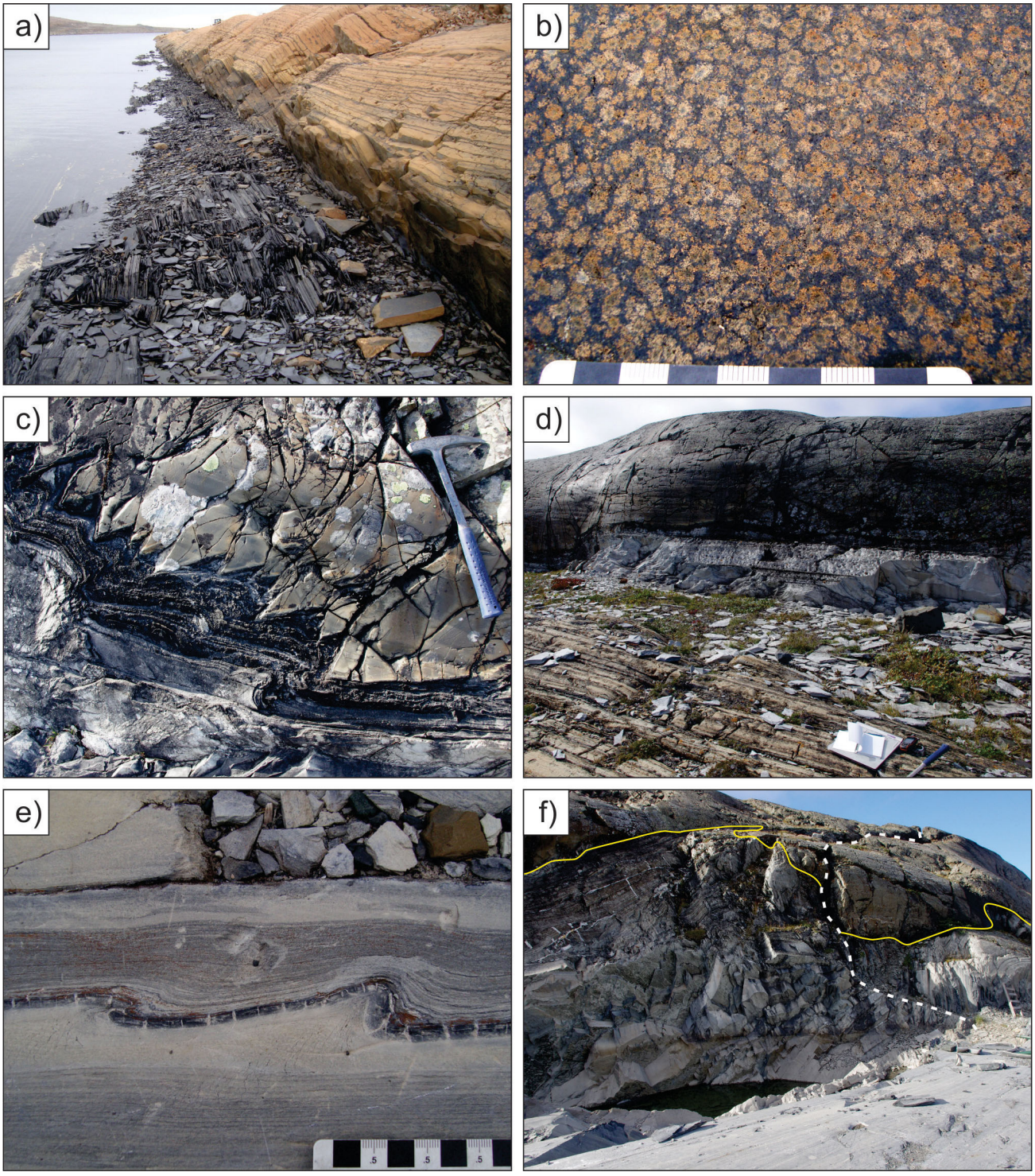

Figure 3: Photographs from the community quarry area on Tukarak Island, Belcher Islands: **a)** contact between the lower, grey shale member (exposed for 1.2 m above the waterline in the foreground) and predominant orange-weathering dolostone with mudstone interbeds of the Costello Formation; **b)** porphyritic texture in the centre of the Haig intrusion west of the active quarry, showing plagioclase phenocrysts with dark cores; **c)** fractured, rotated and displaced blocks of aphanitic gabbro along the chilled margin of the Haig sill, and contact-metamorphosed dolostone that has ductilely deformed around the Haig margin; **d)** white-grey weathering of contact-metamorphosed dolostone adjacent to the black, glacially polished gabbro sill; clipboard, GPS and hammer for scale; **e)** thin black mudstone layer with regular z-folds and concentrations of brown-weathering sulphides within the dolostone and close to the contact with the mudstone layer; **f)** view of the active quarry looking northwest from within the contact aureole (grey polished outcrop in the foreground), showing a minor brittle fault (traced by the white dashed line) that displaces the intrusive contact (yellow lines), and typical white calcite-quartz veins (left) in the contact-metamorphosed Costello Formation; small ladder for scale is approximately 1.2 m tall.

(Figure 3d) and are light to medium grey on fresh surfaces. Although a grain-size change is not visibly apparent, fresh surfaces of the contact-metamorphosed dolostone exhibit a sugary texture, as opposed to the flat, homogeneous fresh face of an unmetamorphosed equivalent. The site where most of the quarrying for soft stone has so far been done is where the contact-metamorphic aureole in the dolostone and mudstone is the broadest in the map area. The sedimentary rocks in this area likely experienced more consistent, prolonged heating due to the large volume of gabbroic magma stratigraphically above, resulting in localized growth of fine-grained metamorphic minerals, possibly including talc, serpentine, brucite, sericite or calcite. Due to the fine-grained nature of these rocks, petrographic analysis is underway to ascertain their precise mineralogy.

A moderately to steeply northeast-dipping cleavage can be observed where contact-metamorphosed beds are highly frost fractured. This fabric is associated with small, north-plunging z-folds that are most easily seen in the glacially polished mudstone layers near the active quarry (Figure 3e). Locally, clusters of sulphide minerals concentrate at the margin between dolostone and mudstone layers, particularly where the mudstone has been folded. These features likely developed during regional deformation of the Belcher Group rocks associated with the Trans-Hudson Orogen.

The Costello Formation and Haig intrusion both preserve relatively late minor veining and brittle faulting. Veins are common along the intrusive contact in pre-existing fractures, cut vertically and horizontally through the contact-metamorphosed sedimentary rocks (Figure 3f), and occur as a narrow concentrated network that follows bedding in the dolostone west of the intrusion and contact-metamorphic aureole. The veins typically contain varying proportions of quartz and calcite, as well as local dolomite and fine-grained talc. The quartz is massive and white in the unmetamorphosed dolostone and occurs as isolated clusters of crystals that are translucent to white, euhedral to subhedral and surrounded by calcite in the contact-metamorphosed areas. In one locality along the intrusive contact margin, thin veins are rimmed by fine-grained talc crystals and infilled by elongated quartz, both being oriented perpendicular to the vein walls and therefore suggesting that crystallization was synchronous with progressive vein opening.

Several late brittle faults are present in the map area, based on minor offsets in the intrusive contact margin and elongate, aligned concentrations of highly fractured gabbro that is more easily traced where the faults intersect the walls of the quarry (Figure 3f). Displacement along any of these faults was likely no more than 5 m in an oblique-slip motion, as indicated by moderately plunging slickensides of recrystallized calcite and rare actinolite.

Other carving stone sites

North of the community quarry, three other carving stone localities were visited to evaluate their geological relationships and petrogenesis, as well as their potential for holding additional carving stone reserves for the territory. These sites are the abandoned quarry, which was used as a carving stone source prior to increased use of the community quarry, and two carving stone showings near Salty Bill Hill (Figure 1b). Based on their locations, all three sites appear to involve sedimentary rocks from the middle member of the McLeary Formation that are closely associated with Haig intrusions (Jackson, 2013).

The abandoned quarry site is located approximately 50 m up a steep, grassy hill from the tideline. The lowest outcrop exposure consists of steeply west-dipping, interbedded dolostone and thinly laminated argillite. A 1.5–2 m thick, pink and grey, crossbedded sandstone layer interrupts the interbedded dolostone and argillite about 4 m up the outcrop. The sedimentary rocks are intruded by a thick Haig sill approximately 6 m up from the sandstone bed. Similar to the community quarry site, it appears as though the heat from the intrusion has contact metamorphosed the outcropping sedimentary rocks below it, and possibly farther down the stratigraphy. Common calcite- and quartz-bearing veins, concentrated mostly in the dolostone and argillite, are also similar to those seen at the community quarry. The dolostone is a light greenish grey and the argillite laminae are buff, grey, dark grey and black.

Carving stone has been harvested primarily from a discrete, 30–40 cm thick layer of contact-metamorphosed, light green dolostone that runs along the base of the outcrop. The extraction of this particular layer has resulted in an 8–10 m deep and 20 m long gap that dips down into the outcrop (Figure 4a). Rusted pry bars and other tools can still be seen at the bottom of the worked layer. Boulders of dolostone have fallen over parts of the gap and, because of this, people no longer attempt to quarry from within it. The desired layer of dolostone continues along strike and reappears at ground level farther to the north, where there is ample evidence of past and recent carving stone harvesting (Figure 4b).

The two carving stone showings near Salty Bill Hill were previously described by Beauregard and Ell (2014), and were visited only briefly this year to conduct a follow-up evaluation of the potential for new carving stone reserves. The first site visited, SBH1 (Figure 1b), comprises two relatively small outcrops (measuring roughly 2 by 2 by 3 m each; Figure 4c) of laminated dolostone adjacent to a north-trending, 4 m wide diabase dyke. The bedding appears to fold with proximity to the dyke, and the outcrop becomes less competent and more frost fractured with distance from the dyke. These two outcrops are the only surface exposures of potential carving stone in the vicinity of the dyke,

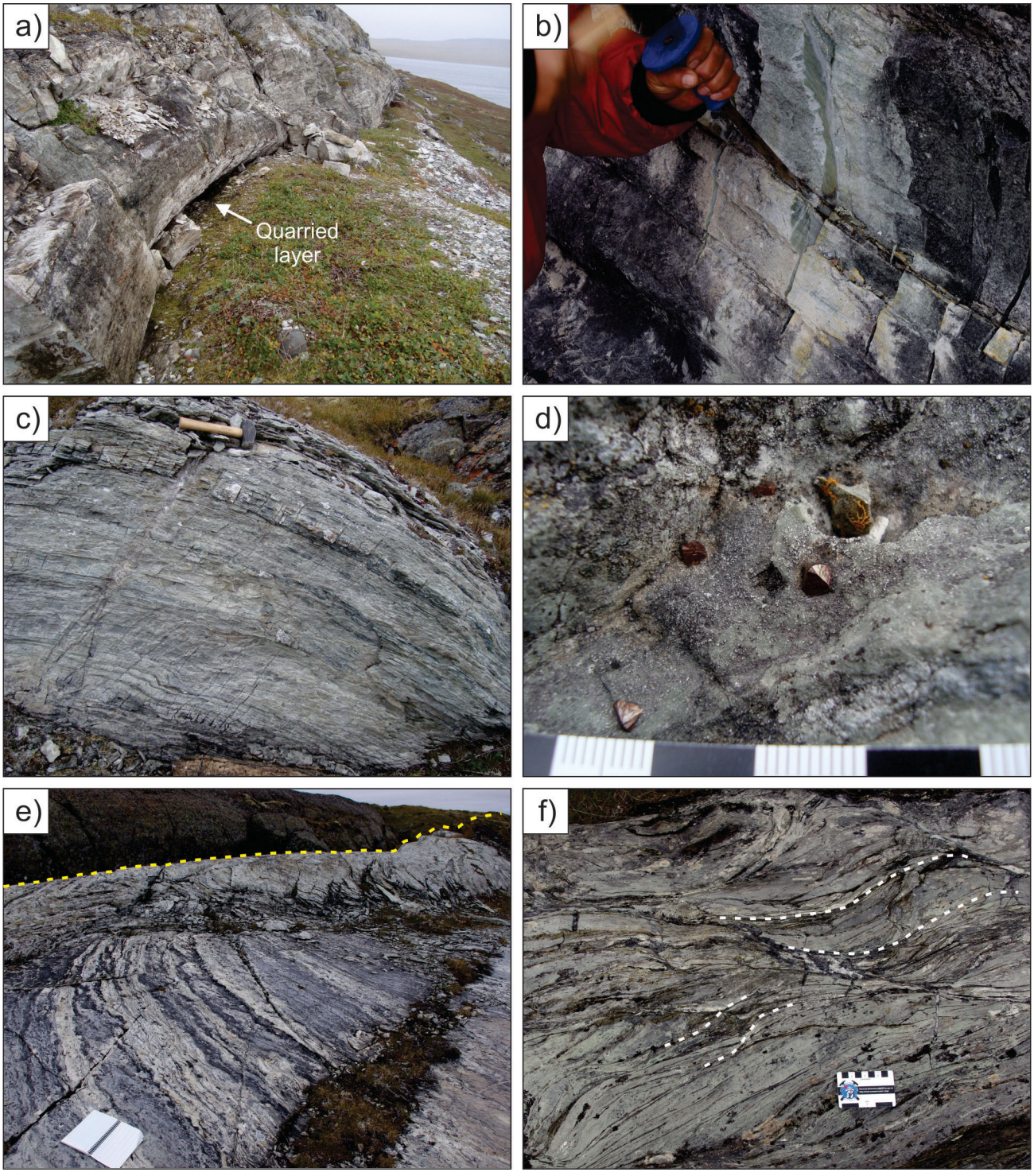

Figure 4: Photographs from other carving stone localities on Tukarak Island, Belcher Islands: **a)** surface opening of the quarried dolostone layer (about 30 cm wide at arrow) at the abandoned quarry site; **b)** the highly desired dolostone layer in photo (a) is well exposed north of the abandoned quarry area along the same outcrop; samples from this site were collected where cuts had already been made with a gas-powered saw; **c)** one of the two exposures of contact-metamorphosed dolostone at SBH1, showing minor folding near the contact with the gabbro dyke just to the right of the image; hammer for scale is 30 cm long; **d)** euhedral sulphide crystals set in pale green dolostone at SBH1; **e)** well-exposed interbedded dolostone and silty dolostone that is broadly folded and lies below the contact (yellow dashed line) with a thick Haig sill (the black rock in the background); spiral binding on the notebook is 22 cm long; **f)** thin beds of dolostone with a weakly developed crenulation cleavage, traced by the white dashed lines.

but there may be additional contact-metamorphosed stone beneath the overburden along the dyke margins.

The contact-metamorphosed dolostone is light green to pale grey and locally contains euhedral sulphide crystals (Figure 4d). Calcite and quartz veins in the dolostone are <1 cm wide and cut the bedding obliquely; in the diabase dyke, they are up to 10 cm wide and also contain sulphide minerals, together with minor malachite and azurite.

The second site visited, SBH2 (Figure 1b), consists of several pavement-style outcrops of interbedded dolostone and silty dolostone directly below the base of a large, extensively exposed Haig sill (Figure 4e) that forms the top of Salty Bill Hill. The dolostone bedding is 10–25 cm thick and broadly folded. A locally developed, weak crenulation cleavage (Figure 4f) is a reflection of this outcrop's position at the hinge of the Tukarak antiform (Jackson, 2013). Dolostone beds are light green on fresh surfaces and locally contain rare, euhedral sulphide minerals. The thin, silty dolostone interbeds are light grey to white and contain laminae with elongate mats of fine-grained talc.

Geological interpretations

The four carving stone sites visited during this study have common geological relationships that have allowed for the genesis of soft, easily carved stone. Each site consists of dolostone beds that have been contact metamorphosed by the Haig intrusive complex. Dolostone within the contact aureoles appears to contain new metamorphic minerals that soften the rock, making it easier to carve. One of many metamorphic reactions that likely occurred in the sedimentary rocks during the intrusion and cooling of the Haig sills is

dolomite silica talc calcite

$$3\ CaMg(CO_3)_2 + 4\ SiO_2 + H_2O \rightarrow Mg_3Si_4O_{10}(OH)_2 + 3\ CaCO_3 + CO_2$$

where the silica may have been sourced partly from the intrusion and partly from the original sedimentary rocks.

Also common to all sites is the relationship between the thickness of the intrusive sill and the resultant thickness of the contact aureole. As documented in the community quarry map area, the extent of the contact-metamorphic aureole also expands where the Haig sill thickens. At the other sites, the tops of the Haig sills are partly eroded, but outcrops still expose a thickness of at least 50 m in places. Also notable is that, where both a top and a bottom contact aureole can be observed (i.e., around the community quarry map area), the aureole below the sill tends to be thicker than that above the sill. It is possible that, after intrusion, the sills may have acted as insulating layers while still progressively cooling. Therefore, rocks below the intrusions may have experienced prolonged heating, allowing more time and energy for the growth of new metamorphic minerals.

Given these observations and interpretations, the petrogenesis of the soft, easily carved stone preferred by local carvers required the intrusion of a thick sill or dyke of gabbroic Haig magma through dolostone beds in the Belcher Group sedimentary strata, followed by persistent, slow cooling of the host strata to allow for the growth of metamorphic minerals. Further prospecting for new carving stone deposits should apply these geological elements and focus particularly around the basal contact surfaces of sills.

Economic considerations

There are numerous locations where the key geological elements identified above exist in the Belcher Islands. Thus, the potential for finding new sites that contain good- to excellent-quality carving stone derived from contact-metamorphosed dolostone is considerable. In terms of access, the Belcher Islands are unique in Nunavut: the land is relatively low-lying, nearly completely accessible with an ATV or boat in the summer and fully accessible by snowmobile in the winter, and bedrock outcrop is extensive. The community quarry and abandoned quarry sites are very close to tidewater, but the Salty Bill Hill sites would require transportation of harvested carving stone for a distance of 2–4 km over uneven tundra to reach a section of the shoreline that is accessible by boat.

Aside from carving stone resources, the Belcher Islands have potential for base metals, such as copper and iron. Many of the sedimentary formations naturally contain disseminated metals, and these appear to be concentrated and recrystallized where associated with the Haig intrusive rocks, and in calcite-quartz veins such as those observed at the SBH1 site.

Finally, the Belcher Islands host a wide variety of Proterozoic sedimentary and volcanic igneous rocks, and preserve many remarkable geological features such as pillow basalts, volcaniclastic-flow deposits, stromatolite reefs and banded iron formations, to name a few. Other examples of these features from the same geological timeframe that are so minimally deformed or metamorphosed are rare throughout the rest of the world. The Belcher Islands could prove to be a significant location for future discoveries regarding Earth's geological history, and is an excellent location for geotourism and geological field schools.

Acknowledgments

The authors thank the community of Sanikiluaq for their interest and support for this project. They are particularly grateful for the expert transportation, guidance and assistance in the field from master carver Jimmy Iqaluq, his son Jack Iqaluq and the rest of the Iqaluq family. Nunavut MLA, Alan Rumbolt, and his family, Garry and Daisy, are thanked for providing accommodations in Sanikiluaq. Mike Beauregard is thanked for his guidance and encour-

agement for furthering work on the Belcher Island carving stone sites; he has invested a great deal of time and effort in the NCSDEP and continues to advocate for carving stone research in Nunavut. The Belcher Islands work was funded by the Community Readiness and Opportunities Planning program of the Canadian Northern Economic Development Agency, and the Qikiqtani Inuit Association. A thoughtful and thorough review of this paper was provided by David Mate.

Natural Resources Canada, Earth Sciences Sector contribution 20160224

References

Beauregard, M.A. and Ell, J. 2015: Nunavut Carving Stone Deposit Evaluation Program: 2013 and 2014 fieldwork in the Kitikmeot Region, Belcher Islands, Hall Peninsula and Repulse Bay, Nunavut; *in* Summary of Activities 2014, Canada-Nunavut Geoscience Office, p. 163–174.

Beauregard, M. and Ell, J. 2015: Nunavut Carving Stone Deposit Evaluation Program: 2015 fieldwork at Rankin Inlet, Cumberland Sound and Arctic Bay, Nunavut; *in* Summary of Activities 2015, Canada-Nunavut Geoscience Office, p. 183–192.

Beauregard, M., Ell, J., Pikor, R. and Ham, L. 2013: Nunavut Carving Stone Evaluation Program (2010–2013), third year results; *in* Summary of Activities 2012, Canada-Nunavut Geoscience Office, p. 151–162.

Corrigan, D., Pehrsson, S., Wodicka, N. and De Kemp, E. 2009: The Palaeoproterozoic Trans-Hudson Orogen: a prototype of modern accretionary processes; *in* Ancient Orogens and Modern Analogues, J.B. Murphy, J.D. Keppie and A.J. Hynes (ed.), The Geological Society of London, Special Publications, vol. 327, p. 457–479.

Government of Canada 1993 (amendments included in 2009): Agreement Between the Inuit of the Nunavut Settlement Area and Her Majesty the Queen in Right of Canada (Nunavut Land Claims Act); Indian and Northern Affairs Canada, Article 19, Title to Inuit Owned Lands: Part 9, Rights to Carving Stone; Government of Canada, p. 149–150.

Nunavut Department of Economic Development and Transportation 2007: Ukkusiksaqtarvik – the place where we find stone: carving stone supply action plan; Nunavut Department of Economic Development and Transportation, 12 p., URL <http://www.gov.nu.ca/sites/default/files/carving_stone_action_plan_english.pdf> [October 2016].

Hoffman, P. 1989: Precambrian geology and tectonic history of North America; *in* Geology of North America – An Overview, A.W. Bally and A.R. Palmer (ed.), Geological Society of America, Chapter 16, p. 447–512.

Jackson, G.D. 2013: Geology, Belcher Islands, Nunavut; Geological Survey of Canada, Open File 4923, 159 p. and map at 1:125 000 scale. doi:10.4095/292434

Steenkamp, H.M., Pizzo-Lyall, M., Wallace, C.J., Beauregard, M.A. and Dyck, B.J. 2014: Geology, history and site-management planning of the Kangiqsukutaaq carving stone quarry, southern Baffin Island, Nunavut; *in* Summary of Activities 2013, Canada-Nunavut Geoscience Office, p. 193–200.

Steenkamp, H.M., Beauregard, M.A. and Mate, D.J. 2015: Carving stone and mineral potential of the Opingivik deposit, southern Baffin Island, Nunavut; *in* Summary of Activities 2014, Canada-Nunavut Geoscience Office, p. 153–162.

Commitment of the Geo-mapping for Energy and Minerals program to community engagement in Nunavut: the Taloyoak Geoscience Field School initiative

M. Sanborn-Barrie[1], E.M. Hillary[2], T. Tremblay[3], A. Ford[4], V.L. Tschirhart[4] and J. Maharaj[5]

[1]*Natural Resources Canada, Geological Survey of Canada, Ottawa, Ontario, mary.sanborn-barrie@canada.ca*

[2]*Dunrobin, Ontario*

[3]*Canada-Nunavut Geoscience Office, Iqaluit, Nunavut*

[4]*Natural Resources Canada, Geological Survey of Canada, Ottawa, Ontario*

[5]*Toronto, Ontario*

Sanborn-Barrie, M., Hillary, E.M., Tremblay, T., Ford, A., Tschirhart, V.L. and Maharaj, J. 2016: Commitment of the Geo-mapping for Energy and Minerals program to community engagement in Nunavut: the Taloyoak Geoscience Field School initiative; *in* Summary of Activities 2016, Canada-Nunavut Geoscience Office, p. 131–140.

Abstract

With a shared commitment to maximize the benefits of geoscience research to northerners, Natural Resources Canada, through its Geo-mapping for Energy and Minerals (GEM) program, and the Canada-Nunavut Geoscience Office (CNGO) partnered in a pilot community field-school initiative. This learning opportunity was offered at an early stage of the GEM Boothia Peninsula–Somerset Island activity, for which bedrock mapping is planned in 2017 and 2018. The Taloyoak Geoscience Field School was designed to stimulate and strengthen interest in geoscience by providing northerners an opportunity to gain a 'hands-on' sense of methods used to gather geological data, and a venue to learn how geoscience data can be accessed and used for planning and decision-making, in a familiar setting. Materials and data from across Nunavut were used in the field school, which engaged some 160 participants of all ages in geoscience topics of relevance to the community and its geological setting. The scientific perspective added to the existing local and traditional knowledge of landmarks, natural materials, topography and travelling routes, in a way that illustrated how both perspectives can coexist agreeably.

Résumé

En raison de leur engagement commun visant à maximiser les avantages de la recherche géoscientifique pour les résidents du Nord, Ressources naturelles Canada, par le biais de son programme de géocartographie de l'énergie et des minéraux, et le Bureau géoscientifique Canada-Nunavut ont lancé une initiative communautaire pilote d'école de terrain. Cette occasion d'apprentissage a été offerte à un stade précoce de l'activité menée dans la péninsule Boothia et l'île Somerset, activité entreprise dans le cadre du programme de géocartographie de l'énergie et des minéraux qui doit porter sur la cartographie du substratum rocheux en 2017 et 2018. L'école de terrain géoscientifique Taloyoak a été conçue dans le but de stimuler et de renforcer l'intérêt des résidents du Nord au sujet des sciences de la Terre en leur permettant d'avoir une expérience pratique des méthodes utilisées en vue de recueillir des données géologiques, tout en leur offrant un lieu où il leur est possible d'apprendre dans un milieu qui leur est familier la façon de procéder afin d'accéder et d'utiliser les données géoscientifiques aux fins de planification et de prise de décisions. Des matériaux et des données provenant de l'ensemble du Nunavut ont été utilisés à l'école de terrain où se sont retrouvés quelque 160 participants de tout âge qui se sont penchés sur certains aspects des sciences de la Terre présentant un intérêt au niveau de la communauté ou en raison de leur contexte géologique. La perspective scientifique est venue s'ajouter aux connaissances locales et traditionnelles touchant les repères terrestres, la végétation naturelle, la topographie et les parcours d'une façon qui a permis de démontrer concrètement comment ces deux perspectives peuvent coexister agréablement.

This publication is also available, free of charge, as colour digital files in Adobe Acrobat® PDF format from the Canada-Nunavut Geoscience Office website: http://cngo.ca/summary-of-activities/2016/.

Introduction

The Geo-mapping for Energy and Minerals (GEM) program is laying the foundation for sustainable economic development in Canada's North through provision of modern public geoscience that will form the basis of long-term decision-making related to investment in responsible resource development. The GEM-2 activity 'Integrated Geoscience of the Northwest Passage' (Figure 1) will involve bedrock mapping, supported by geophysical, geochronological and geochemical datasets, and targeted surficial studies across Boothia Peninsula and Somerset Island. The area is an underexplored frontier region where knowledge stems from 1963 and 1986 mapping (Blackadar, 1967; Frisch, 2011), without benefit of aeromagnetic constraints or modern U-Pb geochronology. New mapping and value-added datasets will 1) significantly upgrade the outdated geoscience framework of this area; 2) expand the impact of the findings from the mainland GEM-2 Rae Thelon activity (Davis et al., 2014; Berman et al., 2015a, b; Berman et al., 2016); and 3) provide relevant data and knowledge to an isolated region of Nunavut that, due to global warming and the resulting increase in shipping activity, will increasingly be exposed to issues related to resource assessment and economic development.

Planning and preparation

Planning related to a community field school was initiated in December 2015 through bilingual (English and Inuktitut) introductory letters from Natural Resources Canada (NRCan) to the Hamlet of Taloyoak, Nunavut and the Spence Bay Hunters and Trappers Association (HTA). Swift, positive support for an experiential learning opportunity focused on the land was communicated to NRCan by a representative from the HTA, who shared the concept with members of the HTA board at its January 2016 meeting. NRCan staff were invited to Taloyoak in mid-March 2016 to deliver presentations to the Hamlet and HTA, to respond to questions and concerns the HTA had in regard to mining activities, and to seek community input on where best to locate a temporary, low-impact, tent-based field

Figure 1: Canada's Far North, highlighting the GEM regions of interest (grey outlines). The area of the Boothia Peninsula–Somerset Island activity 'Integrated geoscience of the Northwest Passage' (blue polygon) is located within the Rae region of interest. The Geoscience Field School described in this paper was located 3.5 km north of Taloyoak (red star).

school to ensure accessibility to as many interested residents as possible. The mid-March visit coincided with the school Science Fair, providing an opportunity to announce the concept of a summer geoscience field school to all science students and many of their parents. A public meeting, held on the evening of March 16, 2016, was used to introduce the initiative, receive input and answer all related questions.

Support for the initiative was communicated by the Hamlet during the visit in March 2016, and endorsement was provided by the HTA on May 16, 2016. Application to the Nunavut Planning Commission was circulated and was determined on June 8, 2016 to be exempt from further screening due to its nature and lack of concern regarding any negative impacts. This paved the way for a Letter of Agreement with the Hamlet of Taloyoak to be drafted as a means to hire local personnel to assist in set-up and take-down of the camp and to co-ordinate storage of equipment after the field school so that it would be available for use during mapping in 2017 and 2018.

Staff from NRCan and CNGO arrived in Taloyoak on the afternoon of August 2, 2016. During the next two days with the support of the Hamlet, researchers posted bilingual brochures and notices around town (Figure 2a, b), set up a low-impact tent camp on an esker adjacent to German lake[5] (Figure 2c), updated information on the Taloyoak Community Facebook page and made arrangements for informa-

[5] *Unofficial place name*

Figure 2: Promoting an accessible community geoscience field school in Nunavut: **a)** brochures distributed at key establishments around the Hamlet of Taloyoak, Nunavut; **b)** bilingual sign postings; **c)** setting of the low-impact, tent-based field school 3.5 km north of Taloyoak, adjacent to a frequently travelled road leading to traditional hunting and fishing grounds near Middle Lake (Figure 5a).

tion to be announced during noon-time community-radio programming. A presentation at the school to teachers and teaching assistants of grades 8 through 12 outlined the scope and intent of the planned activity and its relevance to inspiring youth to realize postsecondary educational opportunities and the variety of career opportunities related to scientific research in the Far North.

The Taloyoak Geoscience Field School held a full-day open house on Friday August 5, hosting more than 160 residents of all ages from Friday, August 5 to the morning of Wednesday, August 10, 2016.

Materials

Mineral specimens from the Government of Nunavut's *Rocks and Minerals of Nunavut Teaching Kit*, distributed to all schools across Nunavut in 2009, formed the foundation of the mineral-identification module (Figure 3a) and complemented a Geological Survey of Canada mineral collection. Rock samples used for demonstration purposes originated from Nunavut, with specimens from Baffin Island, the Committee Bay belt, the Thelon tectonic zone and Southampton Island (Figure 3b). Aerial photographs of distinctive landmarks near Taloyoak and Gjoa Haven were used for stereoscopic viewing to maximize the impact on participants to whom these landmarks would be familiar. Newly acquired airborne geophysical data were used to illustrate one low-impact method of gaining insight into Earth's interior.

Topics covered

Aspects of geoscience relevant to residents of Taloyoak provided the foundation of the field school.

Why and how we map rocks: the story they tell

Several different examples of northern maps were used to illustrate how different types of information can be portrayed (Figure 4a). The geological bedrock map of Nunavut (de Kemp et al., 2006) and locally sourced rock samples, including pink granite, green metavolcanic rocks and beige carbonate rocks, demonstrated how colour on a geological map is designed to correlate with rock type. Everyday uses of a geological map, including locating gem-quality minerals (e.g., garnet) for jewellery making and locating fossil localities for collecting and studying ancient life forms, were discussed.

Theoretical knowledge of the *Periodic Table of the Elements* was put to use to highlight how naturally occurring elements combine to form minerals, and naturally occurring minerals combine to form rocks (Figure 4b). The value of rocks as one of the few recorders of events in the ancient past was realized with the aid of samples from across Nunavut (Figure 4c). These samples provide a record of volcanism (pyroclastic breccia from Cumberland Peninsula), warm oceans (marble from Cape Dorset, Kimmirut) and quiescent ocean basins (iron formation from the Mary River mine, Baffin Island), not only before humans existed but extending back in time some 2–3 billion years.

Ancient ice sheets: why we care

Elements of geomorphology, glacial geology and cartography were integrated through examination of local glacial features, topographic maps, satellite images, airphotos and surficial-geology maps (Dyke, 1984; Tremblay et al., 2007). This enabled an understanding of the fluctuating presence of large ice sheets during the last 2 million years

Figure 3: Geological materials and data from Nunavut: **a)** investigating characteristics of minerals using the Government of Nunavut's *Rocks and Minerals of Nunavut Identification Kit*; **b)** plain-language descriptions of samples allowed self-directed, individual-paced learning.

Figure 4: Rocks and minerals, the story they tell: **a)** recognizing the value of maps to convey different types of information; **b)** appreciating the link between naturally occurring elements, combinations of elements (minerals) and combinations of minerals that form rocks; **c)** marvelling at events in Nunavut's ancient past as learned from its rock record.

(Quaternary Period), and participants easily envisaged the effects of receding ice through identification of swarms of highly elongate drumlins, or flutings, in the Taloyoak area. Limestone erratics, underfoot at the field school site, illustrated how northeast-flowing ice transported Ordovician carbonate rocks from the Rasmussen Basin across the Boothia Peninsula. These dispersed erratics provided a relevant example of how rocks and minerals from economic deposits can be similarly dispersed, and traced 'up ice' to their source. The location of the field school (Figure 5a) on an esker, deposited from meltwaters flowing beneath the glacier during its retreat, emphasized the importance of ancient ice sheets as a source of sand and gravel, critical for the construction of community roads and airstrips. The presence of raised beaches (Figure 5), many of which were notably rich in marine shells, served as a reminder of the long history of sea-level change in this region.

Geophysics: what it reveals

An overview of publicly available potential-field datasets (gravity and magnetics), interpretation techniques for each dataset and a brief overview of instrumentation (gravimeter and magnetic-susceptibility meter) for conducting ground surveys and follow-up fieldwork (Figure 6a) set the stage for 'hands-on' geophysical methods. Participants enjoyed using the magnetic-susceptibility meter to measure various rock samples (Figure 6b) that could be correlated to magnetic-field images over their land. Given that the Aston Bay Holdings Ltd. copper project on northwestern Somerset Island, the closest exploration camp to Taloyoak, relies heavily on gravity data for exploration, a demonstration ground gravity survey was developed. This survey, over a buried object, illustrated the value of gravity as a low-impact method to locate and identify a buried object (Figure 6c).

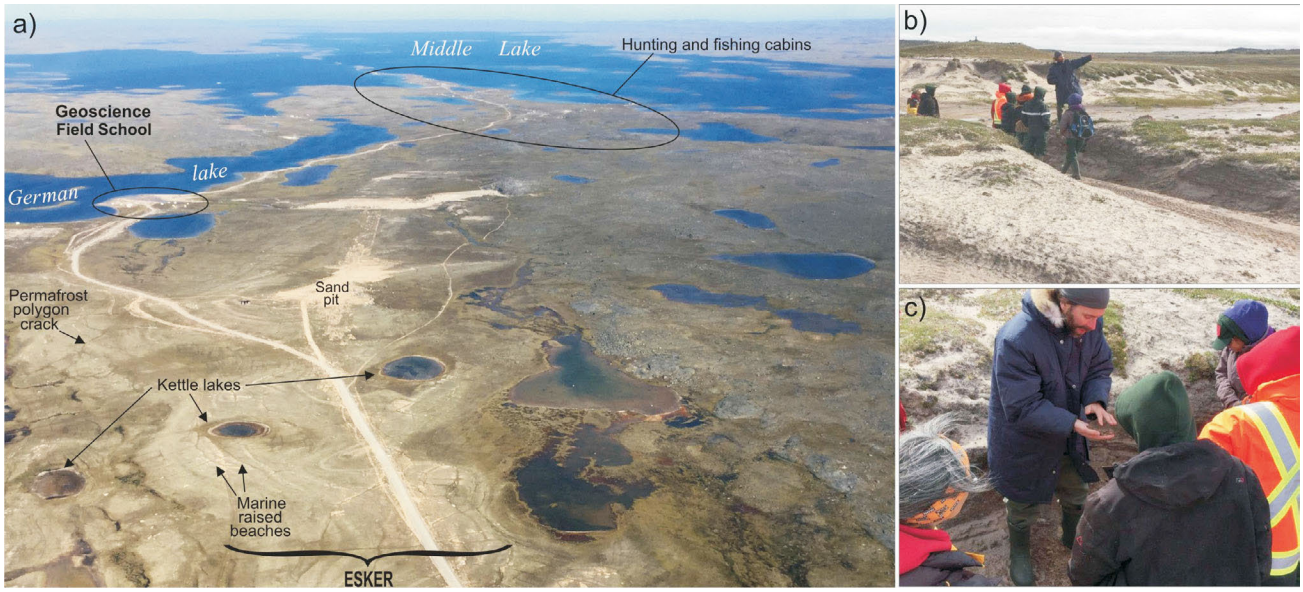

Figure 5: Glacial geology: **a)** site of the Taloyoak Geoscience Field School on an esker, pitted by kettle lakes (formed by large 'cubes' of glacial ice that became entrained in the esker sediment and subsequently melted) and transected by raised beaches marking marine retreat following deglaciation, provided a natural classroom for integrated glacial studies; **b)** roadcut exposing marine littoral sediments; **c)** examination of marine littoral sediments composed of fine sand alternating with layers of ancient plant remains (macrorest layers).

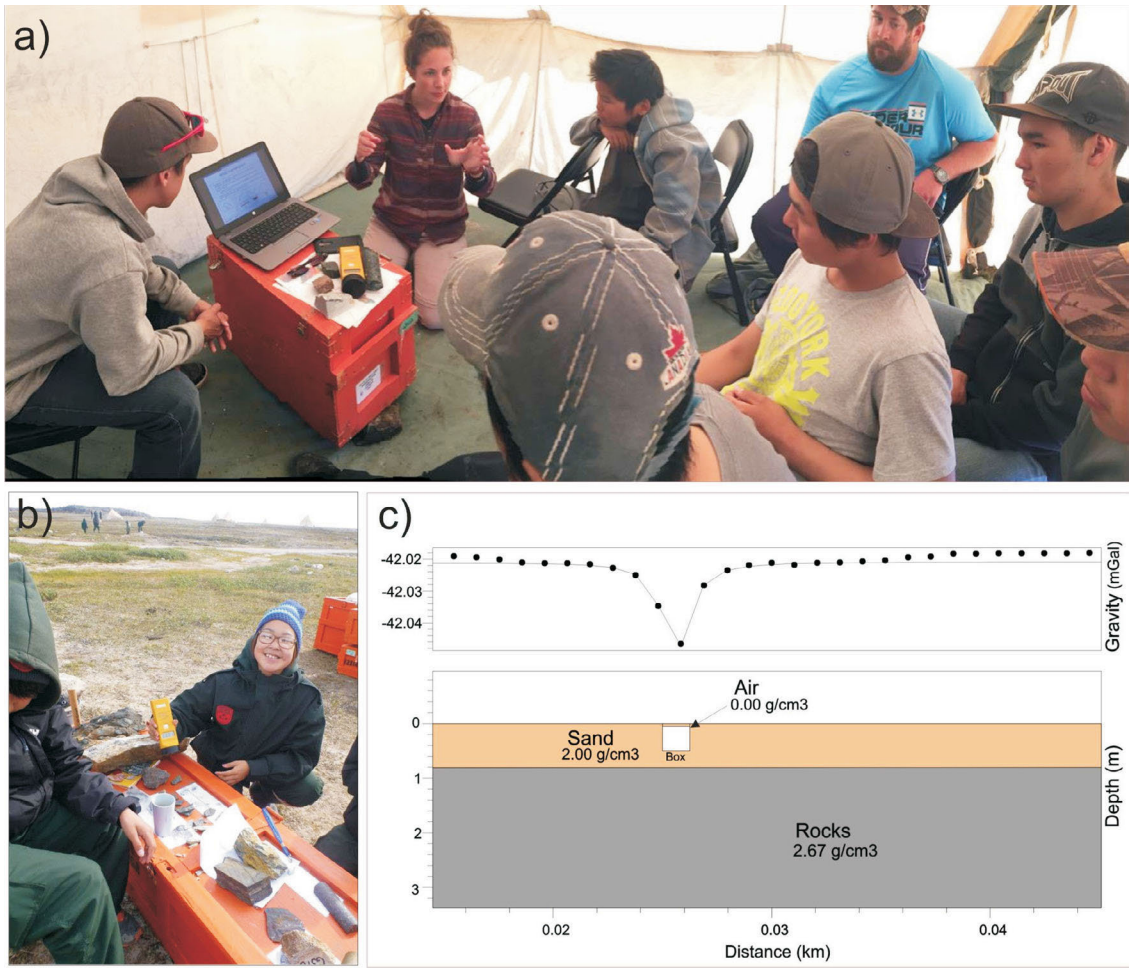

Figure 6: Geophysics, what it reveals: **a)** overview of datasets and methods; **b)** measuring magnetic susceptibility on various samples; **c)** processed data for a simple gravity survey over a buried object.

Mapping in a digital age (GIS)

Field-school participants were introduced to the geographic-information system (GIS), designed to capture, store, manipulate, analyze, manage and present all types of spatial or geographic data, and were provided with an overview of what a GIS specialist does in both office and field settings. 'Hands-on' exploration of a program file containing multiple digital datasets (shapefiles and satellite imagery) using ArcGIS was accomplished in groups of three participants who 'explored' a GIS file of the Taloyoak area for approximately 20–30 minutes. Guidance in selecting features and using basic tools in ArcGIS, such as pan, zoom, measure, identify and find, encouraged participants to locate the homes of friends and family, and to quantify familiar objects, such as the airstrip and Northern store. In addition, various datasets were introduced through an exercise that challenged each GIS team to locate the smallest object visible on the WorldView satellite imagery, and to compare the imagery to the CanVec topographic vectors.

Scratch cooking and nutrition

Two key concepts regarding cooking and nutrition were integrated into a kitchen module offered by the field school. The importance of shifting from highly processed foods to more nutritious, 'from-scratch' cooking was instilled through simple lunches and snacks that combined locally available groceries to produce delicious, yet nutritious lunches and snacks offered to participants each day. Participants contributed to the preparation either by learning a new recipe (Figure 7a) or by sharing a traditional one (Figure 7b, c). The second key concept was that of food management as a career option. Discussions and demonstrations by Toronto-based chef and food activist Joshna Maharaj on the various career paths opening up in the culinary world added to the important role of cooking and meal services centred around northern research and industry camps. Country foods, including arctic char and caribou shoulder, were integrated into the field school meal plan and became an important attraction.

Geocaching using GPS

A popular module offered at the field school involved a hands-on introduction to geocaching (Figure 8a), a treasure-hunting game played by entering co-ordinates into a Global Positioning System (GPS) unit and navigating (Figure 8b) to that position to find a hidden container (cache). Three course configurations, each approximately 3.7 km long, included six caches that held mineral specimens for participants to find and keep. Responsible land-use practices were reinforced through a bonus challenge issued to collect garbage encountered on the route (Figure 8c), with prizes awarded to teams who not only navigated the course successfully but left the environment cleaner than they encountered it.

Key outcomes

The 2016 Taloyoak Geoscience Field School successfully engaged residents in aspects of geology relevant to their community. It allowed dialogue over a sustained period of time in a field setting proximal to Taloyoak, thereby maximizing accessibility for all. It facilitated understanding of the gap in geological knowledge created by out-of-date datasets such as geology maps, and became an important forum for discussing fieldwork planned in the area over the course of the Boothia Peninsula–Somerset Island activity.

The tent-style setting provided a hospitable and receptive destination for residents of all ages (Figure 9) to come to-

Figure 7: Scratch cooking and nutrition: **a)** preparation of scallion cornbread, an alternative to cake; **b)** sharing a bannock recipe; **c)** enjoying a lesson in geology over a nutritious lunch.

Figure 8: Geocaching using GPS: **a)** establishing bearings for the group; **b)** heading to the first cache; **c)** leaving the route cleaner than it was.

gether to learn and appreciate aspects of their land that previously were unfamiliar to them. The respect and commitment demonstrated by the NRCan and CNGO staff throughout the planning and execution of this initiative strengthened support for, and trust of, GEM-2 operations, providing a stronger foundation on which to advance activities related to updating geoscience knowledge across this region.

The geophysics module effectively communicated the low-impact way in which various geophysical surveys can reveal aspects of Earth's interior, while minimizing the human footprint on the land. Presentation of aeromagnetic data garnered appreciation by participants of the type and significance of information acquired by the distinctive-looking aircraft and helicopters that many residents had noticed over their community. The importance of data management in this digital age brought an increased awareness of career opportunities in this field.

The scientific perspective communicated in all aspects of the field school added to the existing local and traditional

Figure 9: The Taloyoak Geoscience Field School reached a broad spectrum of the community and successfully integrated modern science with traditional practices in a respectful and appreciative manner.

knowledge of landmarks, natural materials, topography and travelling routes, in a way that illustrated how both perspectives can coexist. This particularly excited youth who understood that following a career path in geoscience need not exclude traditional learning and living on the land.

Economic considerations

Several participants at the Taloyoak Geoscience Field School had taken the Government of Nunavut's Prospecting Course, most recently offered in July 2016, and welcomed the opportunity to refresh the knowledge gained and to examine a different suite of samples from across Nunavut. Those interested in geoscience were encouraged to register in future prospecting courses. The application of various topics covered at the field school (e.g., geophysics, glacial geology) to mineral exploration helped illustrate that many aspects of mineral exploration do not necessarily impose a significant impact on the environment. In addition, participants came to realize that the usefulness of bedrock and surficial mapping is not solely directed toward exploration for economic resources, but that these mapping activities are critical to understanding the evolution of a region in terms of geological events and ice history. Recognition that we all use metals and minerals to establish infrastructure, for transportation and for technology highlighted the balance between responsible economic sustainability and land use.

Acknowledgments

The authors thank the residents of Taloyoak who took the time to visit the Taloyoak Geoscience Field School and acquire greater knowledge and appreciation of the land we share. They gratefully acknowledge the Taloyoak community support of Jimmy Oleekatalik; Mayor Joe Ashevak; Senior Administrative Officer (SAO) Murtaza Gurmani; Joseph Quqqiaq; Larry Banks; Julie Sarasin; former SAO Greg Holitzki; Kristine, Dennis and Charlie Lyall; and the interest and thoughtfulness of Cathy and Dave Williams. Logistical support essential to delivery of this initiative was provided by the Polar Continental Support Program. The Taloyoak Geoscience Field School was funded through the Geo-mapping for Energy and Minerals (GEM) program and through Strategic Investments in Northern Economic Development (SINED) in partnership with the Canada-Nunavut Geoscience Office. Kate Clark is thanked for her review of this paper and her ongoing role in GEM community-engagement activities.

Natural Resources Canada, Earth Science Sector contribution 20160200

References

Berman, R.G., Nadeau, L., McMartin, I., McCurdy, M.W., Craven, J.A., Girard, É., Sanborn-Barrie, M., Carr, S., Pehrsson, S., Whalen, J.B., Davis, W.J., Roberts, B.J. and Grenier, A. 2015a: Report of activities for the Geology and Mineral Potential of the Chantrey-Thelon Area: GEM-2 Thelon tectonic zone; Geological Survey of Canada, Open File 7693, 14 p. doi:10.4095/295644

Berman, R.G., Nadeau, L., Percival, J.A., Harris, J.R., Girard, E., Whalen, J.A., Davis, W.J., Kellett, D., Jefferson, C.W., Camacho, A. and Bethune, K. 2015b: Geo-Mapping Frontiers' Chantrey project: bedrock geology and multidisciplinary supporting data of a 550 kilometre transect across the Thelon tectonic zone, Queen Maud block, and adjacent Rae craton; Geological Survey of Canada, Open File 7698, 39 p. and 1 map. doi:10.4095/296202

Berman, R.G., Sanborn-Barrie, M., Nadeau, L., Brouillette, P., Camacho, A., Davis, W.J., McCurdy, M., McMartin, I., Weller, O., Chadwick, T., Liikane, D. and Ma, S. 2016: Report of activities for the GEM-2 project 'Geology and Mineral Potential of the Chantrey-Thelon Area: Thelon tectonic zone'; Geological Survey of Canada, Open File 8129, 12 p. doi:10.4095/299386

Blackadar, R.G. 1967: Precambrian geology of Boothia Peninsula, Somerset Island, and Prince of Wales Island, District of Franklin; Geological Survey of Canada, Bulletin 151, 62 p.

Davis, W.J., Berman, R.G., Nadeau, L. and Percival, J.A. 2014: U-Pb zircon geochronology of a transect across the Thelon tectonic zone, Queen Maud region, and adjacent Rae craton, Kitikmeot Region, Nunavut, Canada; Geological Survey of Canada, Open File 7652, 38 p. doi:10.4095/295177

de Kemp, E., Gilbert, C. and James, D.T. 2006: Geology of Nunavut; Geological Survey of Canada–Canada-Nunavut Geoscience Office, scale 1:3 500 000.

Dyke, A.S. 1984: Quaternary geology of Boothia Peninsula and northern District of Keewatin, central Canadian Arctic; Geological Survey of Canada, Memoir 407, 26 p.

Frisch, T. 2011: Geology, Precambrian geology of northern Boothia Peninsula and Somerset Island, Nunavut; Geological Survey of Canada, Open File 6051, scale 1:250 000. doi:10.4095/287896

Tremblay, T., Ryan, J.J. and James, D.T. 2007: Ice-flow studies in Boothia mainland (NTS 57A and 57B), Kitikmeot region, Nunavut; Geological Survey of Canada, Open File 5554, 16 p. doi:10.4095/224165

The **Canada-Nunavut Geoscience Office** conducts new geoscience mapping and research, supports geoscience-capacity building, disseminates geoscience information and develops collaborative geoscience partnerships for Nunavut.

www.cngo.ca